

University of South Bohemia

Faculty of Science



Ph.D. Thesis

**The role of p38-Mapk14/11 as an enabler of primitive endoderm (PrE) maturation and as a sensor of metabolism during mouse preimplantation embryo development**

Vasanth Thamodaran M.Sc.

Supervisor: Asst. Prof. Dr. Alexander W. Bruce Ph.D.

Department of Molecular Biology and Genetics

České Budějovice 2016

Vasanth Thamodaran (2016): **The role of p38-Mapk14/11 as an enabler of primitive endoderm (PrE) maturation and as a sensor of metabolism during mouse preimplantation embryo development.** Ph.D. thesis in English (198 pages), University of South Bohemia, Department of Molecular Biology and Genetics, Faculty of Science, České Budějovice, Czech Republic.

## **ANOTATION**

This thesis describes the role of p38-Mapk14/11 in regulating primitive endoderm (PrE) cell fate and its sensitivity towards exogenously supplemented amino acids during *in vitro* culture of mouse preimplantation embryo development. This study, utilizing various pharmacological inhibitors, gene transcript over-expression and immunofluorescence assisted confocal imaging, has revealed the central role p38-Mapk14/11 in promoting blastocyst stage embryo inner cell mass (ICM) maturation (to yield fully separated PrE and epiblast/ EPI tissue layers) and its potential requirement, as a protector against oxidative stress, under stress conditions, exemplified by amino acid deprived *in vitro* conditions.

## **Financial Support**

The study was supported by the award of a Marie Curie Career Integration Fellowship (to AWB; IDNOVCEL FAT2011) under the European Community's 7<sup>th</sup> framework programme and by an award from the Czech Science Foundation (to AWB; 13-03295S).

## **Declaration**

I hereby declare that my Ph.D. thesis is my work alone and that I have used only those sources and literature detailed in the list of references.

Further, I declare that, in accordance with Article 47b of Act No. 111/1998 Coll. in the valid wording, I agree to the publication of my Ph.D. thesis [in unabbreviated form – in the form arising from the omission of marked parts archived at the Faculty of Science] in electronic form in a publically accessible part of the STAG database operated by the University of South Bohemia in České Budějovice on its webpage, with the preservation of my rights of authorship to the submitted text of this thesis. Further, I agree to the publication, via the same electronic portal, in accordance with the detailed regulations of Act 111/1998 Coll., of the reviews of the supervisor and opponents of the thesis as well as the record of proceedings and result of the defence of the thesis. I also agree to the comparison of the text of my thesis with the Theses.cz database operated by the National Registry of Theses and the Plagiarism Tracing System.

Place and Date

Student's signature

## Statement regarding contribution

- **Thamodaran V**, Bruce AW. 2016. p38 (Mapk14/11) occupies a regulatory node governing entry into primitive endoderm differentiation during preimplantation mouse embryo development. *Open Biology*. 6: 160190.

Vasanth Thamodaran performed the microinjection and inhibition studies, generated the plasmid constructs harboring constitutively active mutants of Mkk6, Mk3, ATF2 and MSK1 and analyzed data. He also helped with writing the manuscript.

- Mihajlović AI, **Thamodaran V**, Bruce AW. 2015. The first two cell-fate decisions of preimplantation mouse embryo development are not functionally independent. *Scientific reports*. 5: 15034.

Vasanth Thamodaran performed supporting experiments to the main author (Mihajlović AI), that whilst not contained within this thesis (as they do not follow the p38-Mapk14/11 narrative) are deserving of merit and recognition here.

.....

Asst. Prof. Dr. Alexander W. Bruce Ph.D.

## Acknowledgment

Firstly, I would like to express my sincere gratitude to my advisor Dr. Alexander. W. Bruce for providing me an opportunity to work in his laboratory and his continuous support of my Ph.D study and related research, for his patience, time, efforts, motivation and giving me hope at difficult times during research. I am grateful and respect his willingness/ readiness to take a risk and provide me with relative theoretical freedoms at work, that I imagine is not typical, even in a well established groups. His guidance has helped me throughout my time of research and during the writing of this thesis. I could not have imagined having a better advisor and mentor for my Ph.D study.

My special thanks to my labmates, Aleksander Mihajlović, Giorgio Virnicchi and Lenka Veselovská for their valuable discussions, continuous support and help throughout my studies. I thank my former colleague Ender Yalçinkaya for helping me with *in vitro* maturation of oocytes and *in vitro* fertilization techniques (during the early part of my studies – not included in this thesis).

I thank Dr. Fournoux Pierre (INRA, France) and Dr. Peter Cheung (York University, Canada) for providing us the CA-ATF2 and CA-MSK1 plasmids respectively. I thank Dr. Lawrence Stanton (Genome Institute of Singapore, Singapore) for providing us the Zscan10 antibody.

I would like to thank my friends for providing their support and for many memorable and joyful moments throughout my stay.

I am grateful to my friends Saranathan. R and Muralidharan. N for helping my parents, when I couldn't be around during my studies.

Last but not the least, I would like to express my sincere gratitude to my parents. I am indebted for their support, the freedom they gave me to chose what I like, the hard work and the sacrifices they made, without which/whom I would haven't made all the way through my career and life in general.

<b>Contents</b>	<b>Page number</b>
Abbreviations	1
1. Summary	3
2. Introduction	5
2.1 An overview of mouse preimplantation embryo development	6
2.2 The first cell fate decision	7
2.3 The second cell fate decision	9
2.4 Factors regulating cell fate decisions in the preimplantation mouse embryo	9
a. Polarization factors: the initiators of cell microenvironment	9
b. Epigenetic modifications: fine tuning cell fate decisions	11
c. Transcription factors: the gatekeepers of specific cell fate	12
d. Transcription factors regulating the trophoectoderm lineage	12
e. Transcription factors regulating primitive endoderm	15
f. Transcription factors regulating pluripotency	16
g. Crosstalk between transcription factors of different lineages	17
2.5 Signal transduction pathways: The messengers that connect external cues with transcriptional regulation and appropriate gene expression	19
a. The Hippo signalling cascade	19
b. The Fgf signalling pathway	22
c. The Tgf- $\beta$ signalling pathway	26
d. The Mitogen activated protein kinase (Mapk) signalling cascade	30
2.6 Metabolism in stem cell fate regulation	45
a. OXPHOS and glycolytic pathways in cell fate regulation	46
b. Signalling mechanisms regulating metabolism and stem cell function	48
c. Metabolism in mouse preimplantation embryo development	50
3. Objectives	55
4. Materials and methods	57

5. Results ( <i>based on Thamodaran V and Bruce AW, 2016. Open Biology.6 : 160190</i> )	61
5.1 Active p38-Mapk14/11 is required for PrE differentiation	62
5.2 p38-Mapk14/11 activity is required during the early stages of blastocyst maturation to permit uncommitted cells to initiate PrE differentiation	72
5.3 Fgf-receptor (Fgfr) mediated cell signalling and the activation of the non-canonically activated BMP-related kinase Tak1, functionally activates p38-Mapk14/11 during PrE derivation	81
5.4 Concluding summary	90
6. Unpublished data	93
6.1 Analysis aimed at identifying downstream factors responsible for the observed p38-Mapk14/11 mediated effects on PrE formation and ICM maturation	94
6.2 Sensitivity of the p38-Mapk14/11 signalling pathway to amino acid (AA) availability in embryo culture media	99
6.3 p38-Mapk14/11 protects against reactive oxygen species (ROS) induced cell death in the preimplantation blastocyst stage embryo	106
6.4 Concluding summary	112
7. Discussion	114
8. Overall conclusion	127
9. References	129
10. Appendix	148

## Abbreviations

AA	amino acid
Atf2	activated transcription factor 2
Bmp	bone morphogenetic protein
Bmpr	bone morphogenetic protein receptor
Cdx2	caudal type homeobox 2
DOHaD	developmental origins of health and disease
EPI	epiblast
Erk	extracellular signal-regulated kinase
Fgf	fibroblast growth factor
Fgfr	fibroblast growth factor receptor
Gata4	GATA binding protein 4
Gata6	GATA binding protein 6
Gsk-3 $\beta$	glycogen synthase kinase-3 $\beta$
ICM	inner cell mass
Jnk	Jun amino-terminal kinases
KSOM	potassium simplex optimized media
Map2k	mitogen activated protein kinase kinase
Map3k	mitogen activated protein kinase kinase kinase
Mapk	mitogen activated protein kinase
Mk3	mitogen-activated protein kinase-activated protein kinase 3
Mkk6	mitogen kinase kinase 6
NAC	N-acetyl cysteine
Oct4	octamer-binding transcription factor 4
p38-Mapk	p38-mitogen activated protein kinase
PrE	primitive endoderm
ROS	reactive oxygen species
RTK	receptor tyrosine kinase
Sox2	SRY (sex determining region Y) -box 2
Sox17	SRY-box 17
Tak1	transforming growth factor- $\beta$ -activated kinase 1
TE	trophoectoderm
Tead4	TEA domain transcription factor 4
Tgf- $\beta$	transforming growth factor- $\beta$
TS	trophoblastic stem cell

Zscan10

zinc finger and SCAN domain containing *10*

# **1. Summary**

Given that the majority of p38-Mapk related work in the preimplantation mouse embryo to date has focused on developmental windows prior to the emergence of correctly specified and segregated primitive endoderm (PrE) and epiblast (EPI) inner cell mass (ICM) populations, the study aims to investigate the potential role of the p38-Mapk pathway during this latter period. Accordingly, a small chemical compound inhibitor (SB220025), that specifically targets the kinase activity of p38 $\alpha$ /Mapk14 and p38 $\beta$ /Mapk11 but does not affect p38 $\gamma$ /Mapk12 or p38 $\delta$ /Mapk13 or any other member of the greater Mapk gene superfamily was employed (Jackson *et al.* 1998) (herein referred to as 'p38-Mapk14/11 inhibition'), to treat embryos from the early (E3.5) to late (E4.5) blastocyst stages and assay for EPI and PrE marker protein expression. The study found that after such p38-Mapk14/11 inhibition, the number of maturing or matured PrE cells, as measured using Sox17 and Gata4 protein expression, is severely diminished compared to DMSO treated vehicle controls [further verified using a second p38-Mapk inhibiting compound, SB203580 (Davies *et al.* 2000), and a non-biologically active compound analogue control, SB202474 (Lee *et al.* 1994)]. Moreover, that the number of cells expressing the EPI marker Nanog is significantly increased, but that this latter phenotype is also profoundly associated with co-expression of the early PrE maker, Gata6, indicating a failure of cells to commit to one of the two ICM cell fates. Further, p38-Mapk14/11 activity occupies a critical window early in the blastocyst maturation, manifesting between the E3.5 and E3.75 developmental time-points. Furthermore, p38-Mapk14/11 functions downstream of Fgf-receptor signalling and the non-canonically and Bmp-ligand activated kinase, Tak1. Collectively, the findings demonstrate a role for p38-Mapk14/11 in mediating the full entry into differentiation/maturation of PrE progenitor cells within the ICM, via as yet uncharacterised mechanisms, that are then enhanced and driven via Mek1/2 dependent pathways. Consequently p38-Mapk14/11 occupies an important 'PrE regulatory node', potentially integrating multiple cell-signalling inputs, that acts to permit germane differentiation and separation of PrE from EPI cell populations, during mouse embryo blastocyst maturation. Further, p38-Mapk signalling is sensitive to availability of amino acids (AA) in the culture media, with blastocyst embryos cultured in KSOM (Potassium Simplex Optimised Media) lacking additional essential and non-essential AA supplementation displaying severe defects in extraembryonic lineages under p38-Mapk inhibited conditions compared to the inhibitor treated groups cultured in KSOM with AA (KSOM+AA) supplementation. In addition, p38-Mapk14/11 also potentially regulates the levels of reactive oxygen species (ROS) during blastocyst maturation, with the cell number deficit in both TE and overall ICM (but not the PrE deficit), induced by p38-Mapk14/11 inhibition, being rescued by the supplementation of culture media with anti-oxidant N-acetyl cysteine (NAC) in KSOM+AA but not in KSOM (lacking AA supplementation). Thus, indicating a possible role for p38-Mapk14/11 in regulating metabolism and associated ROS levels during mouse preimplantation development.

## **2. Introduction**

## 2.1 An overview of mouse preimplantation embryo development

In eutherian mammals, prior to implantation of the embryo in the uterine wall, the sequential events that occur from fertilization to the formation of a vesicular structure called the blastocyst, encompasses preimplantation embryonic development. The blastocyst possesses an epithelial cell layer called the trophoectoderm (TE) encasing the pluripotent epiblast (EPI) that is shielded by primitive endoderm (PrE) from a fluid filled blastocoel (Figure 1). After implantation, the TE gives rise to the extraembryonic ectoderm providing the bulk embryonic part of the placenta, the PrE generates the visceral and parietal endoderm that regulates the supply of nutrients to the developing foetus and the EPI develops into the foetus proper. A remarkable feature of the mammalian preimplantation embryo is its regulative developmental nature. For example, mammalian preimplantation embryos are able to resist interventions such as, cell rearrangement, changes in cell number (Tarkowski *et al.* 1959, 1961) and the removal of either animal or vegetal pole from the zygote (Zernicka-Goetz 1998) and yet recover their development to successfully yield a viable individual. This is in contrast to the deterministic embryos produced in organisms belonging to echinoderms, nematode fish and amphibians. The eggs of these animals have either mRNA or protein (determinants) specifying cell fate that are localized in specific patterns. After fertilization the zygote follows a particular set of cell division patterns and the subsequent cell fates are dictated by the determinants inherited by each cell. So, unlike regulative embryos, in deterministic embryos any interventions, such as those described above, will have profound and often fatal consequences for further development.

In mammalian preimplantation embryos, specification of the three above mentioned lineages from a single cell defines the earliest two cell fate decisions of development. The first cell fate decision commencing at the 8- to 16-cell stage transition generates the pluripotent inner cell mass (ICM) and the outer TE lineage. The second cell fate decision occurring during the early blastocyst stage segregates the ICM into PrE and EPI. The generation of different cell lineages is regulated by both synergistic and antagonistic transcription factor interactions that in turn regulate and respond to intra-cellular polarization and the relative different cell positions within the embryo generated during the 8- to 16-cell transition. The combined function of transcription factors in connection with polarization and cell position is bound together via various signal transduction pathways. Although the role of many of these factors, in relation to spatial and temporal aspects regulating cell fate choice have been uncovered, many aspects regarding preimplantation embryo development remain unclear. For example, the unique regulative nature of the mammalian preimplantation embryo is not clearly understood. Thus, indicating the need to identify other genes that can either work in separate pathways or work in parallel with the factors that have already been studied to address these outstanding questions.

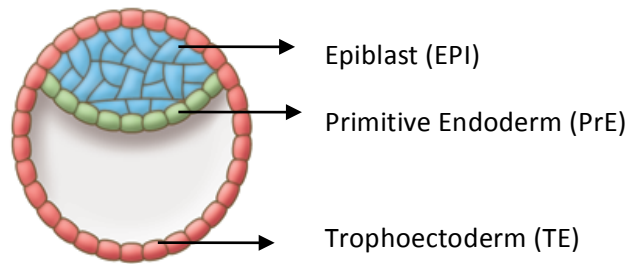


**Figure 1:** Diagrammatic representation of the blastocyst with an outer epithelium trophoectoderm (TE - red), pluripotent epiblast (EPI - blue) and the primitive endoderm (PrE - green). Both TE and PrE represent progenitors of the extraembryonic tissues after implantation and the EPI develops into foetus (taken from Cockburn and Rossant, 2010).

For the past five decades, researchers using mouse models have uncovered many clues to answer questions relating to early mammalian cell fate choice. In mouse, maternal mRNA and protein support development until the mid 2-cell stage after which, most of the mRNA is degraded (Hamatani *et al.* 2006) with some maternal proteins existing beyond the blastocyst stage (Gilbert and Solter 1985). A major transcriptional activation of the embryonic genome occurs during the mid 2-cell stage that is referred to as zygotic genome activation (ZGA), and is responsible for transferring the regulation of the embryo's development from maternal to self-governing control. During preimplantation embryo development, seven cell cleavage stages are accomplished by the mouse zygote. The first two divisions occurring in 18 hours interval with the subsequent divisions being separated by approximately 12 hours, ultimately leading to the formation of an expanded blastocyst (Aiken *et al.* 2004) after a total of 4.5 days (Figure 2). The expanded blastocyst comprising 128 or more cells then hatches out of its protective shell, *zona pellucida*, and becomes implanted in the endometrium wall of uterus. Using mouse as a model, the following sections are attempted to summarize the key features of mammalian preimplantation embryo development and the associated molecular mechanisms guiding its development.

## 2.2 The first cell fate decision

The first cell fate decision begins during the 8- to 16-cell stage transition, generating the progenitors for TE and ICM. During this transition the (outer) cells undergo two types of division, symmetric and asymmetric divisions. When a cell undergoes asymmetric division, a cell divides in an orientation such that one daughter cell is placed inside the embryo and the other outside (either directly following cytokinesis or shortly afterwards). The outer cells form the precursors for the TE lineage and the inside cells form the ICM that segregate in the blastocyst stage into pluripotent EPI and

primitive endoderm (PrE). Cells undergoing symmetric divisions produce two TE progenitor cells that remain on the outside surface of the embryo. Once these populations of cells (inside and outside) are set apart, the inner cells establish pluripotency gene networks involving transcription factors such as Oct4, Nanog and Sox2 that prevent cell differentiation. Whereas, the outer cells become enriched with TE lineage regulating factors like Cdx2 and repress pluripotency gene expression leading to differentiation of outer cells into trophoectoderm (reviewed in, Zernicka Goetz *et al.* 2009). These transcription factors maintain their respective lineages by auto-regulation as in the case of Cdx2 and Oct4 or by exhibiting antagonistic interactions such as the one found between Cdx2 with Sox2 and Nanog to suppress pluripotency in outer cells (Chen *et al.* 2005). These core transcription factors are

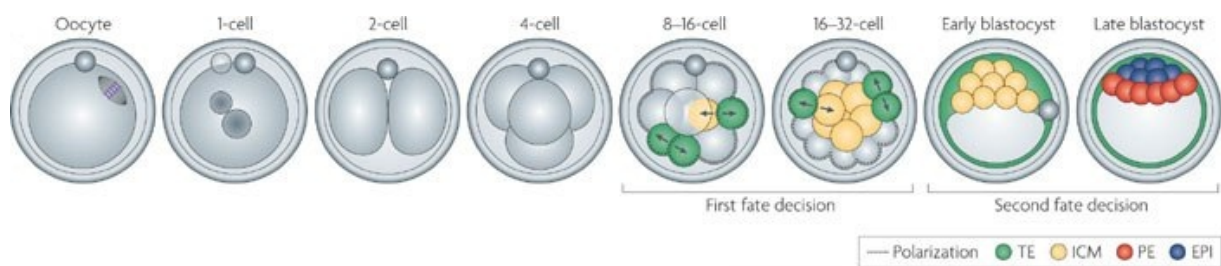


**Figure 2:** Mouse preimplantation embryo development showing the stages from unfertilised oocyte/ zygote to expanded blastocyst. The zygote undergoes three rounds of division to form the 8-cell stage embryo that becomes compacted by increasing cell-to-cell contacts and initiates intra-cellular polarization. During the 8- to 16-cell transition inner (yellow) and outer cells (green) are generated (the first cell fate decision) and again they are generated during 16- to 32-cell stage transition. By the early blastocyst stage the inner cells form the inner cell mass (yellow) and the outer cells form the TE (green). Also at the early blastocyst stage a fluid filled blastocoel/ cavity appears and expands by late blastocyst stage. Around the mid blastocyst stage the ICM sorts into EPI (blue) and PrE (red) cells and they become further segregated into two lineages during late blastocyst stage (the second cell fate decision; taken from Zernicka-Goetz, Morris and Bruce 2009).

also regulated by other transcription factors that work upstream or in parallel in establishing and maintaining specific lineages. For example, Tead4 functions upstream of Cdx2 thereby activating its expression only in TE outer cells. Additionally Gata3 also becomes enriched in TE during the blastocyst stage and works in parallel with Cdx2 to regulate TE maturation during implantation. Moreover, transcription factors are also regulated by signalling and cell polarization factors that are discussed in more detail later.

## 2.3 The second cell fate decision

Following the specification of the TE lineage (*i.e.* the first cell fate decision) the internalized ICM segregates into the primitive endoderm (PrE) and the pluripotent epiblast (EPI) lineages. By the late blastocyst stage the PrE eventually forms a monolayer facing the fluid filled blastocoel with cells of the EPI being located between it and the overlying TE (Figure 1). Resolution of ICM into PrE and EPI requires the expression of *Gata6* (Koutsourakis *et al.* 1999) and *Nanog* respectively in a mutually exclusive manner representing the so-called ‘salt and pepper pattern’ of distribution during the mid blastocyst stage (Chazaud *et al.* 2006; Plusa *et al.* 2008). Segregation of these two lineages is assisted by actin dependent cell sorting, cell death and expression of other transcription factors such as *Sox17* that commits progenitor cells to the PrE lineage (Chazaud *et al.* 2006; Plusa *et al.* 2008; Morris *et al.* 2010 and Niakan *et al.* 2010). The mechanisms behind the initiation of the salt and pepper pattern expression of these lineage markers in EPI and PrE progenitor cells, followed by their segregation is yet to be completely understood.

## 2.4 Factors regulating cell fate decisions in pre-implantation mouse embryo

The ultimate regulation of early cell fate in the pre-implantation embryo relies upon the intricate interplay between various molecular cell circuitries that integrate polarization, signal transduction, epigenetic and transcriptional programs within the three distinct cell lineages. The following sections will summarise the current knowledge of these mechanisms.

### a. Polarization factors: The initiators of differential cell microenvironments

Cell adhesion and cytoskeletal proteins are the first key players in the process of cell polarization. It was first shown in early studies by Hyafil *et al.*, (1980) that culturing mouse pre-implantation embryos with antibodies that inhibited the cell-to-cell adhesive properties of rabbit carcinoma cells, had the same effect on the cells of the embryo thus blocking its compaction during the 8- to 16-cell transition. Further analysis revealed that this effect was mediated by the antibodies recognizing and functionally inhibiting an 84kDa glycoprotein called E-cadherin. In 1983 Shiroysohi *et al.*, demonstrated that E-cadherin is functionally dependent upon  $Ca^{2+}$  ions and that their removal was also enough to inhibit compaction. It is now known that during compaction, E-cadherin in association with  $\beta$ -catenin, is found to polarize along the basolateral regions of blastomere (the name given to cells of preimplantation embryos) plasma membranes (Johnson *et al.* 1986; Sefton *et al.* 1996). Concomitantly, actin containing microvilli are also stabilized exclusively within the apical regions free of cell to cell contacts of blastomeres (Reeve & Ziomek 1981). What is responsible for these differential, yet related, polarization events? The answer lies with the ezrin, radixin and moesin

(ERM) family linker protein ezrin. Ezrin is known to provide a functional link between actin and the plasma membrane and its activity is regulated by phosphorylation at amino acid residue T567 (Hiscox *et al.* 1999). In 2004, Dard *et al.*, reported that a dominant negative point mutation of T567 causes the formation of long chains of abnormal apical microvilli and a failure in E-cadherin mediated cell-to-cell contact that results in the loss of compaction and polarization during the later 8-cell stage. Thus providing the functional link between blastomere polarization and embryo compaction. These two interdependent phenomena can also be induced in early 4-cell stage embryos, by experimentally inducing either protein kinase C or Rho-GTPase (Winkel *et al.* 1990, Clayton *et al.* 1999). These later results demonstrate that polarization molecules are present in the pre-8-cell stage embryo and that their activation at the late 8-cell stage is most likely regulated by post-translational modifications (Dard *et al.* 2004, Sefton 1992). If so, how are these mechanisms specifically activated during the late 8-cell stage? The key players in this case were found to be the PAR family of proteins.

PAR proteins are serine-threonine kinase proteins that were first discovered in *C. elegans*. They become cortically polarized and by regulating the orientation of the mitotic spindle they have been shown to control the first and asymmetric cell division of the worm embryo. During mouse pre-implantation development, there are three detectably expressed PAR homologs. These are Par3, Pard6b and Par1/Emk1 plus the Par/aPkc (aPkc-atypical protein kinase C) complex (Vinot *et al.* 2004, 2005). Pard6b and Emk1 can be observed localized at the mitotic spindle just prior to embryo compaction at the 8-cell stage. However, during compaction they become asymmetrically distributed with Pard6b, independent of cell to-cell-contact, occupying a polarized location along the apical region and Emk1 that is dependent on cell contacts, becoming distributed in the basolateral region (Vinot *et al.* 2005). Furthermore, aPKCzeta co-localizes together with Pard6b in the apical blastomere region during the 16-cell stage, although it is independently present as early as the 8-cell stage, and Par3 joins the complex only in blastocyst tight junctions. These features of asymmetric localization of PAR proteins, at a critical time in which the first inner ICM progenitor cells are being internalized via successive waves of asymmetric division, clearly indicate an important role during blastomere polarization and successful blastocyst morphogenesis. This perspective is reinforced by the work of Plusa *et al.* (2005), showing that down regulation of Par3 by RNAi or overexpression of a dominant negative mutant of aPKC resulted in an increased contribution of cells towards ICM by promoting more asymmetric-like cell divisions. Nevertheless, exactly how PAR proteins effect and are affected by polarization and compaction and exactly how they regulate molecular components such as ezrin, E-cadherin and  $\beta$ -catenin has yet to be fully and satisfactorily experimentally explored. Another noteworthy event that occurs during the radial polarization of 8-cell stage blastomeres is segregation of cells with distinct domains, with the contact free areas of each blastomere forming a distinct apical

domain enriched with microvilli and other actin interacting proteins and the basolateral region enriched with adhesion proteins, like E-cadherin. During further rounds of cell divisions depending on the components enriched in a given daughter cell, the cells either retain an outer position (cells with higher apical domain and lower basolateral related factors) or they take an inner position (if the cells inherit higher levels of basolateral components) (Nance *et al.* 2004).

#### **b. Epigenetic modifications: Fine-tuning cell fate decisions**

During preimplantation embryonic development the mammalian epigenome, (that represents the chemical modifications in DNA and its associated histone proteins that regulate gene expression and hence function and can also be inherited to offspring), undergoes dramatic changes, initially after fertilization after which it remains in dynamic flux until blastocyst formation.

In the blastocyst stage embryo, the repressive post-translational chromatin modifications, mono-, di- and tri-methylated lysine-27 (K27) histone H3 (H3K27me<sub>1/2/3</sub>), typically found in so called 'primed' bi-valent domains (also containing activating K4me<sub>3</sub>) that are associated with developmentally important yet silent differentiation genes, are readily detectable in the nuclei of ICM but less so in differentiating TE cells. In contrast, levels of the alternative repressive chromatin mark, methylation of K9 on histone H3 (H3K9me), display no significant differences between the two lineages (Erhardt *et al.* 2003). In addition to the observed lineage asymmetries in global histone methylation levels there are also known examples of developmentally important genomic gene loci harbouring differential epigenetic histone modifications. For example, in the ICM the *Oct4* and *Nanog* genes are associated with high levels of acetylation of K8 of histone H4 (H4K8ac) and H3K4me<sub>3</sub>, both epigenetic marks associated with actively transcribed chromatin, whereas the same loci are found in association with the transcriptionally repressive H3K9me<sub>2</sub> mark in the cells of the TE. Similarly, the TE specific transcription factor gene *Cdx2* is marked with H3K4me<sub>3</sub> in the TE lineage but associated with repressive histone modifications in the ICM (Vermilyea *et al.* 2009).

Hirasawa *et al.* (2008) showed that the DNA methylases Dnmt3a and Dnmt3b are dispensable throughout the pre-implantation developmental period. However, the DNA methyltransferase Dnmt1 is sufficient, by itself, to maintain the normal DNA methylation patterns, associated with transcriptional repression, and dynamics throughout preimplantation embryo development and moreover its genetic knockout does lead to embryonic lethality. As discussed above with respect to relative global levels of specific histone modifications between the ICM and TE, differential levels of genomic DNA methylation also develop by the blastocyst stage. Accordingly, the genome of the TE lineage is comparatively hypomethylated, although DNA methylation levels are greater than those observed in the 16-cell stage morula, whilst the ICM genome is relatively hypermethylated (Santos *et*

*al.* 2002). In addition to such global DNA methylation asymmetries, functionally important and gene specific differential methylation has also been reported. For example, the promoter of the *Elf5* gene, a transcription factor involved in maintaining TE cell fate, remains hypomethylated and therefore transcriptionally active in differentiating trophoblast. However, in the cells of the ICM the *Elf5* promoter is hypermethylated and consequently inactive. Of specific interest is the fact that Elf5 works together with Cdx2 in a positive feedback mechanism, whereby each transcription factor activates the others transcriptional expression, thus ensuring a 'lock-in' and maintenance of TE cell-fate in the trophoblast, that is dependent on differential inter-lineage DNA methylation (Ng *et al.* 2008).

#### **c. Transcription factors: The gatekeepers of specific cell fate**

The spatially equivalent blastomeres of the polarized 8-cell stage embryo divide to produce both the first outer cells and inner (and therefore spatially distinct) cells of the embryo. As discussed above, this spatial segregation is thought to provide the necessary micro environmental differences that are then sensed by signal transducers and ultimately leads to the required differential gene expression patterns that underpin formation of the three blastocyst cell lineage (Figure 1). The 'effectors' of this process are transcription factors that either activate or repress the genes necessary to influence cell fate in one direction or another (*i.e.* to differentiate or retain pluripotency). For example, in the blastocyst the transcription factor genes *Nanog* and *Oct4* are expressed exclusively in the ICM where they promote pluripotent gene expression programs. In contrast *Cdx2* expression is restricted to the TE lineage and promotes the expression of genes required to promote the differentiation of the trophoblast (Nicholas *et al.* 1998, Strumpf *et al.* 2005) and the transcription factors *Sox17*, *Gata4* and *Gata6* are restricted to progenitor cells of the PrE (Niakan *et al.* 2010).

#### **d. Transcription factors regulating the trophoectoderm lineage**

The development of the TE is regulated by a diverse set of transcription factors. These transcription factors are repressors of pluripotency and act to prime the outer blastomeres at the 16- and 32-cell stages to form fully epithelialized TE by the late blastocyst stage. The following will describe the current understanding regarding the principle transcription factor players involved during this crucial differentiation event.

The caudal homeobox gene family member, *Cdx2*, was first described in *Drosophila* as a regulator of cell-fate specification along the anterior-posterior axis of the embryo (Gamer *et al.* 1993). In the mouse model, *Cdx2* null mutants display embryonic lethality owing to a failure to hatch from the *zona pellucida* and implant into the uterine wall. This developmental failure is associated with

defects in maintaining the blastocoel, consequent to compromised epithelial function of the outer cells. Moreover, such defects are accompanied by abnormal expression of the pluripotency related transcription factors, Oct4 and Nanog, in the outer presumptive TE of the cavitating blastocyst. Readily detectable Cdx2 protein expression during unperturbed development starts at the late 8-cell stage and progressively becomes restricted to the outer, TE-destined, cells of the embryo where it is thought to activate the transcriptional expression of genes required to form the trophoblast (Strumpf *et al.* 2005). The importance of the *Cdx2* gene to successful and appropriate TE specific gene expression and therefore development is underscored by the observation that its own overexpression in pluripotent embryonic stem (ES) cell lines promotes morphological differentiation towards the TE lineage that is accompanied by TE-specific marker gene expression (Niwa *et al.* 2005). RNAi-based experimental down regulation of *Cdx2* expression in one cell of the 2-cell stage mouse embryo leads to an increase in the proportion of progeny blastomeres ultimately contributing towards the ICM, whereas *Cdx2* overexpression using a similar assay increases contribution to the TE (Jedrusik *et al.* 2008). Up-regulation of *Cdx2* has also been found enhance the expression and apical localization of the key polarity factor, aPkc and moreover this has been shown to be associated with increasing the frequency with which a blastomere would undergo a symmetric division that would yield more outside TE progenitor cells, during either the 8- to 16-cell or 16- to 32- cell stage transitions (Jedrusik *et al.* 2008); although other studies (employing only zygotic *Cdx2*<sup>-/-</sup> null embryos) suggest that polarisation is functionally independent of *Cdx2* (Ralston and Rossant 2008). The former described results are in strong accord with similar data that demonstrate that direct experimental down regulation of polarity factors is associated with an increased frequency of differentiative divisions (Plusa *et al.* 2005). Moreover, experiments that removed zygotic (as in the case of the genetic *Cdx2*<sup>-/-</sup> null described above and below) and also maternally contributed *Cdx2* reveal a phenotype of 8- to 16-cell stage arrest, that is associated with profound polarization defects (Jedrusik *et al.* 2014), although this result is disputed by others (Blij *et al.* 2012). Thus *Cdx2* works by up regulating TE specifying genes, down regulating pluripotent genes and fine-tuning apical-basal blastomere/embryo polarity, with knock-on consequences for symmetric/asymmetric divisions and the derivation of inner and outer cells that contributes to the successful formation of a functioning trophoblast lineage.

Whilst zygotic *Cdx2*<sup>-/-</sup> null mutant embryos fail to maintain TE epithelial integrity, the outer cells are still specified towards the TE lineage (Strumpf *et al.* 2005). This suggests the involvement of one or more factors functioning upstream of *Cdx2* in regulating TE specification. One such characterized upstream factor is encoded by the *Tead4* gene. *Tead4*<sup>-/-</sup> null embryos display a pre-implantation lethal phenotype (Yagi *et al.* 2007). This is due to a failure of the embryos to cavitate, hatch and

therefore implant. It is also impossible to derive any viable trophoblastic (TS) stem cell lines from *Tead4*<sup>-/-</sup> embryos, clearly implicating Tead4 in TE derivation. During mouse preimplantation embryo development nuclear localized Tead4 protein is detectable from the 4-cell to blastocyst stages with maximum expression evident at the 8-cell/ morula stages (Yagi *et al.* 2007& Nishioka *et al.* 2009). *Tead4*<sup>-/-</sup> null embryos do not activate the expression of the *Cdx2* gene, thus placing Tead4 functionally upstream of Cdx2 in the TE promoting transcription factor hierarchy. Tead4 and Cdx2 are known to transcriptionally activate two other downstream TE promoting transcription factor genes, *Eomes* and *Elf5*. Although experimental down regulation of either of these genes does not affect the formation of a morphologically recognizable blastocyst it is sufficient to prevent TS differentiation into trophoblast giant cells and extraembryonic ectoderm formation, respectively (Russ *et al.* 2000, Donnison *et al.* 2005).

Other studies have uncovered Gata3 as an independent TE promoting transcription factor, working in parallel with Cdx2 (Homes P *et al.* 2009; Ralston A *et al.* 2010). *Gata3* expression is first detectable at 4-cell stage and becomes restricted to the TE by the blastocyst stage (Home *et al.* 2009). It was revealed that unlike Cdx2, Gata3 is not required for early TE specification. Rather that it is required for TE maintenance, as Gata3 knockdown embryos are able to reach the morula stage but fail to cavitate (65%) despite expressing the early TE lineage markers *Tead4* and *Cdx2*. In addition, overexpression of *Gata3* in TS cells leads to their differentiation into cell types associated with post-implantation development, such as ectoplacental cone (EPC) or extra embryonic ectoderm (ExE), suggestive of a later developmental role for Gata3 (Ralston *et al.* 2010). Interestingly, Home *et al.* (2009) have shown that Gata3 negatively regulates the expression of *Tead4*. Therefore, Gata3 can be viewed as an attenuator of TE development, acting to fine-tune the balance between trophoblast maintenance and maturation. Further studies are required to address exactly how Tead4, Cdx2 and Gata3 cooperate to specify and then maintain the blastocyst trophoectoderm. Two other transcription factors, Klf5 and Tfap2c, have also been implicated in TE development. *Klf5*<sup>-/-</sup> knockout mice display preimplantation embryonic lethality and the embryos fail to cavitate. The embryos lacking *Klf5* show defects in TE and ICM and it was found to be important to suppress PrE specification in ICM lineage. Further, it was found to work downstream of *Fgf4* and upstream of *Cdx2* to regulate TE development (Lin *et al.* 2010). The transcription factor Tfap2c was found to play a key role in regulating the transcription of polarity factors and thereby mediating TE specification. It up-regulates the expression of genes related to apical polarity factors including *Pard6b*, *Rock1* and *Rock2* during 8-cell to morula transition stage and aids in suppressing Hippo signalling (see below) in outer cells to promote TE development. In addition, it also directly regulates the expression of *Cdx2* by binding to an intronic enhancer region in its promoter (Cao *et al.* 2015).

#### e. Transcription factors regulating primitive endoderm

The resolution of pluripotent EPI and differentiating PrE cells within the mature blastocyst ICM (Figure 1) is mediated by the differential expression of transcription factors. In mouse, *Gata*, *Sox* and HNF family proteins are known to play key roles during PrE formation (Koutsourakis *et al.* 1999; Soudais *et al.* 1995 and Niakan *et al.* 2010). Below, will be summarized the current knowledge of the important transcription factors involved in derivation of the PrE lineage.

Utilisation of transgenic embryos expressing a *Gata6-LacZ* fusion construct, led Koutsourakis *et al.*, (1999) to show that *Gata6* expression first starts at the early blastocyst stage (E3.5) in ICM cells in a random fashion with *Gata6* expressing cells resident in both deep locations and also at the surface of the blastocoel. The authors also showed that *Gata6* (and *Gata4* another important PrE-promoting transcription factor acting downstream of *Gata6*) knockout embryos do initiate PrE differentiation but then fail to form one of its later derivative, the visceral endoderm, arguing that functional redundancy or maternally inherited proteins may explain this phenotype. Indeed, the expression of mutated dominant negative *Gata6* in the ICM has been shown to be associated with a reduced contribution of cells to the PrE (Meilhac *et al.* 2009). Moreover, the over-expression of either *Gata6* or *Gata4* is sufficient to initiate ES cells to differentiate towards a PrE-like fate and the clonal co-over-expression of *Gata6* and *Wnt9* within subsets of pre-implantation embryo cells, increases their contribution towards the PrE (Fujikura *et al.* 2002). Recently, Lavial *et al.* (2012) have shown that the polycomb group protein *Bmi1* is specifically up-regulated in endoderm and TS cells and that its expression is repressed by *Nanog* in ES cells. Interestingly *Bmi1* co-segregates with *Gata6* in the PrE progenitors of mouse preimplantation embryo and it has been found to protect *Gata6* from ubiquitin mediated proteasomal degradation, thereby stabilizing *Gata6* function. Finally, the expression of the *Sox17* gene, that begins during the mid blastocyst stage (E3.75), has also been implicated in PrE differentiation. *Sox17* protein also displays the characteristic salt and pepper pattern of expression that becomes restricted to cells lining the ICM surface at the cavity interface (Morris *et al.* 2010; Niakan *et al.* 2010). The *Sox17* protein promotes PrE differentiation by competing with the pluripotency promoting transcription factor *Nanog* for chromatin binding sites at pluripotency-related gene loci. Successful competition leads to transcriptional down-regulation of these genes and provides a 'window of opportunity' for PrE differentiation (Niakan *et al.* 2010). Apart from participating in a functional synergy with *Gata6*, it is also suggested that *Sox17* expression itself is regulated by *Gata6* in a positive feedback mechanism (Frankenberg *et al.* 2011). As *Sox17* competes with *Nanog* for binding sites, it is speculative that *Sox17* may activate *Bmi1*, that in turn stabilizes *Gata6* in PrE progenitor cells. It is noteworthy that in addition to transcription factor related-regulation of PrE lineage formation, cell sorting mechanisms responsible for the segregation of the

two ICM cell lineages that are themselves regulated by various signalling cascades, are also active. Such mechanisms will be addressed in the subsequent sections.

#### **f. Transcription Factors regulating pluripotency**

Oct4 and Nanog are homeodomain transcription factors that were first identified as critical regulators of pluripotency (Palmieri *et al.* 1994; Mitsui *et al.* 2003). Oct4 mRNA and protein are readily detectable in unfertilized oocytes (Scholer *et al.* 1990) however after fertilization these levels rapidly drop, in common with other maternally inherited factors. Oct4 mRNA and protein levels then steadily increase during and after zygotic genome activation (ZGA) and by the 8-cell stage the protein is detected in all cell nuclei (Palmieri *et al.* 1994). However, by the blastocyst stage Oct4 protein expression becomes restricted to the ICM and is undetectable in the TE. This expression profile is consistent with experimental evidence that shows *Oct4*<sup>-/-</sup> null ES cells spontaneously differentiate towards the trophoblast lineage (Nichols *et al.* 1998). Overall, experimental evidence implicates a role for Oct4 in promoting retention of cell pluripotency and places it centrally in the first cell-fate decision, delineating TE and ICM cell populations in the pre-implantation mouse embryo. In marked similarity to the *Oct4* knockout phenotype, the phenotype arising from genetic knockout of the *Sox2* gene also leads to the spontaneous differentiation of ES cells towards the trophoblast lineage (Avilion *et al.* 2003). The common ES cell phenotype exhibited by genetic knockout of the *Sox2* and *Oct4* genes is proposed to result from cooperation between Oct4 and Sox2 proteins in forming heterodimeric complexes that in turn transcriptionally regulate genes required for retention of pluripotency and resist differentiation (Boyer *et al.* 2005). An early study of *Sox2* expression in mouse pre-implantation embryos by Avilion *et al.* (2003) showed that Sox2 protein is universally expressed in all cells until the blastocyst stage after which it becomes restricted to the ICM. Another report by Keramari *et al.* (2010), has described *Sox2* expression in all cells of the blastocyst. Interestingly experimental down-regulation of *Sox2* expression is associated with a reduction in *Tead4* expression (a trophoectoderm regulating transcription factor) and Yap1 (a transcriptional co-factor of Tead4) suggesting a context dependent role of Sox2 in regulating both the ICM and TE lineages. However, a recent study found that the hippo pathway restricts the expression of Sox2 to the inner cells and its expression is suppressed in outer cells by Tead4 (Wicklow E *et al.* 2014). These contradicting observations need future investigations to better define the exact role for Sox2 during mouse preimplantation development.

The Nanog transcription factor has an expression pattern similar to that of Oct4. *Nanog* mRNA is first detectable in oocytes followed by a rapid drop off in levels that then increase during the 16-cell morula stage, with protein expression being restricted to the inner population of cells. This pattern of

inner cell expression is maintained in the blastocyst where only ICM cells display detectable Nanog protein expression. However, Nanog protein does not remain expressed in all ICM cells but rather exhibits the characteristic 'salt and pepper' expression pattern that is also observed for *Gata6/Sox17*, although double immuno-staining has shown that Nanog and *Gata6/Sox17* protein expressing cells are mutually exclusive (Chazaud *et al.* 2006; Morris *et al.* 2010). By the late-blastocyst stage Nanog protein expression becomes restricted to the EPI and is not detectable in the presumptive monolayer of PrE cells in contact with the cavity (Chambers *et al.* 2002). Chromatin immuno-precipitation analysis coupled to genomic DNA microarray hybridization (ChIP-Chip) in mouse ES cell lines has shown that Nanog directly transcriptionally regulates both the *Oct4* and *Sox2* genes to maintain pluripotency. Unlike *Oct4* and *Sox2*, *Nanog* is specifically expressed in the inner cells during the morula stage suggesting Nanog is a key regulator in maintaining pluripotency in these early founder cells that will subsequently populate the ICM and epiblast. Importantly, Nanog was found to maintain the ground state of pluripotency in ES cells (Silva *et al.* 2009). The ground state of pluripotency of ES cells represents a basal proliferative state free of epigenetic restriction and a minimal requirement for extrinsic stimuli. Silva *et al.* (2009), using ES and induced pluripotent stem (iPS) cells showed that *Oct4*, *Sox2* and *Klf4* are sufficient to maintain cells at a de-differentiated pre-pluripotent state characterized by incomplete expression of pluripotency associated genes and many of these genes are regulated by Nanog (Sridharan *et al.* 2009). They also showed that *Nanog*<sup>-/-</sup> null pre-iPS cells cannot attain the ground state of pluripotency and that this block can be overcome by reintroduction of functional Nanog. Besides these important roles for Nanog, it cannot maintain or induce pluripotency on its own (Takashi and Yamanaka, 2006). Silva *et al.* (2009), have shown Nanog is required at the final phase of inducing somatic cells to pluripotency when the cells attain the pre-iPS state in presence of other pluripotency factors. Thus, in this context Nanog functions as the gatekeeper to ground state pluripotency, whereas in the blastocyst embryo it acts to counter entry into ICM cell PrE differentiation (Chambers *et al.* 2002).

#### **g. Crosstalk between transcription factors of different lineages**

Some of the transcription factors introduced above are maternally inherited and their protein can persist until the blastocyst stage. Other transcription factors are initially expressed in all cells and become progressively restricted to specific lineages as the pre-implantation embryo matures. Though such restriction is often linked with symmetrical/ asymmetrical cell divisions (8- to 16-cell and 16- to 32-cell stage transitions) and cross talk between cells via various signalling mechanisms, it also involves regulatory interactions between different transcription factors. For example, pluripotency-related and differentiation-related transcription factors interact with each other antagonistically in order to establish a stable specific lineage.

Niwa *et al.* (2005) first reported such a reciprocal inhibitory interaction between the transcription factors Cdx2 and Oct4 in the delineation of the TE and ICM. Initiation of zygotically derived *Oct4* expression occurs during the 2-cell stage whereas Cdx2 mRNA levels peaks at the 8-to 16 cell stage (Wang *et al.* 2004). As Niwa *et al.* (2005) showed that at the late 16-cell morula stage, Cdx2 protein is expressed more in the outer cells than in the inner cells and that Oct4 is expressed universally in all the cells, it was suggested that an antagonistic interaction of Cdx2 over Oct4 must exist in outer cells in order to establish the TE lineage. Such a hypothesis was consistent with the previous observations that Oct4 protein is detectable in outer TE cells of *Cdx2*<sup>-/-</sup> embryos at early blastocyst stage (Strumpf *et al.* 2005) and the expression of TE markers in the ICM of *Oct4*<sup>-/-</sup> null embryos has been reported (Nichols *et al.* 1998). Thus Niwa *et al.* have suggested that in outer cells Cdx2 forms a protein-protein complex with Oct4 that results in the recruitment of transcriptional co-repressors to Oct4's pluripotency related target genes that then suppress their inappropriate expression. In line with this hypothesis Wang *et al.* (2010) have also demonstrated that Cdx2 recruits the chromatin remodelling factor Brg1 to Oct4 target loci and that this represses their expression independent of DNA methylation. Furthermore, Jedrusik *et al.* (2008) and later Skamagki *et al.* (2013) have shown that *Cdx2* mRNA becomes polarized in the apical region of 8-cell and outer 16-cell stage blastomeres and that it is inherited specifically by the outer TE destined cells following asymmetric cell divisions, thus reinforcing Cdx2 expression in outer cells.

In similarity to the antagonistic interaction between Oct4 and Cdx2, Chen *et al.* (2009) reported using both ES cells and mouse embryos an inhibitory cross talk between Cdx2 and Nanog whereby each transcription factor binds to the other factors' gene promoter to influence their transcriptional expression. The study also revealed that over-expression of *Nanog* reduces the expression levels of TE markers such as *Cdx2*, *Eomes* and *Hand1*. Alternatively, *Nanog* knockdown not only increases the expression levels of the PrE marker gene *Gata6* but also leads to the induction of *Cdx2* and other TE markers. ChIP-chip analysis in ES cells has shown that Nanog represses Cdx2 expression by direct binding to its promoter and reciprocally Cdx2 suppresses *Nanog* and *Oct4* expression by binding their gene promoters in the TE lineage (Chen *et al.* 2009).

In addition to the cross talk between TE and pluripotency factors, the pluripotency factors also interact with PrE regulating transcription factors to sort EPI from the PrE. Using mouse ES cell lines, Singh *et al.* (2007) demonstrated that *in vitro* culture produces a heterogeneous population of cells in which some cells express abnormally high levels of *Gata6* and unusually low levels of Nanog. These '*Gata6* high/*Nanog* low' cells arise spontaneously but can only be maintained only under differentiation-inducing conditions. Over expression of *Nanog* can reduce the heterogeneity of the cultured ES cell lines, thus highlighting Nanog's inhibitory and dominant effect over *Gata6*.

Consistently, ChIP-Chip analysis using human ES cell lines has shown that Nanog protein binds to the *Gata6* gene promoter and recruits the co-repressors Nac1 and Zfp281 to repress *Gata6* transcription (Boyer *et al.* 2005; Wang *et al.* 2006). Interestingly, Silva *et al.* (2009) have reported that *Nanog*<sup>-/-</sup> null mutant embryos are unable to form PrE and do not express the PrE marker genes *Gata4* or *Gata6*. They suggested the reason for this failure to induce PrE formation was due to a lack of an appropriate paracrine relationship between and epiblast and primitive endoderm progenitors. In support of this view, Yamanaka *et al.* (2010) demonstrated that differences between cells of the ICM in responding to Fgf4 (fibroblast growth factor 4) signalling underpins the appropriate sorting of ICM cells into the spatially distinct PrE and EPI lineages (Figure 1) by the late blastocyst stage. Thus transcription factors function in an inter-dependent manner to regulate each other's expression and functions. Consequently, such coordination plays a major role in initiating and maintaining different cell fates during pre-implantation mouse embryo development.

## **2.5 Signal transduction pathways: The messengers that connect external cues with transcriptional regulation and appropriate gene expression**

As described above, transcription factors play the key 'effector' role in regulating specific cell lineage formation. Nevertheless, exactly how their expression becomes enriched in developing specific and spatially distinct cell lineages and at the appropriate developmental time remains a major and largely unresolved question. The following section will summarise some of the current knowledge regarding the role of signal transducing pathways in directing the required gene expression patterns.

### **a. The Hippo signalling cascade**

The Hippo signalling pathway involves a sequential activation of serine/threonine kinases that ultimately regulates the activity of the functionally downstream transcriptional co-activator proteins Yap (Yes-associated protein)/Taz (Tafazzin). The pathway was first described in *Drosophila* with many of its functions conserved in mammals, it regulates a diversified group of cellular mechanisms that includes, embryogenesis, organogenesis, cell proliferation, differentiation and metabolism, with negative control of Yap/Taz proteins in cell proliferation being its key functions (Dong *et al.* 2007 and Santinon G *et al.* 2016). The core signalling cascade includes Mst1/2 kinases that along with the adaptor protein Sav1/WW45 activates Lats1/2 kinases by phosphorylation. The active Lats1/2 protein along with Mob1/2 kinases phosphorylates Yap/Taz leading to their cytoplasmic retention (via an interaction with 14-3-3 proteins) thus preventing their nuclear based transcriptional functions (Yu and Guan. 2013). Cytoplasmic phospho-Yap/Taz then either undergoes degradation or it interacts with other pathways such as Tgf- $\beta$  or Wnt to modulate their function (Azzolin L *et al.* 2014 and

Varelas X *et al.* 2010). However, the nuclear function of non-phosphorylated Yap/Taz, as a co-factor interacting with the members of Tead/Tef transcription factor family (Tead1-4), forms the key transcriptional complex regulating cellular functions, like proliferation and oncogenesis (Zhao B *et al.* 2008). In addition, Yap can also form a complex with Smad1 and Smad2/3 associated transcription complexes, promoting a cross talk between Tgf- $\beta$  family of signalling and the hippo pathway (Huang *et al.* 2016).

The major regulators of the Hippo pathway are cell density associated mechanical cues and to a lesser extent, G-protein coupled receptor (GPCR) and receptor tyrosine kinases (RTKs) (Meng *et al.* 2016). GPCR dependent signalling pathways can both activate and inactivate Hippo signalling depending on the activation of the downstream alpha subunit G protein. For instance, activation of  $G_{\alpha_s}$  results in Lats activation, whereas, GPCR signalling linked with  $G_{\alpha_{12/13}}$  leads to Lats inactivation, resulting in Yap inactivation (phosphorylation) and activation (non-phosphorylation) respectively. Though the GPCR regulated hippo pathway is not fully understood, it has been proposed to be mediated by the F-actin cytoskeleton and Rho-GTPases (Yu *et al.* 2012). In the case of RTK mediated hippo regulation, an epidermal growth factor receptor (EGFR) associated regulation remains the most understood mechanism. Stimulation of EGFR by EGF ligands like amphiregulin (AREG), leads to the activation of phosphoinositide 3-kinase (PI3K) and phosphoinositide dependent-kinase 1 (Pdk1). Mechanistic analyses have revealed that in the absence of liganded growth factors, Pdk1 forms a complex with Sav1 and Lats, thus maintaining hippo signalling in its active state and upon receptor activation Pdk1 becomes recruited to the plasma membrane leading to the disruption of the Sav1-Lats complex that consequently inactivates Lats, resulting in nuclear translocation of unphosphorylated Yap, where it regulates transcription (Fan *et al.* 2013).

As stated Hippo signalling also responds to mechanical cues associated with dynamic changes mediated by an increase or a decrease in cell density (Yu FX and Guan KL. 2013), with high cellular density resulting in cytoplasmic retention of Yap/Taz (*i.e.* Hippo on), whereas at low density Yap/Taz translocates to nucleus (*i.e.* Hippo off). The mechanical response accompanying such changes is reflected among both tight and adherence junction region associated components that include cytoskeleton proteins like F-actin, microtubules and actomyosin. Furthermore, several junctional associated proteins also play a key role in establishing proper apical-basal polarity, indicating an additional layer of control over the Hippo pathway. Accordingly, many Hippo regulators such as Merlin, Kibra, Angiomotins, E-Cadherin and  $\alpha$ -catenin are found to be associated with the cytoskeletal network like F-actin and form parts of junction complexes or regulate cell polarity. Thus disruption of either the cytoskeleton or the above mentioned hippo regulators dictate the nuclear inclusion or exclusion of Yap/Taz and hence hippo signalling activity (Meng *et al.* 2016).

## The role of the Hippo pathway during mouse preimplantation embryo development

As explained in the previous section, the transcription factor gene *Tead4* currently occupies the apex of the regulatory hierarchy of factors mediating TE lineage formation (Nishioka *et al.* 2008; Yagi *et al.* 2007). In contrast to *Cdx2*, *Tead4* protein is expressed in all cells at the 8-, 16-cell and early blastocyst stages, irrespective of relative inner or outer cell position. Therefore, there must exist a mechanism by which *Tead4* only directs its TE promoting regulatory output in the outer, and not inner, cells of the developing preimplantation mouse embryo. In order to function as a transcriptional activator *Tead4* is required to recruit its transcriptional co-activators *Yap/Taz* (Vassilev *et al.* 2001; Zao *et al.* 2008). This functional dependence on *Yap* led to the hypothesis that although *Tead4* may be present in all blastomeres at the 16-cell and early blastocyst stages, does its specific function depend upon the presence or absence of co-recruited *Yap* protein. Consistently, *Yap* is detectable in the nuclei of all 8-cell stage blastomeres but critically its expression becomes restricted to only outer cell nuclei in the subsequent cleavage stages and it is excluded from nuclei of inner cells (Nishioka *et al.* 2009). It is noteworthy that *Yap* displays functional redundancy with its related transcriptional co-activator *Taz* (both factors share approximately 50% similarity), as *Taz* can functionally compensate for the genetic loss of the *Yap* gene (Mahoney *et al.* 2005; Nishioka *et al.* 2009). Thus the relative intra-cellular localization of *Yap/Taz* with respect to a blastomere's relative spatial position in the embryo is responsible for regulating *Tead4* function and therefore specifying appropriate cell fate. Despite this elegant mechanism, what is responsible for *Yap/Taz* cytoplasmic retention in inner cells? *Yap/Taz* localization was found to be regulated by the *Lats1/2* serine/threonine kinases, that in turn are under the influence of the Hippo cell density sensing signalling pathway (Hao *et al.* 2008). Nishioka *et al.* (2009) found that in the inner cells of the embryo (completely surrounded by other cells), the Hippo pathway was sufficiently active to induce *Lats1/2* to phosphorylate *Yap/Taz*, resulting in their cytoplasmic retention, thereby depriving the nuclear localized *Tead4* of any transcriptional co-activators and therefore rendering it unable to activate the expression of genes required for TE differentiation. In contrast, in outer cells where the cell density is less and cells have an exposed apical domain, there is an insufficient level of active Hippo signalling and therefore unphosphorylated *Yap/Taz* is able to accumulate in the nucleus where they cooperate with *Tead4* to regulate TE lineage specification. Accordingly down-regulation of apical polarity factors like *Pard6b* leads to activating of Hippo signalling in outer cells and retention of *Yap* in the cytoplasm in its phosphorylated inactive form (Hirate *et al.* 2013).

Mechanistic studies have also demonstrated the role of Hippo regulators in mouse preimplantation embryo. The FERM domain containing protein Merlin, a component of the Kibra/Expanded complex and a positive regulator of Hippo, functions upstream of *Lats* kinase.

Maternal and zygotic genetic knockout of *Merlin* in mice results in ectopic nuclear localization of Yap in inner cells, leading to *Cdx2* expression and a blockage in ICM lineage specification. Merlin was found to localize to the cellular cortex in both outer and inner cells of the embryo, but to only execute its function in the inner cells (Cockburn *et al.* 2013). Further studies by individual research groups discovered the role of the junctional protein Angiomotin (Amot) in the regulating Hippo pathway in a manner that connects intracellular cell polarity and relative spatial position to lineage specification. In outer cells Amot exists in a non-phosphorylated form that leads to its sequestration in the apical domain by F-actin. In the inner cells it is phosphorylated at residue S176, preventing its interaction with F-actin and prolonging its association with Merlin, this active complex then promotes the activation of Lats kinase, which inactivates and retains Yap/Taz in cytoplasm by phosphorylation (Hirate *et al.* 2013 and Leung & Zernicka-Goetz. 2013). Further recent studies have demonstrated a polarity dependent role of small the GTPase RhoA (Rho-associated, coiled-coil containing protein kinase 1) and Rock (Rho-associated protein kinases 1/2) kinases in regulating Amot/Lats functions to mediate appropriate early cell-fate decisions (Kono *et al.* 2014 and Mihajlovic & Bruce 2016). Thus Hippo signalling plays a central role in regulating the first cell fate decision (TE and ICM specification) during mouse preimplantation embryo development (figure 3).

#### **b. The Fgf signalling pathway**

The fibroblast growth factor family (Fgf) is a group of growth factor ligands showing strong affinity to the cell surface glycoprotein heparin sulphate proteoglycans that promote signal transduction through specific tyrosine kinase receptors. There are 22 identified *Fgf* genes that are characterized by sequence coding for conserved 140 amino acid residue proteins (Ornitz. 2000). The canonical Fgfs (Fgf 1 – 8) display a strong affinity for heparin binding and include five sub family members. The second group of Fgfs are endocrine or hormone-like Fgf ligands displaying relatively lower affinity towards heparin. Both the above mentioned Fgf ligands depend on Fgf receptors (Fgfr), of which there are four in number (Fgfr1 – 4), for signal activation. The canonical ligands play key roles during embryonic development, tissue growth, repair and metabolism, whilst the endocrine Fgfs regulate bile acid, phosphate, lipid and carbohydrate metabolism, apart from functions similar to their canonical counterparts (Zhang. 2006). The third group of ligands are intracellular Fgfs (iFgf, Fgf11 -14) and unlike the other two groups are non-secretory and work independently of Fgfr receptors, functioning as co-factors for voltage gated sodium channels in neuronal and myocardial cells (Zhang X. 2012). Since, the canonical Fgf pathway is a key player during embryonic development, its mode of signalling activation is further explained below.

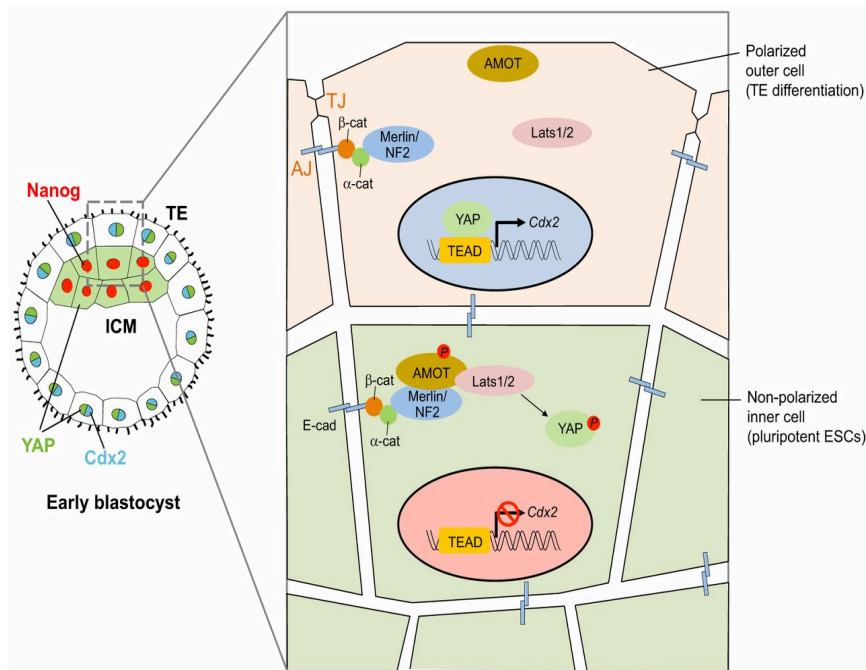


**Figure 3: Regulation of Tead4 activity by Hippo signalling.** The Hippo pathway senses cell density and converts it to a growth regulating signal thereby regulating gene expression. In outer polarised low cell density blastomeres, the hippo activator Amot is rendered inactive by its association with F-actin and potentially other apical polarity proteins leading to the nuclear localisation of Yap/Taz that in association with Tead4 transcriptionally activates genes of the TE, such as *Cdx2*. In high density apolar inner cells, Amot is phosphorylated, making it insensitive to F-actin mediated inactivation, resulting in the formation of an active Merlin/Amot complex that activates Lats kinases leading to Yap/Taz phosphorylation and cytoplasmic retention by binding 14-3-3 proteins. As a result Tead4 is unable to activate *Cdx2* and thus pluripotency is maintained in inner cells (taken from Gumbiner and Kim 2014).

In the canonical Fgf pathway, the secreted Fgf ligands bind the extracellular domain of Fgfr in association with heparin sulphate forming a dimerised complex with two molecules in each component (2:2:2 Fgf:Heparin:Fgfr). The binding leads to the phosphorylation and activation of the intracellular domain of the receptor on its conserved tyrosine residues causing a 500 – 1000 fold increase in its kinase activity (Dailey L. 2005). The activated receptor kinase further regulates downstream intracellular signalling pathways, which includes Rat sarcoma (Ras)-Mitogen activated protein kinase kinase 1/2 (Mek1/2); Extracellular signal related kinase1/2 (Erk1/2), Phosphoinositide 3-kinase (Pi3k), Protein Kinase B (PKB), Phospholipase C-gamma (Plcy), Signal transducers and

activators of transcription (Stat) and other Mitogen activated protein kinases (Mapks) that includes p38-Mapk and Jnk signalling moieties (Dorey K and Amaya E. 2010).

The immediate downstream effector protein of the activated Fgfr receptor is Frs2 and is activated by phosphorylation, resulting in the further recruitment of the adaptor protein Grb2 and its associated nucleotide exchange factor Sos. The Grb2/Sos complex then aids the exchange of GDP bound to the small GTP binding protein Ras for GTP, leading to the activation of the Raf dependent Mek1/2-Erk1/2 signalling pathway. Phosphorylated and active Erk1/2 enzymes then modify the activity of several transcription factors that mostly belong to the ETS group proteins via direct phosphorylation (Schlessinger J. 2000). Furthermore, the adaptor protein Gab1 can also bind Grb2 causing the activation of the Pi3k-Akt serine threonine kinase pathway. Activation of the Pi3k-Akt pathway negatively regulates the forkhead box class transcription factors and also the Tsc2 complex to promote Mtor (Mechanistic target of rapamycin) signalling, thereby regulating cell growth and proliferation (Manning. 2007). Conversely kinases such as Plcy and Jak (or) Stat are activated by their direct interaction with the Fgfr receptors. The active Plcy enzyme hydrolyses phosphatidylinositol-4,5-bisphosphate to inositol-1,4,5-trisphosphate (IP3) and diacylglycerol (DAG). Both IP3 and DAG aid the release of calcium ions from smooth endoplasmic reticulum leading to increased cytoplasmic calcium levels and also promoting the activation of the Protein kinase C (Pkc) signalling pathway (Reilly *et al.* 2000). The Jak-Stat pathway is activated by Fgfr receptor either by phosphorylating and activating Jak kinase or directly phosphorylating receptor bound Stat. Activation of Stat transcription factors via Fgfr has been found to play a key role in cancer cell survival, endothelial cell migration and invasion and tube formation (Dudka *et al.* 2010 and Su *et al.* 1997).

The stress related Mapks, Jnk and p38-Mapk are considered to be activated via a Pi3k-Rac-Mekk3/4/6 dependent axis (see following sections) or by Ras or Pkc dependent mechanisms. In the wound healing process, Fgf dependent activation of the Jnk pathway has been found to promote fibroblast migration to the wound site to initiate the repair process (Kanazawa *et al.* 2010). p38-Mapk is known to be activated by Fgf2 in a Ras dependent manner to promote the activation of Atf1 and Creb during the stress response mediated by opioid peptides in both immune and neural cells (Tan *et al.* 1996). Similarly, the downstream adaptor protein of Fgf signalling, Grb2, was found to regulate the activation of both Jnk and p38-Mapk in a Ras dependent manner to promote T<sub>H</sub> cell maturation (Gong *et al.* 2001). Further, p38-Mapk has been found to regulate the nuclear functions of Fgf, in which, p38-Mapk phosphorylates Fgfr1 to promote the translocation of Fgfr1 bound Fgf1 to the nucleus to regulate gene expression distinct from the canonical Fgf signalling pathway (Sørensen *et al.* 2008). Thus Fgf signalling occupies a molecular cross road of several signalling pathways that regulate a myriad of cellular functions some of which related to p38-Mapk (figure 4).

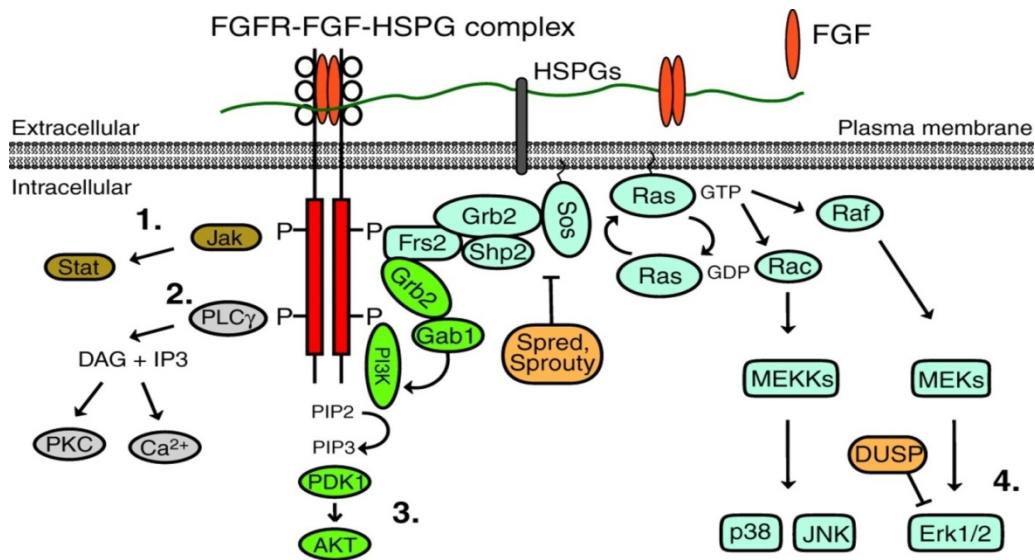


**Figure 4: The Fgf signalling pathway.** The Fgf pathway is activated by the binding of Fgf ligand complexed with heparin proteoglycan to the Fgfr receptor leading to the activation of tyrosine kinase in the receptor's cytoplasmic domain. The tyrosine kinase then promotes further activation of diverse signalling pathways that includes, Jak-Stat, Plcy, Pi3K-Akt and Mapk cascades. (Taken from Lanner and Rossant . 2010).

### Fgf Signalling during mouse preimplantation embryo development

The Fgf signalling pathway forms an important component of TE and ICM cell lineage development. RT-PCR and microarray analyses have revealed that the ligands Fgf4 and Fgf18 are detected in high levels, with the molecules Fgf10 and Fgf11 detected in low and moderate levels respectively from E1.5 to E3.5. Other ligands, like Fgf3, 7, 13, 14 and 23 were not detected during preimplantation stages (Zhong *et al.* 2006). Out of all the 23 ligands analysed by gene knockout, only *Fgf4* displayed blastocyst inner cell mass defects with embryonic lethality by E4.5 indicating its necessity during preimplantation development. In the case of Fgfr receptors both *Fgfr3* and *4* knockout mice are viable and mice lacking *Fgfr1* and *Fgfr2* show embryonic lethality during the gastrulation stage (Dorey & Amaya. 2010). Both Fgfr1 and Fgfr2 are known to display functional redundancy during development (Ornitz. 2005). The presence of Fgfr1 receptor in preimplantation stage embryos has not been analysed though one study reported a reduction in the number of Gata4 positive PrE cells at E4.5 in a mouse strain dependent manner (Brewer *et al.* 2015). Conversely, Fgfr2 mRNA can be detected from the oocyte to blastocyst stage and Fgfr2 protein is detectable in blastocysts with higher expression levels in cells at the abembryonic pole and comparatively decreased expression at embryonic pole; a pattern consistent with its role in regulating TE growth

(Haffner-Krausz et al. 1999). Further, *Fgfr2* knockout mice show visceral endoderm and trophoblast defects, and at the peri-implantation stage (E4.5) display no visible PrE layer; indicating *Fgfr2*'s indispensable role in extraembryonic lineage development even before gastrulation (Arman et al. 1998). Consistently *Fgfr2* protein displays plasma membrane association in both the TE and presumptive PrE lineages in mouse preimplantation embryo at the early blastocyst stage (Mihajlovic et al. 2015).

Fgf dependent PrE specification in the mouse embryo has been demonstrated by Yamanaka et al. (2010), where exogenous supplementation of Fgf4 from E2.5 to E4.5 resulted in complete conversion of all ICM cells to Gata6 expressing PrE cells. Moreover the authors also showed that the ICM becomes insensitive to either Fgf4 supplementation or Mek1/2 inhibition (that results in the opposing phenotype of all ICM cells only expressing Nanog without detectable Gata6 expression) between the E4.0 to E4.25 stage of ICM blastocyst maturation. This observation was further supported by a *Fgf4* knockout mice study that utilized a maternal/ zygotic *Fgf4* knockout strain and showed that Fgf4 plays an essential role during PrE formation in mouse preimplantation embryos. Although the knockout embryos were indistinguishable in regards to *Gata6* expression in the ICM prior to the 64-cell stage relative to wild type embryos, such embryos subsequently lost or displayed weak Gata6/Sox17 expression and retained Nanog in the entire ICM cell population with no detection of Gata4 (a temporally later marker) positive PrE cells. Further, addition of either exogenous Fgf2 or Fgf4 to the mutant embryos resulted in all ICM cells becoming Gata6 positive or ICMs that retained Nanog expression but it was never possible to achieve an appropriately balanced presence of both EPI and PrE cells in the *Fgf4*<sup>-/-</sup> null mutant ICM. Thus, there exists a necessity for local heterogeneity in Fgf concentrations for proper ICM lineage specification to PrE and EPI populations (Krawchuk et al. 2013 and Kang et al. 2013). Consistently it is now known that, specification of PrE is as such non-autonomously dependent on Fgf4 secreted by Nanog positive EPI cells, indeed *Nanog*<sup>-/-</sup> mutant embryos express Gata6 in all ICM cells but lack Fgf4 expression and fail to express the later PrE markers Sox17 and Gata4; a phenotype that can be rescued by supplementing Fgf4 exogenously, further highlighting the importance of Fgfr-Fgf signalling pathway during mouse preimplantation embryo development and ICM maturation (Frankenberg et al. 2011).

### c. The Tgf- $\beta$ family signalling pathway

The Transforming growth factor- $\beta$  (Tgf- $\beta$ ) signalling module is a transmembrane receptor kinase dependent system that regulates a myriad of cellular functions through its downstream Smad dependent and Smad independent pathways. The family includes a group of 33 genes that encodes large propeptide precursor molecules that are processed to produce active ligands from their C-

terminal region that are secreted as disulphide linked homo/heterodimers to activate signalling through Tgf- $\beta$  family receptors. Once activated, the pathway regulates cell growth, differentiation, adhesion, migration, apoptosis and embryonic development (Sakaki-Yumoto 2013).

The ligands include Tgf- $\beta$ , activins, nodal, Gdf (growth differentiation factor) and Bmps (Bone morphogenetic proteins) and transduce signal through heterodimerised type I and type II receptors (Whitman 1998). In mammals the active receptors are formed by the combination of any one class of the molecule from the seven in the type I group and one from a selection of five in the type II receptor group. Binding of a ligand dimer to the type I and II receptor draws receptors together to form a stable tetrameric complex, leading to the phosphorylation driven activation of type I receptor subunits by the kinase activity of the type II receptor, followed by further signal transduction (Shi and Massague 2003). Different ligands bind specific type I receptors, with Bmps binding Alk1/2, BmpRIA/Alk-3 and BmpRIB/Alk-6, whereas, Tgf- $\beta$  and activin function through T $\beta$ RI/Alk-5 and ActRIB/Alk-4 respectively and Nodal functions through Alk4 and Alk-7. The activated type I receptor kinase then induces Smad dependent and non-Smad phosphor-dependent pathways depending on the associated co-receptors, intra cellular co-factors and antagonists (Wu and Hill 2009). Depending on the downstream signalling pathways involved the Tgf- $\beta$  family ligands can promote very diverse effects in the cell.

### **Smad dependent signalling**

There are eight Smad effector proteins (Smad 1 – 8) in vertebrates. The Bmp proteins signal through three Smads (1, 8 and 5) and Tgf- $\beta$ /Nodal/Activin signal through Smad2 and Smad3. These receptor activated Smads (R-Smad) once phosphorylated, trimerises with Smad4 and translocate to the nucleus, where Smad4 functions as a transcriptional co-activator regulating Smad dependent gene expression. The remaining Smad6 and Smad7 molecules function as negative regulators for both Bmp and Tgf- $\beta$ /Nodal/activin signalling (Massague. 2005). Further, the Smad complex can interact with other transcription factors and with the aid of co-activators such as CBP and p300 and repressors such as histone deacetylases to regulate transcription in a context dependent manner (Massague and Wotton 2000). For instance, in mouse EPI stem cells and human ES cells, Tgf- $\beta$ /Activin signalling regulates *Nanog* expression via Smad2/3 to maintain pluripotency. Conversely, upon Bmp signalling, Smad1 was found to interact with the Nanog protein to attenuate its pluripotency promoting function. Furthermore, Smad dependent signalling plays a key role in the early lineage specification of ES cells to primitive streak derivatives that results in mesodermal and endodermal cells, the first step in ES cell differentiation (Sakaki-Yumoto 2013). Thus, diversified cellular

mechanisms are regulated by the Tgf- $\beta$  family ligand activated receptor dependent Smad pathway (figure 5).

### **Smad independent pathway**

The activated/liganded type I and type II receptors either directly or through adaptor proteins activate several non-Smad effector molecules that are mostly characterized as downstream elements of tyrosine receptor kinases and depending on the cell system, such pathways are themselves mediated by Smad dependent signalling. For example, Tgf- $\beta$  has been found to mediate the direct activation of the Mek-Erk pathway; as such liganded/activated Tgf- $\beta$  receptor can phosphorylate and activate the adaptor protein Shc-A that in turn provides a docking site through its phospho-tyrosine residues for Grb2/Sos binding that promotes Ras activation leading to the activation of the Mek-Erk signalling cascade (Lee *et al.* 2007). Further, Tgf- $\beta$  also promotes Tak1 (Tgf- $\beta$  activated kinase 1) stimulation of p38-Mapk and JNK pathways, via Mkk3/6 activation, itself mediated by the ubiquitin ligase Traf6; the TRAF homology domain of Traf6 interacts with the Tgf- $\beta$ I receptor inducing K63-linked polyubiquitination of Traf6 that in turn leads to the binding of Tak1 and the its own activation, possibly by autophosphorylation (Yamashita *et al.* 2008). In addition it also regulates small GTPases like RhoA-Rock, Rac (Ras-related C3 botulinum toxin substrate 1) and Cdc42 (Cell division control protein 42 homolog), thereby regulating cytoskeleton structure and gene expression (Edlund *et al.* 2002). Though detailed studies of Smad independent mechanisms in ES cells are only meagre, one study has demonstrated the positive effect of Bmp4 on ES cell self-renewal is partly achieved via inhibition of both the Erk and p38-Mapk pathways (Qi *et al.* 2004). Thus Tgf- $\beta$  family signalling molecules regulate a variety of non-Smad effectors and thereby promote complex levels of cross-talk between multiple signalling cascades (figure 5).

Since, the present work involved studies only related to Bmp and Tgf- $\beta$  signalling, the role of these pathways in early embryos is described below.

### **The role of Tgf- $\beta$ family signalling during mouse preimplantation embryo development**

In preimplantation mouse embryo, the Hippo pathway has been found to play a key role in regulating Tgf- $\beta$ -Smad signalling, whereby Taz binding to heteromeric Smad complexes influences their nuclear localization in the presence of Tgf- $\beta$ , in a cell density dependent manner (Varelas *et al.* 2008). Additionally this same study also observed a group of inner cells in late blastocysts showing prominent nuclear pSmad2/3 and unphospho-Yap. Therefore given the observation that postimplantation visceral endoderm cells display strong nuclear Smad2/3 signal, the study proposed

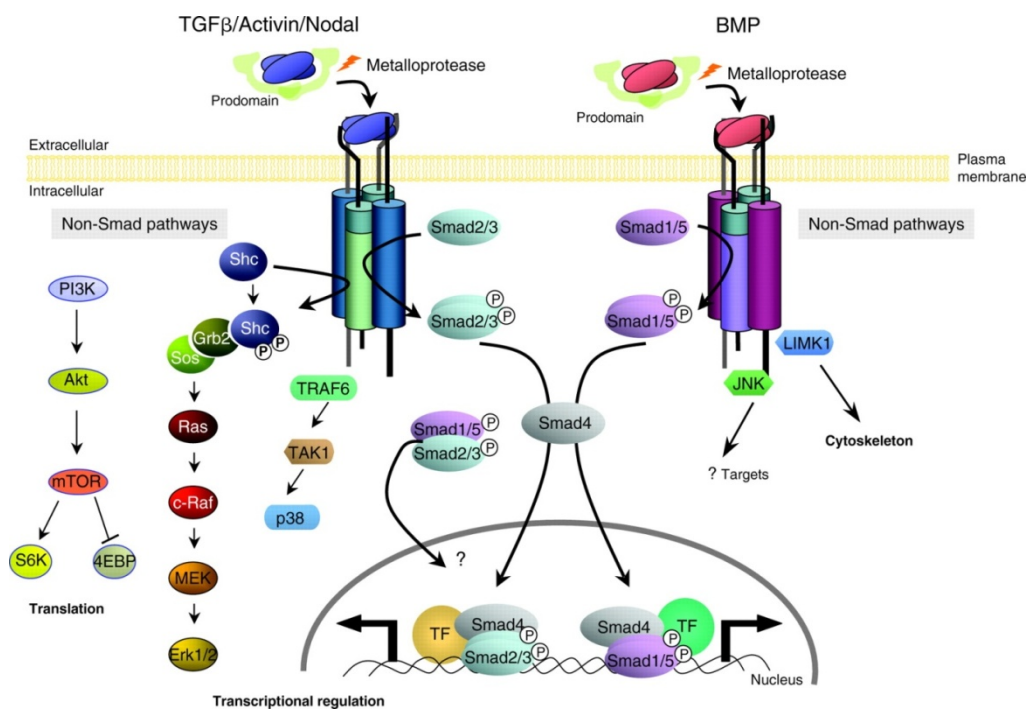


**Figure 5: The Tgf-β family signalling pathway.** The activation of Tgf-β signalling cascade involves the binding of protease processed ligands to the Type I receptor components of the relevant receptors resulting in a stable/liganded tetrameric receptor type I and II complexes that lead to the activation of kinase activity in the receptor’s cytoplasmic domain. In the case of Smad dependent signalling Tgf/Activin/Nodal ligands lead to phosphorylation and activation of Smad2/3(7) and Bmp signals through Smad1/5/8 phosphorylation. The activated Smads then dimerise and enter the nucleus via an interaction with Smad4, where the complex regulates specific gene transcription. In the Smad independent signalling pathways, the liganded/activated receptor phosphorylate and activate multiple signalling domains that includes, mTOR, Mapk and small GTPase dependent pathways (taken from Wharton and Derynck. 2009).

that the observed blastocyst inner cells with nuclear Smad2/3 might undergo PrE differentiation and that the other cells with cytoplasmic pSmad2/3 might give rise to epiblast cells (Varelas *et al.* 2010).

Similar to Tgf-β signalling, the Bmp pathway has also been found to be active in mouse preimplantation embryos (Wang *et al.* 2004). In a recent detailed RNA-Seq analysis in 16-cell stage mouse embryos, a differential spatial enrichment of Bmp ligand and receptor expression was reported between inner and outer cell populations (Graham *et al.* 2014). The ligands Bmp4 and Bmp7 were found to be expressed in inner cells and their receptor Bmpr1a was found in both inner and outer cells. Conversely, Bmpr2, was only expressed in outer cells, indicating a possible role for

Bmp in regulating extraembryonic tissue development, especially relating to the TE. Using a combination of inhibitors (Dorsomorphin), endogenous antagonists (Noggin) and dominant negative constructs for Smad4 and Bmpr2, the study demonstrated an integral role for Bmp in regulating the emergence of both TE and PrE lineages. In addition, it was also reported that a possible Bmp regulated Smad-independent pathway, signalling through Tak1 kinase also modulates ICM maturation into EPI and PrE, as Tak1 inhibition resulted in ICM cells co-expressing both Gata6 and Nanog. Another parallel study has discovered Bmp to be active as early as the 4-cell stage, where it has been found to regulate the rate of cell cleavage up to morula stage. Active Bmp signalling inhibition, either by antagonist or by dominant negative Bmpr1a resulted in the extension of cell cycle length and reduced cell number. Bmp signalling has also been proposed to exert such cell cycle regulating effects by controlling *Id2* and *Id3* gene expression (de Mochel *et al.* 2015).

Taken together both Tgf- $\beta$  and Bmp pathways play major roles during mouse preimplantation development.

#### **d. The Mitogen activated protein kinase (Mapk) signalling cascade**

The Mapk signalling pathway includes a family of conserved serine/threonine kinases that are ubiquitously present in all eukaryotes regulating cell survival, proliferation, differentiation, stress related responses and apoptosis (figure 6). They provide a connection between the extra cellular milieu and specific intra-cellular reactions by relaying signals from membrane receptors and their associated kinases (Chen *et al.* 2001). The Mapks can be grouped as conventional and atypical kinases. The conventional kinase group includes extracellular signal regulated kinases (Erk) 1/2, c-Jun amino (N) terminal kinases 1/2/3 (Jnk 1/2/3), p38-Mapk isoforms ( $\alpha$ ,  $\beta$ ,  $\gamma$  and  $\delta$ ) and Erk5. Atypical Mapks include Erk3/4, Erk7 and Nemo like kinase (Nlk); as they differ from conventional Mapks, their molecular functions are less known. Activation of conventional Mapks in general involves a sequential phosphorylation of Ser/Thr residues in a cascade of upstream kinases; mitogen activated protein kinase kinase kinase (Map3k) phosphorylating and activating mitogen activated protein kinase kinase (Map2k) that then stimulates the relevant Mapks by dual phosphorylation at a conserved Thr-X-Tyr motifs located in their activation loops. Once activated Mapks can activate or enhance other downstream kinases and transcription factors by phosphorylation either at serine or threonine residues in conserved Pro-xxx-Ser/Thr-Pro motifs (Cargnello and Roux 2011). Since, p38-Mapk isoforms fall under the conventional kinase family, the Mapks in this group will be described in detail in the following section.

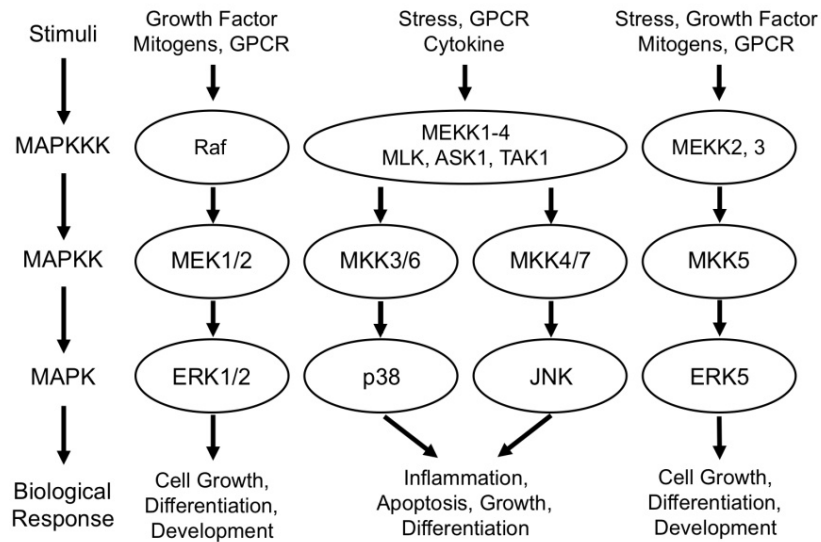


**Figure 6: The conventional Mapk signalling cascade.** The conventional Mapk signalling in general involves the systematic activation of kinases (Mapkkk (Map3k) – Mapkk (Map2k) - Mapk) that leads to a biological response. In case of the Erk1/2 pathway, stimulants include growth factors and mitogens that then activate Raf kinase that in turn activates the Erk1/2 specific activator Mek1/2 leading to further regulation of effectors downstream of Erk1/2 to mediate cell growth and differentiation. Similarly, the stress activated kinases like p38-Mapk and Jnk are stimulated by genotoxic stress or on cytokine receptor activation leading to the activation of a diversified group of Map3ks including Tak1 that results in the activation of Mkk3/6 or Mkk4/7 (Map2ks) that stimulates by phosphorylation both p38-Mapk and Jnk kinases respectively. The most recently described Erk5 pathway follows the same trend as Erk1/2 signalling regulating cell growth and differentiation, with Mek5 being its direct activator (taken from Maki Urushihara and Yukiko Kinoshita 2011).

### The Erk1/2 mediated signalling pathway

The Erk1/2 signalling module is regulated by a diversified number of factors, which includes receptor tyrosine kinases (RTK), G-protein coupled receptors (GPCR) and integrins. Erk1/2 activation commonly depends on its upstream Map2k (Mek1/2) that in turn depends on Map3k (Raf – V-Raf1 Murine Leukaemia Viral Oncogene Homolog 1) for activation (Raf-Mek-Erk). The activation involves phosphorylation of threonine 202 and tyrosine 204 (pT202/pY204) of ERK1 and pT184/pY186 of ERK2 in human. In mouse the orthologous sites are T203/Y205 and T183/Y185 in Erk1 and Erk2 respectively (Roskoski 2012). Activated Erk1/2 kinases can function as monomers exerting their effects on downstream targets in the cytoplasm or they can dimerise and enter the nucleus where

they phosphorylate a variety of transcription and chromatin remodelling factors to regulate gene expression (Shaul and Seger 2007).

Ligand bound activation of GPCR results in the exchange of GDP to GTP in its intracellular receptor bound alpha subunit, resulting in its activation. The GTP bound alpha subunit dissociates from its receptor, as well as its beta and gamma subunits, and stimulates Erk1/2 pathway directly (Raman 2007). Whereas, in a RTK dependent pathway, the binding of a ligand such as a growth factor to the transmembrane receptor results in tyrosine autophosphorylation in its cytoplasmic tail leading to the further phosphorylation on tyrosine residues of the recruited adapter protein Src homology 2 domain containing (Shc). Shc then recruits the Grb2 (Growth factor receptor-bound protein 2)/Sos (Son of sevenless) complex in which Grb2 binds the phospho-tyrosine residue of Shc via its SH2 domain leading to Erk1/2 activation in a Ras dependent manner [*n.b.* Sos is a GDP exchange factor that activates Ras by enabling GDP-GTP exchange leading to Mek1/2 mediated Erk1/2 activation] (Karnoub and Weinberg 2008). In addition, non receptor tyrosine associated kinases like Fak (Focal adhesion kinase) and Src kinase (Sarcoma kinase) that are activated by extracellular matrix associated protein integrins can increase the efficiency of Erk pathway activation and signalling. As such; integrins activate Src kinase that further activates Fak via direct phosphorylation. Its phospho-tyrosine residue provides binding sites for PI3K and the small GTPases proteins like Rac. The activated Rac then stimulates Pak1 (p21 activated kinase) serine/threonine kinase, which can phosphorylate Mek1 and positively regulate Erk1/2 signalling (Zhu *et al.* 2008).

As stated the above mentioned signalling relays converge on the small GTPase molecule Ras. Ras switches between active and inactive states by binding GTP and hydrolysing it to GDP respectively. Its activity is tightly regulated by controlling GTP to GDP ratio, in the presence of functional guanine nucleotide exchange factors (GEF; *e.g.*: Sos1 and Sos2) and GTPase activating proteins (GAPs). In both GPCR and RTK mediated Erk1/2 pathways, Ras is activated by the Sos-Grb2 complex, in which Grb2 brings Sos in close proximity to Ras to enable exchange of GDP with GTP leading to its activation. The active Ras protein then stimulates its downstream effector serine/threonine protein kinases Raf or Rac. Raf further activates mitogen activated protein kinase kinases Mek1/ Mek2, that phosphorylate and activate Erk1/ Erk2. Phosphorylated Erk1/2 dimers then enter the nucleus to activate Ets transcription factors, such as Elk1 (responsible for transcriptional activation of the Fos gene), by phosphorylation (Roskoski 2012). c-Jun also a downstream substrate of Erk, dimerises with Fos to form the active Ap1 (Activator protein 1) transcription factor complex, that is able to stimulate cyclin D proteins that are involved in cell cycle progression. In addition metabolism regulating kinases such as Msk (Mitogen and stress activated protein kinase), Rsk (Ribosomal s6 kinase) and Mnk (Mapk

interacting protein kinase) family members can also function as direct downstream effector proteins of Erk1/2 signalling (Whitmarsh and Davis 1996).

### **The Mek5/ Erk5 Pathway**

The Mek5/Erk5 pathway is perhaps one of the most poorly understood members of the Mapk family, with much of its potential upstream activators and downstream effector proteins only studied to a minor extent. The pathway has been found to be involved in cell survival, proliferation, differentiation and angiogenesis (Drew 2012). Depending on cell type and stimuli, Mek5, the direct activator of Erk5 (*i.e.* Map2k) can be activated by both Mekk2 and Mekk3 (*i.e.* Map3k), with Mekk2 showing a comparatively higher affinity for Mek5 (English *et al.* 1995). One study using the rat PC12 cell line, showed that Erk5 can also be activated by Ras through Egf (Epidermal growth factor) and Ngf (Nerve growth factor) mediated signalling pathways. Yet, Ras was found to be insufficient to activate Erk5 in other studies. In addition, the cytokine Lif (Leukaemia inhibitory factor) has been found to activate Mek5, independently of Mekk2 and Mekk3 kinases (Drew 2012). Hence Erk5 activation may not be restricted to Mek5.

Activated Mek5 promotes the activation of Erk5 by phosphorylation and relieving its auto-inhibition. Though Erk5 has been found to contain a conserved Thr-Glu-Tyr amino acid sequence, as in Erk1/Erk2, it is only activated by Mek5 and not either by Mek1 or Mek2. This C-terminus of Erk5 includes the domain for its activation, auto-phosphorylation and sub-cellular localization (Zhou *et al.* 1995 and Lee *et al.* 1995). It has been proposed that Erk5 in its inactive form exists in a closed 3D conformation, with the N- and C-termini interacting with each other. Once phosphorylated by Mek5, this interaction is disrupted, thus releasing a C-terminal residing nuclear localization signal (NLS) to promote Erk5 nuclear import (Yan *et al.* 2001). Activated nuclear Erk5 is known to phosphorylate and activate various transcription factors, for example Sp1 (Specificity protein 1), Ap1, c-Myc (Myelocytomatosis oncogene) and Mef (Myocyte enhancer factor 2). In addition its C-terminal auto-phosphorylation enables Erk5 to interact with other transcription factors that contain an appropriate SH3 domain (Drew 2012).

The Mek5/Erk5 pathway has been found to be constitutively active in number of cancers including prostate and breast cancer. Given the fact that the C-terminal domain of Erk5 is larger than that of Erk1/2 kinases, this provides a unique opportunity to pharmacologically target Erk5 over-expressing and potentially unhealthy cells and spare the essential Mapk-mediated signalling of neighbouring healthy cell populations.

### **The Jnk signalling pathway**

The c-Jun N-terminal kinase (Jnk) or the stress activated kinase (SAPK) family includes three Jnk genes (*Jnk1*, *Jnk2* and *Jnk3*) that are activated during stress associated stimuli (*e.g.* UV radiation) and mediate cellular responses by promoting Ap-1 transcription factor mediated gene expression. In addition, Jnk signalling has also been found to be involved in cell proliferation, motility, metabolism, DNA repair and apoptosis (Kyriakis *et al.* 1994).

As with other Mapks, the Jnk signalling module involves sequential activation of three kinases (Map3k-Map2k-Mapk/Jnk). The Map2ks (Mkk4 & Mkk7) specific to Jnk signalling activation can be activated by 14 of at least 20 different Map3k kinases. Such Map3ks are themselves under the control of many diverse kinases, such as Pak, Gck (Germinal centre kinase) and Hpk (homeodomain-interacting protein kinase) that are further regulated by GTPases such as Rho and Ras or specific ubiquitin modifications. Once activated in the cytoplasm, a proportion of Jnk enters the nucleus to regulate other downstream substrates via their kinase activity (Zeke *et al.* 2016). In human, C-JUN, a well studied downstream effector protein of JNK signalling is activated by phosphorylation at Serine residues 63/73, resulting in increased c-JUN transcriptional activity, and as mentioned previously, c-JUN forms an integral part of the AP-1 transcriptional complex that positively regulates Cyclin D proteins during cell cycle progression. In addition activated Jnk also regulates other transcription factors including Atf2 (Activating transcription factor 2), p53, Nfatc-1 (Nuclear factor of activated T cells), Elk1 (ETS transcription factor), Stat3, c-Myc and JunB, however, there are thought to be many other cytoplasmic targets that not been studied to such an extent (Weston and Davis 2002).

#### **The p38-Mapk signalling pathway:**

The p38-Mapk signalling pathway is activated in response to environmental stress, growth factor and inflammatory cytokine based signalling. The first kinase to be identified in this Mapk family was a 38kDa protein that it is now referred to as p38-Mapk  $\alpha$  (p38-Mapk14). Subsequently, additional p38-Mapk family members sharing 60% identity with p38-Mapk14 were characterized and were named as p38-Mapk  $\beta$  (Mapk11),  $\gamma$  (Mapk12) and  $\delta$  (Mapk13); all the p38-Mapk isoforms are coded by 4 different genes (Cuadrado and Nebreda 2010) and also display differential tissue expression, with p38-Mapk14 expressed in most adult cell types, whereas, p38-Mapk11/12/13 are preferentially expressed in the adult brain, skeletal muscle and endocrine glands respectively. Although each of the p38-Mapk enzymes exhibits a degree of substrate specificity, they are also capable of considerable functional redundancy. For example, the archetypal p38-Mapk12 substrate, Sap97, can be phosphorylated by other p38-Mapk members in the absence of p38-Mapk12 activity (Sabio *et al.* 2005).

Like other Mapk pathways, p38-Mapk activation relies on sequential activation of a Map3k-Map2k-Mapk (p38-Mapk) cascade. p38-Mapks are activated by phosphorylation on flexible activation loops, harbouring a Thr-Gly-Tyr (TGY) motif, resulting in a relief from internal steric hindrance and thereby promoting an active open conformation. p38-Mapk can be activated by three different Map2ks classified as Mkk3, Mkk4 and Mkk6. Mkk6 can activate all four isoforms, whereas, Mkk3 can activate only  $\alpha$ ,  $\gamma$  and  $\delta$ , with both kinases being highly specific for p38-Mapk members only. The third Mkk protein, Mkk4 is more classically considered a Jnk pathway activator and can only activate p38-Mapk  $\alpha$ . Accordingly, the differential activation of p38-Mapk members can be largely attributed to the differing extent of Map2k protein activation in response to various extracellular cues (Goedert *et al.* 1997; Doza *et al.* 1995 and Brancho *et al.* 2003).

Upstream Map3k kinases activate p38-Mapk related Map2ks, by phosphorylating specific serine/threonine residues in their activation loops. In both mouse and human, Mkk6 is phosphorylated on serine (207)/ threonine (211) residues, resulting in an open conformation and kinase activation. A number of Map3k kinases can activate p38-Mapk related Map2ks including Ask1 (Apoptosis signal-regulating kinase 1), Tak1, Tao 1 and 2 (Thousand and one amino acid protein kinase 1 & 2), Tpl2 (Tumor progression locus 2), Mlk3 (Mixed-lineage protein kinase 3), Mek3 and 4 (Mitogen-activated protein kinase kinase kinase 3 & 4) and Zak1 (Sterile alpha motif and leucine zipper containing kinase 1) (Cuevas 2007). In general Map3ks have broad target specificity; hence they can also activate Mapks of pathways other than those involved in the p38-Mapk pathway. A functionally complex and interdependent network of small GTPase, RTKs and non-RTKs also impacts on Map3k activation. Thus a diversified number of regulatory mechanisms and inputs control p38-Mapk activation and function in response to various cellular milieus.

### **Non-Canonical activation of p38-Mapk**

In addition to canonical Map2k mediated activation, p38-Mapk can also be activated by alternative pathways. In human, one such pathway involves T-cell receptor (TCR) signalling, whereby the TCR proximal tyrosine kinase ZAP70 (Zeta-chain-associated protein kinase 70) directly phosphorylates p38-MAPK14 at tyrosine residue 323, resulting in autophosphorylation on the p38-Mapk14 activation loop and an increase in kinase activity. This phosphorylation at Tyr-323 seems to be specific to T-cells, as genetically modified 'knock in mice' containing a Tyr-323 to phenylalanine mutation are normal and fertile, but their T<sub>H</sub>1 cells display a modest delay in cell cycle (Salvador JM *et al.* 2005). Myeloid cells have been found to utilize another mechanism, in which Tab1 (Tak-1 binding protein 1) binds to p38-Mapk14 (alone) and similarly promotes autophosphorylation in the activation loop (Ge *et al.* 2002).

## Regulation of p38-Mapk pathway

As referred to in the previous sections, p38-Mapks can be stimulated by a diverse number of upstream regulators. However, a strict control over p38-Mapk signalling activity is mediated by specific phosphatases that target the phospho-threonine and tyrosine residues present in the activation loop. p38-Mapk inactivation can be induced by both mono and dual dephosphorylation. Mono dephosphorylation reduces Mapk activity and as such p38-Mapk14 phosphorylated at both threonine 180 and tyrosine 182 residues shows a 10 to 20 fold increased activity compared to the enzyme phosphorylated at the Thr-180 residue alone, Whilst, the Tyr-182 monophosphorylated protein is inactive (Zhang *et al.* 2008). Phosphatase gene families responsible for such a mono-dephosphorylation state include PP2A and PP2C (both obviously serine/ threonine phosphatases). Indeed, the PP2C family protein Wip1 has a wide range of substrate recognition capacity and its functionally antagonistic interaction with p38-Mapk14 is well documented. In response to genotoxic stress, such as UV radiation, the p38-Mapk pathway enhances p53 transcription factor activity by phosphorylation of Ser-33 and Ser-46, thus leading to cell cycle arrest or apoptosis. In such a cell cycle arrest context, p53 in addition to transcriptionally activating many tumor suppressor genes also induces *Wip1*. *Wip1* then functions in a negative feedback loop to promote the removal of the phosphate moiety from Thr-180, leading to a monophosphorylated comparatively inactive form of p38-Mapk14. Therefore, in normal cells, *Wip1* promotes stress endured recovery from cell cycle arrest. However, in an oncogenic state as observed in medulloblastoma cells, endogenously over-expressed *Wip1* activity promotes tumor cell proliferation by overcoming normally arresting cell cycle check points, thus functioning as a classical oncogene (Le Guezennec and Bulavin 2010).

Dual dephosphorylation of Mapks is carried out by a family of dual specificity phosphatases (DUSPs)/Mapk phosphatases (Mkps). They promote the removal of phosphate groups from both threonine and tyrosine residues. These enzymes consist of a domain for Mapk interaction and a domain with phosphatase activity. Similar to the above mentioned PP2A/2C family proteins, Mkps are transcriptionally activated by the same stimuli that activate Mapks and function in negative feedback loops. The Mkps 1, 4, 5 and 7 that are known to dephosphorylate p38-Mapk, can also exert their effects on Jnks (Owens and Keyse 2007). Mkps protect cells from apoptosis caused by genotoxic stress and also reduce the production of pro-inflammatory cytokines. In one study in which mouse RAW (cancerous macrophage cell lines first described by Raschke) cells were exposed to lipopolysaccharides (LPS), the acetylation of the Mkp1 dual phosphatase by p300 was found to promote an inhibitory interaction with p38-Mapk thus causing a reduced innate immune signalling response to cytokines (Cao *et al.* 2008). Additionally, in mouse, negative regulation of p38-Mapk activity has been shown to be induced by phosphorylation at threonine residue 123 caused by the action of the

GPCR protein Grk2 and results in reduced substrate affinity of p38-Mapk14, thereby reducing its functional effect (Peregrin *et al.* 2006).

### **Substrate recognition by p38-Mapk**

p38-Mapks, like other Mapks recognize substrates containing specific docking domains (D-domains) that are rich in positively charged and hydrophobic amino acid residues. The presence of the D-domains is also responsible for inducing conformational changes in the substrate effector proteins necessary for the execution of their function in the p38-Mapk signalling pathway (Tanoue *et al.* 2000). However, some substrates that lack a conserved D-domain can also interact with p38-Mapk in a specific manner, although the criterion for such interaction remains unknown. The interaction between p38-Mapk and their substrates provides an opportunity for specific pharmacological therapeutic intervention; for example, the compound CMPD1 binds to the active site region of p38-Mapks and interferes specifically with Mk2 substrate interactions (Davidson *et al.* 2004). Since, p38-Mapk regulates a wide variety of downstream proteins, compounds like CMPD1 can enable the therapeutic targeting of specific substrates in the wider p38-Mapk pathway. Therefore understanding the mechanisms underlying substrate recognition can aid in the discovery of specific therapeutic leads related to p38-Mapk mediated signalling.

### **Downstream effectors of p38-Mapk pathways**

p38-Mapks can shuttle between cytoplasm and nucleus to execute their function. One report has found that though p38-Mapks do not have a recognisable NLS, the activated phosphorylated form shuttles to nucleus. Conversely, another report have shown that the active form is exported from nucleus to the cytoplasm with the aid of Mk2, suggesting the presence of distinct sub cellular pools of active p38-Mapk executing their functions in both nucleus and cytoplasm (Raingeaud *et al.* 1995 and Ben-Levy *et al.* 1998). About 200-300 proteins substrates are estimated to be as p38-Mapk targets and most published studies have exploited the small chemical inhibitor SB203580 to identify targets, but recent genetic knockout models have also revealed a number of *bona fide* targets. Such confirmed downstream protein substrates include transcription factors, chromatin remodelers, scaffold proteins and cytoskeleton proteins involved in apoptosis, endocytosis and cell motility (Cuadrado and Nebreda 2010).

### **Cytoplasmic targets of p38-Mapks**

p38-Mapk targets a diversified number of substrates in the cytoplasm, ranging from receptors to RNA silencing proteins. Among the earliest studied cytoplasmic targets were the heat shock proteins Hsp25 and Hsp27. Indeed, the Chinese hamster cell line (CCL39) responds to growth factors,

cytokines or stressing agents exposure, by activating p38-Mapk, resulting in nuclear accumulation of Hsp27 protein that intern binds p53 to enhance p21 mediated gene transcription and promote G2/M phase cell cycle arrest (Venkatakrishnan *et al.* 2008). In humans, p38-MAPK promotes phosphorylation and activation of HSP27 at residues Ser-78 and Ser-82 via the effector kinases MK2/MK3. In the cytoplasm, activated Hsp27 can promote actin microfilament stability during oxidative stress and its overexpression in Chinese hamster cell lines increases cortical F-actin concentration and elevates pinocytic (engulfment of fluid like lipid by the cell for energy production) activity dependent on actin polymerization for vesicle transport. In contrast, overexpression of non-phosphorylatable mutant Hsp27 reduces both activities, emphasizing the role of p38-Mapk in stress related cytoskeleton dynamics (Lavoie *et al.* 1993).

Recent reports have suggested a prominent role for the p38-Mapk pathway in regulating autophagy in both positive and negative ways. In one study involving the human embryonic kidney cell line (HEK293A), the autophagy regulating transmembrane protein ATG9 (Autophagy related protein-9) has been found to interact with p38-MAPK interacting protein (p38IP) to promote starvation induced ATG9 trafficking and autophagosome formation. p38IP is known to aid the activation of p38-MAPK14 and inhibition of p38-MAPK14 alters p38IP assisted ATG9 depended autophagosome formation. However, it has also been observed that p38-MAPK14 negatively regulates autophagy by competing with ATG9 to bind p38IP, thereby regulating the homeostatic level of autophagy to prevent autophagy dependent cell death under starvation conditions (Webber and Tooze 2010). In contrast, another study has demonstrated that under amino acid starved conditions, in the presence of glucose supplementation, p38-Mapks promote autophagy necessary for cell survival (Moruno-Manchón *et al.* 2013). In agreement with this report, a recent finding using human neuroblastoma cell lines, showed that p38-MAPKs can enhance autophagy by promoting the activity of the BECN1 (Beclin 1) protein via a MK2 dependent phosphorylation at its serine-89 residue, thus promoting autophagy under nutrient deprived condition. Thus p38-Mapk can function both as positive and negative regulator of autophagy (Wei *et al.* 2015).

p38-Mapks can also phosphorylate plasma membrane associated receptors to target them to endocytic vesicle and thus reduce receptor associated signalling. In humans, EGFR has been shown to undergo phosphorylation, followed by clathrin mediated receptor internalization in the presence of inflammatory cytokines or UV irradiation. Mechanistically, the p38-MAPKs that is activated under both conditions promotes the direct phosphorylation of serine/threonine encompassing amino acid residues 1002-1022 of the receptor (Lambert *et al.* 2010). Furthermore, in mouse fibroblasts, the Rab5 effector proteins Eea1 and Gdi are phosphorylated by p38-Mapks and also contribute to the internalization and functional down-regulation of Egfr (Cavalli *et al.* 2001). Clinically this observation

is of particular relevance, as chemo-resistant tumor cells that are often impaired in respect to EGFR internalization, display increased cell survival rates.

Both Erks and p38-Mapks have been recently implicated in amino acid (AA) signalling. In general, mTOR, the very large molecular complex responsible for sensing AA availability is known to phosphorylate and activates p70-S6 kinase (S6K1), that then can either positively or negatively regulates autophagy. A recent study using the HEK-293 cell line, found that the most widely used commercial antibody used to detect activated p70-S6 kinase (anti-p-T389-S6K1) also recognizes proteins that are insensitive to both mTOR and related PI3K inhibitors, yet are nevertheless sensitive to dynamic changes in AA levels. Comparative sequence analysis revealed MSK and RSK kinases, each containing a region homologous to the Thr-389 containing region of S6K1, as possible candidates for those effects; moreover, p38-MAPKs were shown to target this critical threonine residue. Thus, although this study revealed for the first time the involvement of human MAPKs in AA signalling, via the effector substrate kinases MSK and RSK, their exact function in this context is yet to be fully understood (Casas Tenadellas *et al.* 2008).

### **Nuclear Targets of p38-Mapks**

In the nucleus p38-Mapk activates or enhances the activity of many transcription factors and chromatin related proteins either directly or indirectly. In a classical example, p38-Mapk activates the mitogen and stress activated kinases Msk1/2 that in turn directly activate the transcription factors Creb (CAMP responsive element binding protein), Atf1, RelA (v-rel reticuloendotheliosis viral oncogene homolog A) and Stat3 by phosphorylation. In addition in human, MSK1/2 have been found to phosphorylate H3 histone at Ser-27 and Ser-10 residues. Phosphorylation at Ser-27 of H3 histone, is known to result in stress related activation of immediate early gene expression, such as c-FOS and JUN (Arthur 2008 and Soloaga *et al.* 2003). Such induced transcriptional responses are regulated in an epigenetic manner, by which the presence of phosphor-Ser-27 repels the binding of the polycomb repressive complex-2 (PRC2) to stress related gene DNA sequence elements. Indeed, when human myeloid cells are exposed to LPS, it has been shown to result in increased phosphorylation of histone H3 at Ser-10, via a MSK1 and p38-MAPK dependent mechanism, causing increased expression of IL6, IL8, IL12 and MCP-1 cytokines. This response is brought about by the increased accessibility of the specific gene promoters to the binding of transcription factor (Saccani *et al.* 2002). When cells are irradiated by UV increased Ser-10 histone phosphorylation has also been shown to promote the required chromatin relaxation for nuclear excision repair. Further, p38-MAPK can also directly phosphorylate damaged-DNA-binding complex 2 proteins (DDB2) to promote ubiquitination and their degradation, thus enhancing the repair process (Zhao *et al.* 2008). Additionally, during muscle

differentiation, p38-Mapk regulates chromatin remodelling factors in a gene specific manner; for example, in mouse, p38-Mapk phosphorylates Mef2d (Myocyte enhancer factor 2D) on threonines-308 and -315, that are then recognized and bound by Ash2L (Absent small or homeotic like) methyltransferase, thus promoting histone H3 lysine-4 methylation and hence gene expression. In another example using a mouse model, p38-Mapk was found to phosphorylate the ATPase dependent chromatin remodeller Swi/Snf-Baf60 to promote its association with the *Myod* (Myogenic differentiation factor D) gene and thus facilitate muscle differentiation (Rampalli *et al.* 2007 and Lluís *et al.* 2006).

p38-Mapk can also regulate metabolism by interfering with mitochondrial biogenesis and glucose metabolism. In muscle, increases in cytoplasmic calcium levels activate the calcium/calmodulin dependent protein kinases that in turn promote p38-Mapk phosphorylation and activation. Active p38-Mapk, then phosphorylates the mitochondria biogenesis transcription factor known as peroxisome proliferator activated receptor  $\gamma$  co-activator 1 $\alpha$  (Pgc-1 $\alpha$ ) or activates the chromatin remodeller/histone acetyltransferase (HAT) Atf2 that additionally promotes Pgc-1 $\alpha$  transcription, resulting in mitochondrial biogenesis (Wright *et al.* 2007; Fernandez Marcos *et al.* 2011). In the mouse hepatic system, p38-Mapk directly, via phosphorylation, promotes gluconeogenesis by promoting Cebp- $\alpha$  (CCAAT/enhancer binding protein alpha) activation and lipogenesis by inhibiting Srebp1c (Sterol regulatory element-binding transcription factor 1) (Qiao *et al.* 2006 and Xiong *et al.* 2007).

### **Cross talk with other signalling pathways**

Cross talk between different signalling pathways collectively regulates multiple cellular functions such as cell survival, proliferation and stress response. Although, Mapk proteins have specific activating Map2ks, these can be regulated by common Map3ks indicating a need to consider the broader effects they might have on each distinct Mapk signalling pathway.

Using the p38-MAPK specific inhibitor SB203580 and dominant negative p38-MAPK mutants, Li *et al.* (2003) demonstrated that p38-MAPK promotes a rapid inactivation of MEK1/2 that facilitates the stress induced apoptosis of human skin fibroblasts. In rat cardiac myocytes, p38-Mapk enhances the interaction between the phosphatase Pp2a and the Mek1/2/ Erk1/2 complex to negatively regulate the Erk pathway and promote apoptosis (Liu and Hofmann 2004). This is in contrast to human melanoma cell lines in which, both pathways work synergistically to enhance cell proliferation and migration. Similarly, the stress response Jnk pathway is known to share several upstream regulators with p38-Mapk and both pathways interact either antagonistically or synergistically. In one such synergistic pathway involving mouse sarcoma cell lines, p38-Mapk was found to co-operate with Jnk

signalling to induce Ap1 transcriptional activity by mediating the expression of Jun and its partner c-Fos (Hazzalin *et al.* 1996). In a study involving multiple cell lines treated with p38-Mapk inhibitor SB202190, Muniyappa and Das (2008) demonstrated an induced increase in Jnk signalling, evidenced by increased Ap1 DNA binding. This enhanced Jnk signalling was attributed to the increased activation of its upstream regulator Mlk3, indicating a negative cross talk between the two Mapk pathways.

Two other recent reports have demonstrated positive cross-talk between the p38-Mapk and Wnt (wingless-related integration site) signalling pathways. Gsk-3 $\beta$  (Glycogen synthase kinase-3 $\beta$ ) negatively regulates Wnt signalling by phosphorylating  $\beta$ -catenin and targeting it for ubiquitin mediated degradation. In a canonical mechanism the kinase Akt inactivates Gsk-3 $\beta$  by phosphorylation, resulting in activated unphosphorylated  $\beta$ -catenin that can shuttle into the nucleus and promote Wnt-signalling effects. In brain and thymocytes, p38-Mapk has been found to facilitate nuclear shuttling of  $\beta$ -catenin by inactivating Gsk-3 $\beta$  via distinct phosphorylation at alternative serine residues to those targeted by Akt (Abell *et al.* 2007). However, in a similar mechanism, p38-Mapk has been demonstrated to positively regulate Wnt signalling in mouse embryonal carcinoma cells to promote PrE differentiation (Bikkavilli *et al.* 2008).

In response to stresses such as UV radiation or LPS stimulation, mouse Stat1 is known to be activated by phosphorylation (at amino acid residue Ser-727). Using a p38-Mapk14 deficient mouse fibroblast cell line, Ramsauer *et al.* (2002) have reported that p38-Mapk14, under stress conditions, promotes this phosphorylation allowing Stat1 to bind its target gene *Irf9* (Interferon regulatory factor 9). In another study, p38-Mapk has been found to interact with Smad3 in murine chronic-myelogenous leukaemia (CML) stem cells to promote stem cell identity and survival. These cells were found to accumulate an unusually higher level of dipeptide species, compared to their normal hematopoietic stem cell counterparts, resulting in p38-Mapk dependent amino acid signal activation. Upon p38-Mapk activation, Smad3 was phosphorylated at residue Ser-208, leading to its nuclear translocation, where it interacted with the transcription factor Foxo3a to promote CML stem cell maintenance (Naka *et al.* 2015).

Thus, p38-Mapk pathways are under the influence of, and also influence various signalling pathways to maintain varied cellular functions under different circumstances.

### **Inhibitors targeting p38-Mapks**

Therapeutic targeting of p38-Mapks using specific chemical inhibitors is of great interest, as p38-Mapks are involved in various medical conditions ranging from cancer, arthritis, psoriasis and chronic

obstructive pulmonary disease (COPD). The earliest described chemical inhibitors of p38-Mapk are a family of pyridinyl and pyrimidinyl imidazole compounds collectively grouped under the name CSAID™ (cytokine suppressive anti-inflammatory drugs). They were shown to inhibit LPS induced synthesis of cytokines such as IL-1 and TNF in human monocytes by specifically inhibiting p38-MAPK activity. These compounds were marketed by Smith Kline Beecham (SB) and three p38-MAPK targeting drugs SB203580, SB202190 and SB220025 are widely used in research (also in mice). They are found to have an IC<sub>50</sub> values ranging between 10-100nM, targeting both active and inactive enzyme by competing with ATP to bind the enzyme's active site. The inhibitors SB203580, SB202190 specifically inhibit p38 $\alpha/\beta$ -Mapk 14/11, but the compound SB220025 was also found to have activity against p38 $\delta$ -Mapk13 as well. None of the compounds inhibit other closely related Mapks, like Erks or Jnks (Coulthard *et al.* 2009 and Kanaji *et al.* 2012). These compounds are found to be active against arthritis, bone resorption and hippocampal apoptosis. In the present study, SB inhibitor SB220025 was primarily used to target p38-Mapk14/11 and it has a IC<sub>50</sub> value of 60nM and a 2000 fold greater selectivity for p38-Mapk14/11 over Erk1/2, 500 fold over Pka, 50 fold over Pkc and >1000 fold over Egfr, in murine cells (Jackson *et al.* 1998). Therefore at the concentrations used it is highly selective for p38-Mapk14/11 inhibition.

Other potent and selective p38-Mapk14/11 inhibitors include VX-702, Pamapimod, Losmapimod, Dilmapiomod, BMS-582949, ARRY-797 and PH797804, these are found to have lower IC<sub>50</sub> values compared to their SB counterparts (Arthur and Ley 2013.) but are not widely available for research. These inhibitors have been used in clinical trials to test their effectiveness against rheumatoid arthritis, Crohn's disease and COPD. Another recent addition to the list of p38-Mapk targeting compound is BIRB796, unlike the conventional SB inhibitors the molecule allosterically binds p38-Mapk leading to its structural deformation preventing its interaction with ATP. This molecule inhibits all four members of the p38-Mapk family and at higher concentrations it also inhibits the Jnk pathway kinases. However, although BIRB0796 affects Jnk2 *in vitro* it does not affect the activation of Jnk pathway *in vivo* (Pargellis *et al.* 2002).

Though p38-Mapk inhibitors have shown promising results in pre-clinical animal model trials, they have also been shown to have toxic effects against the liver and neural cells in clinical studies, indicating the existence of yet to be identified off target effects of the drugs. One study has reported a strategy to overcome such toxic effects *in vivo*, by utilizing a drug delivery polymer called PCADK (polycyclohexane-1,4,diylacetone dimethylene ketol) to maintain restriction of the inhibitor to a specific organ; in this case to treat myocardial infarction affected cardiac tissue (Sy *et al.* 2008). Overall the identification of p38-Mapk targeting compounds (preferably without any off-targets) is of great importance in treating various clinical manifestations.

## The Role of Mapks during mouse preimplantation embryo development

### Erk1/2 and Erk5 cascade

Spatial and temporal microarray based expression analysis by Wang *et al.* (2004), demonstrated that all components of Erk1/2 and Erk5 pathway are present in mouse preimplantation embryos at the mRNA level. In their analysis all the upstream components of the Erk1/2 pathway, including Frs2 $\alpha$  (Fibroblast Growth Factor Receptor Substrate 2), Grb2, Gab1, Sos1, Ha-Ras, Raf1/RafB, Mek1/2 and downstream effectors Rsk1/2/3 were analysed by real time PCR and immuno-staining and were found to be expressed from the oocyte to the blastocyst stage. Similar observations were also made for Erk5 and its upstream activator Mek5 (Wang *et al.* 2004).

Knockout studies of all the above mentioned *Erk1/2* and *Erk5* components have been performed and all with the exception of the *H-Ras* (Esteban *et al.* 2001) and *Rsk1/2/3* (Dumont *et al.* 2005) knockouts, are embryonic lethal (summarised in Wang *et al.* 2004). In mice genetic ablation of *Frs2 $\alpha$* , a key player in Fgf signalling, results in post-implantation embryo death at E8.0 with defects in anterior-posterior (A-P) axis formation and it was found to be essential for trophoblast self-renewal in response to Fgf4. In addition the epiblasts of *Frs2 $\alpha$*  mutant embryos showed reduced expression of Bmp4 and Smad1/5 activation demonstrating a potential cross-talk between the Fgf and Bmp pathways (Gotoh *et al.* 2005). Null mutation of the SH2/ SH3-domain containing adaptor protein *Grb2*, that binds a number of phospho- activated RTKs and docking proteins, such as Frs-2 through its SH2 binding domain, and Sos1 (a GEF protein for Ras) by its SH3 binding domain, shows embryonic lethality between E5.5 – E7.5 with defects in ICM differentiation towards the endoderm lineage (Cheng *et al.* 1998). Consistently, when embryos lacking *Grb2* are analysed at E3.5, they show loss of Gata6 expression, with all ICM cells expressing Nanog (*i.e.* a failure to adopt the salt and pepper pattern of expression), indicating a defect in primitive endoderm specification as early as the preimplantation blastocyst stage (Chazaud *et al.* 2006). Similarly, the lack of another SH2/ SH3 adaptor protein *Gab1*, which interacts with *Grb2* to activate Plc- $\gamma$  signalling, also results in lethality between E13.5 – E18.5 with defects in placenta, heart, eye, muscle and skin development (Itoh *et al.* 2000). Homozygous null mutation of *Sos1* exhibit placental and cardiac defects with embryonic death around the mid-gestation stage (Qian *et al.* 2000). *B-Raf* (directly phosphorylates and activates Mek1/2) a well studied positive regulator of Erk1/2 signalling also shows defects in placental development when it is knocked out in mice and this trend of placental defect was observed for other Mapk components including *Mek1*, *Erk2* and *Mek5* (Galabova-Kovacs *et al.* 2006; Giroux *et al.* 1999; Hatano *et al.* 2003 and Wang *et al.* 2005). Taken together the Erk1/2 and Erk5 pathway

represents indispensable players in extraembryonic tissue development with the Mek/Erk1/2 pathway most well explored during preimplantation mouse embryo development.

Utilizing ES cells, Kunath *et al.* (2007) demonstrated a role for Fgf4 and the associated activation of the Mek1/2 pathway in priming cells from a self-renewal state towards lineage commitment. Using chemical inhibitors for Mek1/2 (PD184352) and Fgf receptors (SU5402), plus accompanying genetic ablation of the relevant genes, the study reported a block in the ability of ES cells to differentiate towards neural and mesodermal lineages that did not affect the undifferentiated state of ES cells (that retained the expression of the characteristic pluripotency markers Oct4, Nanog and Rex1). Further, Ying *et al.* 2008, using a combination of three inhibitors targeting Mek1/2/Fgfr/Gsk-3 $\beta$  (3i) and genetic *Stat3*<sup>-/-</sup> null mutations showed that ES cells do not require Mapks for survival. Moreover, they showed factors like Stat3/ Bmp/ Smad/ Id (Inhibitor of DNA binding) actually work as suppressors of Fgf activated Mapk signalling to inhibit differentiation and to maintain a ground state of pluripotency. This *in vitro* study was found to be applicable to the preimplantation stage ICM of the mouse embryo; as subjecting embryos to Mek1/2 + Fgf inhibition from E2.5 to E4.5, results in an ICM with no PrE and all cells expressing the epiblast marker Nanog, suggesting that segregation of ICM into EPI and PrE is a Fgf/Mapk pathway dependent in mice (Nichols *et al.* 2009). Taken together an Fgf dependent Mek-Erk1/2 pathway plays an indispensable role during PrE mouse preimplantation embryo development. Interestingly in humans PrE formation has been found to be independent of FGF dependent MEK-ERK1/2 pathway and the signalling pathway that regulates PrE formation in humans is still unknown (Roode *et al.* 2012).

### **The Jnk and p38-Mapk Cascades**

Similar to the Erk pathways, Jnk and p38-Mapk signalling is activated in response to external stimuli and regulates cell cycle/ cell proliferation, differentiation and apoptosis, but unlike the Erk pathways, they also respond to stress stimuli such as UV-irradiation, osmotic shock and inflammatory cytokines. Maekawa *et al.* (2005) have shown that inhibiting the p38-Mapk and Jnk pathways individually, using the respective specific chemical inhibitors SB203580 and SP600125, from the 8-cell to E4.5 stage, results in cavitation failure and embryo arrest at the 16-32 cell morula – blastocyst transition stage. Though the defects observed for p38-Mapk inhibition are consistent with an earlier report by Natale *et al.* (2003), it seems that Jnk is dispensable for preimplantation embryo development, when cultured in optimised media such as KSOM (Potassium simplex optimized media) supplemented with amino acids (KSOM+AA). Moreover, that its function is necessary for maintaining normal homeostasis when cultured in sub-optimal media such as Ham's F10 or M16 (Xie *et al.* 2006); presumably due to modulating a stress induced response. In contrast, p38-Mapk inhibition shows

developmental defects in both the described sub-optimal medias (Maekawa *et al.* 2005), KSOM without AAs (present study) and in optimal media KSOM+AAs (Natale *et al.* 2003); demonstrating an absolute requirement for p38-Mapk function during embryo development. Furthermore, genetic mutant mice individually lacking the *Jnk1/2/3* genes individually are viable, whereas the *p38-Mapk14*<sup>-/-</sup> knockout mouse is embryonic lethal displaying defects in placental development at E10.5 (Coffey 2014 and Mudgett *et al.* 2000).

Preliminary analysis by Natale *et al.* (2003) utilizing immuno-staining and RT-PCR has shown that all four isoforms of p38-Mapk are present in the mouse preimplantation embryo, as are both of its upstream activator Map3ks (Mkk3/6). Moreover, the well characterized downstream effectors Mk2 and Hsp25 are also present from the oocyte to blastocyst stage and in their active phosphorylated forms; indicating the p38-Mapk pathway is active throughout the entire preimplantation development period (Fong *et al.* 2007). In addition, Natale *et al.* (2003) and Paliga *et al.* (2005) have shown that p38-Mapk dependent Hsp25/ 27 activation regulates cytoskeleton organization and that inhibition of p38-Mapk results in disruption of the F-actin network and embryo arrest at the morula stage with associated cavitation failure. A recent study by Yang *et al.* (2015) demonstrated a role for Fgfr2-Fgf2 dependent p38-Mapk activation to promote TE development by regulating cavitation via a mechanism involving the maintenance of genes such as aquaporins. Though most of the above studies have concentrated on early embryo cavitation and associated TE development, none have addressed the role of p38-Mapk during ICM maturation and the separation of EPI and PrE despite p38-Mapks being active in ICM cells at this time (Natale *et al.* 2003 & Maekawa *et al.* 2005).

## **2.6 Metabolism in stem cell fate regulation**

When a stem cell either becomes quiescent or differentiates towards a different cell types, the process is always accompanied by a change in its metabolic status. Accordingly, various studies have found that stem cells that have the potential to self-renew and exhibit the plasticity to form varied different cell types, are more dependent on the glycolytic pathway for their energy needs and as a consequence have less mitochondrial content. Conversely, differentiating cells rely more on mitochondria dependent oxidative phosphorylation (OXPHOS) for their energy production and as such differentiation is typically followed by an increase in mitochondrial content (Teslaa and Teitell. 2015). Apart from serving as the cellular power-house, mitochondria also functions as sites of regulation for amino acid, fatty acid and steroid metabolism. They also generate reactive oxygen species (ROS) molecules that can often function as secondary messengers (second messengers are small molecules, such as cyclic AMP, that relay a signal from a receptor to other protein targets in cytoplasm or nucleus) in some specific signalling pathways. In addition, other signalling homeostatic

mechanisms such as mTOR and AMPK (AMP-activated protein kinase) can sense the metabolic status of inter-/ intra-cellular environments to regulate cellular processes such as autophagy, a process found to play a key role in regulating pluripotency during human induced pluripotent stem (iPS) cell generation (Murakami *et al.* 2004 and Vazquez-Martin *et al.* 2012).

#### **a. OXPHOS and glycolytic pathways in cell fate regulation**

##### **Mitochondrial dynamics and energy dependence during self-renewal and differentiated cell states**

Transmission electron microscopic (TEM) analysis of human and mouse ES cells has revealed that their mitochondria display perinuclear localisation and immature globular structural form containing poorly developed cristae. However, in differentiated cells such as fibroblasts, the mitochondria appear mature, elongated, electron dense with well developed cristae. These mitochondrial phenotypes appear reversible, as mitochondria can remodel when stem cell pluripotency is altered, for example in response to differentiating stimuli (Teslaa and Teitell 2015). Further, with the induction of stem cell differentiation an OXPHOS shift in metabolism is known to occur and is accompanied by enhance mitochondrial biogenesis and increased oxygen consumption, ROS production and intracellular ATP levels, plus decreased lactate production/ secretion. Similarly, during the reprogramming of somatic cells to iPS cells, an increase in glycolytic enzymes and a down regulation of mitochondrial subunits of complex I and II expression can be observed in proteomic analyses (Folmes *et al.* 2011).

However, OXPHOS targeting chemical inhibitors have revealed contradictory requirements for OXPHOS dependent ATP production in stem cells. In one study, exposing iPS cells and human/ mouse ES cells to the mitochondrial uncoupling agent CCCP (Carbonyl cyanide m-chloropheryl hydrazone) lead to a drop in intracellular ATP levels with a concomitant reduction in cell proliferation rate. Similarly, when mouse ES cells are subjected to inhibition by antimycin A (an inhibitor of complex III of the electron transport chain) an increase in the AMP/ATP ratio was observed (Pereira *et al.* 2013). Whereas in another study, inhibiting OXPHOS with oligomycin, only resulted in a 5% drop in ATP levels, indicating a minimal dependence of pluripotent stem cells on OXPHOS for ATP generation. This discrepancy between the studies is attributed to the dependence of mitochondria on dissociated  $F_1-F_0$  synthase components for their proliferation and viability (Zhang *et al.* 2011). Thus, it is possible that the pluripotent cells are dependent on mitochondria for carrying out metabolic pathways like lipid metabolism, but not for the ATP energy production. Further, exposing ES cells to inhibitors of mitochondria OXPHOS function, like antimycin A, leads to an increase in the expression of the pluripotency marker *Nanog* and decreases in mRNA levels related to differentiation (Pereira *et al.* 2013). Similarly, treating ES cells with an uncoupler, like CCCP, or over-expressing uncoupling protein

2, results in an up-regulation of the pluripotent genes *Nanog*, *Sox2* and *Oct4*, thus impairing embryonic differentiation. Accordingly, stimulation of mitochondrial biogenesis, using the chemical S-nitrosoacetyl penicillamine (SNAP) or by over-expressing the mitochondrial biogenesis stimulating transcription factor Pgc-1 $\alpha$ , results in down-regulation of pluripotency markers and promotes ES cell differentiation towards the hepatocyte and adipocyte lineages (Huang *et al.* 2011). Thus, mitochondria and their associated metabolic mechanisms play a key role in stem cell renewal and differentiation.

### **The role of the glycolytic pathway in pluripotency maintenance**

Highly proliferative pluripotent cells are more dependent on the glycolytic pathway for their energy needs, despite the glycolytic pathway being relatively inefficient compared to OXPHOS generated yields of ATP production, it does play key roles in generating various co-factors components and intermediate substrates, in the biosynthetic pathways necessary for cell proliferation (De-Berardinis *et al.* 2008). Consistently, pluripotent cells, like mouse ES cells, display elevated levels of enzymatic genes related to glycolytic pathway and a low mitochondrial oxygen consumption rate (Kondoh *et al.* 2007). Further, in human adult pluripotent cells, the phosphorylated and inactive form of the Pyruvate dehydrogenase (PDH) enzyme is elevated leading to a reduction in substrates entering into the TCA cycle. Accordingly, the expression of the *pyruvate dehydrogenase kinase (PDK) 2* and *4* genes responsible for the inactivation of the PDH complex is also elevated, thus favouring glycolysis (Takubo *et al.* 2013). In addition UCP2, an uncoupling protein that prevents mitochondria dependent oxidation and diverts glycolytic intermediates towards biosynthetic pathways was also found to be up-regulated in stem cells and its ectopic over-expression in differentiated cells has been shown to result in defects associated with the differentiated state (Zhang *et al.* 2011). An added advantage of the dependence of stem cells on the glycolytic pathway is the reduction in the generation of ROS molecules that can be deleterious to the cell if overproduced. Therefore, as pluripotent stem cells are known to exhibit an inefficient G1 to S phase transition cell cycle check-point (despite the relative shortness of this transition) it makes sense to keep ROS production to a minimum to prevent ROS mediated DNA damage and associated DNA mutation. Additionally, minimizing ROS at lower levels also counteracts the promotion of cell differentiation that ROS production can induce (Maryanovich and Gross 2013). Indeed, exposing mouse ES cells to cyclosporin A (thus increasing ROS levels),  $\pm$  antioxidant supplement control, promotes mitochondrial biogenesis, and favours spontaneous cardiomyocyte differentiation (Cho *et al.* 2014).

Thus, a balance between mitochondria dependent OXPHOS and the glycolytic pathway regulates self-renewal, proliferation and differentiation in a wide spectrum of stem cell models and types.

## **b. Signalling mechanisms regulating metabolism and stem cell function**

Signalling pathways play a major role in sensing the extracellular milieu and integrating such information intra-cellularly, by communicating with downstream effectors that can also function as regulators of metabolism; thereby influencing stem cell maintenance and differentiation. The well studied signalling pathways in the context of metabolism are summarised below.

### **The mechanistic target of rapamycin (mTOR) signalling pathway**

The mTOR signalling pathway is one of the most well studied homeostatic and metabolic pathways; it functions as a nutrient sensor that is sensitive to various factors including molecular oxygen, energy status, exposure to extra-cellular growth factors and amino acid availability. It regulates cell growth, proliferation, survival and positively influences anabolic metabolism and negatively regulates catabolic pathways like autophagy. The mTOR pathway is guided by two functionally redundant and distinct multi protein complexes, termed mTORC1 and mTORC2. mTORC1 is sensitive to the antibiotic rapamycin and functions as a nutrient sensor regulating cell metabolism and protein synthesis. The mTORC2 complex is rapamycin insensitive and in addition to its role in regulating cell survival and metabolism, it also regulates the cytoskeleton by influencing F-actin, paxillin, RhoA, Rac1, Cdc42 and Pkc- $\alpha$  (Laplante and Sabatini 2009). mTORC1 functions as a key regulator of pluripotency (the ability of a cell to generate lineages of all three germ layers) in ES and iPS cells, as well as in the ICM of mouse blastocyst embryos (Murakami *et al.* 2004).

Based on the status of the cell (pluripotent or differentiated), the mTORC pathway is necessary for both maintaining pluripotency and promoting differentiation. In stem cells, it is the magnitude of the mTOR signal rather than it functioning in a complete binary on/off mechanism that is important. In agreement with this, mTORC1 is known to be required for the proliferation of human and mouse ES cells and its inhibition causes pluripotency defects associated with reductions in *Oct4*, *Sox2* and *Nanog*; with cells differentiating towards both endodermal and mesodermal lineages. Conversely, a transient inhibition of mTORC1 at the initial stages of nuclear reprogramming during the derivation of iPS cells has been found to enhance the efficiency of obtaining pluripotent cells (He *et al.* 2012). Mechanistic analysis has revealed that the initial inhibition of mTORC1 by rapamycin was found to promote autophagy, the cellular process that is normally activated in response to nutrient depletion and causes degradation of cytoplasmic macromolecules and organelles to provide substrates for cellular metabolic needs. However, it has also been shown that during reprogramming, Sox2 inhibits mTOR gene expression by recruiting the nucleosome remodelling and deacetylase (NuRD) repressor complex to the *mTORC1* gene promoter, thereby suppressing the mTOR pathway, and that this also promotes autophagy (Wang *et al.* 2013a); thus suggesting an integral role for *mTORC1* during the

establishment of the induced pluripotent state. Consistently, exposure of cells to spermine, an autophagy agonist also enhances the efficiency of mouse iPS cell generation. However, Deftor an endogenous inhibitor of mTORC1/2 activity can also maintain pluripotency and repression of Deftor expression triggers differentiation of mouse and human ES cells towards neuronal lineages. Similarly, in somatic stem cells, such as hematopoietic stem cells, a reduction in mTORC1 activity preserves the self-renewal nature of the cell, by inhibiting mitochondrial biogenesis and ROS production (Chen *et al.* 2008). Thus the mTORC pathway is heavily implicated in the regulation of metabolism and influences cell fate specification under a variety of contexts that can sometimes appear conflicting. Notwithstanding this point, the regulatory metabolic effects associated with the mTOR pathway are heavily implicated in the balance between pluripotency and cellular differentiation, but in an as yet poorly understood and context dependent manner.

### **The AMP-activated protein kinase (Ampk) signalling pathway**

The Ampk pathway is an intracellular energy sensor that is activated by an increase in the AMP/ATP ratio that represents a reduction in the availability of energy in the form of ATP. Ampk activation causes the stimulation of catabolic pathways that include autophagy, fatty acid oxidation and glucose uptake, that are also coupled to reductions in anabolic pathways and thereby maintain a homeostatic energy balance (Hardie *et al.* 2012).

Similar to the mTOR pathway, Ampk can function as a positive regulator of stem cell maintenance and also promote differentiation in a context dependent manner. Accordingly, both human ES and iPS cells display typically low expression levels of the Ampk catalytic  $\alpha 1$  subunit and consistently activation of Ampk activity by metformin impedes reprogramming during the derivation of human iPS cell (Vazquez-Martin *et al.* 2012). In contrast to human ES cells, human and mouse iPS and mouse ES cells retain an active Ampk pathway that positively regulates pluripotency gene expression (Shi *et al.* 2013). Thus, Ampk is not so much a regulator of cell fate towards either pluripotency and/ or differentiation; rather it indicates an individual cell's specific metabolic state at different stages of pluripotency and/ or differentiation. Accordingly, active Ampk levels differ according to the degree of differentiation towards specific lineages. Thus, its activation inhibits mouse myoblast differentiation, but promotes endothelial and cardiac differentiation (Williamson *et al.* 2009). Further, both Ampk and mTOR pathways are known to have opposing roles in regulating autophagy, with Ampk promoting autophagy by activating Ulk1 (Unc-51 Like Autophagy Activating Kinase 1) and mTOR inhibiting it by phosphorylation mediated inactivation of Ulk1, under nutrient deficient and sufficient conditions respectively (Akers *et al.* 2012). Thus a possible cross talk between these two pathways is

responsible for the general homeostatic control of metabolism, that in turn can influence stem cell self-renewal and/or differentiation.

### **c. Metabolism in mouse preimplantation embryo development**

#### **Developmental origins of health and disease (DOHaD)**

In 1999 Barker proposed the hypothesis of “Fetal origins” that is now termed the “Developmental Origins of Health and Disease (DOHaD)”, that centres around the hypothesis that environmental cues, especially nutrition availability, during the pre and peri-conceptual days continue to influence metabolic homeostasis extending to adulthood with potential pathological consequences (O’Brien *et al.* 1999). DOHaD investigations studying the influence of the environmental milieu surrounding the embryo during its development have revealed metabolic and epigenetic changes as having key roles in early embryonic growth (Chason *et al.* 2011). Recent studies involving embryos from different animal models, plus ES cells, have provided mechanistic insight into how metabolism impacts foetal development and the corresponding long-term implications manifest in adulthood. The standard model species of preimplantation development, the mouse, has been utilized in such studies. Mouse embryos unlike the embryos from other large mammals such as cattle, pigs and rabbits, have relatively smaller fat storage capacity that in the other species provides the embryo with a buffering window; responsible for altering growth through a few extra cell cycles without additional exogenous nutrient supplementation. Thus, mouse embryos poor in storage fat, are known to be sensitive to metabolic perturbations with embryos cultured in non-supplemented conditions arresting within 10-15 hours; thus highlighting how mouse and other rodent embryos are potentially more vulnerable to maternal dietary changes. Although mouse embryos have the potential to serve as sensitive models to study metabolism associated DOHaD, caution should be applied when attempting to extrapolate results to the human system, since human embryos (like the other domestic animal models referred to above) are speculated to have high levels of buffering storage fat. Nevertheless, an increase in blood pressure among offspring from mouse embryos cultured under restrictive dietary conditions has been found to be applicable in humans conceived through the *in vitro* fertilization (IVF) technique, indicating that mice can still serve as a valuable, if not tentative, tool to study DOHaD (Leese 2012).

#### **Mitochondria and oxidative metabolism**

Mammalian preimplantation embryos in general use ATP as their energy source, most of which they obtain via oxidative phosphorylation. Organisms exhibiting external development, such as birds, reptiles, fish and amphibians obtain their energy and required substrates for development by

mitochondria mediated oxidation of lipids and proteins stored in the yolk bulk. In contrast, mammalian embryos develop from microlecithal eggs, which lack a bulky energy providing yolk and during preimplantation development, they rely on the undefined complex of the extracellular nutrient milieu; including pyruvate, lactate, amino acids and other ions that maintain the embryo's metabolic homeostasis (Kane *et al.* 1997 and O'Neill 2008). The mammalian embryo, like any other vertebrate embryos, uses mitochondria to oxidize pyruvate, lactate (after its conversion to pyruvate via lactate dehydrogenase in the inter-membrane space of mitochondria) and amino acids to obtain ATP. However, until the compaction stage the embryo directly utilizes pyruvate and not glucose. Yet, by the blastocyst stage the rate of both oxygen consumption and glycolysis is increased, indicating glucose is now also metabolized; consequently producing the required pyruvate that in turn enters the OXPHOS system to generate ATP (Houghton *et al.* 1996 and Jansen *et al.* 2008). The notion of this metabolic switch towards glucose dependence is supported by the findings that depleting glucose transporters only induces apoptosis in blastocyst stage embryos and not at prior developmental stages (Chi *et al.* 2000).

In mouse embryos about 70% of the consumed oxygen has been found to be utilized in non-mitochondrial pathways. It has been proposed that it is utilized during ROS generation via the activity of enzymes such as NADPH oxidases during blastocyst stage. It has also been proposed that the ROS produced is used to stimulate the phospholipase and cyclooxygenase activities required for the decidual response during embryo implantation (Manes and Lai 1995). Since, high levels of ROS are associated with generally deleterious cellular effects, limiting their levels either by providing a low oxygen supply (*e.g.* 5%, similar to the levels in oviduct) or by supplementing EDTA to *in vitro* culture media, has been found to promote embryo development from the zygote to blastocyst stages (Orsi and Leese. 2001). Similarly, adding a minimal amount of NO (nitric oxide) donor (0.1 $\mu$ M sodium nitroprusside) to culture media has been found to stimulate embryo development, by reducing oxygen consumption and thereby potentially limiting ROS production (Amiri *et al.* 2003). Further, in the *in vivo* situation NO is known to be produced by supporting cumulus cells and found to regulate the mitochondrial polarity required to promote meiotic maturation in oocytes (Bu *et al.* 2003). Taken together these studies highlight the importance of mitochondria and the associated OXPHOS pathway that utilizes varied substrates in response to distinct physiological needs, during preimplantation embryo development.

### **Amino acid (AA) supplementation in preimplantation *in vitro* embryo culture**

Brinster (1965) first introduced AA supplementation into preimplantation embryo culture media as a replacement for serum and typically during his early studies usually used a single or chemically

related group of AAs. Later Juetten and Bavister (1983) discovered that the presence of four AAs (glutamic acid, isoleucine, methionine and phenylalanine) aided golden hamster embryos to pass through the problematic 2-cell stage block and also increased cell cleavage rates; thus enhancing the proportion of blastocyst that could be derived *in vitro*. Although AA supplementation has been found to support *in vitro* culture of other pre-implantation embryos including mouse, the exact requirement for each animal model still remains unknown. For instance, hamster embryos were found to arrest at the 8-cell stage if the media was supplemented with all 20 AAs and adding either essential or non-essential AAs alone was found to reduce the proportion of embryos reaching the blastocyst stage. Subsequent studies revealed that the reported inhibitory nature of AA supplementation could be attributed to high concentrations used in the media recipes, since the preparations are mostly based on blood composition rather than the reproductive tract fluid composition. Accordingly, when mouse embryos are *in vitro* cultured in KSOM media supplemented with AAs, at concentrations comparable to the follicular fluid, it was found to improve the rate of blastocyst formation (Sturmey 2008).

The effect of AAs in media also depends on the animal model under investigation. Thus, in contrast to the hamster embryos, that show reduced development in the presence of all AAs, mouse embryos exhibit an improved blastocyst hatching rate when all AA are supplemented. Mechanistic analyses have subsequently revealed that AAs generally reduce the levels of metabolic stress *in vitro* (Lane and Gardner 1998). Indeed, the presence of all 20 AAs (ordinarily found in proteins) has been found to reduce the abnormally high glycolytic levels, observed in the mouse blastocyst when cultured under sub-optimal culture conditions; *i.e.* those levels that not only provide required substrates for biosynthetic pathways, but also contribute to increased detrimental ROS production (see above). Therefore, the presence of exogenously supplemented AAs is proposed to reduce the embryo's reliance on glycolysis, thereby reducing stress that can be further augmented by the addition of other exogenously provided vitamins and anti-oxidants (Lane and Gardner 1998).

### **AAs in early embryo metabolic homeostasis regulation**

Preimplantation embryos cultured *in vitro* can grow without any exogenous AA supplementation by recycling their endogenous proteins to generate the required substrates for both biosynthetic and energy producing pathways up to the blastocyst stage (Thompson *et al.* 1998). However, recent studies involving mice fed with low protein/ AA diets during the preconception stage, has revealed that embryos derived from such mice are affected both at the metabolic and epigenetic levels, leading to DOHaD phenotypes; thus highlighting the importance of the exogenous AA supply to

appropriate embryo foetal development (Fleming *et al.* 2015). The specific roles of a few AAs studied in the context of *in vitro* cultured preimplantation embryo development are discussed below.

Glutamine is one of the most commonly supplemented AAs in culture media, and can be metabolized to produce glutamate and then  $\alpha$ -ketoglutarate, that is subsequently oxidized in the TCA cycle to produce ATP. Glutamine, when added as the sole AA to the culture media does improve the hatching rate of blastocyst in porcine, hamster and mouse embryos. This effect has been found to act through its influence on oxidative metabolism, plus providing substrates for purine and pyrimidine synthesis, rather than just an AA precursor for protein synthesis, hence it is its metabolic role in energy production that is important (Sturmey 2008). NO in modest levels has been found to be an absolute requirement for early embryo development (Meininger and Wu 1997). Consistently, media supplemented with arginine and glutamine, both known to have key roles in NO signalling by enabling the synthesis of NO through the activation of NO synthase and glutaminase respectively, have also been shown to improve the rates of mouse blastocyst formation in *in vitro* culture. Similarly, aspartate and methionine have been found to aid *in vitro* embryo culture by forming part of a Malate-aspartate shuttle that regulates lactate metabolism and DNA methylation pathways (Lane and Gardner 2005).

AAs also function as precursors for molecules involved in paracrine signalling. In the porcine and human systems, blastocyst secreted histidine is decarboxylated via histidine decarboxylase to generate histamine and it is proposed that this histidine plays a role in preparing the uterus for implantation (Wood *et al.* 2000). Furthermore, glycine, glutamine, alanine and the non-protein AAs taurine and hypotaurine, serve as a substrates for the Glyt1 glycine transporter that is known to protect the embryo from osmolytic stress (Steeves *et al.* 2003). Thus exogenous supplementation of AAs to *in vitro* culture media is known to regulate a spectrum of mechanisms (plus the potential undiscovered mechanisms) that act to maintain early appropriate embryo homeostasis associated with optimized preimplantation stage development.

#### **DOHaD associated with AA deficiency**

Extensive studies from the Fleming lab (eluded to above) have highlighted the importance of the maternal diet, and more specifically on AAs, during the peri-conceptual stage of development. During this stage, the gametes and embryos that represent the primitive stages of development are hypersensitive to environmental changes that in turn can influence their metabolism, epigenetics and subsequent development (Fleming *et al.* 2015). For example, studies on mouse and rat pups born to mothers fed on low protein diet (LPD; with 9% casein as protein source) during their first 4.5 days of *in vivo* development and then switched to a normal protein diet (NPD; with 18% casein)

showed substantially and significantly increased body weight (in both male and females), compared to control groups derived from females fed with NPD throughout gestation. Moreover, new born female and postnatal (4 - 11 weeks old) male pups had increased systolic blood pressure; male kidney weight was increased and both male and female livers exhibited abnormal gene imprints. Furthermore, female mice showed hyperactive behaviour and a poor memory. Importantly the above mentioned abnormalities observed were very similar to those observed in offspring derived from females exposed to low protein diet throughout the whole gestation period (Kwong *et al.* 2000, 2006 and 2007). Thus protein derived nutrient deprivation during the preimplantation development alone has long term physiological effects that can extend to the prenatal stage of development and beyond into adulthood. Indeed E3.75 stage embryos derived from females fed with LPD (from the point of mating) exhibit a greater number of proliferating TE cells and increased levels of endocytosis (also associated with robust increases in the mRNA and protein expression levels of the receptor megalin). The observed stimulation of endocytosis was indicative of a plasticity to adjust to the protein deprived conditions and to draw upon more exogenous nutrients and was shown to be dependent on RhoA-GTPase dependent actin cytoskeleton rearrangements. Although an increase in lysosomal vesicles was observed, the number of autophagic vesicles remained unaltered; thereby demonstrating the dependence on exogenous protein uptake, likely by endocytosis, is the major contributor for maintaining an appropriate AA homeostatic balance during otherwise unperturbed preimplantation development, rather than catabolism dependent recycling of proteins to derive AAs (Sun *et al.* 2014)(although autophagosomes do exist, highlighting the presence of concomitant and active catabolism). Similar to the changes observed in the TE, the emerging PrE lineage also showed similar adaptations that could aid in nutrient uptake. Accordingly there was up-regulation in cell proliferation, megalin receptor distribution, endocytosis and the number of lysosomes. When embryoid bodies were derived from LPD derived embryos, these compensatory responses were still maintained in the peripheral PrE-like cells of the resulting embryoid bodies; indicating a possible epigenetic modification based mechanism that is responsible for the persistence of the phenotype. Further, ChIP analysis revealed that the PrE specific transcription factor *Gata6* gene showed reduced H3 and H4 acetylation with accordingly up-regulated *Histone deacetylase 1 (Hdac1)* and reduced *Gata6* gene expression, resulting in impaired PrE differentiation and an increase in the size of the embryoid bodies (Sun *et al.* 2015). Thus these data demonstrate that AA availability during preimplantation mouse embryo development is able to regulate key events relating to the emergence of the differentiating extraembryonic cell lineages that have the potential to mediate long lasting effects on embryo development and adulthood.

## **3. Objectives**

### 3.1 Objectives

The presented thesis study aims are to elucidate the previously unexplored role of p38-Mapk14/11 in second cell fate decision during mouse preimplantation embryo development (*i.e.* the separation of EPI and PrE cell populations in the blastocyst ICM). In addition, to uncover the metabolic sensitivity of the p38-Mapk14/11 pathway to the availability of exogenous amino acids in the embryo culture media, in the stated cell-fate context. Accordingly, the following objectives were defined.

- To investigate the existence of possible PrE lineage formation associated functions of p38-Mapk14/11, by utilizing pharmacological inhibitors.
- To identify the developmental window period during which, p38-Mapk14/11 could be essential for PrE development.
- To deduce the possible upstream and downstream regulators of p38-Mapk14/11 that can regulate its PrE related function.
- To investigate if the presence or absence of exogenously supplemented amino acids in the culture media can influence the outcome of p38-Mapk14/11 related functions during preimplantation embryo development, in respect to blastocyst ICM cell-fate maturation.

## **4. Materials and methods**

#### 4.1 Embryo culture, specific inhibitors and microinjection treatments.

Two-cell stage (E1.5) embryo collection and *in vitro* culture, in KSOM (Potassium simplex optimised media) supplemented with amino acids, KSOM+AA (non essential amino acids and amino acid solution, from Gibco, diluted to working concentration of 0.5x from 100x and 50x stock solutions, respectively) was conducted as previously described (Mihajlovic *et al.* 2015). Specific chemical inhibitor embryo treatments were administered in KSOM+AA (unless otherwise stated) and targeted the stated proteins/pathways and were conducted at the follow concentrations; (i) p38-Mapk14/11; SB220025 (Calbiochem, Millipore) at 20  $\mu$ M from either E2.5–E4.5 or E3.5–E4.5 and in experiments aimed at identifying the developmental timeframe of p38-Mapk14/11 inhibition sensitivity, during blastocyst maturation, from E3.5 to E4.0 or from E3.75/E4.0 to E4.5 (ii) p38-Mapk14/11; SB203580 (plus non-biologically active analogue control SB202474, Calbiochem, Millipore) at 20  $\mu$ M from E3.5 to E4.5, (iii) Mek1/2; PD0325901 (Sigma-Aldridge) at 1  $\mu$ M, in the same time periods as described p38-Mapk14/11 inhibition using SB220025, plus E2.5–E4.5, (iv) Tak1; (5Z)-7-Oxozeaenol (Tocris) at 700 nM from E2.5 to E4.5, (v) Fgf-receptor; SU5402 (Calbiochem) at 10  $\mu$ M from E3.0 to E4.5 and (vi) GSK-3 $\beta$ ; CHIR99021 (Selleckchem) at 3  $\mu$ M from E2.5 to E4.5. Note, that in the cases of SB220025 and PD0325901 inhibition from E3.5 to E4.0, if embryos were not to be immediately fixed, they were washed through 25 approximately 9  $\mu$ l drops of normal pre-warmed KSOM+AA growth media (to wash out the drug) and returned to *in vitro* culture and fixed at the late-blastocyst (E4.5) stage (to assay if inhibition effects were irreversible). As all inhibitors used were either supplied or reconstituted in DMSO solvent, parallel vehicle control condition embryo groups to each experimental/inhibition condition group were also established; these contained equivalent concentrations of DMSO diluted in the same KSOM+AA media (and were therefore slightly different in relation to which experimental/inhibition group they acted as control for). Single blastomere microinjections were performed on two-cell stage embryos (in both blastomeres) according to previously described and defined protocols (Zernicka-Goetz *et al.* 1996) using apparatus formerly described (Mihajlovic *et al.* 2015). Mutant mRNA, were microinjected, and represented constitutively active mouse-derived Mkk6 (Mkk6-EE; were serine-207 and threonine-211 were replaced with glutamate to provide phospho-mimetic function), ATF2 (CA-ATF2; were the phosphorylation dependent domain of rat Atf2 was replaced with constitutively active domain of human CREB2), Mk3 (CA-Mk3; were threonine-315 residue of mouse Mk3 was replaced with glutamate to provide phospho-mimetic constitutively active function) and MSK1 (CA-MSK1; were the hydrophobic motif of human MSK1 (amino acid residues 1-379) was replaced with the constitutively active hydrophobic residue of PRK2 with a N-terminally tagged NLS sequence for nuclear transport). Mkk6-EE was microinjected at a concentration of 500 ng/ $\mu$ l; both CA-ATF2 and CA-Mk3 at 350ng/ $\mu$ l and CA-MSK1

at 50ng/μl (GFP mRNA microinjection control groups were also included at the relevant concentrations). All mRNAs were co-microinjected with Oregon green-conjugated dextran beads (OGDBs; 1 μg/μl —to confirm successful microinjection). Microinjected embryos were then *in vitro* cultured and potentially exposed to defined chemical inhibitor treatments, as described above, until the desired developmental stage, in 20 μl culture drops overlaid with mineral oil at 37°C in a 5% CO<sub>2</sub> containing atmosphere. Non-microinjected embryos (2–3 per experiment, per plate) served as culture sentinels to confirm successful *in vitro* development. To study amino acid associated metabolic role of p38-Mapk14/11, embryos were cultured both in KSOM+AA and in a commercially available KSOM (cKSOM; EmbryoMax®KSOM embryo culture media – Millipore) and the inhibitor SB220025 was employed to inhibit p38-Mapk14/11 pathway in embryos from the early (E3.5) to late (E4.5) blastocyst stage. Further, the anti-oxidant N-acetyl cysteine (NAC; Sigma-Aldridge) at a concentration of 1mM was used in both KSOM+AA and cKSOM culture conditions under p38-Mapk14/11 inhibition (SB220025) from the early (E3.5) to late (E4.5) blastocyst stage, to investigate any role for p38-Mapk14/11 inhibited embryos in the protection from reactive oxygen species (ROS).

#### **4.2 mRNA preparation for microinjection.**

The microinjected mRNA constructs were derived, and purified, by *in vitro* transcription of linearized (2 μg; using Sfil) pRN3P (Zernicka-Goetz *et al.* 1997) plasmid containing the appropriate cDNA cloned downstream of the T<sub>3</sub> bacteriophage-derived RNA polymerase promoter with 5' and 3' flanking untranslated region (UTR) sequences from the frog β-globin gene, according to the kit manufacturer's protocols (T<sub>3</sub> MessageMACHINE, Ambion). pRN3P:GFP is described elsewhere (Zernicka-Goetz *et al.* 1996), but pRN3P:Mkk6-EE and CA-Mk3 were newly derived for this study by PCR amplifying wild-type mouse Mkk6 and Mk3 cDNA insert from either brain or spleen-derived cDNA libraries respectively, and cloning into the multiple cloning site of pRN3P (by virtue of included *BamHI* and *NotI* recognition sequences in the forward and reverse PCR primers, respectively), followed by PCR-based site-directed mutagenesis to derive the required activating mutations (S207E and T211E in Mkk6; designated as Mkk6-EE, T315E in Mk3; designated as CA-Mk3) and DNA sequence verified; all using standard molecular biology techniques. pRN3P:CA-ATF2 and pRN3P:CA-MSK1 were created by sub-cloning from a previously described ATF2-CREB2 and NLS-CA-MSK1 constructs (Steinmuller L & Thiel G. 2003 and Frodin *et al.* 2000) into the pRN3P vector using the *EcoRI/BamHI* and *EcoRI/NotI* sites respectively, again using standard linker mediated PCR-based strategies to generate the required insert.

### 4.3 Immuno-fluorescent staining and confocal imaging

Embryos of appropriate developmental stage were prepared, fixed, immuno-fluorescently stained and imaged by confocal microscopy as previously detailed (Mihajlovic *et al.* 2015). Primary antibodies targeting specific proteins were obtained from the following suppliers and used at the stated concentration: (i) eBioscience, Nanog (14-5761-80); 1 : 200 dilution. (ii) Abcam, Nanog (ab80892); 1 : 200 dilution. (iii) Cell Signalling Technologies, phospho-p38-Mapk14/11 (9216), phospho-Erk1/2 (9106) and cleaved caspase 3 (9661); 1 : 200 dilution. (iv) R&D Systems, Gata6 (AF1700) and Sox17 (AF1924); 1 : 200 dilution. (v) Santa Cruz, Gata4 (sc-9053) and Gata4 (sc-1237); 1 : 200 dilution. (vi) ThermoFisher scientific, phospho-Nanog pSer71 antibody (PA5-13078); 1 : 200 dilution. (vii) Zscan10 (a gift from Lawrence W. Stanton). The following secondary antibodies were purchased from Life Technologies and used at 1 : 500 dilutions to detect the following epitopes: (i) Alexa647-conjugated donkey-anti rabbit (A31573); Nanog (ab80892). (ii) Alexa488-conjugated donkey-anti-goat (A11055); Gata4 (sc-1237) and Sox17. (iii) Alexa647-conjugated donkey-anti-rabbit (A31573); Nanog (ab80892), phospho-p38-Mapk14/11, Gata4 (sc-9053) and Caspase-3. (iv) Alexa488-conjugated donkey-anti-goat (A11055); Gata6. (v) Alexa488-conjugated goat-anti-mouse (A11029); phospho-Erk1/2. (vi) Cy3-conjugated rat-anti-mouse (A10521); Nanog (14-5761-80). (vii) Alexa555-conjugated donkey anti-rabbit (A31572); phospho-Nanog pSer71 (PA5-13078), Zscan1. Please note that owing to the non-specific interaction between microinjected OGDBs and the goat-derived anti-Gata4 antibody (sc-1237), any embryos that had been microinjected and were to be co-immuno-fluorescently stained for Nanog and Gata4, were done so using the following explicit primary antibody combination (hence the reason why two Nanog and Gata4 primary antibodies are listed; in non-microinjected embryos immuno-stained for Nanog and Gata4, the alternative primary antibody combination was used); mouse-derived anti-Nanog (14-5761-80) and rabbit-derived anti-Gata4 (sc-9053).

### 4.4 Image analysis/cell counting.

Individual E4.5 (and E4.0) stage blastocyst cell contributions to specific cell lineages (deduced by presence and/or absence of specific immunofluorescence/ IF detected signal for the relevant marker protein expression), or within inner or outer cell populations, were determined in both experimental and control embryos by inspection of confocal micrograph z-sections using FLUOVIEW v. 1.7.a (Olympus), IMARIS (Bitplane) and IMAGEJ software. These contributions were individually tabulated for each embryo (see appendix) and the mean of cells within defined populations plus the standard error of means (mean  $\pm$ s.e.m.) calculated (and presented in graphical format). The statistical significance between relevant experimental and control groups was determined using two-tailed Student's t-tests.

## 5. Results

The result section explained below forms the basis of the accepted and published paper:

**p38 (Mapk14/11) occupies a regulatory node governing entry into primitive endoderm differentiation during preimplantation mouse embryo development.** Thamodaran V, Bruce AW. 2016. *Open Biol.* rsob.160190.

### 5.1 Active p38-Mapk14/11 is required for PrE differentiation

Previous studies investigating the role of p38-Mapk14/11 during preimplantation mouse embryo development have utilised small compound pharmacological inhibition strategies and uncovered a requirement during the morula/ blastocyst transition stage, with p38-Mapk14/11 inhibited embryos typically exhibiting arrested development, associated with failures in blastocoel formation and associated TE cell function (Bell and Watson 2013; Natale *et al.* 2004; Yang *et al.* 2015). Given that both the TE and PrE can be considered as somewhat similar extraembryonic and highly polarised epithelial blastocyst tissues, it was hypothesised that p38-Mapk14/11 may also have a role in the differentiation of PrE and hence blastocyst maturation. Moreover, that this potential role could be assayed using a similar pharmacological inhibition approach, only modified to provide the p38-Mapk14/11 inhibiting drug (SB220025) after the described sensitive morula to blastocyst transition. First, to confirm the results of previous studies and the efficacy of the utilised p38-Mapk14/11 inhibitor SB220025, 8-cell stage (E2.5) embryos were *in vitro* cultured to the late blastocyst (E4.5) stage in the presence of the inhibitor or DMSO vehicle control [*n.b.* the same concentrations were used as previously reported (Natale *et al.* 2004)]. As shown in figure 7a, embryos specifically in the SB220025 treated group were developmentally arrested; DMSO treated embryos developed normally to form expanded/ hatching blastocysts. Moreover, this phenotype was consistent with blocked development at the morula to blastocyst transition, as embryos typically consisted ~30 cells (figure 7b) and failed to form a blastocoel. This data hence agrees with previous reports and demonstrates the efficacy of the p38-Mapk14/11 inhibition. Further, immuno-fluorescent (IF) staining was performed, using antibodies specific for pairwise combinations EPI and TE, or EPI and PrE lineage markers (figure 7c). These analyses showed that whilst the majority of outer cells in p38-Mapk14/11 inhibited embryos did express the TE marker *Cdx2*, indicating TE had been correctly specified (figure 7d' & 7e'), virtually all ICM cells were positive for both the EPI marker, *Nanog* and the early PrE marker *Gata6*, but not the later PrE marker *Sox17* (figure 7d & 7e). This result suggested that there could indeed be a block in PrE differentiation within the ICM of p38-Mapk14/11 inhibited embryos but was tempered by the fact the embryos were arrested, in terms of cell total number, at the morula to blastocyst transition. Therefore, having now confirmed the efficacy of the inhibition approach, experiments to address the question of PrE differentiation sensitivity to p38-Mapk14/11 inhibition more directly were employed. As referenced above, cavitated early blastocyst stage embryos (E3.5), that had therefore successfully transited the p38-Mapk14/11 sensitive morula/ blastocyst stage, were transferred into culture conditions supplemented with SB220025 or control DMSO and allowed to develop to the late blastocyst (E4.5) stage. Embryos were then fixed and processed for immuno-fluorescent (IF) staining for lineage specific marker proteins, whereby *Nanog*

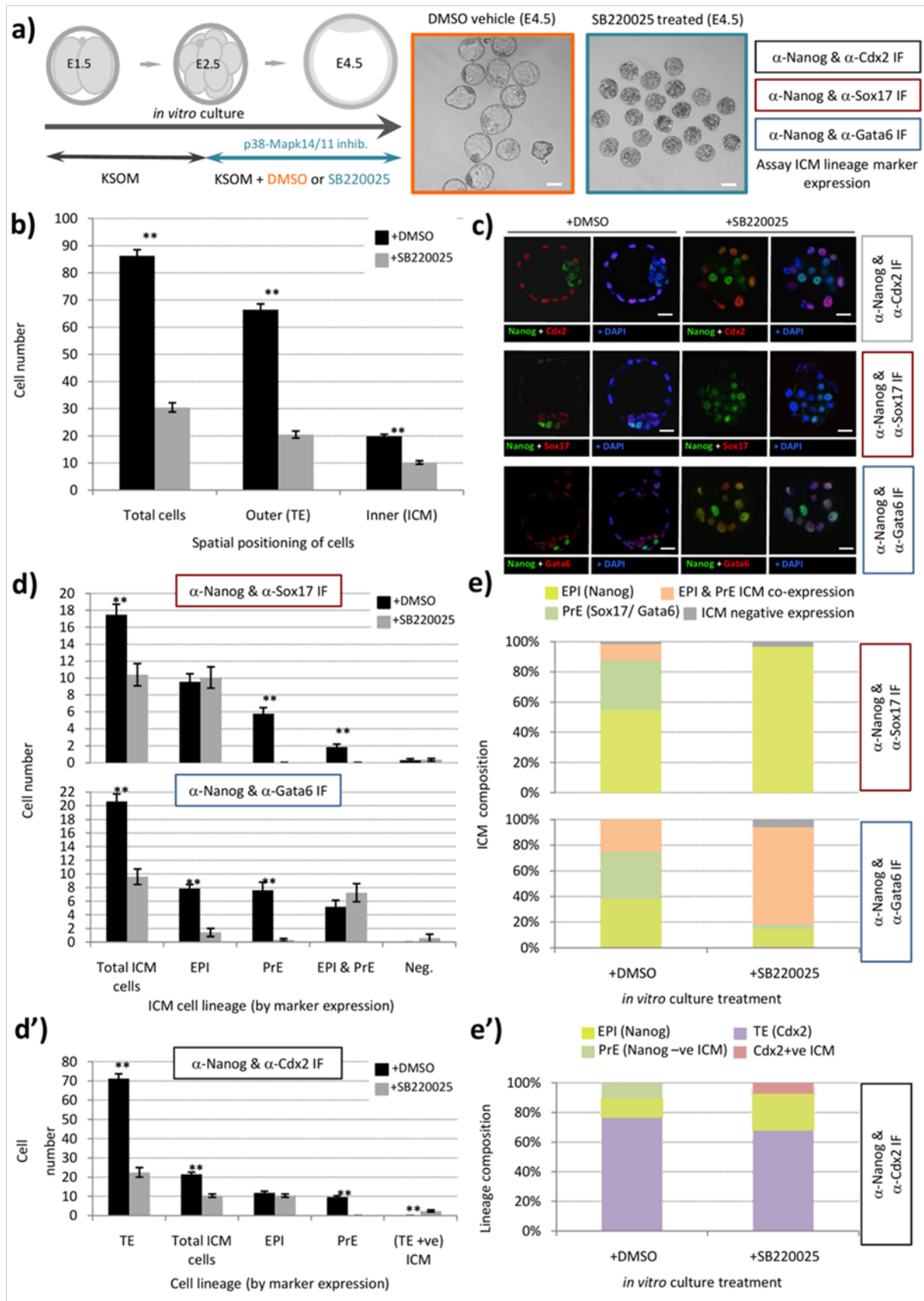


Figure 7. (legend overleaf)

**Figure 7: p38-Mapk14/11 inhibition (+SB220025) from the 8-cell (E2.5) to late blastocyst (E4.5) stage.** **a)** Experimental schema of *in vitro* cultured embryos subject to p38-Mapk14/11 inhibition (+SB220025; highlighted in sea-green), or vehicle control treatment (DMSO; highlighted in orange), from the 8-cell (E2.5) to late-blastocyst (E4.5) stage and the details of the antibodies used to analyse (ICM) cell lineage marker protein expression by immuno-fluorescence (IF); denoted by black box, Nanog and Cdx2 (+DMSO n=14, +SB220025 n=18), denoted by red box, Nanog and Sox17 (+DMSO n=15, +SB220025 n=15) and denoted by blue box, Nanog and Gata6 (+DMSO n=13, +SB220025 n=12). Bright-field micrographs detail exemplar late-blastocyst (E4.5) stage embryos at the end of the *in vitro* culture/inhibition period, prior to fixation and IF. Note defective blastocoel formation in SB220025 treated group. Scale bar = 15µm. **b)** Average number of outer- (defined as TE) and inner- (ICM) cells in embryos stained by IF for indicated ICM markers [*i.e.* as in **a)**] in either control (+DMSO) or p38-Mapk14/11 inhibited (+SB220025) conditions. Error bars reflect s.e.m and statistically significant divergence between conditions, determined by 2-tailed student t-test, are highlighted (\* p<0.05 and \*\* p 0.005). Data represent the composite of the three IF regimes employed. **c)** Representative single z-plane confocal micrographs of embryos stained by IF for the indicated ICM makers [*i.e.* as in **a)**] in control (+DMSO) or p38-Mapk14/11 inhibited (+SB220025) conditions. Nanog derived staining in green, Cdx2, Sox17 and Gata6 signal in red are shown in merged images with additional DNA DAPI counterstain merge in blue. Scale bars = 15µm. **d)** and **d')** Bar charts showing average number of cells allocated to each specified ICM lineage, as judged by the indicated IF staining regime employed [as in **a)**]. Error bars represent s.e.m. and \* and \*\* denote statistical significant differences in cell number between the vehicle control (+DMSO, black bars) and p38-Mapk14/11 inhibited (+SB220025, grey bars) embryo groups, according to 2-tailed students t-test, with p<0.05 and p<0.005 confidence intervals, respectively. Note ICM cells solely expressing Nanog or Sox17/Gata6 were classified as EPI or PrE respectively or EPI & PrE if both markers were detectable. Cells negative for both ICM markers were designated negative (Neg.). A similar classification was applied to the embryo group immuno-stained for Nanog and Cdx2 [see **d')**], although PrE cells were classified as those expressing neither Nanog or Cdx2 and instead of Neg. cells, ICM cells exhibiting ectopic expression of Cdx2 were noted (TE +ve ICM). The total number of outer-residing Cdx2 positive TE cells is additionally provided. **e)** and **e')** Percentage bar charts detailing the averaged relative cell lineage composition of ICMs from vehicle control (+DMSO) and p38-Mapk14/11 inhibited (+SB220025) embryo groups, [classified according to the scheme described for **d)** and **d')**], immuno-stained for the indicated cell lineage marker proteins. All individual embryo data used in the preparation of this figure are contained within appendix tables T1 and T2.

was assayed in combination with either Gata6, Sox17 or the late PrE marker Gata4 (figure 8) or Cdx2 (figure 9), to permit blastocyst cell lineage allocation to be compared. In regard to the ICM cell lineages, p38-Mapk14/11 inhibition was associated with a striking and statistically robust reduction in the number/ proportion of cells expressing any of the three assayed PrE lineage markers alone (*i.e.* not also expressing Nanog; this effect was also observable in the ICMs of blastocysts immunofluorescently stained for Nanog and Cdx2, when assuming Nanog negative ICM cells belong to the PrE). Indeed, on average the percentage contribution of such cells to the ICMs of each assayed and p38-Mapk14/11 inhibited group only represented 14.2%, 10.8%, and 14.1% (when assaying for Gata6, Sox17 and Gata4, respectively) compared to an average of 36.9% in control embryo groups (when considered together across the three assayed conditions); PrE cell number reductions were associated with highly significant p-values (*i.e.* <0.005, 2-tailed students t-test;  $p=2.21^{E-12}$ ,  $8.40^{E-7}$  and  $2.54^{E-12}$ , when respectively assaying Gata6, Sox17 and Gata4). A similar and significant reduction in the number of PrE cells (judged by immuno-fluorescently staining for Nanog and Gata4) was also observed when an alternative p38-Mapk14/11 inhibitor SB203580 (Natale *et al.* 2004) was employed, corresponding to 10.4% of the ICM ( $p=3.82^{E-9}$  compared to DMSO vehicle control and  $p=2.96^{E-8}$  compare to non-active drug analogue SB202474 treated groups; figure 10), thus independently confirming the SB220025 derived phenotype. In contrast to the reduction in total ICM cell number in SB220025 treated embryos, SB203580 treated embryos displayed a statistically significant increase in ICM cell number (with 2-tailed student t-test p-value;  $p=1.48^{E-05}$  compared to DMSO treated group; figure 10d). Further, the readily observed cells of control, DMSO treated, embryos that solely expressed the assayed PrE markers, had appropriately sorted to the blastocoel facing surface of the ICM in a manner indicative of successful PrE differentiation (figure 8), therefore confirming the suitability of the *in vitro* culture conditions used.

Accordingly, the above data were interpreted as demonstrating a significant failure in PrE differentiation/ blastocyst ICM maturation that is associated with the inhibition of p38-Mapk14/11 activity. However, it should be noted that the PrE differentiation inhibition phenotype was not completely penetrant, at the concentration of SB220025 used, and likely reflects heterogeneity within ICM cells to successfully integrate PrE promoting cues. Additionally and consistent with observations made of embryos inhibited from the 8-cell (E2.5) stage, a notable and statistically significant increase ( $p = 1.83^{E-3}$ ) in the number/ proportion of cells expressing both Nanog and Gata6 was recorded, indicative of ICM cells of uncommitted fate (figure 8); manifest in an increased ICM percentage contribution of such uncommitted cells to 52% versus 26.4% in DMSO treated controls (a similarly significant increase,  $p=2.00^{E-7}$ , to 70% uncommitted ICM cells was also observed using the alternative SB203580 p38-Mapk14/11 inhibitor; figure 11). There was no similar increase in co-

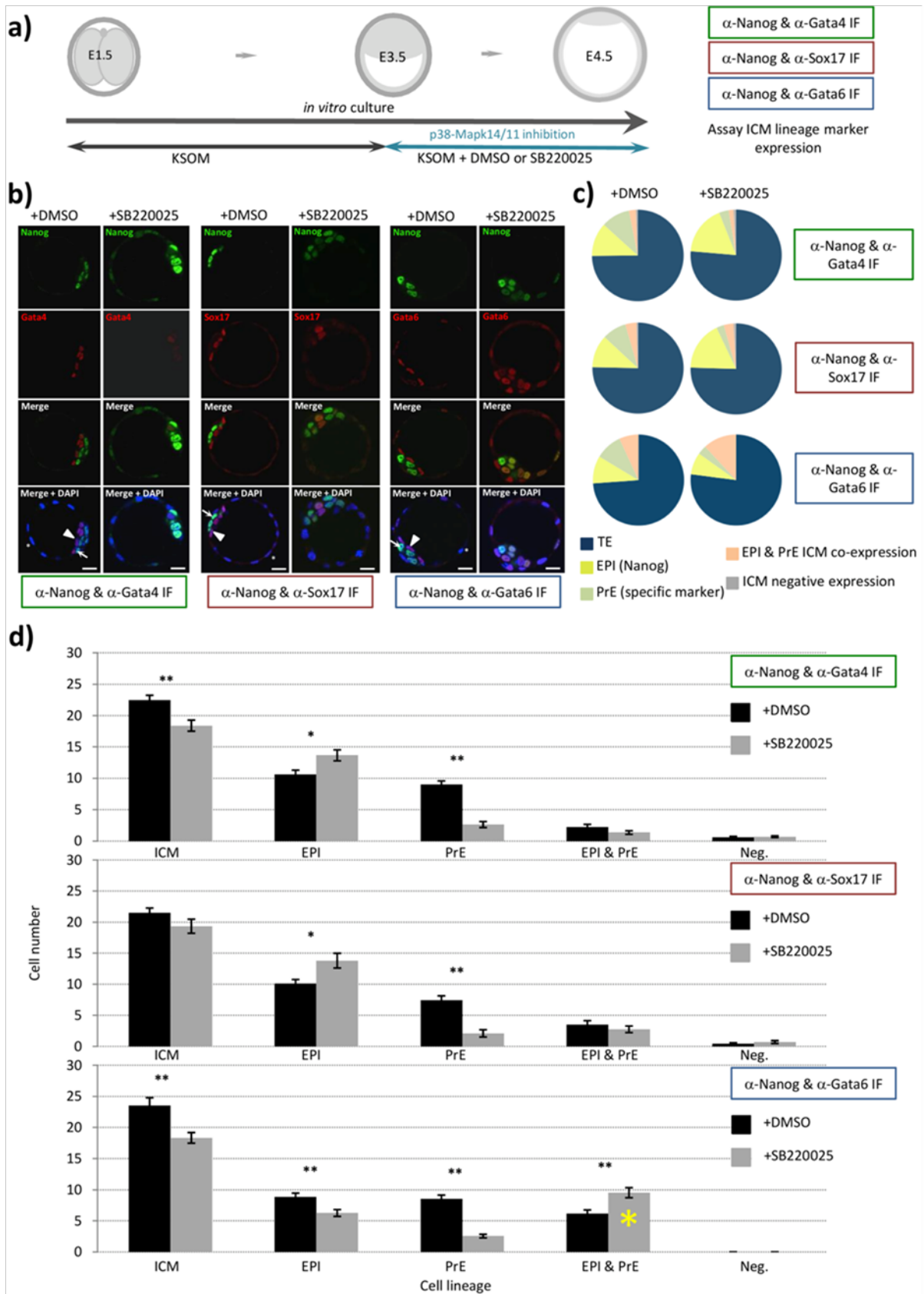


Figure 8. (legend overleaf)

**Figure 8: p38-Mapk14/11 inhibition during blastocyst maturation (from E3.5 to E4.5) blocks PrE differentiation/ maturation. a)** Experimental schema of p38-Mapk14/11 inhibition (+SB220025), plus vehicle control (+DMSO), and the details of antibodies used to analyse ICM cell lineage marker protein expression by immuno-fluorescence (IF) in late blastocysts (E4.5); Nanog & Gata4 (+DMSO n=27, +SB220025 n=33) - green, Nanog and Sox17 (+DMSO n=18, +SB220025 n=20) – red, and Nanog and Gata6 (+DMSO n=24, +SB220025 n=27) - blue. **b)** Representative single confocal z-plane micrographs of vehicle control treated (+DMSO) or p38-Mapk14/11 inhibited (+SB220025) late-blastocyst stage/ equivalent embryos, immuno-fluorescently (IF) stained for indicated ICM cell lineage markers (Nanog in green and Gata4, Sox17 and Gata6 in red, plus DAPI DNA stain in blue). Examples of cells classified as TE, PrE and EPI are marked with an asterisk, arrow-head and arrow, respectively. Scale bar = 15µm. **c)** Pie charts of the relative cell lineage contribution in vehicle control (+DMSO) and p38-Mapk14/11 inhibited (+SB220025) blastocyst as judged by immunofluorescence (IF) to detect the stated ICM lineage marker proteins. Blue = trophoctoderm (TE), yellow = Epiblast (EPI – ICM exhibiting exclusive Nanog expression), green = Primitive Endoderm (PrE - ICM exhibiting exclusive Gata4/6 or Sox17 expression, as appropriate), orange = uncommitted ICM cells (exhibiting co-expression of both Nanog and Gata4/6 or Sox17, as appropriate) and grey = ICM cells negative for either assayed marker. **d)** Bar charts showing average number of cells allocated to each specified ICM lineage, as judged by the indicated IF staining regime employed. Error bars represent s.e.m. and \* and \*\* denote statistical significant differences in cell number between the vehicle control (+DMSO, black bars) and p38-Mapk14/11 inhibited (+SB220025, grey bars) embryo groups, according to 2-tailed students t-test, with  $p < 0.05$  and  $p < 0.005$  confidence intervals, respectively. Yellow asterisk denotes increase in cells positively immuno-fluorescently staining for both EPI and PrE ICM markers using anti-Nanog and anti-Gata6 (an early PrE marker) antibodies. All data used to prepare this figure are described in appendix tables T3.

---

expressing cells in p38-Mapk14/11 inhibited groups immuno-fluorescently stained for Nanog and the later PrE markers Sox17 or Gata4 (although there was an enhanced level of ectopic Nanog co-expression with Cdx2 in outer TE cells; figure 9). Importantly, p38-Mapk14/11 inhibition mediated phenotypes were not associated with altered levels of activated phospho-Erk1/2 kinase [Erk1/2(p)], extensively implicated in PrE differentiation via reports using inhibitors of its upstream activating mitogen activated kinases, Mek1/2 (Frankenberg *et al.* 2011; Kang *et al.* 2011; Nichols *et al.* 2009; Yamanaka *et al.* 2010) as judged by specific immuno-fluorescence after p38-Mapk14/11 inhibition using SB220025 (figure 12).

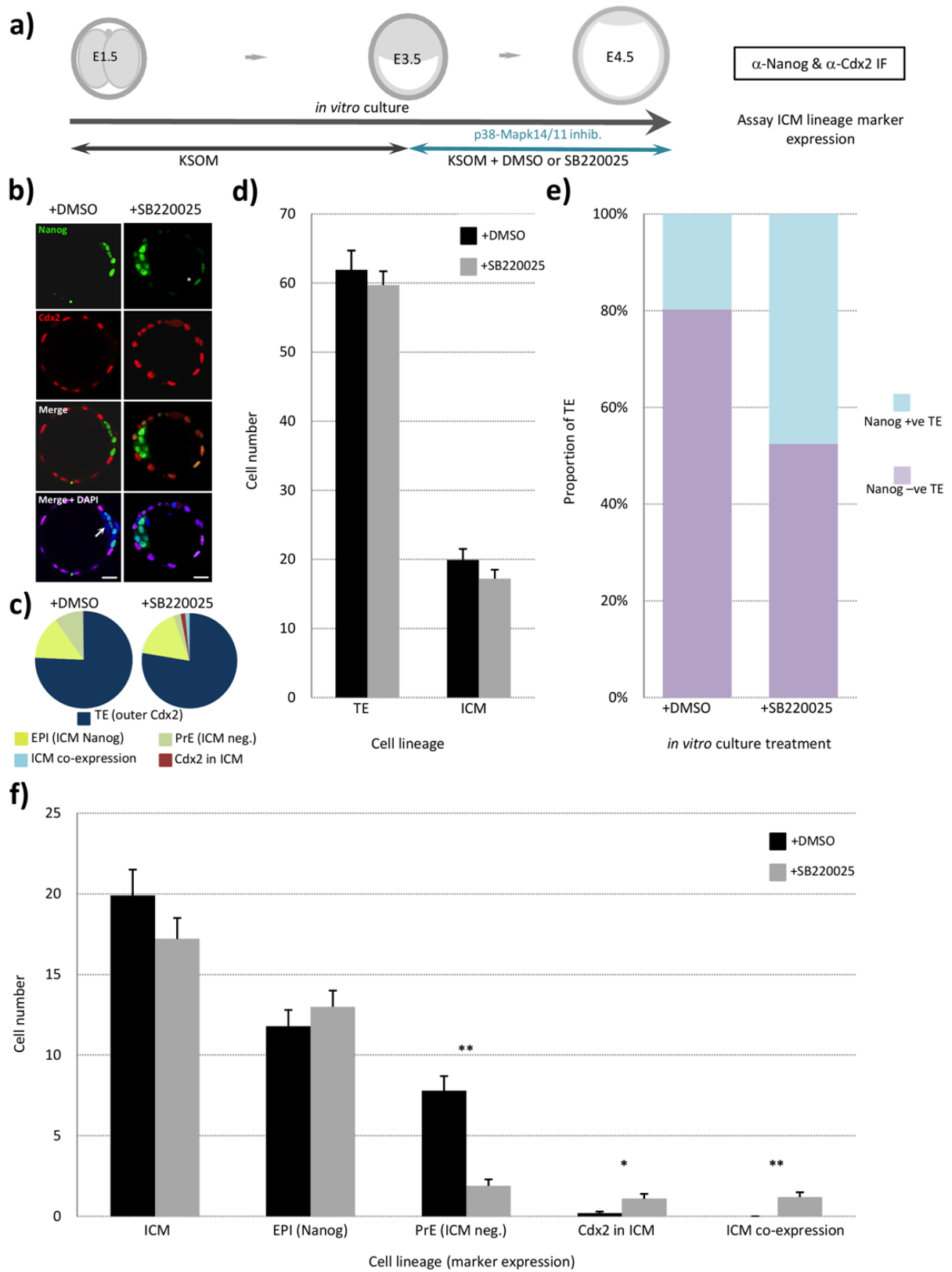


Figure 9. (legend overleaf)

**Figure 9: p38-Mapk14/11 inhibition from the early- (E3.5) to late blastocyst (E4.5) stages also effects outer TE cells.** **a)** Experimental schema of *in vitro* cultured embryos subject to p38-Mapk14/11 inhibition (SB220025) or vehicle control treatment (DMSO) from the early- (E3.5) to late-blastocyst (E4.5) stage and immuno-fluorescently (IF) stained for Nanog and Cdx2 (+DMSO n=17, +SB220025 n=26). **b)** Representative single z-plane confocal micrographs of IF stained embryos in control (+DMSO) or p38-Mapk14/11 inhibited (+SB220025) groups. Nanog derived staining in green, Cdx2 signal in red (also merged) plus additional merged image with DNA DAPI counterstain merge in blue. Scale bars = 15µm. Note, arrow in the control image (+DMSO) denotes ICM cells devoid of detectable Nanog signal, designated as PrE; asterisk denotes ectopic Nanog expression in the outer TE cells of p38-Mapk14/11 inhibited embryos. **c)** Pie charts of the relative cell lineage contribution in vehicle control (+DMSO) and p38-Mapk14/11 inhibited (+SB220025) blastocyst as judged by anti-Nanog/ Cdx2. Blue = trophoctoderm (TE – outer cells expressing Cdx2), yellow = Epiblast (EPI – ICM exhibiting exclusive Nanog expression), green = Primitive Endoderm (PrE - ICM devoid of staining), light blue = co-expressing ICM cells (exhibiting co-expression of both Nanog and Cdx2) and maroon = ICM cells ectopically expressing Cdx2. **d)** The averaged number of outer/ TE and inner/ ICM cells in p38-Mapk14/11 inhibition (SB220025; grey) or vehicle control treatment (DMSO; black) groups. Errors stated as s.e.m. **e)** Percentage bar charts detailing the averaged relative ectopic expression of Nanog in outer TE cells in p38-Mapk14/11 inhibition (+SB220025) or vehicle control treatment (+DMSO) groups. Light blue denoting ectopic expression in the TE and purple an absence of detectable Nanog in the TE. Note, increased number of outer TE cells ectopically expressing Nanog. **f)** Bar chart showing average number of cells allocated to each indicated ICM lineage, as judged by the indicated IF staining pattern detected. Error bars represent s.e.m. and \* and \*\* denote statistical significant differences in cell number between the vehicle control (+DMSO, black bars) and p38-Mapk14/11 inhibited (+SB220025, grey bars) embryo groups, according to 2-tailed students t-test, with p<0.05 and p<0.005 confidence intervals, respectively. Note, ectopic Cdx2 expression in the ICM. All individual embryo data used in the preparation of this figure are contained within appendix tables T4.

---

Therefore, it was concluded that blastocyst stage p38-Mapk14/11 inhibition is associated with a profound cell-fate commitment failure of ICM cells. Interestingly, in the Nanog/Gata6 assayed experimental group using the SB220025 inhibitor a statistically significant reduction in the number of cells expressing Nanog or Gata6-alone was observed ( $p= 3.18^{E-3}$  and  $2.21^{E-12}$ , respectively), suggesting an inhibition to commit to both EPI and PrE cell-fates. However, p38-Mapk14/11 inhibition was also associated with overall reduction in total ICM cell number (on average 3.5 fewer cells). Therefore,

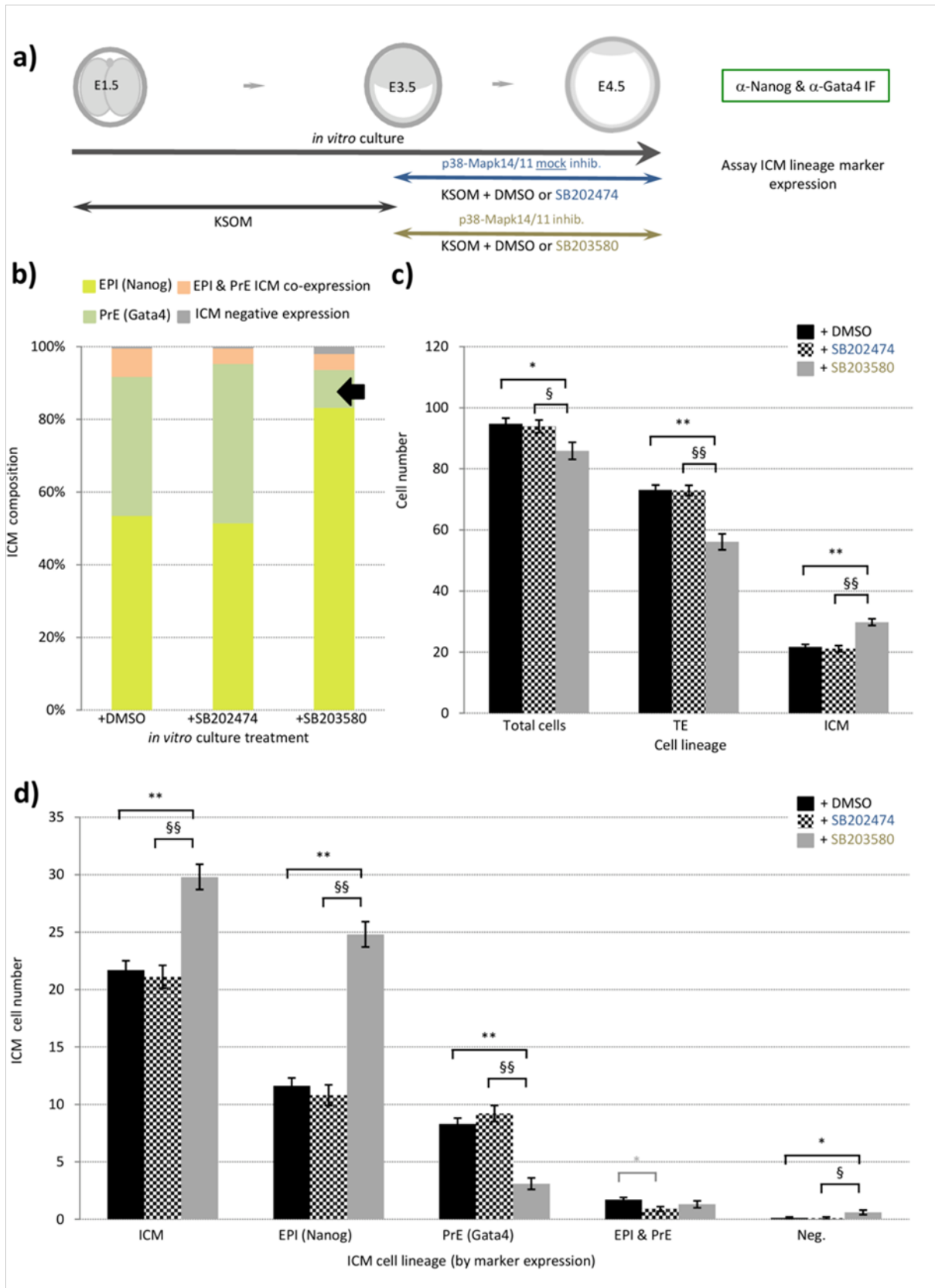


Figure 10. (legend overleaf)

**Figure 10: The alternative p38-Mapk14/11 inhibitor SB203580 also impairs PrE formation in the ICM (when administered from E3.5 to E4.5) whereas its inactive analogue SB202474 does not. a)** Experimental schema detailing the regime of p38-Mapk14/11 inhibition (+SB20350) or mock inhibition with inactive drug analog (+SB202474), at 20 $\mu$ M concentrations, with attendant vehicle control (+DMSO) condition, from the early to late blastocyst (E3.5-E4.5) stages employed. Immunofluorescence (IF) antibody details used to analyse ICM cell lineage marker protein expression in late blastocysts (E4.5) are also given (*n.b.* Gata4 used as PrE marker). **b)** Averaged percentage makeup of the ICMs of each stated condition in relation to each specified ICM lineage; EPI or PrE (yellow and green, exclusively immuno-stained for either Nanog or Gata4, respectively), EPI & PrE co-expressing cells (orange, representing cells uncommitted to either lineage) and cells negative for either studied lineage marker (grey). The black arrow denotes the decreased percentage contribution of Gata4-alone positive PrE cells in the ICM of +SB203580 treated embryos compared to +DMSO vehicle or inactive analog (+SB202474) controls. In the +DMSO treated group n = 32, in the +SB202474 mock group n = 19 and in the +SB203580 p38-Mapk14/11 inhibition group n = 18. **c)** Averaged total cell number and contribution to the TE and ICM blastocyst cell lineages, based on relative spatial location in each of the stated experimental conditions. Errors are represented as s.e.m. and appropriate statistically significant differences, derived from 2-tailed students t-tests, highlighted by one or two significance markers (\*/\$ p<0.05 and \*\*/\$\$ denoting p<0.005). **d)** Averaged contribution of cells to each ICM cell lineage, based on exclusive expression of either EPI (Nanog) or PrE (Gata4) lineage marker (or both or neither marker), in each of the stated experimental conditions. s.e.m and statistical significance numbers as in **c)**. All data used to prepare this figure are described in appendix tables T5.

---

when the proportional effect is considered, the phenotype is stronger in regard to PrE than EPI (*i.e.* despite exhibiting smaller ICMs the percentage of EPI cells within Mapk14/11 inhibited blastocyst ICMs is largely maintained, whereas the percentage of PrE cells is reduced; figure 8c). Indeed, when plotted as a function of overall ICM cell size (Figure 13), the number of Gata6-alone positive (*i.e.* PrE), cells in p38-Mapk14/11 inhibited E4.5 blastocysts are clearly underrepresented compared to controls whereas there is no difference in the representation of Nanog-alone positive (*i.e.* EPI) cells. Moreover, there is a consistent overrepresentation of uncommitted Nanog/Gata6 positive cells in such ICMs. Thus, these data demonstrate that whilst p38-Mapk14/11 inhibited blastocysts do on average present with smaller ICMs (under the SB220025 inhibitor conditions), accounting for fewer EPI cells, there is also a profound block in the commitment of cells to differentiate to PrE that is independent of this effect and reflected in the increased number/ proportion of uncommitted ICM

cells (co-expressing Nanog and Gata6; as described above). The possible reason for the observed reduced ICM numbers in p38-Mapk14/11 inhibited blastocysts is described in the unpublished data results section (relating to an identified anti-oxidant role of p38-Mapk14/11) and could arise from reduced cell proliferation and/ or increased apoptosis, potentially of uncommitted cells. Indeed immuno-fluorescent staining for cleaved caspase 3 indicates significantly elevated levels of apoptosis in p38-Mapk14/11 inhibited embryos versus vehicle controls (figure 14) that could account for this difference.

Therefore, in summary, it is concluded that p38-Mapk14/11 activity is required during blastocyst ICM maturation to promote appropriate differentiation of the PrE by participating in the resolution of the uncommitted state by which cells co-express the EPI marker Nanog and the early PrE marker Gata6 (*i.e.* the formation of the salt and pepper pattern of mutually exclusive EPI and PrE marker expression – see introduction).

## **5.2 p38-Mapk14/11 activity is required during the early stages of blastocyst maturation to permit uncommitted cells to initiate PrE differentiation.**

As described in the introduction, the role of active Mek1/2 during PrE differentiation in the ICM has been well characterised. Indeed, pharmacological experiments investigating the developmental timing of Mek1/2 requirement, albeit in combination with concomitant Fgf-receptor (Fgfr) inhibition, demonstrate a developmental plasticity of ICM cells up to a point between E4.0 and E4.5, when cell-fate becomes irreversibly committed (*i.e.* the inhibitor treatment is no longer able to convert, nearly all, ICM cells to an EPI fate) (Yamanaka *et al.* 2010). Accordingly, in a similar manner the temporal requirement for p38-Mapk14/11 activity was assayed, during PrE formation, and directly compared with that for active Mek1/2 (assayed by targeting Mek1/2 alone, as in Nichols *et al.* 2009, and not in combination with Fgfr inhibition, as previously described; Yamanaka *et al.* 2010). Therefore, a series of experiments were conducted in which embryos were *in vitro* cultured to the late blastocyst (E4.5) stage in the presence of either p38-Mapk14/11 (SB220025) or Mek1/2 (PD0325901) inhibitor, from either the early blastocyst (E3.5) (as previously assayed for p38-Mapk14/11 inhibition – see figure 8, 9, 12, 13 & 14), E3.75 or mid blastocyst (E4.0) stages and assayed for EPI (Nanog) and late PrE (Gata4) lineage marker expression within the ICM (*n.b.* Gata4 marker was selected to ensure only specified PrE was assayed). An additional condition in which embryos were cultured in the presence of inhibitor from E3.5 to E4.0 and then returned into normal growth media for continued culture until the assayed late blastocyst (E4.5) stage was also included (*i.e.* an experimental condition assaying the potential reversibility of inhibitor induced phenotypes), as were control conditions for all inhibitor permutations in which embryos were exposed to appropriate concentrations of vehicle control

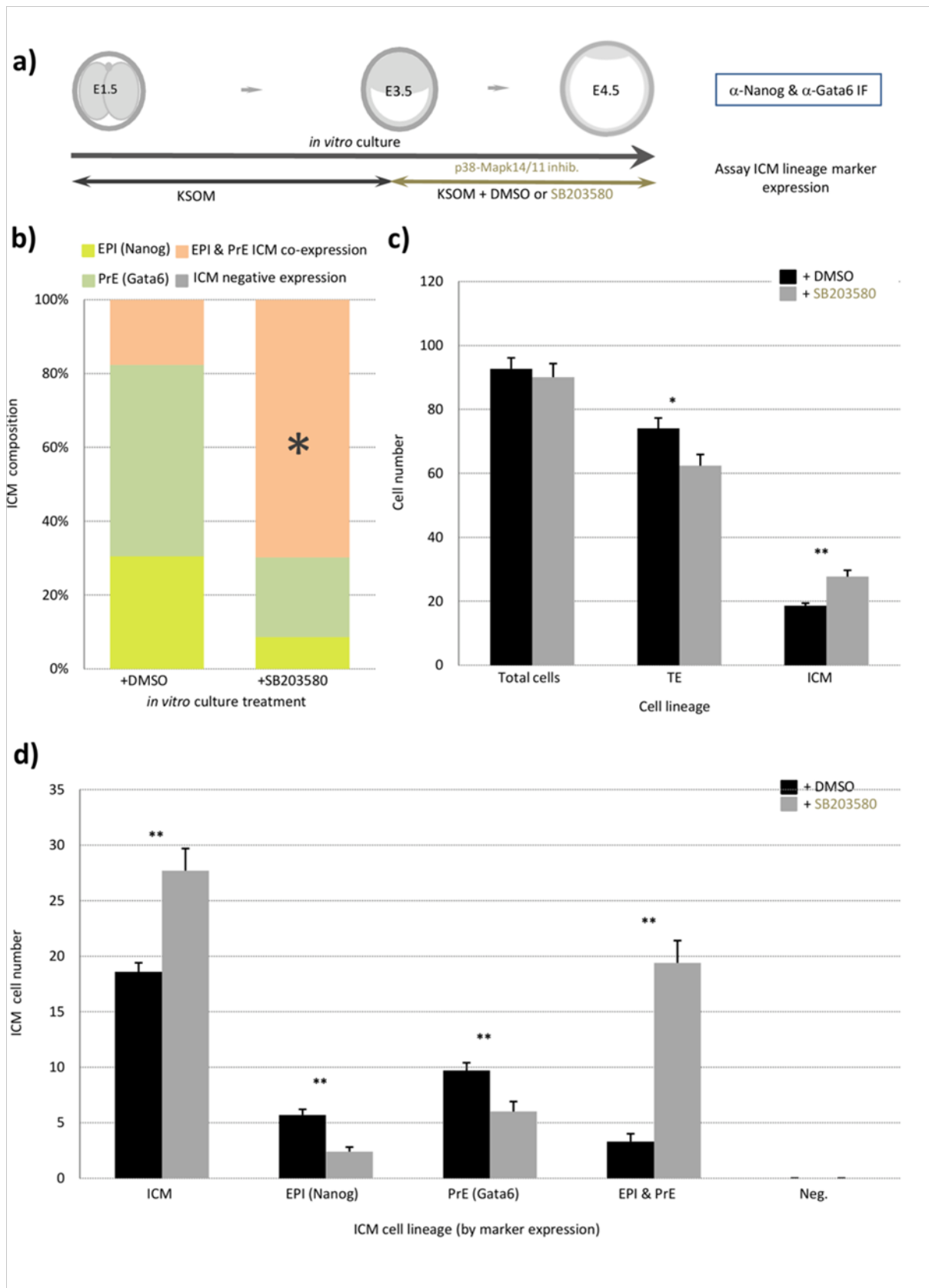
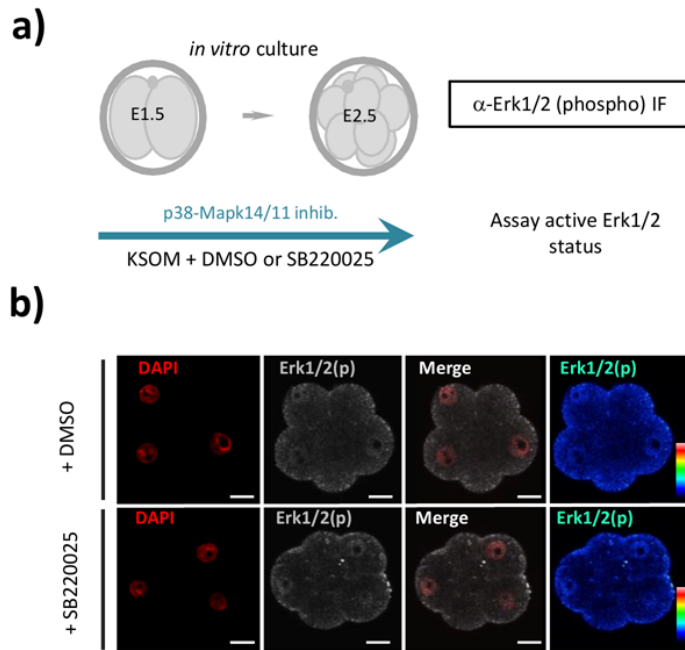


Figure 11. (legend overleaf)

**Figure 11: The alternative p38-Mapk14/11 inhibitor SB203580 also causes increased number of uncommitted ICM cells expressing both EPI (Nanog) and early PrE (Gata6) markers (when administered from E3.5 to E4.5)** **a)** Experimental schema detailing the regime of p38-Mapk14/11 inhibition (+SB203580, 20 $\mu$ M), with attendant vehicle control (+DMSO) condition, from the early to late blastocyst (E3.5-E4.5) stages employed. Immuno-fluorescence (IF) antibody details used to analyse ICM cell lineage marker protein expression in late blastocysts (E4.5) are also given (*n.b.* Gata6 used as PrE marker). **b)** Averaged percentage makeup of the ICMs of each stated condition in relation to each specified ICM lineage; EPI or PrE (yellow and green, exclusively immuno-stained for either Nanog or Gata6, respectively), EPI & PrE co-expressing cells (orange, representing cells uncommitted to either lineage) and cells negative for either studied lineage marker (grey). Asterisk denotes the increased percentage contribution of uncommitted ICM cells (expressing both Nanog and Gata6) in SB203580 treated embryos versus +DMSO vehicle control. In the +DMSO treated group n=12 and in the +SB203580 p38-Mapk14/11 inhibition group n=14. **c)** Averaged total cell number and contribution to the TE and ICM blastocyst cell lineages, based on relative spatial location in each of the stated experimental conditions. Errors are represented as s.e.m. and appropriate statistically significant differences, derived from 2-tailed students t-tests, highlighted by one or two significance markers (\* p<0.05 and \*\* denoting p<0.005). **d)** Averaged contribution of cells to each ICM cell lineage, based on exclusive expression of either EPI (Nanog) or PrE (Gata4) lineage marker (or both or neither marker), in each of the stated experimental conditions; s.e.m and statistical significance numbers in **c)**. All data used to prepare this figure are described in appendix tables T6.

---

DMSO (figure 15). Consistent with the previous experiments (figure 8), the study found that p38-Mapk14/11 inhibition from E3.5 to E4.5 was again associated with a profound, although not entirely penetrant, block in PrE formation (also associated with an increased number/proportion of Nanog-alone positive 'EPI-like' cells; represented by an average 11.2% PrE and 81.1% EPI-like make up, the remaining ICM cells either co-expressing or negative for the assayed proteins). The identical treatment regime targeting Mek1/2 resulted in near 100% conversion of all ICM cells to Nanog-alone expression status, with virtually no evidence of Gata4 expression (on average yielding 1.0% PrE and 97.4% EPI-like ICM cell contribution); in marked similarity to previously reported data inhibiting Mek1/2 (plus Fgfr) from E2.5 to E4.5 (Yamanaka *et al.* 2010). Whilst both treatments highlight the requirement for both p38-Mapk14/11 and Mek1/2 activity during the appropriate derivation of PrE, the latter results suggest that Mek1/2 activity has a more profound effect than p38-Mapk14/11, at least at the inhibitor concentrations used. Thus, the data suggest that even in the presence of normal levels of activated p38-Mapk14/11, inhibition of Mek1/2 is sufficient to block PrE differentiation;



**Figure 12: Treatment of embryos with the p38-Mapk14/11 inhibitor SB220025 does not alter the levels of detectable activated phospho-Erk1/2 [Erk1/2 (p)].** **a)** Experimental schema by which 2-cell (E1.5) stage embryos were *in vitro* cultured to the 8-cell (E2.5) stage in control (+DMSO) or p38-Mapk14/11 inhibitor (+SB220025) treated media, fixed and immuno-fluorescently (IF) stained for activated Erk1/2(p). **b)** Representative central confocal z-plane sections of (IF) stained embryos from each group. Erk1/2(p) signal is shown in both grey and spectral pixel intensity palettes and red pseudo-coloured DAPI DNA counterstain is also provided (merged and unmerged images shown). Scale bar = 15 $\mu$ m.

whereas even if the p38-Mapk14/11 pathway is inhibited some PrE differentiation, potentially driven by active Mek1/2 is able to occur. PD0325901 treated, Mek1/2 inhibited, embryos remained sensitive to Mek1/2 inhibition administered from E3.75 or E4.0, leading to appreciable and statistically significantly increased levels of EPI conversion, compared with vehicle control ( $p = 7.00^{E-7}$  and  $1.91^{E-8}$ , respectively); as represented by the respective averaged PrE and EPI percentage contributions of 6.1% and 91.9% in embryos treated from E3.75 and 9.1% and 87.4% in group treated from E4.0 (*n.b.* some Gata4-alone positive and lineage marker co-expressing ICM cells did appear, in these latter two treatment conditions, suggesting some cells had already committed, or begun commitment, to PrE fate before the inhibitor was provided). However, the administration of p38-Mapk14/11 inhibitor (SB220025) after E3.75 had no significant effect on ICM cell lineage specification/ segregation, when compared with appropriate DMSO treated control embryos; for

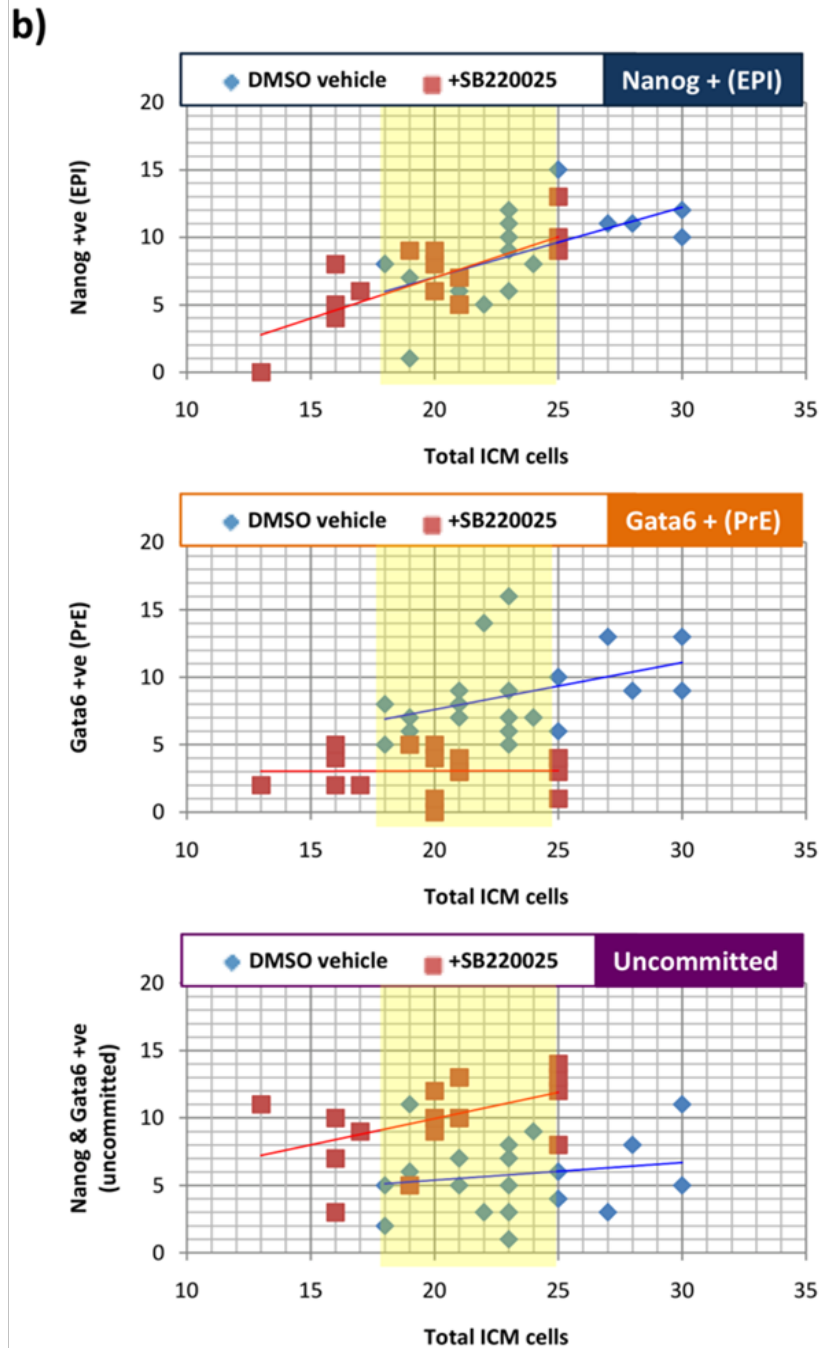
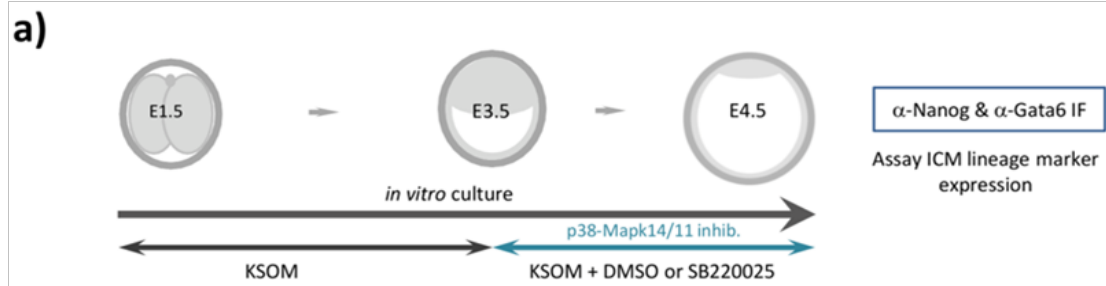


Figure 13. (legend overleaf)

**Figure 13: The reduction in PrE cells induced by p38-Mapk14/11 (+SB220025) inhibition is not due to a general and temporal delay in ICM cell-fate separation, despite smaller total ICM cell number.**

**a)** Experimental schema of the blastocyst maturation (E3.5–E4.5) p38-Mapk14/11 inhibition (+SB220025, n=15), plus vehicle control (+DMSO, n=14), strategy employed and the immunofluorescent (IF) staining regime used to assay resulting individual ICM cell-fates; cells exhibiting exclusive Nanog or Gata6 expression being designated EPI and PrE, respectively, and those expressing both markers denoted as uncommitted to either cell lineage. **b)** Three x versus y scatter plots, detailing the number of cells immuno-staining positive for either Nanog (EPI) or Gata6 (PrE) alone (upper-blue and central-orange plots, respectively) or both markers (representing uncommitted cells, lower-purple plot) per embryo, as a function of total ICM cell number in control (+DMSO vehicle; blue diamonds) and p38-Mapk14/11 inhibited (+SB220025; red square) groups. Trend lines (blue for control and red for p38-Mapk14/11 inhibited embryo groups), plus regions where the two datasets overlap in terms of total ICM cell number (yellow shaded highlights) are also shown to aid interpretation. Note, that despite p38-Mapk14/11 inhibited embryos on average presenting fewer ICM cells (see figure 8 and figure 9), they still constitute a number of EPI cells appropriate to this size, whereas they contain disproportionately fewer PrE cells and more uncommitted cells; hence the deficit in mature PrE cells observed after p38-Mapk14/11 inhibition (see figure 8 and figure 9) cannot simply be a function of generally delayed development, as EPI cells have segregated, but is indicative of a block in the maturation of the PrE lineage.

---

example the PrE and EPI percentage contributions in embryo groups treated from E3.75 to E4.5 were 37.6% and 53.7% for DMSO controls and 34.0% and 52.1% for p38-Mapk14/11 inhibited embryos.

These results suggest that the developmental window at which p38-Mapk14/11 activity is required for appropriate PrE differentiation is before E3.75 (*i.e.* in the context of the experiment it is between E3.5 and E3.75, but as it is not possible to study the effect of p38-Mapk14/11 inhibition on PrE differentiation by providing the inhibitor before E3.5, due to the induced morula to blastocyst arrest, see figure 7, it could start before E3.5), whereas the Mek1/2 inhibition sensitive window extends beyond E4.0; again in agreement with previous studies (Yamanaka *et al.* 2010). This conclusion was confirmed when embryos that had been exposed to inhibitor treatment from E3.5 to E4.0 and then transferred back to normal growth media were assayed. In such embryos exposed to a pulse of p38-Mapk14/11 inhibition, the classically observed PrE deficit (*i.e.* as achieved when inhibiting continuously from E3.5 to E4.5) was still robustly and statistically significantly evident; the averaged percentage ICM contribution of PrE cells was 12.6% versus 42.2% in similarly treated DMSO

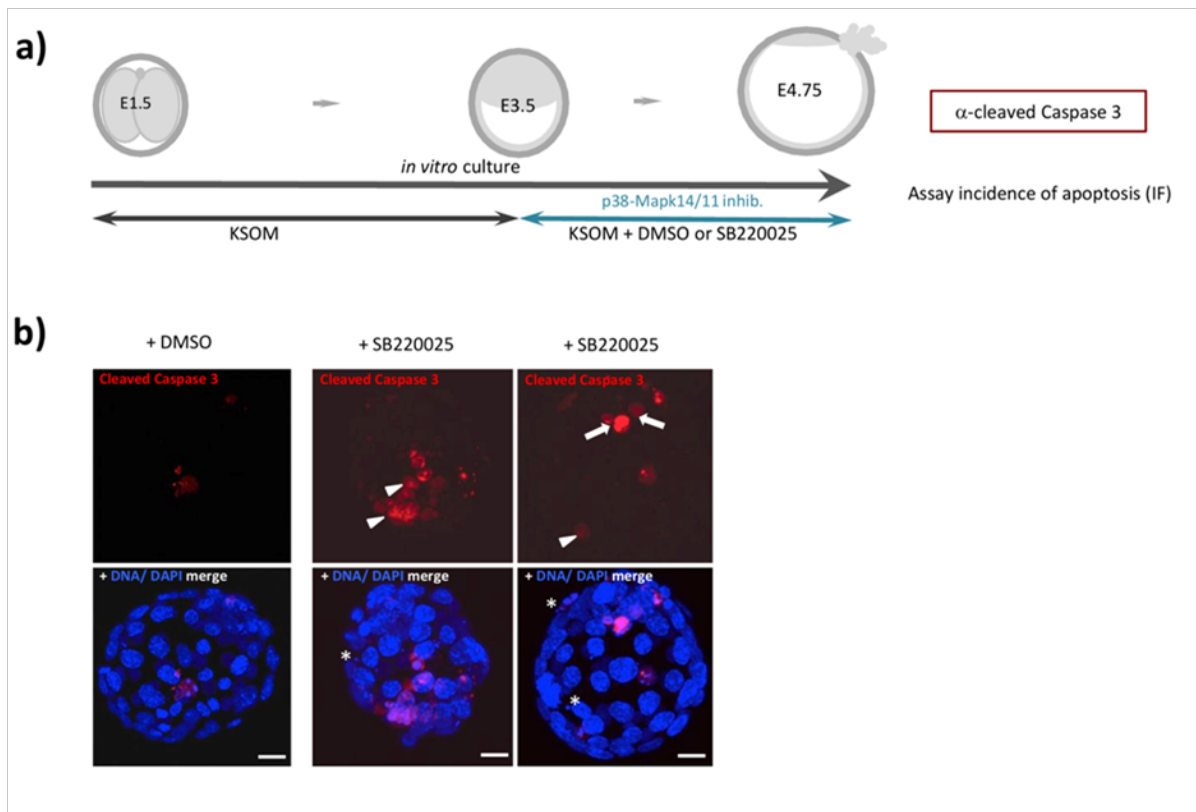


**Figure 14: p38-Mapk14/11 inhibition (+SB220025) during blastocyst maturation is associated with increased incidence of apoptosis in both TE and ICM cells. a)** Experimental schema by which recovered 2-cell (E1.5) stage embryos were *in vitro* cultured until the early blastocyst (E3.5) stage and transferred into media containing p38-Mapk14/11 inhibitor (+SB220025) or vehicle control (+DMSO) and further cultured to the late/ hatching blastocyst (E4.75) stage. Embryos were fixed and immuno-fluorescently stained with anti-cleaved caspase 3 (an intracellular marker of activated apoptosis) antibody for confocal microscopy-based assay of the incidence of apoptosis. **b)** Exemplar confocal z-plane projections of control (+DMSO) and p38-Mapk14/11 inhibitor treated (+SB220025) blastocysts; cleaved caspase signal in red and DNA DAPI counterstain in blue. Arrows and arrowheads highlight apoptotic cells, positive for cleaved caspase 3, in the outer TE and ICM cells, respectively, of p38-Mapk14/11 inhibited embryos. Asterisks in +DNA/DAPI merge micrographs highlight apoptotic bodies in p38-Mapk14/11 inhibited embryos, that are not positive for cleaved caspase 3 immuno-staining. Scale bar = 15µm.

control groups ( $p = 1.10^{-8}$ ). However, in embryos treated with a pulse of Mek1/2 inhibition, the number of Nanog-alone (EPI) and Gata4-alone (PrE) cells (plus co-expressing cells and cells negative for expression of either marker) were statistically equivalent to DMSO vehicle control treated embryos; indicative of the reversible and plastic nature of Mek1/2 driven PrE differentiation, not

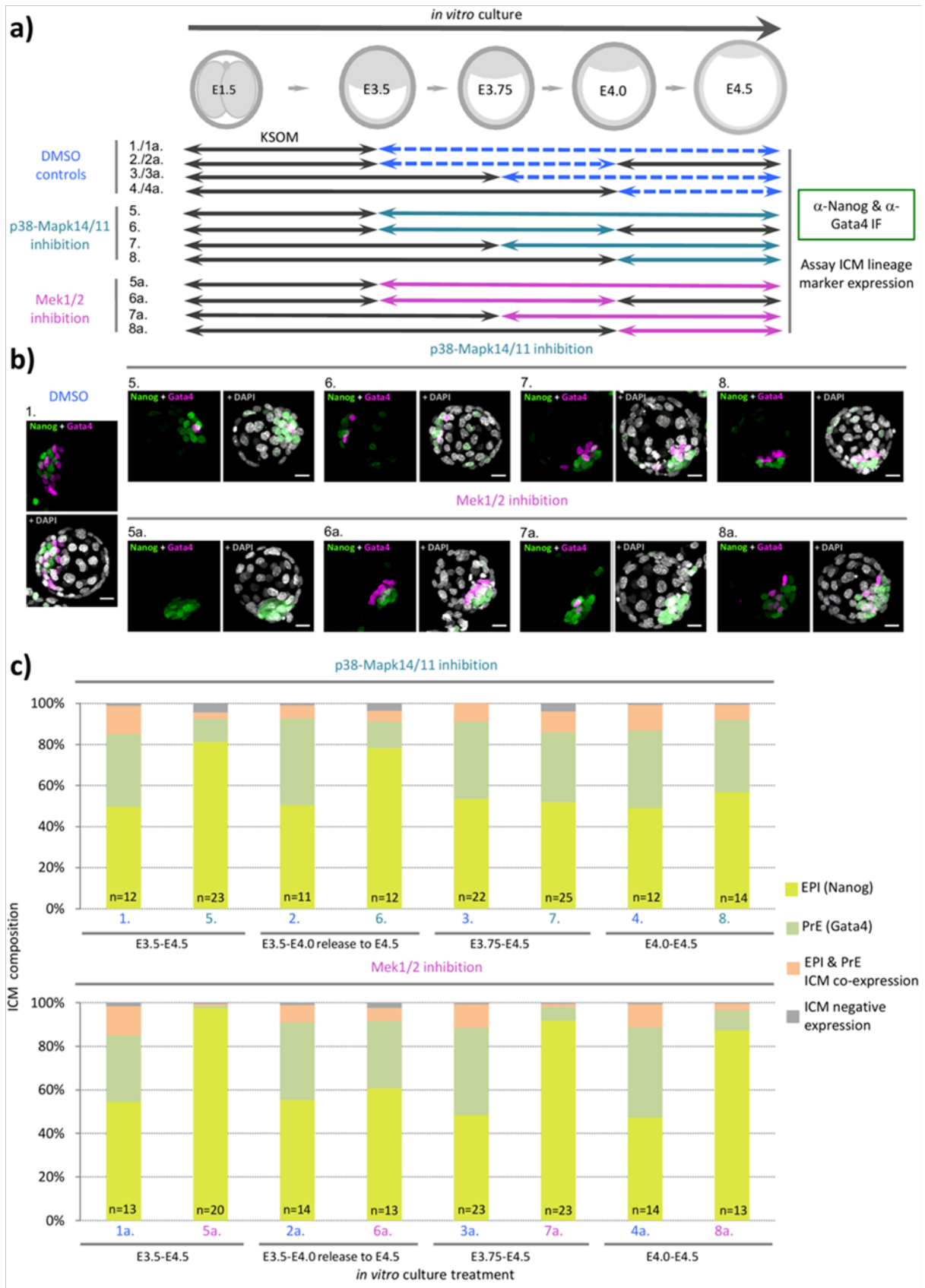


Figure 15. (legend overleaf)

**Figure 15: p38-Mapk14/11 is required for appropriate PrE derivation during early blastocyst maturation and precedes Mek1/2 mediated PrE differentiation.** **a)** Experimental schema employed to identify the developmental time-point at which p38-Mapk14/11 is required for PrE differentiation, compared to Mek1/2 activity. 2-cell (E1.5) stage embryos were *in vitro* cultured to varied blastocyst stages (ranging from E3.5 to E4.0, as indicated) and transferred into media supplemented with either p38-Mapk14/11 inhibitor (+SB220025) or Mek1/2 inhibitor (+PD0325901) or +DMSO vehicle controls (note that the required concentrations of DMSO to control the p38-Mapk14/11 and Mek1/2 inhibition were not the same; hence the nomenclature of DMSO controls relating to Mek1/2 inhibition is suffixed here, and throughout the figure, with 'a'). Embryos were then cultured to the late-blastocyst (E4.5) stage and fixed for immuno-fluorescent (IF) staining against the ICM cell lineage markers Nanog and Gata4. Note that a second embryo group transferred at the early-blastocyst (E3.5) stage was removed from vehicle control/ inhibitor treatment at the mid-blastocyst (E4.0) stage and returned to normal growth media before being similarly processed at the late-blastocyst (E4.5) stage. **b)** Representative examples of immuno-fluorescently stained embryos as projected confocal z-stacks, from each of the above described treatment regimes [in **a**]; note the consistent use of nomenclature (for ease of presentation only one example of a DMSO-treated embryo is provided). Pseudo-coloured merges of detected Nanog (green) and Gata4 (magenta) protein are provided together with a further merge containing DAPI-derived DNA counterstain (pseudo-coloured white). Scale bar = 15µm. **c)** Percentage bar charts detailing the averaged relative cell lineage composition of ICMs from embryos derived from each of the above described treatment regimes [in **a**] note the consistent use of nomenclature (and the change in the order of the treatments – for ease of interpretation DMSO vehicle control embryos are labelled in blue, p38-Mapk14/11 inhibited embryos in sea green and Mek1/2 inhibited embryos in magenta). The averaged percentage contribution of ICM cells to each lineage, within the chart, is highlighted; EPI (yellow), PrE (Green), EPI & PrE ICM co-expression (orange) and ICM negative expression (grey). The number of embryos analysed in each group is highlighted within each percentage bar. All individual embryo data used in the preparation of this figure are contained within appendix tables T7 and T8.

---

shared by p38-Mapk14/11. Therefore, these data demonstrate a requirement for active p38-Mapk14/11 mediated signalling during the earliest stages of blastocyst ICM maturation that is needed to appropriately derive the PrE and EPI cell lineages.

Given the findings that germline differentiation of the PrE is not sensitive to p38-Mapk14/11 inhibition subsequent to the E3.75 stage (figure 15), the stage at which the salt and pepper pattern

of EPI and PrE marker expression begins to resolve (Chazaud *et al.* 2006; Niakan *et al.* 2010; Plusa *et al.* 2008), and that the ICMs of blastocysts *in vitro* cultured in the presence of p38-Mapk14/11 inhibitor from E3.5 to E4.5 display significantly increased numbers/ proportions of Nanog positive and Gata6 positive uncommitted co-expressing cells (figure 8 and figure 11), it was hypothesised that p38-Mapk14/11 inhibition during the sensitive window would also result in significantly increased levels of uncommitted ICM cells. Therefore early blastocysts were treated from E3.5 until E4.0 with either p38-Mapk14/11 or Mek1/2 inhibitor and then fixed and immuno-fluorescently stained for Nanog and Sox17 (figure 16). The DMSO vehicle control treated embryo ICMs contained a substantial number/ proportion of Nanog and Sox17 co-expressing uncommitted cells (representing an average of 39.7% of ICM cells, between the two control groups), appropriate to the temporal mid-point of blastocyst maturation (*n.b.* in relation to p38-Mapk14/11 and Mek1/2 inhibitor treated blastocysts groups different concentrations of DMSO vehicle control were administered). However, the number/ proportion of similarly uncommitted cells observed in the p38-Mapk14/11 group was significantly increased (to 76.7% of all ICM cells,  $p = 1.23^{E-3}$ ), mostly at the expense of specified EPI (*i.e.* Nanog-alone expressing) but also specified PrE (*i.e.* Sox17-alone expressing) cells, whilst there were no uncommitted cell differences in Mek1/2 inhibited embryo ICMs, despite the fact the number/ proportion of EPI and PrE specified cells was respectively increased (to an ICM average contribution of 60.2% from 48.3%) and decreased (to 7.6% from 20.4%). Furthermore, p38-Mapk14/11 inhibition does not alter detectable levels of activated Erk1/2(p) (figure 12) or Mek1/2 inhibition does not affect activated phosphorylated-p38-Mapk14/11 [p38-Mapk14/11(p)] levels (figure 17) thereby excluding cross-reactivity effects of the chemical inhibitors used. Therefore the data is interpreted as p38-Mapk14/11 supporting a relatively early role in facilitating the resolution of uncommitted ICM cells and a role for Mek1/2 in driving PrE differentiation (without itself affecting the fate resolution of uncommitted ICM cells), that is subsequent to, or concomitant with, the emergence of the salt and pepper expression pattern of ICM lineage markers.

### **5.3 Fgf-receptor (Fgfr) mediated cell signalling and the activation of the non-canonically activated Bmp-related kinase Tak1, functionally activates p38-Mapk14/11 during PrE derivation.**

As previously discussed, the role of Fgf-ligands in the specification of the PrE cell lineage is well described (Frankenberg *et al.* 2011; Kang *et al.* 2013; Nichols *et al.* 2009; Yamanaka *et al.* 2010). It was therefore decided to assay if Fgfr mediated cell signalling during specification of the PrE was acting, in part, via the activation of p38-Mapk14/11, as has recently been shown during TE specification (Yang *et al.* 2015). Accordingly, the well-characterised and specific chemical inhibitor, SU5402 (SU5402 inhibits Fgfr1 and Fgfr3, Sun *et al.* 1999), that has been widely used in preimplantation mouse embryo studies (Guo *et al.* 2010; Nichols *et al.* 2009) to functionally block

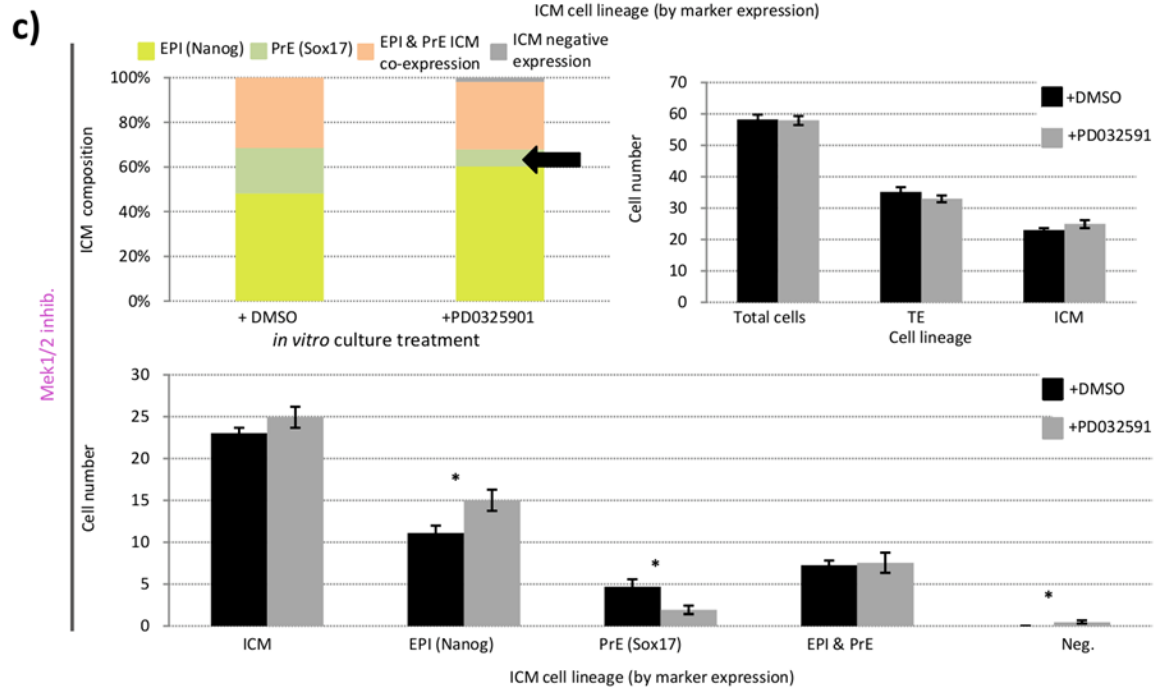
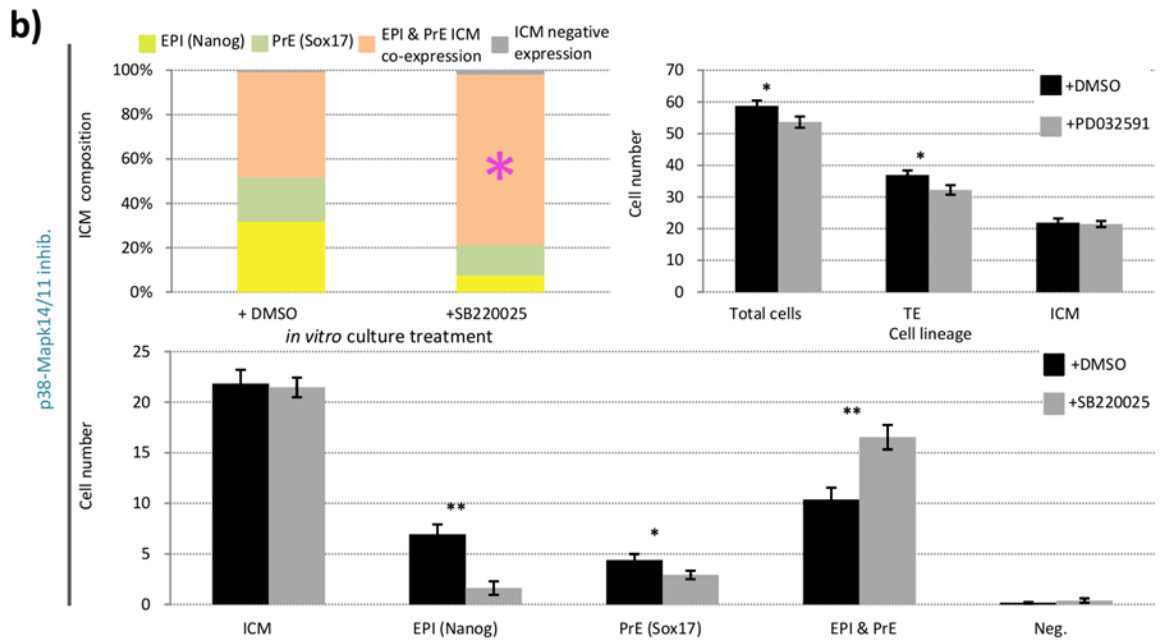
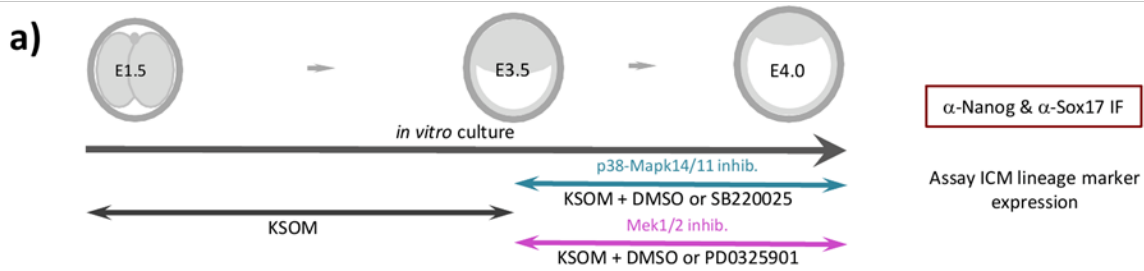
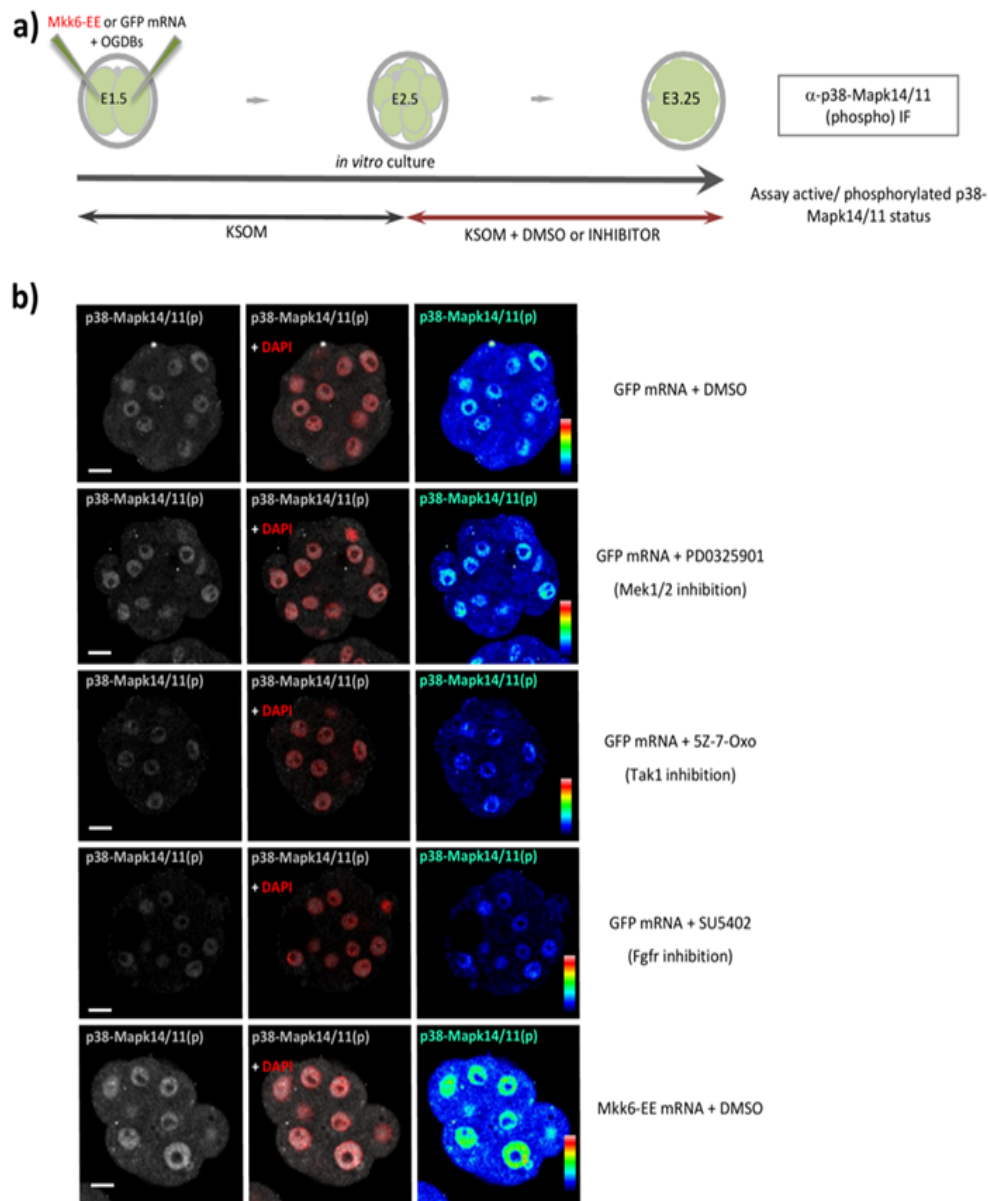


Figure 16. (legend overleaf)

**Figure 16: p38-Mapk14/11 inhibition during early blastocyst maturation produces ICM cells of uncommitted fate, whereas Mek1/2 inhibition prevents differentiation to the PrE lineage. a)** Experimental schema employed to study the effect on ICM lineage separation of p38-Mapk14/11 and Mek1/2 inhibition during early blastocyst maturation. Cultured embryos were transferred to growth media supplemented with vehicle control (+DMSO; note two concentration used depending on the specific inhibitor to be used – see below) or inhibitor against p38-Mapk14/11 (+SB220025) or Mek1/2 (+PD0325901) and permitted to develop to the mid-blastocyst (E4.0) stage, fixed and immuno-fluorescently (IF) stained for EPI (Nanog) and PrE (Sox17) marker proteins. **b)** Relating to p38-Mapk14/11 inhibition (n=13 and 13 for control and inhibitor treated groups, respectively), and **c)** relating to Mek1/2 inhibition experiments (n=12 and 13 for control and inhibitor treated groups, respectively); percentage bar charts showing the relative contribution of ICM cells to respective lineages (EPI in yellow, PrE in green, uncommitted cells expressing both EPI and PrE markers in orange and cells not expressing either marker in grey). Note, decreased maturation of EPI and PrE in p38-Mapk14/11 inhibited embryos is due to increased proportion of uncommitted cells (highlighted by magenta asterisk), whereas in Mek1/2 inhibited embryos the proportion of uncommitted cells is no different to controls but the contribution of solely *Sox17* expressing PrE cells is diminished (highlighted by black arrow) and solely *Nanog* expressing EPI cells is increased. The average number of cells in each treatment and accompanying control regime, contributing to total embryo cell number, outer TE and inner ICM lineages are shown as bar charts, as is the average number of cells in each ICM lineage. Errors are representative of s.e.m. and \* and \*\* denote statistical significant differences in cell number between the vehicle control (black bars) and p38-Mapk14/11 or Mek1/2 inhibited (grey bars) embryo groups, according to 2-tailed students t-test, with p<0.05 and p<0.005 confidence intervals, respectively. All individual embryo data used in the preparation of this figure are contained within appendix tables T9 and T10.

---

Fgfr was utilised and p38-Mapk14/11 dependent PrE phenotypes were assayed. Treatment of *in vitro* cultured embryos from the 8-cell (E2.5) to the late morula (E3.25) stage with SU5402 revealed reduced levels of activated p38-Mapk14/11(p), as detected by confocal microscopy based immuno-fluorescent staining (see figure 17), confirming p38-Mapk14/11 activation is susceptible to Fgfr mediated cell signalling levels in the preimplantation mouse embryo. Next using identical inhibitor regimes to those previously described for SU5402 (Guo *et al.* 2010), confirmation that Fgfr inhibition results in defective PrE formation and was sought and further assays performed to ascertain if any component of this phenotype was dependent on active p38-Mapk14/11 were undertaken. Therefore, isolated 2-cell (E1.5) stage embryos were microinjected, in both blastomeres, with



**Figure 17: Activated phospho-p38-Mapk14/11 [p38-Mapk14/11(p)] levels in late morula (E3.25) stage embryos, following over-expression of the constitutive active p38-Mapk14/11 targeting Map2k kinase, ‘Mkk6-EE’ mutant or incubation in various specific and relevant chemical inhibitors.**

**a)** Experimental scheme describing how 2-cell (E1.5) stage embryos were microinjected in both blastomeres with Oregon-green conjugated dextran beads (as an injection marker control) and either control GFP or constitutively active mutant Mkk6-EE mRNA, and *in vitro* cultured until the 8-cell (E2.5) stage. GFP microinjected embryos were then transferred into growth media supplemented with either Mek1/2 (+PD0325901), Tak1 (+5Z-7-Oxo) or Fgfr (+SU5402) specific inhibitors, or vehicle control (+DMSO), whereas Mkk6-EE microinjected embryos were only transferred into media supplemented with control DMSO. All embryo groups were then further cultured until the late morula (E3.25) stage, before being fixed and processed for immuno-fluorescent (IF) staining using an

antibody specific to activated phospho-p38-Mapk14/11 [p38-Mapk14/11(p)]. Therefore the effect of the various chemical inhibitions and Mkk6-EE over-expression on activated p38-Mapk14/11(p) levels could be appropriately assayed against the same GFP microinjected and DMSO exposed control embryos. **b)** Representative single central z-plane confocal sections of immuno-fluorescently (IF) stained embryos [as described in **a)**]. Activated p38-Mapk14/11(p) staining shown in a spectral pixel intensity scale (on right), in grey-scale (on left) or merged with red pseudo-coloured DAPI derived DNA counterstain (central panels). Note all images of central z-plane sections were acquired using the same confocal microscopy settings. Scale bar = 15 $\mu$ m.

---

recombinant control GFP mRNA or transcript for a constitutively active form of the p38- Mapk14/11 targeting and activating (Map2k) kinase, Mkk6, also known as Map2k6 (*n.b.* Oregon-green conjugated dextran beads/OGDBs were also microinjected to confirm construct delivery). The mutant, mouse sequence derived, Mkk6 kinase contained two phospho-mimetic amino acid substitutions, S207E and T211E (and was thus designated Mkk6-EE) and when expressed in the preimplantation mouse embryo resulted in increased activated p38-Mapk14/11(p) levels (figure 17) without effecting activated Erk1/2(p) levels (figure 18); moreover, extensive structural and biochemical studies have confirmed that Mkk6 specifically targets all p38-Mapks (and preferentially targets p38-Mapk14/11) and does not effect extracellular signal-regulated kinases (*e.g.* Erk1/2 and Erk5) or c-Jun N-terminal kinase (Jnk) substrates (Han *et al.* 1996; Stein *et al.* 1996). Microinjected embryos, from each group, were then cultured until the 16-cell (E3.0) stage and transferred into media containing either Fgfr inhibitor (+ SU5402) or vehicle control (+DMSO) and further cultured until the late blastocyst (E4.5) stage. An additional group of Mkk6-EE microinjected and SU5402 treated embryos were subject to an extra experimental step, whereby the Fgfr inhibitor containing media was further supplemented with p38-Mapk14/11 inhibitor (+SB220025) at the early blastocyst (E3.5) stage, before continued culture to the late blastocyst (E4.5) stage. ICM cell lineage derivation was then determined in each experimental and control group by confocal microscopy-based immuno-fluorescent staining for Nanog (as an EPI marker) and Gata4 (as a late PrE marker). As can be seen (figure 19) the treatment of GFP microinjected control embryos with Fgfr inhibitor caused a statistically significant decrease and increase in the number/ proportion of derived PrE (from an averaged ICM percentage contribution of 34.7% in DMSO treated controls to 9.6%,  $p = 8.08^{E-10}$ ) and EPI (from 57.4% to 82.3%,  $p = 1.18^{E-2}$ ), respectively, without significantly altering overall ICM cell number; a phenotype in agreement with previous studies (Guo *et al.* 2010; Nichols *et al.* 2009). Strikingly, this Fgfr inhibitor mediated PrE deficit phenotype could be largely rescued, in terms of total PrE cell number and the proportion of PrE specified ICM cells (increasing to an ICM contribution

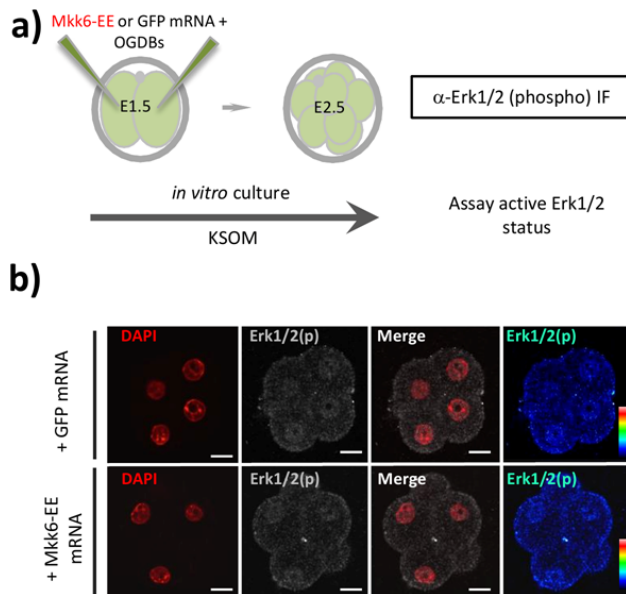


**Figure 18: Over-expression of the constitutively active p38-Mapk14/11 targeting Map2k kinase. Mkk6-EE mutant in preimplantation stage mouse embryos does not alter activated phospho-Erk1/2 [Erk1/2(p)] levels. a)** Experimental scheme describing how 2-cell (E1.5) stage embryos were microinjected in both blastomeres with Oregon-green conjugated dextran beads (OGDBs, as an injection marker control) and either control GFP or constitutively active mutant Mkk6-EE mRNA, were *in vitro* cultured until the 8-cell (E2.5) stage, fixed and processed for immuno-fluorescent (IF) staining using an antibody specific to activated phospho-Erk1/2 [Erk1/2(p)]. **b)** Representative central single z-plane confocal sections of immuno-fluorescently (IF) stained embryos [as described in **a)** and indicated]. Activated Erk1/2(p) staining shown in a spectral pixel intensity scale (far right panels), in grey-scale (panels second from left) or in grey-scale merged with red pseudo-coloured DAPI derived DNA counterstain (panels second from right). DAPI derived DNA staining alone is also shown (far left panels) Note all images of central z-plane sections were acquired using the same confocal microscopy settings. Scale bar = 15 $\mu$ m.

of 48.8%,  $p = 5.28^{E-5}$ ), by the over-expression of the Mkk6-EE construct; albeit Mkk6-EE microinjected embryos presented with fewer total and ICM cells (compared to GFP microinjected controls). This result suggests that p38-Mapk14/11 is functionally activated downstream of Fgfr mediated PrE specification, indeed expression of the Mkk6-EE construct in DMSO vehicle control embryos alone was enough to result in 74.5% of derived ICM cells to adopt a PrE fate. This interpretation is confirmed by the fact that when Fgfr inhibited and Mkk6-EE microinjected embryos were subject to additional p38-Mapk14/11 inhibition, the PrE rescue effect of Mkk6-EE expression was completely

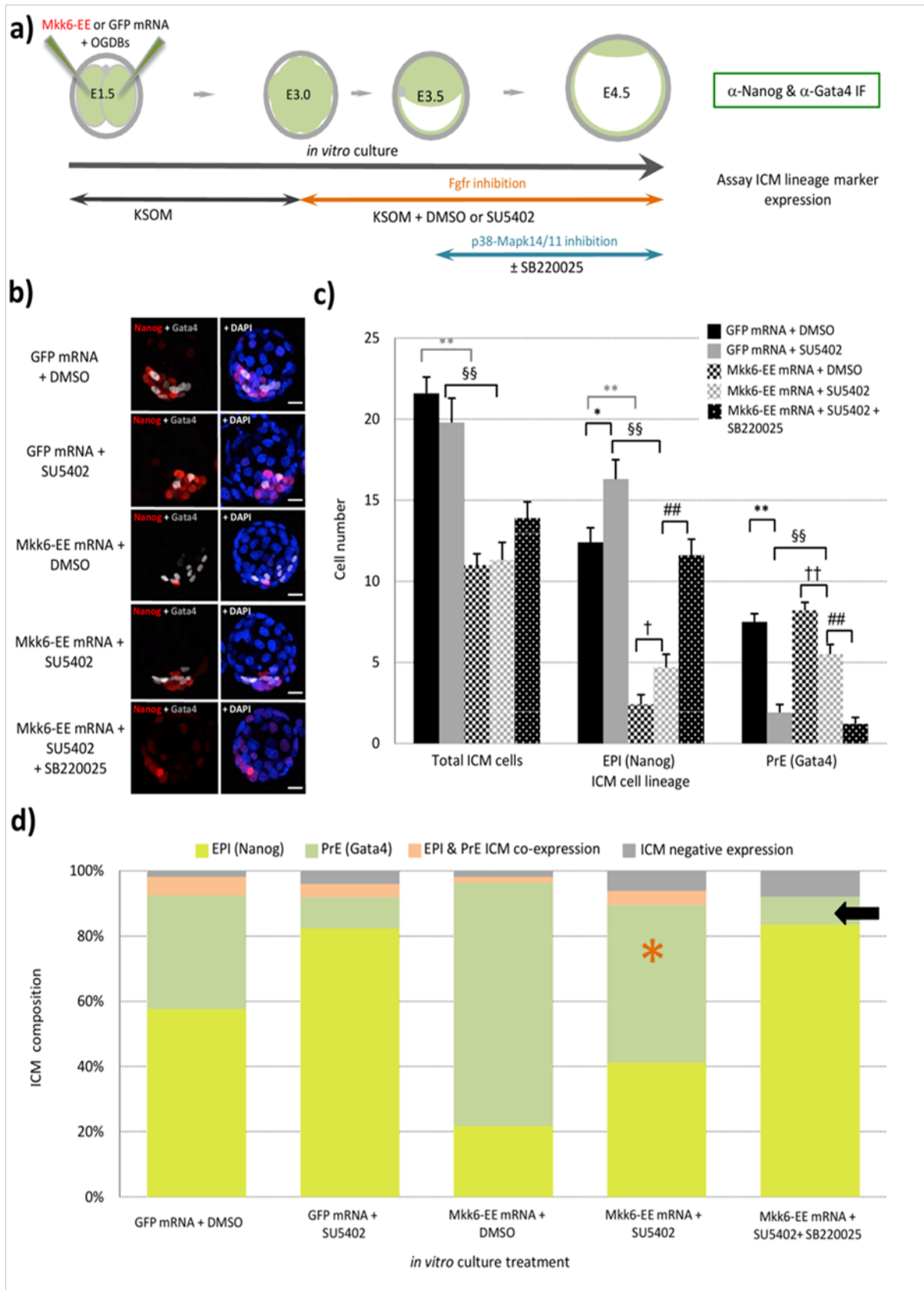


Figure 19. (legend overleaf)

**Figure 19. Inhibition of Fgf-receptors (Fgfr) inhibits PrE formation in a p38-Mapk14/11 dependent manner.** **a)** Experimental schema detailing the regime of Fgf-receptor (Fgfr) inhibition (+SU5402), with attendant vehicle control (+DMSO) condition, from the 16-cell to late blastocyst (E3.0-E4.5) stages and optional p38-Mapk14/11 co-inhibition ( $\pm$ SB220025, from E3.5-E4.5), employed. Also highlighted are mRNAs microinjected (together with Oregon-green conjugated dextran beads/OGDBs, to confirm successful mRNA delivery) into both blastomeres at the 2-cell (E1.5) stage; the constitutive active, p38-Mapk14/11 targeting Map2k kinase, 'Mkk6-EE' mutant or microinjection control 'GFP'. Immuno-fluorescence (IF) antibody details used to analyse ICM cell lineage marker protein expression in late blastocysts (E4.5) are also given. **b)** Representative confocal z-plane projections of ICM lineage marker expression (Nanog, for EPI, in red and Gata4, for PrE, in grey-scale, plus DAPI DNA counter-stain in blue) in each of the studied conditions in late-blastocyst (E4.5) stage embryos; GFP microinjection control plus DMSO vehicle control (GFP mRNA +DMSO; n=23), GFP microinjection control plus Fgfr inhibition (GFP mRNA +SU5402; n=23), Mkk6-EE microinjection plus DMSO vehicle control (Mkk6-EE mRNA +DMSO; n=24), Mkk6-EE microinjection plus Fgfr inhibition (Mkk6-EE mRNA +SU5402; n=23) and Mkk6-EE microinjection plus Fgfr and p38-Mapk14/11 inhibition (Mkk6-EE mRNA +SU5402 +SB220025; n=22). Scale bar = 15 $\mu$ m. **c)** Averaged contribution of cells to each ICM cell lineage, based on exclusive expression of either EPI (Nanog) or PrE (Gata4) lineage marker, in each of the stated experimental conditions. Errors are represented as s.e.m. and appropriate statistically significant differences, derived from 2-tailed students t-tests, highlighted by one or two significance markers (one, representing  $p < 0.05$  and two denoting  $p < 0.005$ ) described thus; asterisks (\*) showing differences between the 'GFP mRNA + DMSO' and 'GFP mRNA +SU5402' or 'Mkk6-EE mRNA +DMSO' (in grey) groups, the symbol § highlighting significant difference between the 'GFP mRNA +SU5402' and 'Mkk6-EE +SU5402' groups, crosses (†) between the 'Mkk6-EE +DMSO' and 'Mkk6-EE +SU5402' groups and hashtags (#) denoting divergence between the 'Mkk6-EE +SU5402' and 'Mkk6-EE +SU5402 +SB220025' groups. **d)** Averaged percentage makeup of the ICMs of each stated condition in relation to each specified ICM lineage; EPI or PrE (yellow and green, exclusively immuno-stained for either Nanog or Gata4, respectively), EPI & PrE co-expressing cells (orange, representing cells uncommitted to either lineage) and cells negative for either studied lineage marker (grey). Orange asterisk denotes the rescue of the PrE component of ICM cells in Fgfr inhibited embryos expressing the p38-Mapk14/11 activating kinase mutant, Mkk6-EE ('Mkk6-EE mRNA +SU5402' group) compared to the appropriate control Fgfr inhibited condition (the 'GFP mRNA +SU5402' group). Similarly, the black arrow highlights the ablation of this rescue effect by additional p38-Mapk14/11 inhibition (in the 'Mkk6-EE mRNA +SU5402 +SB220025' group). Data also presented in appendix tables T11.

ablated, with both the proportional PrE make-up of the ICM and the total PrE cell number returning to statistically equal levels observed in control GFP mRNA microinjected embryos treated with Fgfr inhibitor; this phenotype was also accompanied by a similar increase in EPI (Nanog-alone positive) cells. The collective interpretation of these data demonstrates functional role for p38-Mapk14/11 that is downstream of PrE promoting cell signalling mediated by activated Fgfr in the maturing ICM of preimplantation mouse blastocysts.

A relatively recent study identified a role for secreted Bmp-ligands and activated Bmp-receptors (Bmpr), in the derivation the PrE (and TE) during mouse blastocyst ICM cell lineage specification and segregation. In addition to classical Smad-dependent mechanisms, this study also uncovered a non-canonical/ Smad-independent mechanism of PrE derivation that functionally requires the active (Map3k) kinase, Tak1 (also known as Mkk7/ Map3k7)(Graham *et al.* 2014). As Tak1 kinase is able to target and activate both Mkk6 and Mkk3 (each Map2ks), that themselves are known to be the only targeting and activating enzymes of p38-Mapks (Huang *et al.* 2006; Kim *et al.* 2007), it was desirable to test if any of the reported Tak1 mediated inhibitory effects on PrE derivation (Graham *et al.* 2014) were mediated by p38-Mapk14/11. As with embryos cultured in the presence of Fgfr inhibitor, it was found incubation of 8-cell (E2.5) stage embryos *in vitro* cultured to the late morula (E3.25) stage in the specific Tak1 inhibitor, (5Z)-7-Oxozeanol [(Ninomiya-Tsuji *et al.* 2003), abbreviated herein to 5Z-7-Oxo], resulted in reduced levels of activated p38-Mapk14/11(p) protein (figure 17); demonstrating p38-Mapk14/11 activation is susceptible to functional Tak1 levels in the preimplantation mouse embryo. Therefore, it was next decided to conduct a Tak1/ Mkk6-EE/ p38-Mapk14/11 inhibition experiment, conceptually similar to that described above for Fgfr inhibition but with the difference that the 5Z-7-Oxo Tak1 inhibitor was provided from the 8-cell (E2.5) stage rather than the 16-cell (E3.0) stage, as has previously been reported for uncovering PrE deficit phenotypes (Graham *et al.* 2014) (figure 20). As can be observed, results extremely similar to the Fgfr inhibition experiment were obtained (figure 19), in that Tak1 inhibition in GFP microinjected control embryos caused a significant reduction in overall PrE cell number and the proportional make up of the ICM (down to 18.3% from the 40.9% observed in DMSO treated control embryos,  $p = 5.53^{E-8}$ ). This PrE deficit phenotype was concomitant with an increase in the number/ proportion of ICM cells solely expressing the EPI marker Nanog (up to 69.5% versus 50.5% in controls). Moreover, the PrE phenotype caused by Tak1 inhibition was rescued by over expression of the p38-Mapk14/11 activating Mkk6-EE construct but the rescue could also be ablated by subsequent direct inhibition of p38-Mapk14/11 itself; thereby confirming Tak1 activity, itself functionally downstream of activated Bmpr (Graham *et al.* 2014), functions to promote PrE derivation in the mouse blastocyst ICMs by contributing to the activation of p38-Mapk14/11.

#### 5.4 Concluding summary

Collectively the published data demonstrate that p38-Mapk14/11 is required during mouse blastocyst ICM maturation to appropriately ensure the specification and segregation of the EPI and PrE lineages. Specifically, that functional p38-Mapk14/11 ensures the resolution of cells of uncommitted cell-fate, expressing both Nanog and earlier PrE markers (*e.g.* Gata6 and Sox17), in a developmental time window coinciding with the earliest stages ICM maturation (*i.e.* before the E3.75 stage) and the ordinarily observed adopting of the classical salt and pepper pattern of mutually exclusive EPI and PrE marker gene expression. Moreover, that it is the resolution of uncommitted cells towards the PrE fate that is most severely affected. Indeed, it is shown that the regulation of p38-Mapk14/11 activity, and hence function, is downstream of already known and well characterised PrE promoting cell signalling pathways represented by Bmpr/Tak1 and Fgfr and that in the case of the latter, p38-Mapk14/11 likely cooperates with the Mek1/2 activated component of the same pathway to allow the driving of PrE cell-fate.

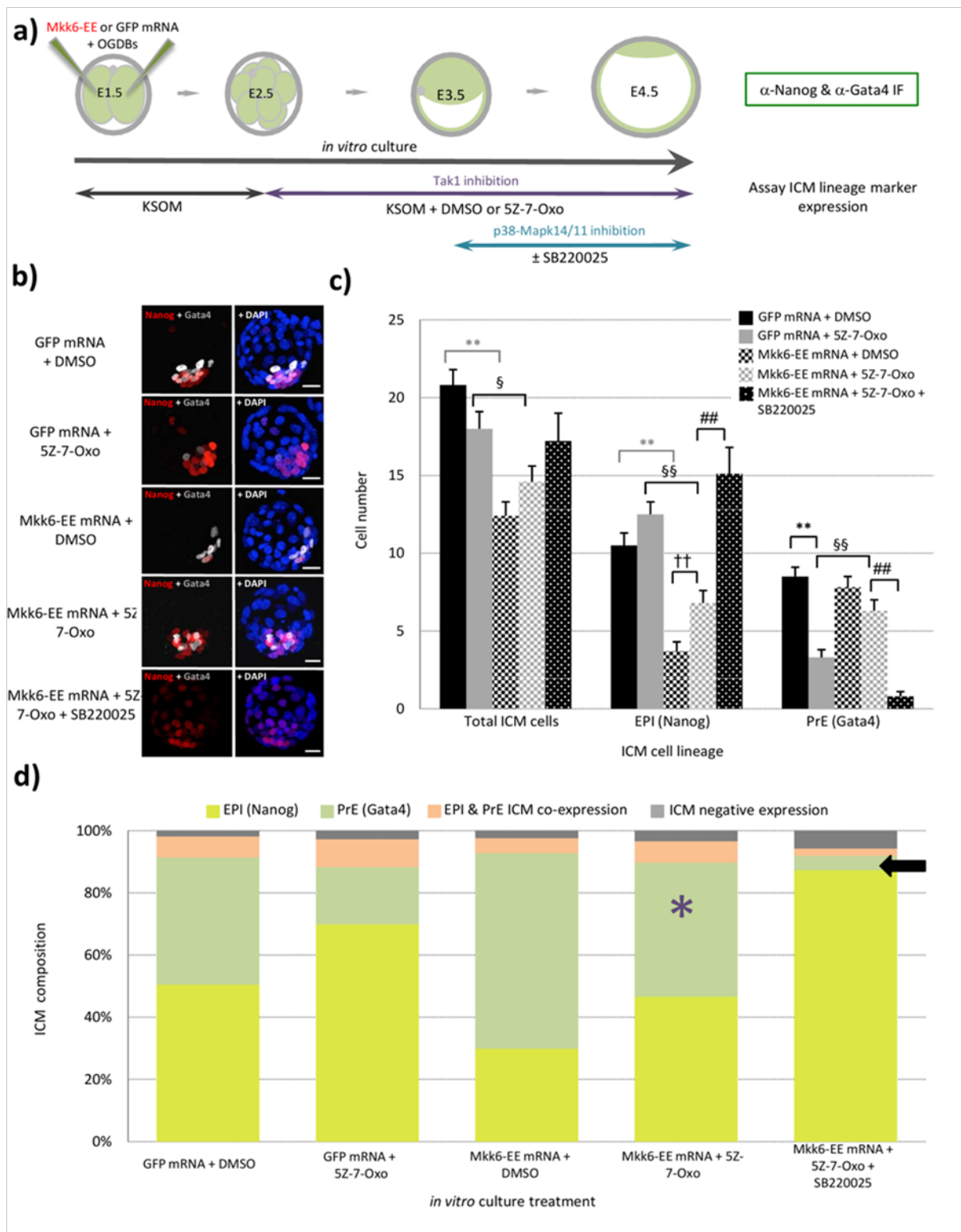


Figure 20. (legend overleaf)

**Figure 20. Inhibition of Tak1 impairs PrE formation in a p38-Mapk14/11 dependent manner. a)** Experimental schema detailing the regime of Tak1 inhibition (+5Z-7-Oxo), with attendant vehicle control (+DMSO) condition, from the 8-cell to late blastocyst (E2.5-E4.5) stages and optional p38-Mapk14/11 co-inhibition ( $\pm$ SB220025, from E3.5-E4.5), employed. Also highlighted are mRNAs microinjected (together with Oregon-green conjugated dextran beads/ OGDBs, to confirm successful mRNA delivery) into both blastomeres at the 2-cell (E1.5) stage; the constitutive active, p38-Mapk14/11 targeting Map2k kinase, 'Mkk6-EE' mutant or microinjection control 'GFP'. Immunofluorescence (IF) antibody details used to analyse ICM cell lineage marker protein expression in late blastocysts (E4.5) are also given. **b)** Representative confocal z-plane projections of ICM lineage marker expression (Nanog, for EPI, in red and Gata4, for PrE, in grey-scale, plus DAPI DNA counterstain in blue) in each of the studied conditions in late-blastocyst (E4.5) stage embryos; GFP microinjection control plus DMSO vehicle control (GFP mRNA +DMSO; n=22), GFP microinjection control plus Tak1 inhibition (GFP mRNA +5Z-7-Oxo; n=23), Mkk6-EE microinjection plus DMSO vehicle control (Mkk6-EE mRNA +DMSO; n=25), Mkk6-EE microinjection plus Tak1 inhibition (Mkk6-EE mRNA +5Z-7-Oxo; n=25) and Mkk6-EE microinjection plus Tak1 and p38-Mapk14/11 inhibition (Mkk6-EE mRNA +5Z-7-Oxo +SB220025; n=21). Scale bar = 15 $\mu$ m. **c)** Averaged contribution of cells to each ICM cell lineage, based on exclusive expression of either EPI (Nanog) or PrE (Gata4) lineage marker, in each of the stated experimental conditions. Errors are represented as s.e.m. and appropriate statistically significant differences, derived from 2-tailed students t-tests, highlighted by one or two significance markers (one, representing  $p < 0.05$  and two denoting  $p < 0.005$ ) described thus; asterisks (\*) showing differences between the 'GFP mRNA +DMSO' and 'GFP mRNA +5Z-7-Oxo' or 'Mkk6-EE mRNA +DMSO' (in grey) groups, the symbol § highlighting significant difference between the 'GFP mRNA + 5Z-7-Oxo' and 'Mkk6-EE +5Z-7-Oxo' groups, crosses (†) between the 'Mkk6-EE +DMSO' and 'Mkk6-EE +5Z-7-Oxo' groups and hashtags (#) denoting divergence between the 'Mkk6-EE +5Z-7-Oxo' and 'Mkk6-EE +5Z-7-Oxo + SB220025' groups. **d)** Averaged percentage makeup of the ICMs of each stated condition in relation to each specified ICM lineage; EPI or PrE (yellow and green, exclusively immuno-stained for either Nanog or Gata4, respectively), EPI & PrE co-expressing cells (orange, representing cells uncommitted to either lineage) and cells negative for either studied lineage marker (grey). Purple asterisk denotes the rescue of the PrE component of ICM cells in Tak1 inhibited embryos expressing the p38-Mapk14/11 activating kinase mutant, Mkk6-EE ('Mkk6-EE mRNA +5Z-7-Oxo' group) compared to the appropriate Tak1 inhibited condition (the 'GFP mRNA +5Z-7-Oxo' group). Similarly, the black arrow highlights the ablation of this rescue effect by additional p38-Mapk14/11 inhibition (in the 'Mkk6-EE mRNA +5Z-7-Oxo +SB220025' group). Data also presented in appendix tables T12.

## **6. Unpublished data**

The following section describes the unpublished data relating to that discussed above (published), detailing experiments aimed at identifying the functionally downstream mechanism of p38-Mapk14/11 action during blastocyst ICM maturation. Moreover, further data relating to a potential amino acid sensing role of p38-Mapk14/11 during mouse preimplantation embryo development is presented.

## 6.1 Analysis aimed at identifying downstream factors responsible for the observed p38-Mapk14/11 mediated effects on PrE formation and ICM maturation.

As mentioned previously in the introduction section, p38-Mapks have been estimated to directly phosphorylate approximately 200-300 functionally downstream effector proteins. Given the huge number of effector proteins that could be responsible for the ICM maturation role identified (see previous results section) a candidate gene approach, drawing on published stem cell renewal/differentiation precedents in the literature, was employed to mechanistically investigate how p38-Mapk14/11 may execute this role (Cuadrado A & Nebreda AR 2010). Indeed a survey of the literature revealed that Nanog stability can be affected by direct phosphorylation events, reported to be imparted by Erk1/2 signalling, at serines-52, -71 and -78 that results in proteasomal degradation of Nanog and during mouse ES cell differentiation (Kim *et al.* 2014). Therefore, given the observation that there is an increase in the number of uncommitted Nanog/ Gata6 co-expressing ICM cells in p38-Mapk14/11 inhibited blastocysts an immuno-fluorescent staining assay for any differences in phospho-Nanog (p-Nanog) levels between the control (+DMSO) and inhibitor (+SB220025) treated group ICMs (using a commercially available anti-p-Nanog antibody specific for phospho-serine-71) was conducted. However, this assay failed to identify any significant changes in p-Nanog (Ser71) levels in p38-Mapk14/11 inhibited embryos (figure 21b), suggesting direct regulation of Nanog stability via p38 dependent phosphorylation is not a component of the observed PrE (increased uncommitted ICM cells) defect. However, it is noteworthy that it was only possible to assay a single p-Nanog isoform, due to a lack of required primary antibody reagents, therefore not totally excluding p38-Mapk14/11 mediated destabilising phosphorylation of Nanog as a possible mechanism. Similarly, a comparative analysis of protein expression levels of another pluripotency regulating transcription factor Zscan10 was performed, given that its paralogous gene *Mzf1*, was found to contain a domain susceptible to p38-Mapk phosphorylation (as indicated in the phosphosite.org website) that in turn negatively effects its stability. However, once more, no differences in Zscan10 expression were detected between control (+DMSO) and p38 inhibited (+SB220025) blastocyst ICMs, thereby also ruling out this potential mechanism (figure 21b). Additionally a further published study in F9 tetra carcinoma cells, has reported that p38-Mapk positively regulates the Wnt3a dependent Wnt-signalling pathway by a phosphorylation dependent inhibition of the negative Wnt regulator Gsk-3 $\beta$ , thus resulting in the nuclear accumulation of the transcriptional co-factor  $\beta$ -catenin, that in turn promotes PrE differentiation (Bikkavilli *et al.* 2008). It was therefore hypothesized that p38-Mapk14/11 inhibition in preimplantation mouse embryos, might render Gsk-3 $\beta$  active, leading to an attenuation of Wnt signalling and thus blocked PrE differentiation. Therefore, according to this hypothesis it was reasoned that if p38 inhibition mediated, even in part, its effect on blocked PrE

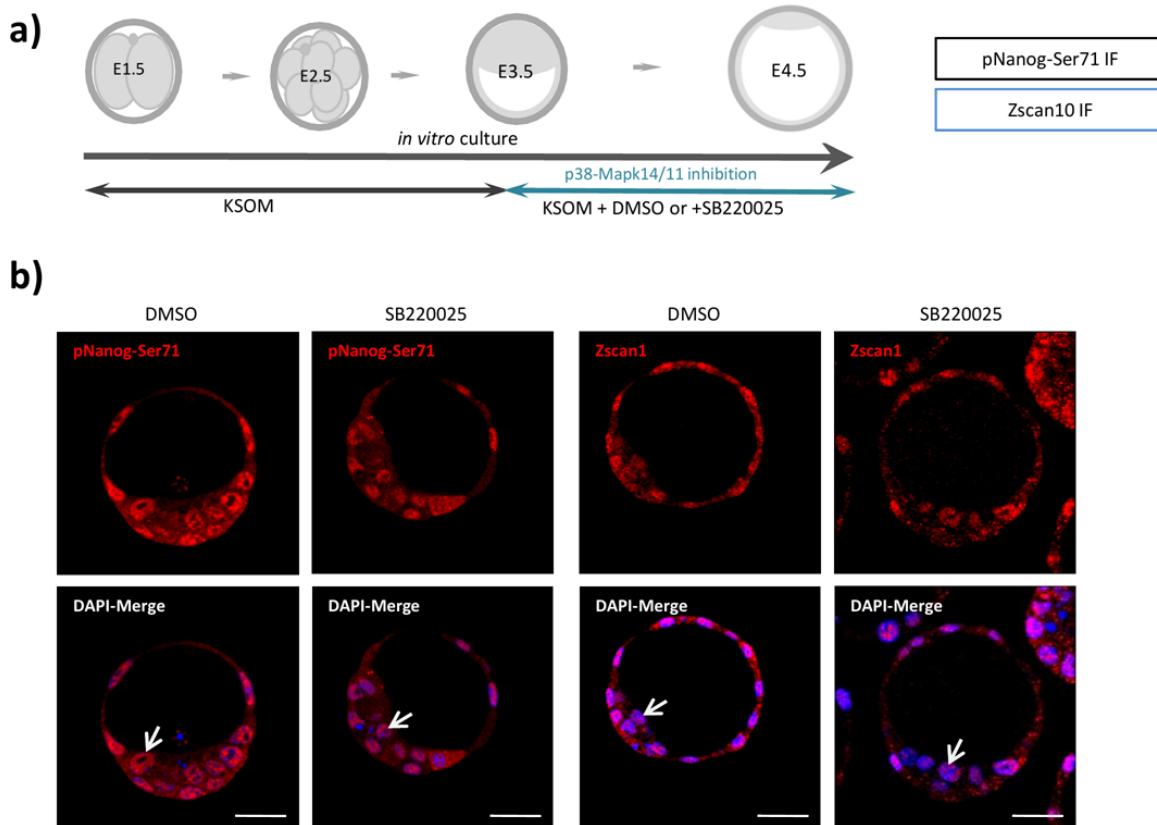


**Figure 21. Treatment of embryos with the p38-Mapk14/11 inhibitor SB220025 does not alter the levels of either phospho-Ser71-Nanog or Zscan10.** **a)** Experimental schema of p38-Mapk14/11 inhibition (+SB220025), plus vehicle control (+DMSO) culture conditions during blastocyst maturation (E3.5-E4.5) and the details of antibodies used to analyse protein expression by immuno-fluorescence (IF) in derived late blastocysts (E4.5); pNanog-Ser71 (+DMSO & +SB220025) – black and Zscan10 (+DMSO & +SB220025) – blue. **b)** Representative central confocal z-plane sections of (IF) stained blastocyst embryos from each culture group IF stained for the indicated protein. pNanog-Ser71 and Zscan10 signal is shown in red and DAPI DNA counterstain (blue) is also provided (unmerged and merged images shown) with white arrows indicating the nuclear staining for either p-Ser71-Nanog and Zscan10 as appropriate. Scale bar = 15 $\mu$ m.

differentiation via failure to inactivate Gsk-3 $\beta$ , direct pharmacological inhibition of Gsk-3 $\beta$  itself would be able to partially restore PrE formation even in the presence of continued p38-Mapk14/11 inhibition. To explore such a possibility the Gsk-3 $\beta$  inhibitor CHIR99021 (widely employed in various studies; *e.g.* Nichols *et al.* 2009) was utilised. Consequently, embryos were cultured in four groups and assayed for EPI (Nanog) and late PrE (Gata4) marker gene expression at the late blastocyst stage by confocal microscopy, to ascertain the average cell-fate make up of the derived ICM cells. The first

two groups comprised embryos cultured in the sole presence of either SB220025 (p38-Mapk14/11 inhibitor) or vehicle control DMSO from the early blastocyst (E3.5) stage to the late blastocyst (E4.5) stage, whilst a third group comprised embryos cultured in the presence of CHIR99021 from the 8-cell (E2.5) stage to the late blastocyst (E4.5) stage. The last group of embryos were cultured in the presence of CHIR99021 from the 8-cell (E2.5) stage until the early blastocyst (E3.5) stage and then transferred into fresh media further supplemented with SB220025 and CHIR99021 before continued culture to the assayed late blastocyst (E4.5) stage. As indicated in figure 22 and in agreement with previous reports in mouse early embryos (Nichols *et al.* 2009), Gsk-3 $\beta$  inhibition alone did not cause any statistically significant effect on ICM lineage derivation compared to the control (+DMSO), representing 50% and 43.1% for EPI and PrE respectively. Whereas, the SB220025 alone treated embryos displayed the usual defect in PrE formation (presenting with PrE contribution of 8.8% compared to the DMSO control value of 43.3%,  $p = 8.93^{E-08}$ ). Similarly and crucially, the SB220025/CHIR99021 double inhibitor treated group also retained the PrE deficit (13.27% PrE contribution to the ICM compared to DMSO control, value of 43.3%,  $p = 2.35^{E-06}$ ). Furthermore, it also resulted in an overall decrease in cell number by the late blastocyst stage (E4.5), with the majority of the decreased cell number observed in the TE; possibly highlighting a synergy between p38-Mapk and Wnt based signalling in the TE not evident in the ICM. Therefore, the conclusion of these experiments is that the p38-Mapk mediated effect on PrE differentiation, revealed by solely inhibiting p38-Mapk14/11 during blastocyst ICM maturation, is not processed via regulating the activity of Gsk-3 $\beta$  and the Wnt/ $\beta$  catenin pathway, as suggested from previous *in vitro* studies in F9 carcinoma cells.

Further analysis of other direct downstream targets of p38-Mapk signalling, including the Activating transcription factor-2 (Atf2), a cAMP-responsive element (CRE) binding protein with an additional histone acetyltransferase activity that is activated by p38-Mapk dependent phosphorylation (Ouwens *et al.* 2002) was conducted. As it has been reported by proteomic analysis in ES cells that Oct4 interacts with Atf2 (Pardo *et al.* 2010) and that Oct4 is required (albeit no-cell autonomously) during PrE formation (Frum *et al.* 2013), it was hypothesized that such an interaction in the ICM cells of preimplantation mouse embryos may promote PrE required gene expression and differentiation. Therefore, mRNA for constitutively active human ATF2 (CA-ATF2), that had been created by fusing the constitutively active domain of the human CREB2 transcription factor with the C-terminal region of ATF2 (182-326aa), that retains ATF2 specific functions and Oct4 binding (Steinmuller L & Thiel G. 2003), was microinjected in both cells of 2-cell stage embryos that were then cultured until the early blastocyst (E3.5) stage. Embryos were then transferred into culture media containing either DMSO (vehicle control) or SB220025 (p38-Mapk14/11 inhibitor) and cultured up to late blastocyst (E4.5) stage, to see if CA-ATF2 expression could rescue the PrE defect ordinarily

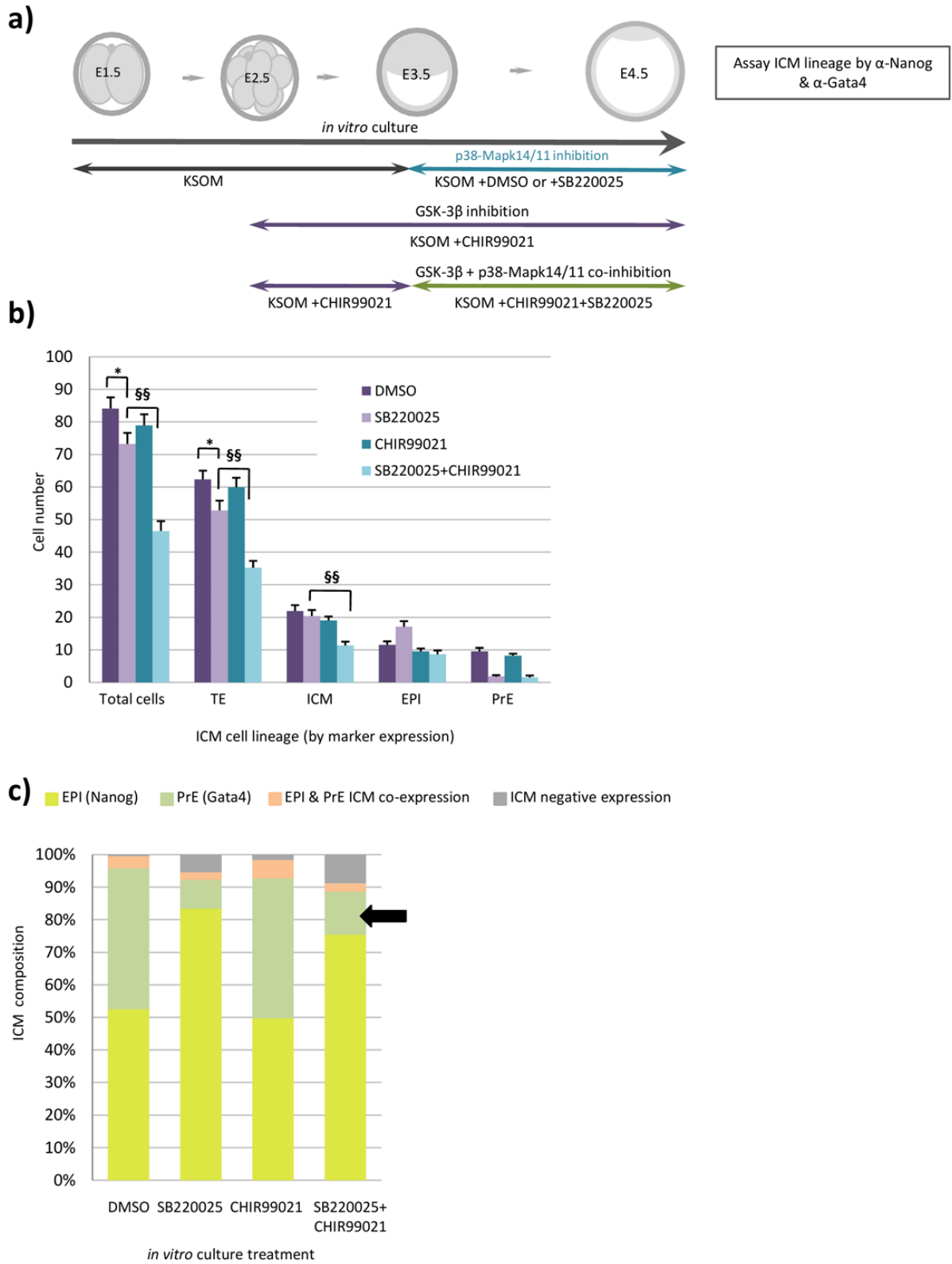


Figure 22. (legend overleaf)

**Figure 22. p38-Mapk14/11 regulation of PrE differentiation does not act through the canonical Wnt-signalling pathway.** **a)** Experimental schema detailing the regime of sole p38-Mapk14/11 inhibition (+SB220025), from the early blastocyst (E3.5) to late blastocyst (E4.5) stages with attendant vehicle control (+DMSO), Gsk-3 $\beta$  inhibition (+CHIR99021) from the 8-cell to late blastocyst (E2.5-E4.5) stage, and Gsk-3 $\beta$ / p38-Mapk14/11 co-inhibition [typified by +CHIR99021 supplementation from 8-cell (E2.5) to early blastocyst (E3.5) stage, followed by a co-inhibition regime with +CHIR99021 and +SB220025 from early blastocyst (E3.5) to late blastocyst (E4.5) stage] experimental conditions employed and the details of antibodies used to analyse ICM cell lineage marker protein expression by immuno-fluorescence (IF) in late blastocysts (E4.5); Nanog (EPI) and Gata4 (PrE) – green box. For each of the studied conditions in late-blastocyst (E4.5) stage embryos; DMSO vehicle control (+DMSO, n=13 ), p38-Mapk14/11 inhibition (+SB220025, n=17), Gsk-3 $\beta$  inhibition (+CHIR99021, n=15), and Gsk-3 $\beta$  plus p38-Mapk14/11 co-inhibition (+SB220025 +CHIR99021, n=12). **b)** Averaged contribution of cells to all blastocyst lineages in each of the stated conditions, with total cell number and TE number calculations based on DAPI staining and the exclusion of ICM markers respectively, and the ICM lineage numbers based on exclusive expression of either EPI (Nanog) or PrE (Gata4) lineage markers. Errors are represented as s.e.m. and appropriate statistically significant differences, derived from 2-tailed students t-tests, highlighted by one or two significance markers (one, representing  $p < 0.05$  and two denoting  $p < 0.005$ ) described thus; asterisks (\*) showing differences between the '+DMSO' and '+SB220025' groups, the symbol (§) highlighting significant difference between the '+SB220025' and '+SB220025 +CHIR99021' groups. **c)** Averaged percentage makeup of ICMs in each of the stated experimental groups in relation to each specified ICM lineage; EPI or PrE (yellow and green, exclusively immuno-stained for either Nanog or Gata4, respectively), EPI & PrE co-expressing cells (orange, representing cells uncommitted to either lineage) and cells negative for either studied lineage marker (grey). The black arrow indicates that the p38-Mapk 14/11 inhibition effect was not rescued (in the 'SB220025 +CHIR99021' group) by co-inhibition of Gsk-3 $\beta$ . All data used to prepare this figure are described in appendix tables T13.

---

associated with p38-Mapk inhibition. Embryos similarly microinjected with GFP mRNA were cultured in identical conditions served as controls. As shown in figure 23, the over-expression of CA-ATF2 in vehicle control treated conditions (+DMSO) actually resulted in a significant increase in Nanog alone immuno-stained EPI cells, compared to embryos injected with control GFP mRNA (*i.e.* an increase to 69.2% versus the more typical 47.5% in the controls,  $p = 4.25 \times 10^{-3}$ , that ran contrary to the predicted hypothesis). Therefore suggesting CA-ATF2 was unlikely to rescue the p38-Mapk14/11 inhibition induced deficient PrE phenotype. This indeed was the case as both CA-ATF2 and GFP microinjected

embryo groups exposed to SB220025 exhibited statistically indistinguishable and robust PrE deficient phenotypes (Gata4 alone positive PrE cells making up 6.2 and 9.0% of derived ICM populations in CA-ATF2 and GFP microinjected embryos, respectively  $p = 2.78^{E-01}$ ). Thus, the over-expression of constitutively active, and functionally downstream in relation to p38-Mapk14/11, CA-ATF2 was unable to rescue p38-Mapk14/11 inhibition mediated effects, suggesting it is not a paucity of activated Atf2 that is responsible for the observed PrE deficiency. Similar experiments were performed by over-expressing constitutively active forms of self-derived mouse Mk3 (CA-Mk3) and obtained human MSK1 (CA-MSK1), both known to be direct effectors of activated p38-Mapk14/11 that positively regulate gene expression by targeting epigenetic regulators including the polycomb group proteins (PcG) and histones, respectively. Indeed, Mk3 is known to be a chromatin regulator activated by p38-Mapk and Erk1/2 mediated phosphorylation leading to its nuclear translocation, where it phosphorylates and destabilizes the PcG protein Bmi1. Since, Bmi1 is itself known to promote the stabilization of the early PrE transcription factor Gata6 in mouse preimplantation embryos, thus stimulating PrE specification (Lavial *et al.* 2012), it was reasoned that the observed increase in Nanog/ Gata6 co-expressing and uncommitted ICM cells observed in SB220025 treated embryos may be due to attenuated Mk3 activation; resulting in Bmi1 stabilization and consequently prolonged *Gata6* presence/ expression. However, just as with the above described CA-ATF2 experiments over-expression of mouse derived CA-Mk3 also failed to rescue the classically observed p38-Mapk inhibition induced PrE deficient phenotype (Figure 24). Msk1 was selected for further investigation and for similar reasons, as it is also imported to the nucleus in response to p38-Mapk or Erk1/2 mediated phosphorylation/ activation, where it in turn phosphorylates histone H3 at serine-10 and-28 residues to displace bound PcG proteins from chromatin to facilitate gene activation (Gehani *et al.* 2010). However, over-expression of CA-MSK1 was also unable to rescue the p38-Mapk inhibition induced PrE deficit phenotype (data not shown). Thus, given the fact that p38-Mapk pathway includes a myriad of downstream effectors, it was concluded that more than one of these proteins could be involved in p38-Mapk14/11 regulated PrE development and that functionally targeting such proteins in isolation may not be sufficient to reveal their role. Alternatively, it is also possible that the candidate gene approach adopted had failed to identify the relevant effector, thus necessitating a future need to assay for the potential effector(s) in a more empirical/ experimental approach.

## **6.2 Sensitivity of the p38-Mapk14/11 signalling pathway to amino acid (AA) availability in embryo culture media.**

Previous studies in mouse preimplantation embryos have shown that inhibiting p38-Mapk activity results in the down regulation of glucose transporters 1 and 4 (*Glut1* & 4) expression both at the

mRNA and protein levels, leading to developmental arrest during the morula stage (Sozen *et al.* 2015). Further, many studies using non-embryonic cells have demonstrated metabolism dependent p38-Mapk signalling in the regulation of various cellular mechanisms, including amino acid (AA) availability dependent signalling pathways and autophagy (Casas-terradellas *et al.* 2008 and Moruno-manchon *et al.* 2013). Given the findings that amino acid availability is known to affect the phenomenon of 'developmental origin of health and disease' (DOHaD) during preimplantation embryo development (as discussed in the introduction section to this thesis), the uncovered cell-fate role of p38-Mapk during ICM maturation in relation to AA availability was investigated. To this end, p38-Mapk14/11 inhibition was performed from E3.5 to E4.5 with blastocyst embryos cultured in two different media conditions; one comprising KSOM supplemented with essential and non-essential amino acids (KSOM+AA, as previously described above) and the other representative of KSOM without any additional essential or non-essential AA supplementation commercially purchased from Millipore (under the trade name EmbryoMax<sup>®</sup>, referred to here as cKSOM). Both media conditions comprised inhibitor treated embryo groups (+SB220025) and vehicle control embryo groups (+DMSO). The embryos were fixed at late blastocyst (E4.5) stage and immuno-fluorescently stained (IF) and analysed by confocal microscopy for the expression of the EPI marker Nanog and each of the available PrE markers *i.e.* Gata6, Sox17 and Gata4. In agreement with the previous findings of embryos cultured in KSOM+AA, the embryos inhibited by SB220025 yet cultured in cKSOM also showed a profound PrE deficit (Figures 25 and 26; micrographs and quantification respectively). Moreover, an increase in uncommitted ICM cells co-expressing both the EPI marker Nanog and early PrE marker Gata6 was also similarly and consistently observed (Figures 25 and 26). Interestingly, the defect in general extraembryonic development (both of TE and PrE) was more severe in the inhibitor (+SB220025) treated embryos cultured in cKSOM than in the equivalent embryos inhibited in KSOM+AA culture media (Figure 26; plus the previously described experiments in the preceding results section); for example a range of 40-45 TE cells were observed in the cKSOM (+SB220025) group compared to 53-56 TE cells in the KSOM+AA (+SB220025) group, with the number of PrE cells ranging between 0.8-1 cells in the cKSOM (+SB220025) group, as opposed to 2.8-3.2 cells in KSOM+AA inhibitor treated embryos. It is noteworthy that though there are statistically significant differences in the average cell lineage cell numbers after inhibitor treatment in different culture conditions, these defects when expressed in proportional terms, are broadly similar in either culture conditions, that is to state that the shared trend is for the average number of extraembryonic TE and PrE cells to be diminished, whilst the number of uncommitted ICM cells are concomitantly enhanced after inhibition of p38-Mapk14/11, irrespective of supplemented amino acid availability. However, these phenotypes are exacerbated by a lack of amino acid supplementation (Figure 26). Thus, p38-

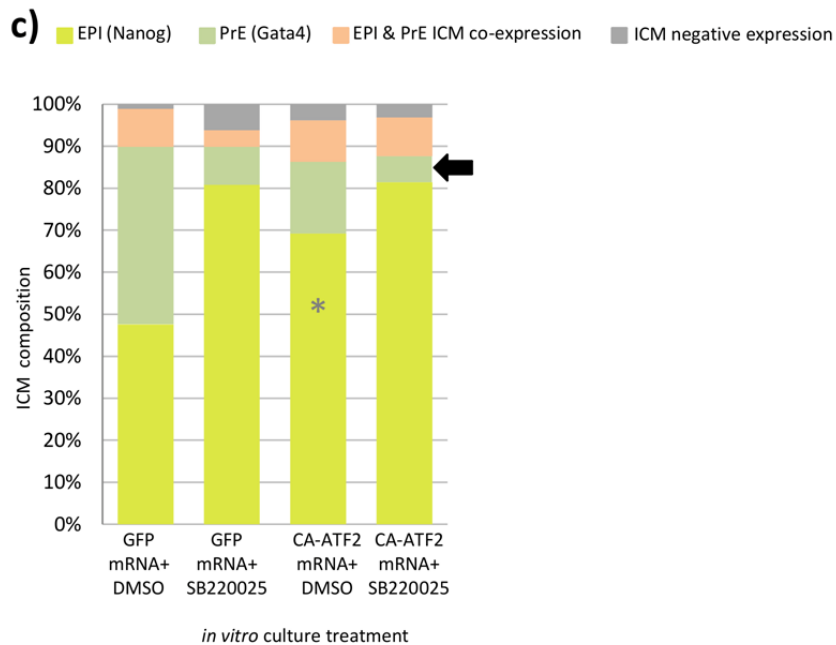
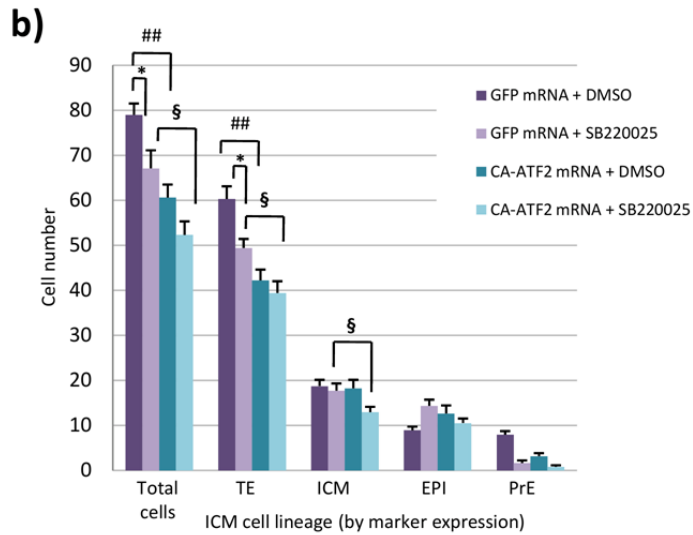
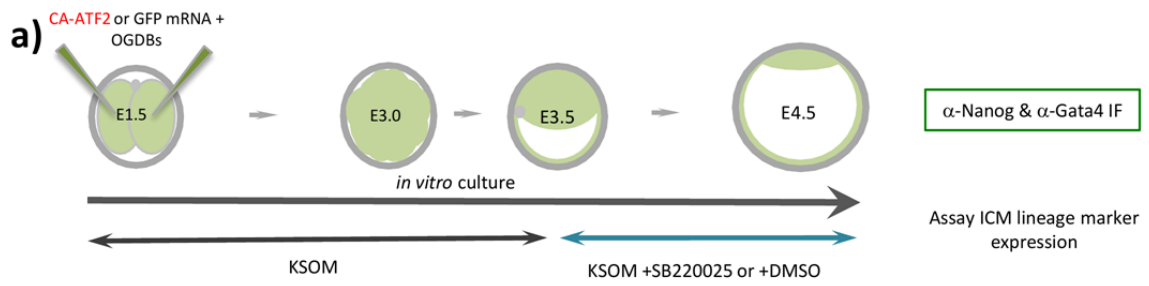


Figure 23. (legend overleaf)

**Figure 23. An attempt to rescue the PrE defect caused by p38-Mapk14/11 inhibition by overexpressing constitutively active ATF2 (CA-ATF2).** **a)** Experimental schema detailing the regime of p38-Mapk14/11 inhibition (+SB220025), with attendant vehicle control (+DMSO) condition, from the early to late blastocyst (E3.5-E4.5) stages, employed. Also highlighted are mRNAs microinjected (together with Oregon-green conjugated dextran beads/OGDBs, to confirm successful mRNA delivery) into both blastomeres at the 2-cell (E1.5) stage; the constitutively active, p38-Mapk14/11 downstream target, 'CA-ATF2' mutant or microinjection control 'GFP'. Immuno-fluorescence (IF) antibody details used to analyse ICM cell lineage marker protein expression in late blastocysts (E4.5) are also given – green box. In each of the studied conditions in late-blastocyst (E4.5) stage embryos for CA-ATF2; GFP microinjection control plus DMSO vehicle control (GFP mRNA +DMSO n=12), GFP microinjection control plus p38-Mapk14/11 inhibition (GFP mRNA +SB220025 n=15), for CA-ATF2 microinjection plus DMSO vehicle control (CA-ATF2 mRNA +DMSO n=12), and CA-ATF2 plus p38-Mapk14/11 inhibition (CA-ATF2 mRNA +SB220025 n=14). **b)** Averaged contribution of cells to all embryonic lineages, with total cell number and TE number based on DAPI and exclusion of ICM markers respectively, whilst, the ICM lineage number was based on exclusive expression of either EPI (Nanog) or PrE (Gata4) lineage marker, in each of the stated experimental conditions. Errors are represented as s.e.m. and appropriate statistically significant differences, derived from 2-tailed students t-tests, highlighted by one or two significance markers (one, representing  $p < 0.05$  and two denoting  $p < 0.005$ ) described thus; asterisks (\*) showing differences between the 'GFP mRNA + DMSO' and 'GFP mRNA +SB220025' groups, the hash tags (#) highlighting significant difference between the 'GFP mRNA + DMSO' and 'CA-ATF2 mRNA + DMSO groups, and the symbol § denoting the divergence between the 'GFP +SB220025' and 'CA-ATF2 +SB220025' groups. **c)** Averaged percentage makeup of the ICMs of different experimental groups after overexpressing CA-ATF2 in relation to each specified ICM lineage; EPI or PrE (yellow and green, exclusively immuno-stained for either Nanog or Gata4, respectively), EPI & PrE co-expressing cells (orange, representing cells uncommitted to either lineage) and cells negative for either studied lineage marker (grey). The black arrow indicates that the p38-Mapk 14/11 inhibition effect was not rescued (in the CA-ATF2 +SB220025 group) and the grey asterisk indicates the increase in percentage of Nanog positive EPI cells in CA-ATF2+DMSO group. All data used to prepare this figure are described in appendix table T14.

---

Mapk regulates extra-embryonic cell lineages number during mouse preimplantation embryo development in a manner that is indeed sensitive to amino acid availability.

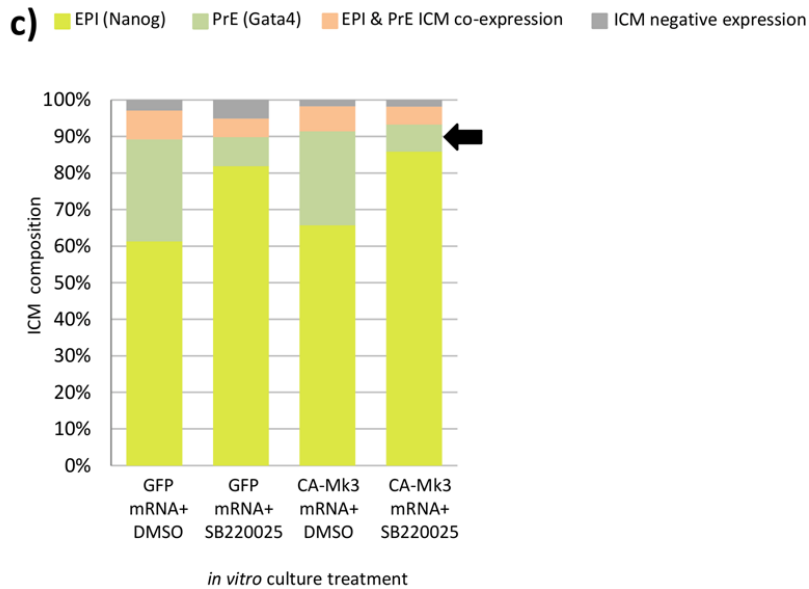
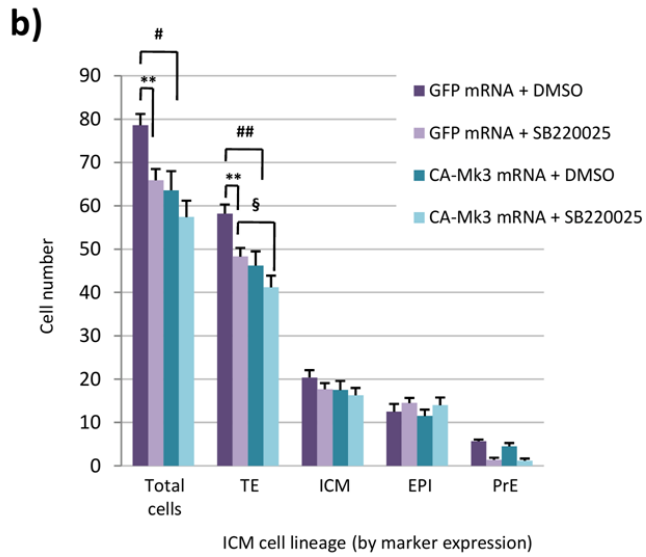
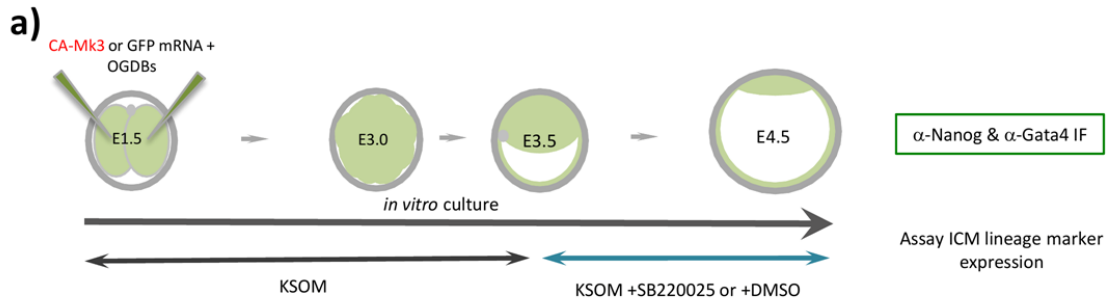


Figure 24. (legend overleaf)

**Figure 24. An attempt to rescue the PrE defect caused by p38-Mapk14/11 inhibition by overexpressing constitutively active Mk3 (CA-Mk3).** **a)** Experimental schema detailing the regime of p38-Mapk14/11 inhibition (+SB220025), with attendant vehicle control (+DMSO) condition, from the early to late blastocyst (E3.5-E4.5) stages, employed. Also highlighted are mRNAs microinjected (together with Oregon-green conjugated dextran beads/ OGDBs, to confirm successful mRNA delivery) into both blastomeres at the 2-cell (E1.5) stage; the constitutive active, p38-Mapk14/11 downstream target, 'CA-Mk3' mutant or microinjection control 'GFP'. Immuno-fluorescence (IF) antibody details used to analyse ICM cell lineage marker protein expression in late blastocysts (E4.5) are also given – green box. In each of the studied conditions in late-blastocyst (E4.5) stage embryos for CA-Mk3; GFP microinjection control plus DMSO vehicle control (CA-MK3, GFP mRNA +DMSO n=13), GFP microinjection control plus p38-Mapk14/11 inhibition (CA-Mk3, GFP mRNA +SB220025 n=15), for CA-Mk3 mRNA microinjection plus DMSO vehicle control (CA-Mk3 mRNA +DMSO n=11), and CA-Mk3 mRNA plus p38-Mapk14/11 inhibition (CA-Mk3 mRNA +SB220025 n=12). **b)** Averaged contribution of cells to all embryonic lineages, with total cell number and TE number based on DAPI and exclusion of ICM markers respectively, whilst, the ICM lineage number was based on exclusive expression of either EPI (Nanog) or PrE (Gata4) lineage marker, in each of the stated experimental conditions. Errors are represented as s.e.m. and appropriate statistically significant differences, derived from 2-tailed students t-tests, highlighted by one or two significance markers (one, representing  $p < 0.05$  and two denoting  $p < 0.005$ ) described thus; asterisks (\*) showing differences between the 'GFP mRNA +DMSO' and 'GFP mRNA +SB220025' groups, the hash tags (#) highlighting significant difference between the 'GFP mRNA +DMSO' and 'CA-Mk3 mRNA +DMSO' groups, and the symbol § denoting the divergence between the 'GFP +SB220025' and 'CA-Mk3 mRNA +SB220025' groups. **c)** Averaged percentage makeup of the ICMs of different experimental groups after overexpressing CA-Mk3 in relation to each specified ICM lineage; EPI or PrE (yellow and green, exclusively immuno-stained for either Nanog or Gata4, respectively), EPI & PrE co-expressing cells (orange, representing cells uncommitted to either lineage) and cells negative for either studied lineage marker (grey). The black arrow indicates that the p38-Mapk 14/11 inhibition effect was not rescued (in the CA-Mk3 +SB220025 group). All data used to prepare this figure are described in appendix table T15.

---

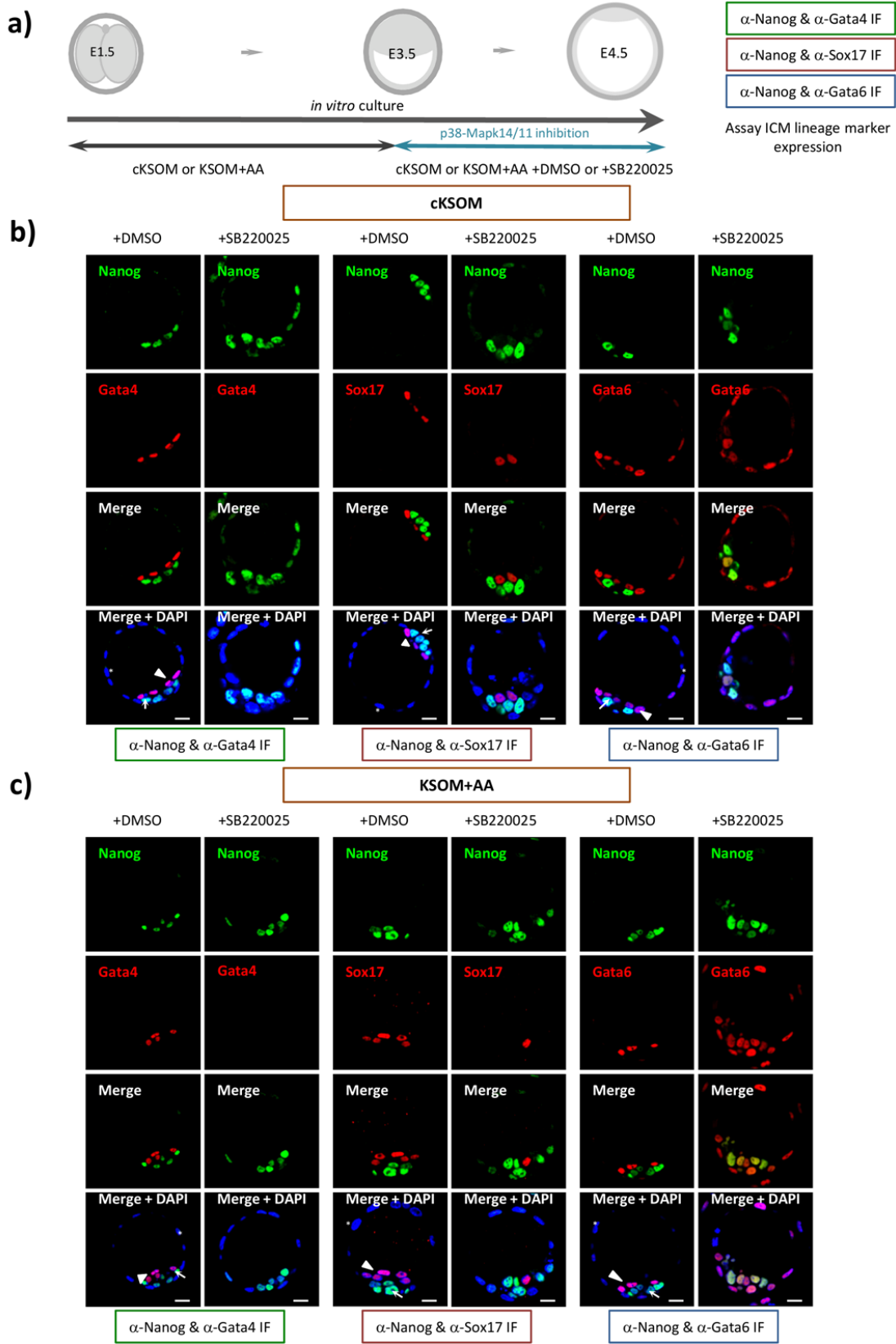


Figure 25. (legend overleaf)

**Figure 25. The PrE deficit associated with p38-Mapk14/11 inhibition (E3.5 - E4.5) is retained in embryos cultured in both commercial KSOM (cKSOM without amino acids supplementation) and KSOM supplemented with AAs (KSOM+AA); illustrative examples of embryo micrographs, see figure 26 for cell fate quantification analysis. a)** Experimental schema of blastocyst p38-Mapk14/11 inhibition (+SB220025), plus vehicle control (+DMSO), cultured in commercial KSOM without essential and non-essential AA cocktail supplementation (cKSOM) and preparatory KSOM media supplemented with AA (KSOM+AA, as routinely used) from early blastocyst (E3.5) to late blastocyst (E4.5) stage. The details of antibodies used to analyse ICM cell lineage marker protein expression by immuno-fluorescence (IF) in late blastocysts (E4.5) are given; Nanog & Gata4 (cKSOM +DMSO=22, +SB220025=24; KSOM+AA +DMSO n=14, +SB220025 n=18) – green box, Nanog and Sox17 (cKSOM +DMSO=20, +SB220025=24; KSOM+AA +DMSO n=17, +SB220025 n=17) – red box and Nanog and Gata6 (cKSOM +DMSO=24, +SB220025=22; KSOM+AA +DMSO n=16, +SB220025 n=17) – blue box. **b) & c)** Representative single confocal z-plane micrographs of cKSOM and KSOM+AA cultured, vehicle control treated (+DMSO) or p38-Mapk14/11 inhibited (+SB220025) late-blastocyst stage (E4.5)/ equivalent embryos, IF stained for the indicated ICM cell lineage markers (Nanog in green and Gata4, Sox17 and Gata6 in red, plus DAPI DNA stain in blue). Examples of cells classified as TE, PrE and EPI are marked with an asterisk, arrow-head and arrow, respectively. Scale bar = 15µm.

---

### **6.3 p38-Mapk14/11 protects against reactive oxygen species (ROS) induced cell death in the preimplantation blastocyst stage embryo.**

As previously stated in this thesis, inhibition of the p38-Mapk14/11 pathway during blastocyst maturation by SB220025 is associated with increased cell death (Figure 14); most probably accounting for the observed decreases in cell number (both in the TE and ICM). Previous studies have reported that p38-Mapk signalling induces the expression of anti-oxidant genes, under conditions of oxidative stress. For example in response to an increase in reactive oxygen species (ROS), thus promoting cell survival (Gutierrez-Uzquiza *et al.* 2012). As described in the previous section, p38-Mapk14/11 inhibition is known to negatively impact glucose transporter expression, both at mRNA and protein levels, leading to embryo arrest at the morula stage; potentially due to associated glucose deprivation necessary for morula to blastocyst transition (Sozen *et al.* 2015). Studies in various cancer cell lines have revealed that glucose deprivation is very often associated with increases in ROS levels, that are responsible for cytotoxicity and cell death (Graham *et al.* 2012). From these combined reports, it was speculated if a situation of glucose deprivation induced in blastocysts subjected to p38-Mapk14/11 inhibition (+SB220025) may not result in ROS levels that in

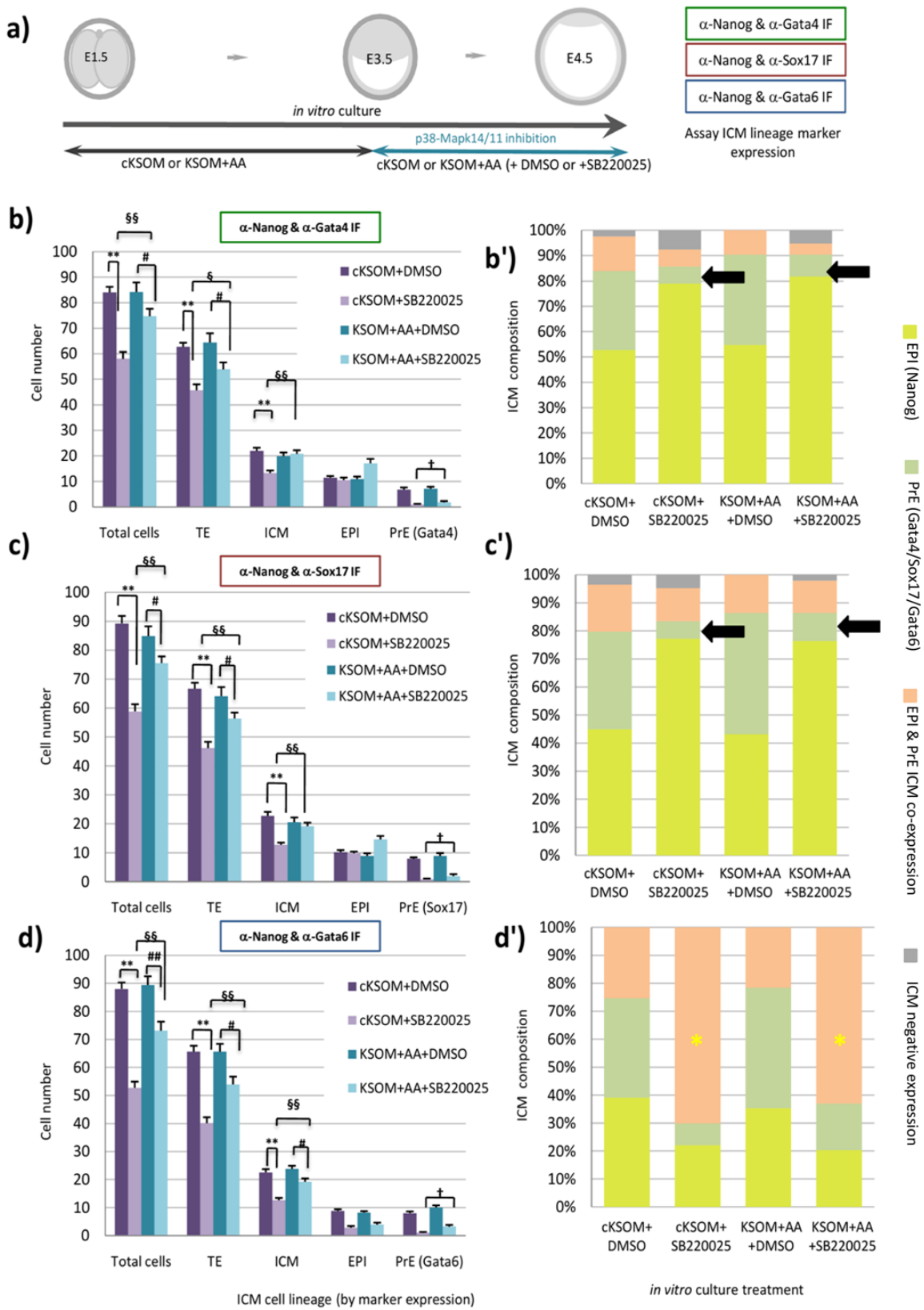


Figure 26. (Legend overleaf)

**Figure 26. p38-Mapk14/11 inhibition during blastocyst maturation (E3.5 – E4.5) in both cKSOM and KSOM+AA media is associated with significant reductions in extra-embryonic lineage cell number.**

**a)** Experimental schema of blastocyst p38-Mapk14/11 inhibition (+SB220025), plus vehicle control (+DMSO), cultured in commercial KSOM without essential and non-essential AA cocktail supplementation (cKSOM) and preparatory KSOM media supplemented with AA (KSOM+AA, as routinely used). The details of antibodies used to analyse ICM cell lineage marker protein expression by immuno-fluorescence (IF) in late blastocysts (E4.5) are given; Nanog & Gata4 (cKSOM, +DMSO=22, +SB220025=24; KSOM+AA, +DMSO n=14, +SB220025 n=18) – green box, Nanog and Sox17 (cKSOM, +DMSO=20, +SB220025=24; KSOM+AA, +DMSO n=17, +SB220025 n=17) – red box, and Nanog and Gata6 (cKSOM, +DMSO=24, +SB220025=22; KSOM+AA, +DMSO n=16, +SB220025 n=17) – blue box.

**b), c) & d)** Averaged contribution of cells to all embryonic lineages, with calculated total cell number and TE number based on DAPI fluorescence and the exclusion of ICM markers respectively, whilst, the ICM lineage number was determined by the exclusive expression of either EPI (Nanog) or PrE (Gata4, Sox17 and Gata6) lineage marker, in each of the stated experimental conditions. Errors are represented as s.e.m. and appropriate/ relevant statistically significant differences, derived from 2-tailed students t-tests, highlighted by one or two significance markers (one, representing  $p < 0.05$  and two denoting  $p < 0.005$ ) described thus; asterisks (\*) showing differences between the 'cKSOM+DMSO' and 'cKSOM+SB220025' groups, the hash tags (#) highlighting significant difference between the 'KSOM+AA+DMSO' and 'KSOM+AA+SB220025' groups, the symbol § denoting the divergence between the 'cKSOM+SB220025' and 'KSOM+AA+SB220025' groups and † indicating the difference in the number of PrE cells, with 'cKSOM+SB220025' having an even less number of PrE less compared to 'KSOM+AA+SB220025' . **b') c') & d')** Averaged percentage makeup of the ICMs of the different stated experimental groups cultured in cKSOM and KSOM+AA in relation to each specified ICM lineage; EPI or PrE (yellow and green, exclusively immuno-stained for either Nanog or Gata4, respectively), EPI & PrE co-expressing cells (orange, representing cells uncommitted to either lineage) and cells negative for either studied lineage marker (grey). The black arrow in **b')** and **c')** panels indicate that irrespective of culture conditions the proportion of PrE defect caused by p38-Mapk14/11 inhibition remains broadly similar in both cKSOM and KSOM+AA media (*i.e.* reduced). In **d')** panel the asterisks (yellow) indicates the increased proportion of Nanog and Gata6 co-expressing uncommitted ICM cells under the p38-Mapk14/11 inhibited conditions cultured in either cKSOM or KSOM+AA. All individual embryo data used in the preparation of this figure are contained within appendix tables T16, T17 and T18

turn could be responsible for the increased incidence of cell death observed. Therefore, to explore the possibility that p38-Mapk14/11 can regulate intracellular ROS levels and thus promote cell survival, early blastocyst (E3.5) stage embryos were cultured to the late blastocyst (E4.5) stage in both cKSOM and KSOM+AA under control (+DMSO) or p38-Mapk14/11 (+SB220025) inhibited conditions in the presence or absence of the characterized anti-oxidant N-acetyl cysteine (NAC) (Kawamura *et al.* 2010). The blastocyst were then fixed and immuno-stained for Nanog (EPI) and Gata4 (PrE) protein expression and analysed by confocal imaging. As depicted in the figure 27b, embryos cultured in cKSOM and treated with SB220025, consistently with respect to and treated with SB220025, consistently with respect to the above elucidated data, displayed a severe defect in both TE and PrE cell number [average cell number of 44.4 (TE) and 0.6 (PrE) in inhibitor group compared to 64.8 (TE) and 6.4 (PrE) in DMSO group,  $p = 7.21^{E-07}$ ;  $p = 1.06^{E-12}$  between TE and PrE values, respectively]. Furthermore, the p38-Mapk14/11 inhibited embryos that were cultured in cKSOM and in the presence of supplemented NAC also showed a similar trend of reduced TE and PrE lineages [average cell number 39.0 (TE) and 0.2 (PrE) in SB220025+NAC against 44.4 (TE) and 0.6 (PrE) in SB220025 group,  $p = 1.60^{E-01}$ ;  $p = 1.81^{E-01}$  between TE and PrE values, respectively]. Indicating that under p38-Mapk inhibited conditions, the addition of the anti-oxidant NAC to cKSOM without AA supplementation was unable to rescue any extraembryonic cell death/ deficit associated with loss of p38-Mapk14/11 activity. However, different results were observed when similar experiments were performed on embryos cultured in KSOM+AA; whilst SB220025 treatment displayed the classical PrE defect with an associated decrease in total ICM and a minor but statistically significant reduction in TE cell number (not as robust as for cKSOM cultured embryos), the supplementation of KSOM+AA with 1mM NAC resulted in rescued numbers of both TE and total ICM cells [68.5 (TE) and 20.0 (ICM) cells on average in SB220025+NAC, opposed to 67.4 (TE) and 20.7 (ICM) average cells in DMSO control,  $p = 7.91^{E-01}$ ;  $p = 6.20^{E-01}$ ]. However and importantly, despite the observed rescue in TE and total ICM cell number, the classically observed PrE deficit phenotype associated with p38-Mapk inhibition was still readily observed. Thus under culture conditions of AA supplementation and increased availability, the antioxidant NAC is able to rescue total ICM and TE cell number deficits associated with p38-Mapk inhibition during blastocyst ICM maturation but not the derivation of PrE cells [2.0 (PrE) average number in SB220025+NAC relative to 7.3 (PrE) in DMSO,  $p = 2.87^{E-10}$ ] (Figure 27c). Furthermore, as adding NAC to KSOM+AA+DMSO resulted in statistically equal numbers of cells in both TE and ICM, NAC does not have any autonomous effects on cell proliferation. Thus it can be reasoned that during blastocyst maturation p38-Mapk14/11 functions to counteract the production of deleterious ROS species that would otherwise contribute to TE and ICM cell death, but that this role is more likely to significant in stress induced conditions associated with reduced AA availability (*i.e.* in cKSOM), as it is not rescuable by NAC anti-oxidant supplementation; whereas it is in KSOM+AA

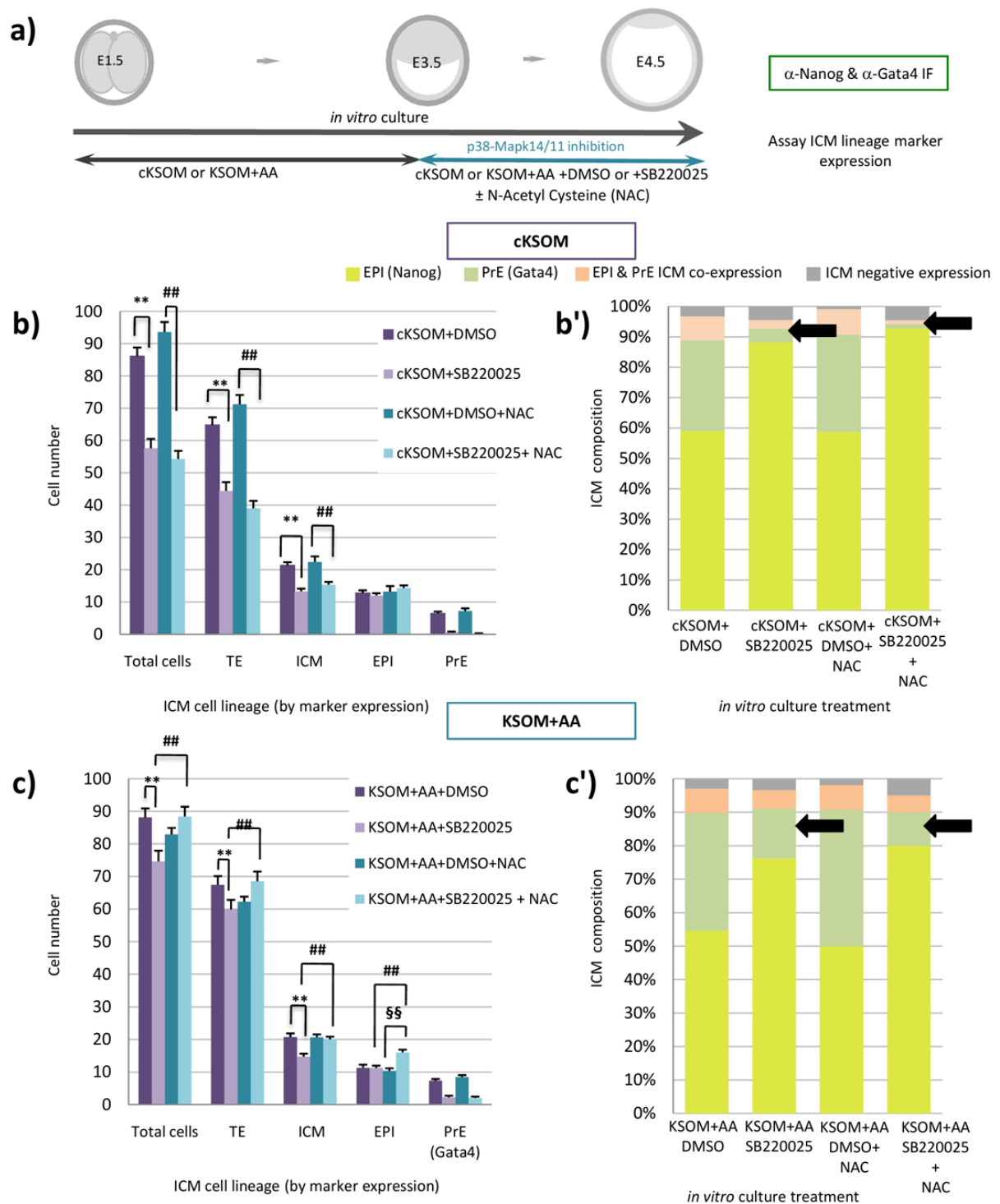


Figure 27. (legend overleaf)

**Figure 27. p38-Mapk protects against ROS induced cell death in the maturing mouse blastocyst stage embryo.** **a)** Experimental schema of blastocyst maturation under p38-Mapk14/11 inhibition (+SB220025), plus vehicle control (+DMSO), and inhibitor & vehicle control conditions & Gata4. In each of the studied late-blastocyst (E4.5) stage conditions; DMSO vehicle control (cKSOM, +DMSO n=27 & KSOM+AA, +DMSO n=24 ), p38-Mapk14/11 inhibition (cKSOM, +SB220025 n=28 & KSOM+AA, +SB220025 n=24), DMSO plus NAC (cKSOM, DMSO+NAC n=13 & KSOM+AA, DMSO+NAC n=17), and p38-Mapk14/11 inhibition plus NAC (cKSOM, SB220025+NAC n=20 & KSOM+AA, SB220025+NAC n=23). **b) & c)** Averaged contribution of cells to all blastocyst lineages, with derived total cell number and TE number based on DAPI fluorescence and the exclusion of ICM markers respectively, whilst, the ICM lineage number was calculated based on exclusive expression of either EPI (Nanog) or PrE (Gata4) lineage marker, in each of the stated experimental conditions. Errors are represented as s.e.m. and appropriate/ relevant statistically significant differences, derived from 2-tailed students t-tests, highlighted by one or two significance markers (one, representing  $p < 0.05$  and two denoting  $p < 0.005$ ) described thus; asterisks (\*) showing differences between the 'cKSOM+DMSO' and 'cKSOM+SB220025' or 'KSOM+AA+DMSO' and 'KSOM+AA+SB220025' groups, the hash tags (#) highlighting significant difference between the 'cKSOM+DMSO+NAC' and 'cKSOM+SB220025+NAC' or 'KSOM+AA+DMSO+NAC' and 'KSOM+AA+SB220025+NAC' groups, and the symbol § denoting the significant divergence in EPI lineage numbers between the 'KSOM+AA+DMSO+NAC' and 'KSOM+AA+SB220025+NAC' groups, (*i.e.* the ICM rescue effect associated with NAC antioxidant supplementation), note that the rescued ICM cell number observed in KSOM+AA cultured embryos under p38-Mapk14/11 inhibition conditions, supplemented with NAC is associated with an increase in EPI cells, but the PrE deficit phenotype persists; indicating that the PrE deficiency observed in non NAC supplemented condition, was not due to cell death but rather a *bona fide* defect in PrE specification **b) & c')** Averaged percentage makeup of the ICMs of different experimental groups cultured in cKSOM and KSOM+AA, p38-Mapk14/11 inhibitor or DMSO control in the presence or absence of NAC in relation to each specified ICM lineage; EPI or PrE (yellow and green, exclusively immuno-stained for either Nanog or Gata4, respectively), EPI & PrE co-expressing cells (orange, representing cells uncommitted to either lineage) and cells negative for either studied lineage marker (grey). The black arrows indicate that irrespective of culture conditions the proportion of PrE defect caused by p38-Mapk14/11 inhibition remains similar in both cKSOM and KSOM+AA supplemented with NAC (despite rescued ICM cell number in KSOM+AA+NAC cultured embryo groups). All individual embryo data used in the preparation of this figure are contained within appendix tables T19 and T20.

media. Moreover, that such a ROS protective role is distinct from its role in governing entry into PrE differentiation. Consistent with this interpretation, the increased incidence of apoptosis (observed by confocal IF imaging for cleaved caspase 3) ordinarily observed in late blastocyst (E4.5) stage embryos matured in the presence of p38-Mapk14/11 inhibition (figure 14) is reduced to levels observed in DMSO control treated groups after supplementing KSOM+AA media with antioxidant NAC (figure 28).

#### **6.4 Concluding summary**

Taken together, the described experiments have uncovered a metabolically associated/ sensitive role for p38-Mapk14/11 (centred on AA availability) during preimplantation mouse blastocyst development. As such, the inhibition of the p38-Mapk14/11 pathway under AA deprived conditions is associated with more severe defects in the emergence of the extraembryonic lineages (TE and PrE), compared to culture conditions of AA supplementation. Moreover, p38-Mapk14/11 acts to protect blastocyst cells (both in the TE and ICM) from oxidative stress, potentially associated with the known generation of enhanced ROS levels at this developmental time. However, this effect is also sensitive to AA availability. Notwithstanding these conclusions, p38-Mapk14/11 inhibition is consistently associated with profound blocks in PrE differentiation, during blastocyst maturation, irrespective of AA availability or anti-oxidant NAC supplementation; indicating p38-Mapk14/11 inhibition does not cause reduced PrE cell numbers in the ICM via a mechanism of selective PrE progenitor cell death (potentially related to induced oxidative stress) but rather acts as *bona fide* block to such cells successful differentiation.

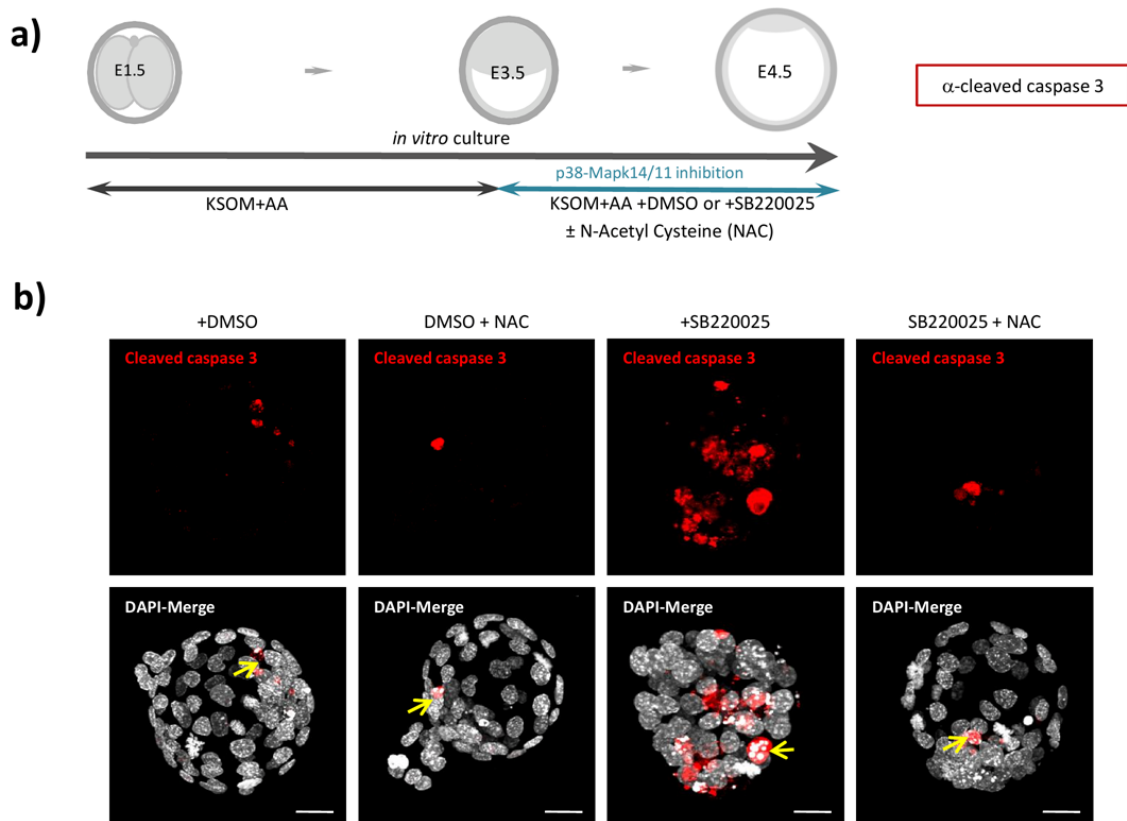


**Figure 28: Increased p38-Mapk14/11 inhibition associated incidence of apoptosis in both TE and ICM cells of KSOM+AA cultured embryos can be reduced in the presence of the antioxidant NAC. a)** Experimental schema by which recovered 2-cell (E1.5) stage embryos were *in vitro* cultured in KSOM+AA until the early blastocyst (E3.5) stage and transferred into media containing the p38-Mapk14/11 inhibitor +SB220025 or +DMSO vehicle control and further cultured to the late/hatching blastocyst (E4.5) in the presence or absence of supplemented NAC. Embryos were fixed and immunofluorescently stained with anti-cleaved caspase 3 antibody for a confocal microscopy-based assay of the incidence of apoptosis. **b)** Exemplar confocal z-plane projections of control (+DMSO & DMSO+NAC) and p38-Mapk14/11 inhibitor treated (+SB220025 & SB220025+NAC) blastocysts; cleaved caspase signal in red, DNA DAPI counterstain in pseudo coloured grey and apoptotic cells represented by yellow arrows. Scale bar = 15 $\mu$ m.

## **7. DISCUSSION**

At the early blastocyst (E3.5) stage, the ICM of mouse embryos presents as a population of apparently bi-potent cells expressing both EPI (Nanog) and PrE (Gata6) markers. Although the extent to which all cells are indeed truly bipotent or biased towards one or the other ICM cell lineages by their previous developmental history (*e.g.* by the relative timing of ICM founder cell internalization) remains open to debate (Morris *et al.* 2013; Mihajlovic *et al.* 2015; Krupa *et al.* 2014; Yamanaka *et al.* 2010 & Ohnishi *et al.* 2014) and further research. However, by the mid blastocyst stage the ICM resolves into a heterogeneous population of cells mutually expressing EPI or PrE markers (*i.e.* the salt and pepper pattern) that then further segregates into the deeply residing EPI population, overlaid by the blastocoel facing PrE monolayer, by the late blastocyst (E4.5) stage. As has been extensively reviewed elsewhere (Hermitte and Chazaud 2014), such ICM maturation is mediated by the antagonistic interactions of Nanog and the active Erk1/2 pathway (functionally downstream of Mek1/2), that is itself potentiated by active receptor tyrosine kinase signalling; and although many studies have elegantly demonstrated, by means of genetic knockout and chemical inhibitor based strategies, some of the key components involved (also reviewed in the introduction section), the initial mechanism that promotes the emergence of the salt and pepper state remains relatively poorly understood. In the present study, p38-Mapk14/11 was found to play an important role in this context and functions prior to, or at least concomitantly with, Erk1/2 pathway activation to promote germane ICM maturation.

The data described in this thesis indicate that inhibition of p38-Mapk14/11 from E3.5 to E4.5 results in a severe PrE deficit. However, notwithstanding such a profound PrE defect, it was nevertheless possible to observe some solely Gata4 positive PrE cells (on average 2.6 cells per embryo in embryos cultured in KSOM supplemented with AAs). The reason why these cells appear insensitive to the administered p38-Mapk14/11 inhibition regime is not clear. However, it may be explained by such cells having already past a temporal PrE commitment point, governed by p38-Mapk14/11, by the developmental time the inhibitor was provided; a commitment point not passed for the remaining ICM cells. Indeed, to avoid causing arrested development at the morula to blastocyst transition [as observed when the p38-Mapk14/1 inhibitor was provided from the 8-cell/E2.5 stage, see figure 7 and in other reported literature (Bell and Watson 2013; Natale *et al.* 2004; Yang *et al.* 2015)] the inhibitor was provided from the E3.5 developmental time-point at the earliest (*i.e.* after specification of the TE and formation of the blastocoel). It is therefore possible the observed p38-Mapk14/11 insensitive cells had embarked to a path of PrE differentiation before E3.5 and moreover, as the activity of the Erk1/2 pathway remains unaffected by p38-Mapk14/11 inhibition (figure 12), such cells were free to respond to these PrE differentiation promoting cues. The fact that a couple of cells, on average, were insensitive to the p38-Mapk14/11 inhibition also

supports the notion that functionally significant heterogeneity amongst cells of the same embryo ICM already exists by the early blastocyst (E3.5) stage. Furthermore, that such p38-Mapk14/11 insensitive cells may have already committed to a path towards PrE differentiation may reflect their ancestral cell history. For example, reports suggest that ICM cells derived from founder cells internalized during the 8- to 16-cell stage transition are biased to form EPI, but that if atypically large numbers of cells are internalized (*i.e.* >3) the extra cells will contribute to PrE, potentially by an Fgf4-dependent mechanism (Krupa *et al.* 2014; Morris *et al.* 2013; Morris *et al.* 2010). It is therefore possible that the p38-Mapk14/11 inhibition insensitive cells observed may be derived from such supernumerary inner cells derived during the 8- to 16-cell stage transition, that have had a comparatively longer time to integrate PrE promoting cues and commit to their fate comparatively early compared with PrE progenitors internalised during the 16- to 32-cell stage transition. Additionally, it is noteworthy that in embryos inhibited for p38-Mapk14/11 under cKSOM culture conditions the PrE defect is more severe, this may be because the specification of cells in ICM towards PrE lineage is happening late compared to the embryos cultured in KSOM supplemented with AAs. This is speculated from the observation that embryos cultured in KSOM+AA cavitate earlier than the embryos cultured in cKSOM (unpublished observation). Alternatively, it would reflect the inherent susceptibility of p38-Mapk14/11 to AA availability (as considered in the previous chapter). Additionally, it is noteworthy that in contrast to inhibiting p38-Mapk14/11 by SB220025, inhibition using SB203580 resulted in an increase in ICM cell number. A recent study found that SB220025 can affect p38 $\delta$ -Mapk 13 function (Kanaji *et al.* 2012), whereas SB203580 affects only p38-Mapk14/11 kinases, thus it is possible that SB220025 inhibitor's influence of p38 $\delta$ -Mapk13 could have affected the ICM cell number; possibly reflecting an anti-oxidant role, specific for p38 $\delta$ -Mapk13.

The present experiments also show that p38-Mapk14/11 inhibition from the early (E3.5) to late blastocyst (E4.5) stages resulted in a significant increase in the number/ proportion of uncommitted ICM cells co-expressing both Nanog and the early PrE marker Gata6 (figure 8 and figure 11); indicating p38-Mapk14/11 activity is required to permit germane progression of ICM cells, through the mutually exclusive salt and pepper expression pattern of EPI and PrE markers, to the fully segregated tissue layers of the mature ICM. However, because this p38-Mapk14/11 inhibition regime also lead to late blastocysts containing on average fewer overall and specifically fewer ICM cells, it could be argued the observed effect of increased numbers/ proportion of uncommitted cells was due to a general temporal delay in development. There are multiple lines of evidence that refute this interpretation. Firstly, whilst p38-Mapk14/11 inhibited embryos on average presented with fewer ICM cells they still contained an appropriate number of EPI cells, equivalent to vehicle control treated embryos, per unit of total ICM cell number, but fewer PrE specified and more uncommitted cells

(figure 13). Secondly, there are examples of embryos in the p38-Mapk14/11 inhibited group that do contain equivalent numbers of ICM cells compared to controls, indicating similar developmental progression, yet these also present with significantly greater numbers of uncommitted cells, fewer PrE specified cells and equivalent EPI specified cells (figure 13). Thirdly, when the p38-Mapk14/11 inhibition was given between the early (E3.5) and mid (E4.0) blastocyst stages and ICM lineage marker expression immediately assayed (figure 16), the p38-Mapk14/11 inhibited embryos comprised significantly enhanced levels of uncommitted/ co-expressing cells, versus the vehicle treated controls, despite presenting with ICMs of statistically equivalent size. Fourthly, the incidence of reduced ICM cell number in p38-Mapk14/11 inhibited embryos is also accompanied by increased incidence of apoptotic cell death in both the ICM and TE (figure 14), potentially accounting for the smaller observed numbers, rather than generally delayed development. Indeed, the total number of ICM cells in the embryos treated with vehicle DMSO control from the early (E3.5) to either mid (E4.0) or late (E4.5) blastocyst stages is statistically equal (approx. 22 cells, indicating a lack of ICM cell division during this twelve hour period) and this number is statistically equal to that observed in p38-Mapk14/11 inhibited embryos cultured to the mid (E4.0) blastocyst stage; thus, the reduced number of ICM cells associated with prolonged p38-Mapk14/11 inhibition to the late (E4.5) blastocyst stage (approx. 2-3 cells versus DMSO control) is most probably accounted for by the observed increase in ICM apoptosis causing a loss of cells and not generally delayed development. Moreover, though the decrease in cell number (TE and ICM) was rescued in KSOM+AA+NAC culture conditions, the PrE defect is still strong (actually the same as without NAC supplementation), also the +NAC mediated rescue of these ICM cells that would have ordinarily died does not lead to extra PrE, but solely extra EPI cells (*i.e.*, the antioxidant effect can be separated from cell fate effect; indicating extra cells cannot differentiate). Furthermore, in p38-Mapk14/11 inhibited experimental conditions using lower SB220025 concentrations (data not shown), the ICM cell number was found to be equal with vehicle (+DMSO) controls but assayed PrE numbers were still robustly and significantly decreased; again separating the cell survival role from the cell-fate regulating p38-Mapk14/11 function. Hence, the compound data is interpreted as a true indication of a p38-Mapk14/11 mediated role for resolving the fate of uncommitted ICM cells towards the PrE.

It has also been discovered that the timing of the p38-Mapk14/11 inhibition sensitive developmental window, in relation to the separation of ICM cell lineage fate, overlaps with the earliest stages of blastocyst maturation, becoming insensitive by the E3.75 stage (although as acknowledged above, it may also precede the E3.5 stage, but the observed inhibitor induced morula to blastocyst transition block, associated with temporally earlier drug administration, precludes a direct assay). Moreover, that a pulse treatment of p38-Mapk14/11 inhibition between the early

(E3.5) and mid (E4.0) blastocyst stage is sufficient to achieve the same PrE/ ICM defects at the late (E4.5) blastocyst stage as observed by continual inhibition. However, it was also discovered that during this same developmental window, Mek1/2 activity appears dispensable; as evidenced by the fact embryos can be cultured in Mek1/2 inhibitor between the early (E3.5) and mid (E4.0) blastocyst stages and then released back into normal growth media and still correctly specify and segregate the late (E4.5) blastocyst ICM cell lineages (figure 15). Moreover, it was found that Mek1/2 inhibition sensitive effects on PrE derivation were also observable (all be they progressively weaker) at developmental time points after which p38-Mapk14/11 inhibition had no effect; for example when the drug was administered from E3.75 or E4.0 to the late blastocyst (E4.5) stage (figure 15); in agreement with previous data combining Mek1/2 and Fgfr inhibition in similar experiments (Yamanaka *et al.* 2010). It is of note that the emergence of p38-Mapk14/11 inhibition insensitivity at E3.75 is temporally coincident with the initial appearance of the salt and pepper expression pattern of mutually exclusive EPI (Nanog) and PrE (Gata6/ Sox17) markers (Chazaud *et al.* 2006). Moreover, that p38-Mapk14/11 inhibition also results in statistically significant elevated levels of uncommitted cells (be it at the mid/ E4.0 or late/ E4.5 blastocyst stages, figures 16 and 8, respectively) that are apparently unable to fully differentiate (evidenced by the substantially reduced numbers/ ICM proportion of cells expressing the late PrE marker, Gata4, at the late blastocyst stage, figures 8 and 15). Such uncommitted cells appear to resist differentiation, despite the presence of a non-inhibited and a partially/ temporally downstream active Mek1/2 (Erk1/2) pathway [*n.b.* p38-Mapk14/11 inhibition does not alter levels of activated Erk1/2(p), figure 12], known to ordinarily induce PrE formation. Given that the uncommitted cells, by definition express Nanog, and that continued Nanog expression in mouse embryos and ES cells is known to prevent differentiation (Mitsui *et al.* 2003; Silva *et al.* 2009), the present data support a role for p38-Mapk14/11 in governing the commitment of ICM cells to fully enter into the PrE differentiation program by down-regulating Nanog expression and becoming receptive to Mek1/2 directed mechanisms of differentiation. Indeed, other ES cell studies have identified just such a role for p38-Mapks in regulating entry in to cardiac or neurogenic differentiation (Barruet *et al.* 2011) or being the targets for functional Bmp4-derived inhibition, resulting in the promotion of self-renewal (Qi *et al.* 2004). Moreover, other reports have shown that small molecule inhibition of p38-Mapks results in the promotion of naïve pluripotency in primate and human stem cell cultures, *in vitro* (Fang *et al.* 2014; Gafni *et al.* 2013; Weinberger *et al.* 2016). Interestingly, although it was found that functional Mek1/2 sensitivity temporally extended beyond that of p38-Mapk14/11, the study did find that the extreme PrE deficit phenotype (resulting in a virtual absence of Gata4 positive ICM cells) observable after prolonged Mek1/2 inhibition alone [from either the 8-cell/ E2.5 (data not included) or early blastocyst/ E3.5 to late/ E4.5 blastocyst stages, figure 15] could be partially rescued using the microinjected, p38-Mapk14/11 activating,

Mkk6-EE mRNA construct (data not shown). Such data imply that whilst Mek1/2 inhibition is very successful in blocking full PrE differentiation to Gata4-alone expressing ICM cells, some otherwise uncommitted cells, co-expressing Nanog and early PrE markers (*e.g.* Gata6) may exist after Mek1/2 inhibition and that enhanced levels of p38-Mapk14/11, caused by Mkk6-EE expression, may be sufficient to drive these cells to fully differentiate to PrE. Consistent with this theory, after Mek1/2 inhibition from the early (E3.5) to late (E4.5) blastocyst stages, the ICM of treated embryos do indeed contain a number of uncommitted Nanog and Gata6 co-expressing cells (data not shown). Also it is interesting that the profound PrE-deficit phenotypes associated with Mek1/2 inhibition are associated with large increases in EPI number/ proportion, despite the presence of non-inhibited p38-Mapk14/11. Therefore, it is probable that some ICM cells that had resolved from their uncommitted state, by the action of p38-Mapk14/11 causing reduced Nanog levels, may reactivate *Nanog* expression as a default response to the lack of active and Mek1/2 driven PrE differentiation.

The role of Mek1/2 in activating the Erk1/2 pathway downstream of Fgfr activation during the emergence of PrE has been well described (Kang *et al.* 2013; Yamanaka *et al.* 2010; Nichols *et al.* 2009 and Frankenberg *et al.* 2011) but the data presented here suggest that activation of the same receptor also leads to functional activation of p38-Mapk14/11 that is relevant for full entry into PrE differentiation. Indeed, a retrospective review of the literature supports a mechanism by which activated Fgfr activates two distinct mitogen-activated protein kinase pathways during PrE differentiation. For example, it is known that the ICMs of *Fgf4*<sup>-/-</sup> null embryos fail to express Gata6 or a transgenic Pdgfra promoter driven early PrE reporter gene at the early blastocyst (E3.5) stage, indicative of a block in PrE specification. However, if wild-type embryos are treated with Mek1/2 inhibitor from the 8-cell (E2.5) stage, in combination with a Gsk3- $\beta$  inhibitor they are able to express the same early PrE reporter gene (Kang *et al.* 2013). Hence, the functional inhibition of just one component downstream of the Fgfr is not able to phenocopy the absence of the activating ligand, thus suggesting the existence of at least one other functional pathway acting beneath the receptor itself, most likely to involve p38-Mapk14/11 as described here. Indeed, there are numerous non-preimplantation mouse embryo related studies reporting incidences of p38-Mapk pathway activation consequent to Fgf-based signalling (Matsumoto *et al.* 2002; Tan *et al.* 1996 and Sorensen *et al.* 2008) and more recently, Fgfr2 mediated Fgf2 signalling has been demonstrated to depend on the p38-Mapk pathway to regulate TE development in mouse preimplantation embryos (Yang *et al.* 2015). Furthermore, genetic evidence from models of T-cell activation suggest that Grb2, most often considered in the preimplantation mouse embryo context for its potential role of activating the Erk1/2 pathway (via Mek1/2) to promote PrE differentiation in the ICM (Chazaud *et al.* 2006), can also activate p38-Mapks (plus Jnks) in manner that is preferential to its activation of Erk1/2 (Gong *et*

*al.* 2001). Hence, there exists precedent for Fgfr mediated activation of the p38-Mapk pathway, from both the earlier stages of preimplantation mouse embryo development and other cellular/developmental systems. Moreover, that these precedents are similar to the Fgfr results described, in conjunction with Mek1/2 (Erk1/2) activation and in the context of ICM cell-fate resolution, herein. Interestingly, the chemical inhibition of Fgfr in preimplantation embryos only reduced, rather than abolished, detectable levels of activated phosphorylated p38-Mapk14/11(p) (figure 17), suggesting multiple activating inputs are in play, as would be in keeping with the known general biology of p38-Mapks (Cuadrado and Nebreda 2010). Indeed, it was found that chemical inhibition of the catalytic activity of the serine/ threonine kinase Tak1 (also known as Mekk7/Map3k7) also reduces the levels of activated p38-Mapk14/11(p) in the preimplantation mouse embryo (figure 17). Moreover, Tak1 has previously been described as being a component of the non-canonical and Smad-independent pathway of Bmpr mediated/directed PrE differentiation in mouse blastocyst ICMs (Graham *et al.* 2014) and the results of the Tak1 inhibition (using 5Z-7-Oxozeanol) presented here (figure 20), are consistent with this earlier study. Despite having a broad range of substrate specificity, Tak1 is known in other cell contexts to target and activate the p38-Map14/11 specific activating Map2k kinases Mkk6 and Mkk3 (Huang *et al.* 2006; Xin *et al.* 2011), suggesting that it is by failing to activate one or both of these intermediate kinases, that Tak1 inhibition leads to reduced levels of activated p38-Mapk14/11(p); this assertion is substantiated by the fact PrE deficits caused by Tak1 inhibition can be rescued by over-expression of the constitutively active Mkk6-EE mutant (figure 20). Hence, it would appear that p38-Mapk14/11 activation, and the attendant full entry of mouse blastocyst ICM cells into PrE differentiation, is under the control of at least two independent cell signalling pathways, based on secreted Fgf- and Bmp-ligands. Although, it is noteworthy that activated Fgfr3-based signalling has been shown to be Tak1 dependent in the context of multiple myeloma and bladder cancers (Salazar *et al.* 2014), therefore not excluding the possibility that mouse blastocyst Fgf-signalling may also activate Tak1 (indicated by the dashed arrow in the model present in figure 29). Further, the decrease in the total cell number observed in Mkk6-EE microinjected embryos (figures 19 and 20) are most probably attributed to the hyper-activation of p38-Mapk14/11 from the early stages prior to morula. It would therefore be advantageous to have a system by which Mkk6-EE expression could be tightly temporally controlled. This issue could be addressed by using a transgenic mouse models harbouring a TET-ON (tetracycline- on) inducible Mkk6-EE activation genetic system, that would enable Mkk6-EE activation at a specific stage; in the present context, the late morula stage. Moreover, such a system could be employed to overexpress dominant negative constructs of p38-Mapk14/11 during the sensitive early blastocyst stages of ICM maturation. If the presence of other isoforms block the desired phenotype, the dominant negative forms of other two p38-Mapks (*i.e.* p38-Mapk12/13) could also be employed.

Activated p38-Mapk14/11(p) have been implicated in the phosphorylation of a plethora of downstream target proteins, in a wide range of cellular contexts, with functional consequences for such fundamental processes as protein turnover, transcription and chromatin remodelling and cytoskeleton structure (Cuadrado and Nebreda 2010). With such a broad spectrum of potential downstream functional effects it is, and has proved, difficult to identify those responsible for the p38-Mapk14/11 inhibition mediated effects, in relation to ICM cell-fate specification and segregation. As discussed above, the phenotype that was observed is best described as a block of uncommitted cells to resolve their fate and in particular, fully initiate their differentiation towards PrE. Consequently, a series of experiments were conducted, cognisant of this commitment block, to try and resolve the mechanism behind the p38-Mapk14/11 inhibition phenotype, but to no avail. These included, assaying for the relative abundance of phospho-specific forms of Nanog [Nanog(p)], that in ES cells have been shown to destabilise the protein and thus potentiate differentiation [by the action of Erk1/2, (Kim *et al.* 2014)], but no differences could be observed between control and p38-Mapk14/11 inhibited embryo groups [although not all the necessary antisera to probe all the known Nanog(p) isoforms were available to this study] (figure 21). Similarly, no differences were observed in the protein expression of Zscan10, a known ES cell pluripotency-related factor (Wang *et al.* 2007) whose paralogous gene, *Mzf1*, is listed as a p38-Mapk14 substrate in the 'phosphosite.org' database and the stability of which is sensitive to p38-Mapk phosphorylation, were uncovered (figure 21b). Further, over-expressing the known p38-Mapk14/11 effector kinase, Mk3 (also known as Mapkapk3), in an attempt to overcome the p38-Mapk14/11 inhibition mediated, uncommitted ICM cell phenotype was also attempted. This was because activated phosphorylated Mk3 has been shown to phosphorylate the Gata6 interacting and stabilising poly-comb group (PcG) protein Bmi1 (Lavial *et al.* 2012), leading to its instability and degradation (Voncken *et al.* 2005); hence it was speculated that p38Mapk14/11 inhibition might be stabilising Bmi1 and so Gata6, thus contributing to the assumed uncommitted cell fate state, by a failure to activate Mk3. However, over-expression of a constitutively activated Mk3 mRNA had no effect on the p38-Mapk14/11 inhibition mediated ICM phenotype (figure 24). An attempt to rescue the phenotype by over-expressing a constitutively activated form of another confirmed p38-Mapk14/11 effector, Msk1; known to promote transcriptional activation (potentially of target genes required for full entry into PrE differentiation) by phosphorylating chromatin on histone H3 (at serines-10 and -28) to repel PcG protein binding (Soloaga *et al.* 2003) was also undertaken. However, Msk1 over-expression in the early stage of preimplantation mouse embryo was associated with cell division arrest (data not shown) and direct pharmacological inhibitor targeting of the Msk1 protein, during blastocyst maturation, had no effect on ICM lineage specification and segregation (data not shown). Similarly the over-expression of the histone acetyl-transferase Atf2 [actually a constitutively active fusion protein of human ATF2 linked

to the transcriptional activation domain of CREB, (Steinmuller and Thiel 2003)], another well characterised downstream p38-Mapk14/11 effector (Breitwieser *et al.* 2007), was also unable to rescue the p38-Mapk14/11 inhibition mediated uncommitted ICM phenotype (figure 23). Interestingly it actually caused reduced PrE contribution with an increased proportion of EPI cells compared to DMSO treated control embryos. Lastly, given that PrE-like differentiation in F9 teratocarcinoma cells has been shown to require p38-Mapk14/11 mediated inhibition of Gsk3- $\beta$  function (Bikkavilli *et al.* 2008), it was tested if the observed uncommitted ICM phenotype could be rescued by direct pharmacological inhibition of Gsk3- $\beta$  itself and found that it could not (figure 22). As referenced above, the potential wide range of downstream p38-Mapk14/11 effectors and pathways makes it difficult to identify any one in isolation as a candidate for the observed ICM specification defects in the present thesis. Notwithstanding, a substantial and concerted effort was made to mechanistically assay candidate effector components functionally downstream of p38-Mapk14/11 activation. It is possible that the failed attempts to rescue the observed ICM phenotype, as described above, may largely reside in the fact that p38-Mapk14/11 touches many related and important effector pathways and that the perturbation of just one of many, may not be sufficient to reveal a mechanistic role. Therefore a more empirical approach to identify the relevant p38-Mapk14/11 effector is required. Accordingly a current approach utilising mass spectrometry to identify changes in the abundance of specific phospho-protein levels, across the whole phospho-proteome, subsequent to p38-Mapk14/11 blastocyst maturation inhibition is being developed.

Studies using non-embryonic and embryonic models have well documented the functional interplay between dynamic metabolism and p38-Mapk signalling (Gehart *et al.* 2010). For example, it has been demonstrated that active p38-Mapk is required to enhance Glut4 transporter translocation to the plasma membrane of ischaemic porcine myocardial cells to enhance glucose uptake and protect them from necrotic cell death (McFalls *et al.* 2004). Additionally, under amino acid starvation conditions, glucose has been found to promote autophagy (a catabolic process that allows extraction of amino acids by degradation of cytoplasmic components under starvation conditions) in NIH 3T3 cell lines (embryonic fibroblasts) in a p38-Mapk dependent manner (Moruno-Manchón *et al.* 2013). Other studies involving animal cell lines have also demonstrated conflicting roles for p38-Mapk during amino acid sensing as both a positive and negative regulator in mediating autophagy. In one study activated p38-Mapk14 was found to compete with the autophagy promoting protein Atg9 for binding to the p38-Mapk interacting protein (p38IP), a positive regulator of Atg9 mediated autophagy; thus under p38-Mapk14 activation conditions, the phosphorylated p38-Mapk14 preferentially binds the p38IP protein, leading to a reduction in Atg9 dependent autophagy (Webber *et al.* 2010). Conversely, under amino acid deprived conditions, glucose has been found to promote

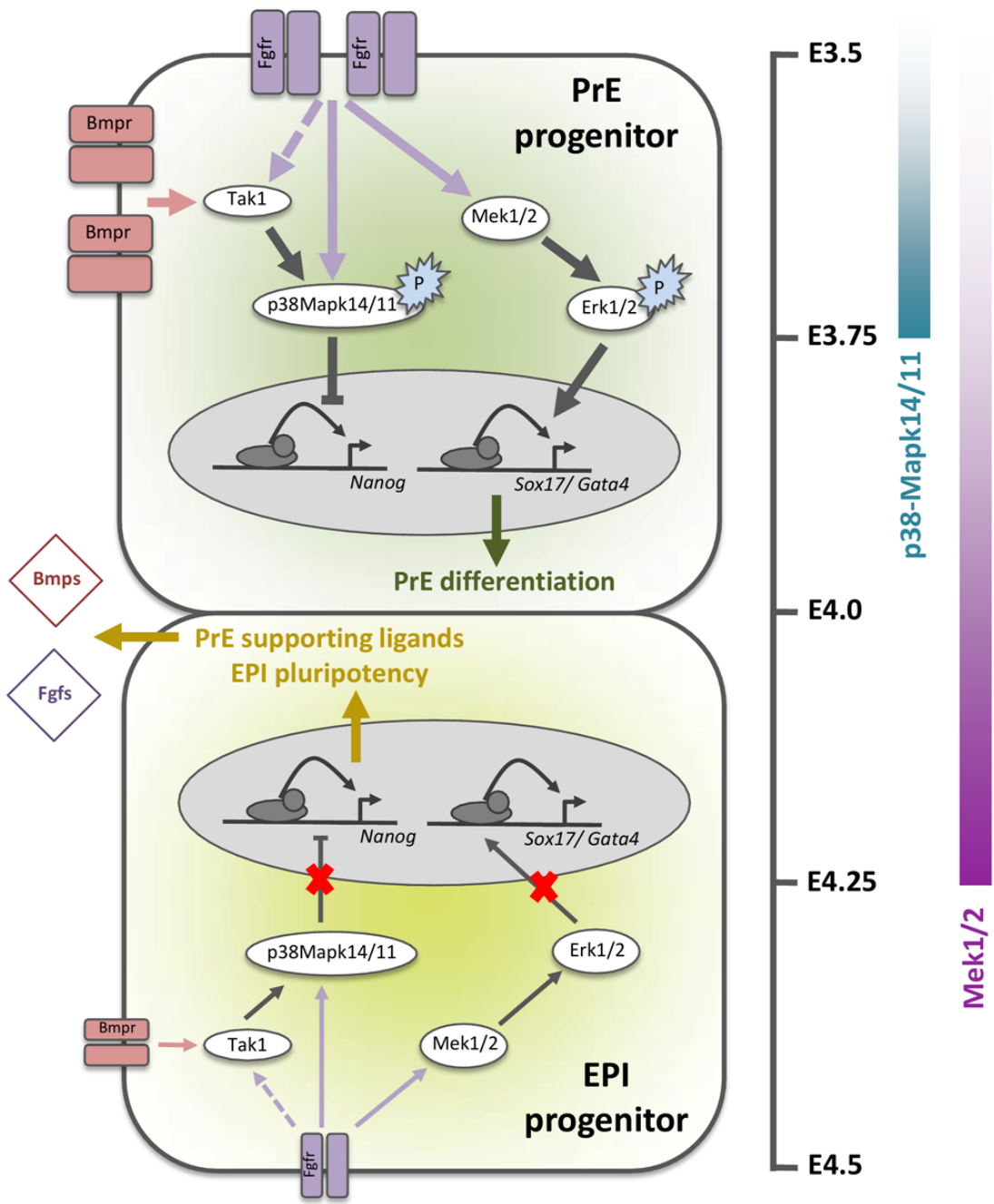


Figure 29. (legend overleaf)

**Figure 29: Revised model of PrE and EPI cell-fate specification and segregation during mouse blastocyst ICM maturation.** In PrE progenitors, activated/ liganded Bmp and Fgf receptors cause the activation of p38-Mapk14/11, via a mechanism at least partly dependent on Tak1 (note, theorised activation of Tak1 functionally downstream of Fgf receptors is denoted by dashed line). Activation of p38-Mapk14/11, before E3.75, inhibits the expression the pluripotency marker Nanog. Simultaneously, and for a period after E3.75 (until E4.25), activation of Mek1/2 and downstream Erk kinases (Erk1/2), also functionally down-stream of Fgf receptor signalling, promotes the expression of PrE markers (e.g. *Sox17* and *Gata4*) required to drive PrE cell fate. Hence the combined effect of activating both p38-Mapk14/11 and Mek1/2 contributes to the emergence of the so-called ‘salt and pepper’ pattern of exclusive PrE and EPI ICM marker protein expression, that arises from initially uncommitted cells expressing both *Nanog* and the early PrE marker *Gata6*, at around the E3.5 – E4.0 developmental window. Ultimately, the derived salt and pepper pattern resolves into the two segregated ICM lineages by the late blastocyst (E4.5) stage. Alternatively, in EPI progenitors an insufficiency of p38-Mapk14/11 and Mek1/2 activating signalling (due to relatively reduced expression levels of Fgf and Bmp receptors) fails to block Nanog or induced required PrE-related gene expression, respectively. Consequently, Nanog levels remain high and PrE differentiation is resisted in favour of retention of pluripotency. This effect also augments the expression of secreted Bmp- and Fgf-related ligands that further reinforce the promotion of PrE differentiation of neighbouring receptive cells, in a paracrine manner.

---

autophagy in a p38-Mapk dependent manner (Moruno-Manchón *et al.* 2013). Glucose is a key nutrient supplement in preimplantation mouse embryo culture media, since it is required for the transition from the morula to blastocyst stage (Brown, Whittingham. 1991). A recent study investigating p38-Mapk signalling in the early pre-blastocyst, stage mouse preimplantation embryo has found that under pharmacologically induced p38-Mapk inhibited conditions, the glucose transporters *Glut1* and *Glut4* are down-regulated both at mRNA and protein levels leading to a reduction in glucose uptake and embryonic arrest at morula stage (Sozen *et al.* 2015). It was speculated in this report that inhibiting p38-Mapk14/11 from the early blastocyst (E3.5) to late blastocyst (4.5) stage might also lead to similar reductions in glucose availability. Therefore, since, supplemented amino acids in preimplantation embryo culture media are potentially an alternative source of carbon and given the findings that p38-Mapk signalling senses and responds to amino acid availability (Casas-terradas *et al.* 2008; Moruno-Manchon *et al.* 2013), it was assayed whether under p38-Mapk14/11 inhibition, the presence or absence of amino acid supplementation in embryo culture media could influence blastocyst cell lineage development. Accordingly, embryos were

cultured in the presence of SB220025 from E3.5 to E4.5 in KSOM media supplemented with AA cocktail (KSOM+AA) or a commercially obtained KSOM (cKSOM); that contained only L-glutamine and BSA as its AA source. Consistent with the previous observation p38-Mapk14/11 inhibition in KSOM+AA showed a severe PrE deficit and a minor but statistically significant reduction in TE cell number and an increase in Nanog positive EP-like cells (*n.b.* IF was conducted against Nanog and Gata4). On the other hand, embryos inhibited in cKSOM, displayed a more severe cell number reduction in both TE and PrE (and hence ICM as a whole) than their KSOM+AA counterparts, while the EPI number remained similar to the control. These data indicate that the extraembryonic lineages are specifically susceptible to AA availability in a manner dependent on p38-Mapk (14/11) activity, thus confirming a functional link between p38-Mapk activity and metabolism in the preimplantation stage embryo/blastocyst. However and crucially consistent with the previous data discussed herein the inhibitor treated embryos in cKSOM also displayed profound PrE defects, similar yet slightly stronger to those observed in the KSOM+AA cultured embryos, demonstrating that media composition does not alter the cell fate regulating role of p38-Mapk. The identification of a link between on p38-Mapk signalling and its sensitivity towards AA availability is of particular interest in relation to DOHaD (Developmental Origin of Health and Diseases, discussed in the introduction). For example, recent studies have demonstrated the importance of AA availability in extraembryonic tissue development in preimplantation mouse embryos, eventually affecting behavioural patterns, blood pressure, body mass and cardiovascular functions in adult mice (Fleming *et al.* 2015). Consistent with this, *p38-Mapk14*<sup>-/-</sup> knockout mice, present with an embryonic lethality that is associated with a massive reduction in myocardial cells due to placental defects affecting the proper supply of oxygen and nutrients to the developing embryonic heart (Adams *et al.* 2000). Thus, apart from the already suggested role of mTOR (specifically in its role to sense branched chain AA availability) in DOHaD (Fleming *et al.* 2015), it will be interesting to investigate in the light of data presented her, a potential role for p38-Mapk14/11 in preimplantation extraembryonic tissue AA signalling and potential knock on consequences for the developmental origin of health and disease (DOHaD) hypothesis.

The transit of *in vitro* cultured embryos from the morula to blastocyst stage is known to be associated with increased oxygen consumption and enhanced production of reactive oxygen species (ROS) (Leese HJ. 2012). In general, an increase in ROS levels is associated with an arrest in cellular growth and subsequent apoptosis (Thannickal VJ & Fanburg BL. 2000). p38-Mapk signalling is sensitive to stress related stimuli, including ROS and p38-Mapk has been found to up-regulate various anti-oxidant genes to ameliorate the negative impact of high ROS levels, responsible for cell death if not kept under tight control (Gutiérrez-Uzquiza *et al.* 2012). In the experiments described

herein, associated with p38-Mapk inhibition, an increase in apoptosis was observed that was postulated to be caused by induced and abnormally high levels of ROS, thus contributing to the observed decrease in TE and ICM cell number. To test this theory of p38-Mapk inhibition induced ROS accumulation, experiments in which embryos were cultured in both cKSOM and KSOM+AA in the presence or absence of SB220025 and the antioxidant NAC were undertaken. As described previously, NAC did not rescue the cell number defect under cKSOM culture conditions, but it did rescue the total TE/ICM cell number defect in the KSOM+AA cultured embryos; although the PrE defect was maintained in both culture mediums. There are two possible mechanisms that could explain the selective cell number rescue in the KSOM+AA group; firstly, AAs apart from functioning as the building blocks of proteins and peptide molecules can in themselves act as antioxidants, (especially the acidic and basic groups and AAs containing sulphhydryl moieties) (Udenigwe CC & Aluko RE. 2011). In fact NAC is a derivative of the amino acid L-cysteine (*i.e.* contains a sulphhydryl group) that has also been demonstrated to be a metabolic precursor in the formation of the antioxidant peptide glutathione (Wu *et al.* 2004). Thus, it is possible that a combination of a general anti-oxidant effect provided by specific AAs in the supplemented cocktail in KSOM+AA media, along with NAC, could have contributed to the rescued reduction in cell number associated with p38-Mapk14/11 inhibition. Alternatively, as mentioned in the previous section, p38-Mapk14/11 can also positively regulate the catabolic autophagic pathway, under starvation conditions to keep AA supply in balance. Thus, the second possibility may be that p38-Mapk along with regulating the induction of specific anti-oxidant genes, might function as part of internal/ intra-cellular AA homeostatic system by positively influencing autophagy. Thus in cKSOM media the embryo could well be more dependent on the recycled AAs generated by autophagy due to a lack of supplemented AAs, meaning the inhibition of p38-Mapk14/11 and hence autophagy has a more profound negative effect on individual cell survival. Whereas, in the presence of exogenous AA supplementation (*i.e.* in KSOM+AA media) the embryo is able to obtain sufficient AA supply from the external source, rendering p38-Mapk14/11 dependent activation of autophagy dispensable for cell survival. Further, the minor extraembryonic cell number defect observed in such embryos cultured in KSOM+AA may be attributable to the high ROS levels known to be associated with p38-Mapk14/11 inhibition (Gutiérrez-Uzquiza Á *et al.* 2012). However, such induced ROS levels are able to be rescued by the anti-oxidant effect imparted by the presence of NAC, something not possible in embryos cultured in cKSOM. Notwithstanding these informed conjunctures the combined data from observing the effect on total TE/ ICM cell number in p38-Mapk14/11 inhibited embryos cultured in KSOM supplemented, or not, with additional AAs and/or NAC is that p38-Mapk14/11 activity is required to modulate/ regulate the presence of cell toxic ROS, in a manner actually sensitive to overall AA availability.

## **8. Overall Conclusion**

In conclusion, the present study reports how Fgfr and non-canonical Bmpr/Tak1 mediated cell signalling converge upon and activate p38-Mapk14/11 during a critical early window of blastocyst maturation contributing to the germline specification and segregation of the ICM cell lineages. The study also shows how this activation is indispensable and required for the resolution of uncommitted cells to begin their full differentiation towards a PrE fate; concomitantly and then subsequently facilitated by the classically appreciated active Mek1/2 (and hence Erk1/2) signalling pathway. Therefore, within the context of the maturing mouse blastocyst ICM, the activation of p38-Mapk14/11 can be considered as the 'enabler' of PrE differentiation, whilst activation of Mek1/2 is the 'driver' (summarised in figure 29). Further, it was discovered that p38-Mapk14/11 inhibition (and hence function) is sensitive to amino acid availability in a manner that affects its role as a protector of ROS induced cell death/damage. It will be of great interest to uncover the functionally downstream mechanisms by which p38-Mapk14/11 executes its PrE differentiation enabling role and how via sensing amino acid availability it contributes to the emergence/survival of the extraembryonic lineages in future studies.

## **9. References**

- Abell AN, Granger DA, Johnson GL. MEKK4 stimulation of p38 and JNK activity is negatively regulated by GSK3 $\beta$ . *J. Biol. Chem.* 282:30476–30484. (2007).
- Adams RH. Essential role of p38 $\alpha$  MAP kinase in placental but not embryonic cardiovascular development. *Mol. Cell.* 6:109-116. (2000).
- Aiken CEM, *et al.* The direct measurement of embryogenic volume and nucleo-cytoplasmic ratio during mouse preimplantation development. *Reproduction.*128:1–10. (2004).
- Alers S, *et al.* Role of AMPK-mTOR-Ulk1/2 in the regulation of autophagy: cross talk, shortcuts, and feedbacks. *Mol. Cell Biol.* 32:2-11. (2012).
- Amiri I, *et al.* The effect of nitric oxide on mouse pre-implantation embryo development and apoptosis. *Iran. Biomed. J.* 7, 107–111. (2003).
- Arman E, *et al.* Targeted disruption of fibroblast growth factor (FGF) receptor 2 suggests a role for FGF signalling in pregastrulation mammalian development. *Proc. Natl. Acad. Sci. U S A.* 95:5082-5087. (1998).
- Arthur JS. and Ley SC. Mitogen-activated protein kinases in innate immunity. *Nat. Rev. Immunol.* 9:679-692. (2013).
- Arthur JS. MSK activation and physiological roles. *Front. Biosci.*13:5866–5879. (2008).
- Avilion AA, *et al.* Multipotent cell lineages in early mouse development depend on SOX2 function. *Genes & Dev.* 17:126–140. (2003).
- Azzolin L, *et al.* YAP/TAZ incorporation in the  $\beta$ -catenin destruction complex orchestrates the Wnt response. *Cell.* 158:157-170. (2014).
- Barruet E, *et al.* p38 mitogen activated protein kinase controls two successive-steps during the early mesodermal commitment of embryonic stem cells. *Stem Cells Dev.* 20:1233-1246. (2011).
- Bell CE. and Watson AJ. p38 MAPK regulates cavitation and tight junction function in the mouse blastocyst. *PLoS One.* 8:e59528. (2013).
- Ben-Levy R, *et al.* Nuclear export of the stress-activated protein kinase p38 mediated by its substrate MAPKAP kinase-2. *Curr. Biol.* 8:1049–1057. (1998).
- Bikkavilli RK, Feigin ME, Malbon CC. p38 mitogen-activated protein kinase regulates canonical Wnt-beta-catenin signaling by inactivation of GSK3beta. *J. Cell Sci.* 121:3598-3607. (2008).
- Boyer L A, *et al.* Core transcriptional regulatory circuitry in human embryonic stem cells. *Cell.* 122:947–956. (2005).

Brancho D, *et al.* Mechanism of p38 MAP kinase activation in vivo. *Genes & Dev.* 17:1969–1978. (2003).

Brewer JR, *et al.* Fgfr1 regulates development through the combinatorial use of signaling proteins. *Genes & Dev.* 29:1863-1874. (2015).

Brown JJ. and Whittingham DG. The roles of pyruvate, lactate and glucose during preimplantation development of embryos from F1 hybrid mice in vitro. *Development.* 112:99-105. (1991).

Bu S, *et al.* Dual effects of nitric oxide on meiotic maturation of mouse cumulus cell-enclosed oocytes in vitro. *Mol. Cell Endocrinol.* 207:21-30. (2003).

Cao W, *et al.* Acetylation of mitogen-activated protein kinase phosphatase-1 inhibits Toll-like receptor signaling. *J. Exp. Med.* 205:1491–1503. (2008).

Cargnello M. and Roux PP. Activation and function of the MAPKs and their substrates, the MAPK-activated protein kinases. *Microbiol. Mol. Biol. Rev.* 75:50-83. (2011).

Casas-Terradellas E, *et al.* ERK and p38 pathways regulate amino acid signalling. *Biochim. Biophys. Acta.* 1783:2241-2254. (2008).

Cavalli V, *et al.* The stress-induced MAP kinase p38 regulates endocytic trafficking via the GDI:Rab5 complex. *Mol. Cell.* 7:421–432. (2001).

Chambers I, *et al.* Functional expression cloning of Nanog, a pluripotency sustaining factor in embryonic stem cells. *Cell.* 113:643–655. (2003).

Chason RJ, *et al.* Environmental and epigenetic effects upon preimplantation embryo metabolism and development. *Trends in Endo. and Metab.* 22:412–420. (2011).

Chazaud C, *et al.* Early lineage segregation between epiblast and primitive endoderm in mouse blastocysts through the Grb2-MAPK pathway. *Dev. Cell.* 10:615-624. (2006).

Chen C, *et al.* TSC-mTOR maintains quiescence and function of hematopoietic stem cells by repressing mitochondrial biogenesis and reactive oxygen species. *J. Exp. Med.* 205:2397–2408. (2008).

Chen L, *et al.* Cross-regulation of the Nanog and Cdx2 promoters. *Cell Res.* 19:1052–1061. (2009).

Chen Z, *et al.* MAP kinases. *Chem. Rev.* 101:2449-76. (2001).

Cheng AM, *et al.* Mammalian Grb2 regulates multiple steps in embryonic development and malignant transformation. *Cell.* 95:793-803. (1998).

Chen Z, *et al.* MAP kinases. *Chem. Rev.* 101(8):2449-2476. (2001).

Chi MM, *et al.* Decreased glucose transporter expression triggers BAX-dependent apoptosis in the murine blastocyst. *J. Biol. Chem.* 275(51):40252-40257. (2000).

Cho SW, *et al.* Dual modulation of the mitochondrial permeability transition pore and redox signaling synergistically promotes cardiomyocyte differentiation from pluripotent stem cells. *J. Am. Heart Assoc.* 3:e000693. (2014).

Clayton L, Hall A, Johnson MH. A role for Rho-like GTPases in the polarisation of mouse eight-cell blastomeres. *Dev. Biol.* 205:322–331. (1999).

Cockburn K, *et al.* The Hippo pathway member Nf2 is required for inner cell mass specification. *Curr. Biol.* 23:1195-1201. (2013).

Cockburn K. and Rossant J. Making the blastocyst: lessons from the mouse. *J. Clin. Invest.* 120: 995–1003. (2010).

Coffey ET. Nuclear and cytosolic JNK signalling in neurons. *Nat. Rev. Neurosci.* 15:285-299. (2014).

Coulthard LR, *et al.* p38(MAPK): stress responses from molecular mechanisms to therapeutics. *Trends Mol. Med.* 8:369-379. (2009).

Cuadrado A. and Nebreda AR. Mechanisms and functions of p38 MAPK signalling. *Biochem. J.* 429:403-417. (2010).

Cuevas BD, Abell AN, Johnson GL. Role of mitogen-activated protein kinase kinase kinases in signal integration. *Oncogene.* 26:3159–3171. (2007).

Dailey L, *et al.* Mechanisms underlying differential responses to FGF signaling. *Cyto. Gro. Fact. Rev.* 16:233–247. (2005).

Dard N, *et al.* Phosphorylation of ezrin on threonine T567 plays a crucial role during compaction in the mouse early embryo. *Dev. Biol.* 271:87–97. (2004).

Davidson W, *et al.* Discovery and characterization of a substrate selective p38 $\alpha$  inhibitor. *Biochemistry.* 43:11658–11671. (2004).

DeBerardinis RJ, *et al.* The biology of cancer: metabolic reprogramming fuels cell growth and proliferation. *Cell Metab.* 7:11-20. (2008).

de Mochel NS R, *et al.* BMP signaling is required for cell cleavage in preimplantation-mouse embryos. *Dev. Biol.* 397:45–55. (2015).

Dong J, *et al.* Elucidation of a universal size-control mechanism in Drosophila and mammals. *Cell.* 130:1120-1133. (2007).

Donnison M, *et al.* Loss of the extraembryonic ectoderm in Elf5 mutants leads to defects in embryonic patterning. *Development*. 132:2299–2308. (2005).

Dorey K. and Amaya E. FGF signalling: diverse roles during early vertebrate embryogenesis. *Development*. 137:3731-3742. (2010).

Doza NY, *et al.* Activation of the MAP kinase homologue RK requires the phosphorylation of Thr-180 and Tyr-182 and both residues are phosphorylated in chemically stressed KB cells. *FEBS Lett*. 364:223–228. (1995).

Drew BA, Burow ME, Beckman BS. MEK5/ERK5 pathway: the first fifteen years. *Biochim.Biophys. Acta*. 1825:37-48. (2012).

Dudka AA, Sweet SM, Heath JK. Signal transducers and activators of transcription-3 binding to the Fibroblast Growth Factor receptor is activated by receptor amplification. *Cancer Res*. 70:3391–3401. (2010).

Dumont J, *et al.* p90Rsk is not involved in cytostatic factor arrest in mouse oocytes. *J Cell Biol*. 169:227-231. (2005).

Dzeja PP, *et al.* Developmental enhancement of adenylate kinase-AMPK metabolic signaling axis supports stem cell cardiac differentiation. *PLoS One*. 6:e19300. (2011).

Eckert JJ, *et al.* Metabolic induction and early responses of mouse blastocyst developmental programming following maternal low protein diet affecting life-long health. *PLoS ONE*. 7, e52791. (2012).

Edlund S, *et al.* Transforming growth factor-beta-induced mobilization of actin cytoskeleton requires signaling by small GTPases Cdc42 and RhoA. *Mol. Biol. Cell*. 13:902–914. (2002).

English JM, *et al.* Isolation of MEK5 and differential expression of alternatively spliced forms. *J. Biol. Chem*. 270:28897-28902. (1995).

Erhardt S, *et al.* Consequences of the depletion of zygotic and embryonic enhancer of zeste 2 during preimplantation mouse development. *Development*. 130:4235–4248. (2003).

Esteban LM, *et al.* Targeted genomic disruption of H-ras and N-ras, individually or in combination, reveals the dispensability of both loci for mouse growth and development. *Mol. Cell Biol*. 21:1444-1452. (2001).

Fan R, Kim NG, Gumbiner BM. Regulation of Hippo pathway by mitogenic growth factors via phosphoinositide 3-kinase and phosphoinositide-dependent kinase-1. *Proc. Natl. Acad. Sci. U S A*. 110:2569-2574. (2013).

Fernandez-Marcos PJ. and Auwerx J. Regulation of PGC-1 $\alpha$ , a nodal regulator of mitochondrial biogenesis. *Am. J. Clin. Nutr.* 93:884S-90. (2011).

Fleming TP, *et al.* Do little embryos make big decisions? How maternal dietary protein restriction can permanently change an embryo's potential, affecting adult health. *Reprod. Fertil. Dev.* 27:684-692. (2015).

Folmes CD, *et al.* Somatic oxidative bioenergetics transitions into pluripotency-dependent glycolysis to facilitate nuclear reprogramming. *Cell Metab.* 14:264–271. (2011).

Fong B, Watson PH, Watson AJ. Mouse preimplantation embryo responses to culture medium osmolarity include increased expression of CCM2 and p38 MAPK activation. *BMC Dev. Biol.* 10;7:2. (2007).

Frankenberg S, *et al.* Primitive endoderm differentiates via a three-step mechanism involving Nanog and RTK signaling. *Dev. Cell.* 21:1005–1013. (2011).

Fujikura J, *et al.* Differentiation of embryonic stem cells is induced by GATA factors. *Genes & Dev.* 16:784–789. (2002).

Galabova-Kovacs G, *et al.* Essential role of B-Raf in ERK activation during extraembryonic development. *Proc. Natl. Acad. Sci. U S A.* 103(5):1325-1330. (2006).

Gamer LW. and Wright C V. Murine Cdx-4 bears striking similarities to the Drosophila caudal gene in its homeodomain sequence and early expression pattern. *Mech.Dev.* 43:71-81. (1993).

Ge B, *et al.* MAPKK-independent activation of p38 $\alpha$  mediated by TAB1-dependent autophosphorylation of p38 $\alpha$ . *Science.* 295:1291–1294. (2002).

Gehart H, *et al.* MAPK signalling in cellular metabolism: stress or wellness?. *EMBO Rep.* 11:834-840. (2010).

Gilbert SF. and Solter D. Onset of paternal and maternal Gpi-1 expression in preimplantation mouse embryos. *Dev.Biol.* 109:515–517. (1985).

Giroux S, *et al.* Embryonic death of Mek1-deficient mice reveals a role for this kinase in angiogenesis in the labyrinthine region of the placenta. *Curr. Biol.* 9:369-372. (1999).

Goedert M, *et al.* Activation of the novel stress-activated protein kinase SAPK4 by cytokines and cellular stresses is mediated by SKK3 (MKK6): comparison of its substrate specificity with that of other SAP kinases. *EMBO J.* 16:3563–3571. (1997).

Gong Q, *et al.* Disruption of T cell signaling networks and development by Grb2 haploid insufficiency. *Nat. Immunol.* 2:29-36. (2001).

Gotoh N, *et al.* The docking protein FRS2alpha is an essential component of multiple fibroblast growth factor responses during early mouse development. *Mol. Cell. Biol.* 25:4105-4116. (2005).

Graham SJ, *et al.* BMP signalling regulates the pre-implantation development of extra-embryonic cell lineages in the mouse embryo. *Nat. Commun.* 5: 5667. (2014).

Gumbiner BM. and Kim NG. The Hippo-YAP signaling pathway and contact inhibition of growth. *J. Cell Sci.* 127:709-717. (2014).

Gutiérrez-Uzquiza Á, *et al.* p38 $\alpha$  mediates cell survival in response to oxidative stress via induction of antioxidant genes: effect on the p70S6K pathway. *J. Biol. Chem.* 287:2632-2642. (2012).

Haffner-Krausz R, *et al.* Expression of Fgfr2 in the early mouse embryo indicates its involvement in preimplantation development. *Mech. Dev.* 85:167-172. (1999).

Hamatani T, Ko MSH, Yamada M, Kuji N, Mizusawa Y, *et al.* Global gene expression profiling of preimplantation embryos. *Hum. Cell.* 19:98–117. (2006).

Hardie DG, Ross FA, Hawley SA. AMPK: a nutrient and energy sensor that maintains energy homeostasis. *Nat. Rev. Mol. Cell Biol.* 13:251–262. (2012).

Hatano N, *et al.* Essential role for ERK2 mitogen-activated protein kinase in placental development. *Genes Cells.* 8:847-856. (2003).

Hazzalin CA, *et al.* p38/RK is essential for stress-induced nuclear responses: JNK/SAPKs and c-Jun/ATF-2 phosphorylation are insufficient. *Curr. Biol.* 6:1028-1031. (1996).

He J, *et al.* An elaborate regulation of Mammalian target of rapamycin activity is required for somatic cell reprogramming induced by defined transcription factors. *Stem Cells Dev.* 21:2630–2641. (2012).

Hirasawa R, *et al.* Maternal and zygotic Dnmt1 are necessary and sufficient for the maintenance of DNA methylation imprints during preimplantation development. *Genes & Dev.* 22:1607–1616. (2008).

Hirate Y, *et al.* Polarity-dependent distribution of angiominin localizes Hippo signaling in preimplantation embryos. *Curr. Biol.* 23:1181-1194. (2013).

Hiscox S, Jiang W. Ezrin regulates cell–cell and cell–matrix adhesion, a possible role with E-cadherin/beta-catenin. *J. Cell Sci.* 112:3081–90. (1999).

Ho Y, *et al.* Preimplantation development of mouse embryos in KSOM: augmentation by amino acids and analysis of gene expression. *Mol. Reprod. Dev.* 41:232-8. (1995).

Home P, *et al.* GATA3 is selectively expressed in the trophectoderm of peri-implantation embryo and directly regulates Cdx2 gene expression. *J. Biol. Chem.* 284: 28729-28737. (2013).

Houghton FD, *et al.* Na<sup>+</sup>,K<sup>+</sup> ATPase activity in the human and bovine preimplantation embryo. *Dev. Bio.* 263:360–366. (2003).

Houghton FD, *et al.* Oxygen consumption and energy metabolism of the early mouse embryo. *Mol. Reprod. Dev.* 44:476–485. (1996).

Huang PI, *et al.* Enhanced differentiation of three-gene-reprogrammed induced pluripotent stem cells into adipocytes via adenoviral-mediated PGC-1 $\alpha$  overexpression. *Int. J. Mol. Sci.* 12:7554-7568. (2011).

Hyafil F, *et al.* A cell surface glycoprotein involved in the compaction of embryonal carcinoma cells and cleavage stage embryos. *Cell.* 21:927–934. (1980).

Itoh M *et al.* Role of Gab1 in heart, placenta, and skin development and growth factor- and cytokine-induced extracellular signal-regulated kinase mitogen-activated protein kinase activation. *Mol. Cell. Biol.* 10:3695-3704. (2000).

Jackson JR, *et al.* Pharmacological effects of SB220025, a selective inhibitor of P38 mitogen-activated protein kinase, in angiogenesis and chronic inflammatory disease models. *J. Pharmacol. Exp. Ther.* 284:687-692. (1998).

Jansen S, Pantaleon M, Kaye PL. Characterisation and regulation of monocarboxylate cotransporters Slc16a7 and Slc16a3 in preimplantation mouse embryos. *Biol. Reprod.* 79:84–92. (2008).

Jedrusik A, *et al.* Role of Cdx2 and cell polarity in cell allocation and specification of trophectoderm and inner cell mass in the mouse embryo. *Genes & Dev.* 22:2692–2706. (2008).

Jedrusik A, *et al.* Maternally and zygotically provided Cdx2 have novel and critical roles for early development of the mouse embryo. *Dev. Biol.* 344:66-78. (2010).

Johnson MH, Maro B, Takeichi M. The role of cell adhesion in the synchronisation and orientation of polarisation in 8-cell mouse blastomeres. *Development.* 93:239–255. (1986).

Kanaji N, *et al.* The p38 mitogen-activated protein kinases modulate endothelial cell survival and tissue repair. *Inflamm. Res.* 61:233-244. (2012).

Kanazawa S, *et al.* bFGF regulates PI3-kinase-Rac1-JNK pathway and promotes fibroblast migration in wound healing. *PLoS One.* 5:e12228. (2010).

Kane MT, Morgan PM, Coonan C. Peptide growth factors and preimplantation development. *Hum. Reprod. Update.* 3:137–157. (1997).

Kang M, *et al.* 2013. FGF4 is required for lineage restriction and salt-and-pepper distribution of primitive endoderm factors but not their initial expression in the mouse. *Development.* 140:267-279. (2013).

Karnoub AE, and Weinberg RA. Ras oncogenes: split personalities. *Nat. Rev. Mol. Cell. Biol.* 9:517-531. (2008).

Kawamura Y, *et al.* Sirt3 protects in vitro-fertilized mouse preimplantation embryos against oxidative stress-induced p53-mediated developmental arrest. *J. Clin. Invest.* 120:2817-2828. (2010).

Keramari M, *et al.* Sox2 is essential for formation of trophectoderm in the preimplantation embryo. *PLoS ONE* 5:e13952. (2010).

Kondoh H, *et al.* A high glycolytic flux supports the proliferative potential of murine embryonic stem cells. *Antioxid. Redox Signal.* 9:293–299. (2007).

Kono K, Tamashiro DA, Alarcon VB. Inhibition of RHO-ROCK signaling enhances ICM and suppresses TE characteristics through activation of Hippo signaling in the mouse blastocyst. *Dev. Biol.* 394:142-155. (2014).

Koutsourakis M, *et al.* The transcription factor Gata6 is essential for early extraembryonic development. *Development.* 126:723–732. (1999).

Krawchuk D, *et al.* FGF4 is a limiting factor controlling the proportions of primitive endoderm and epiblast in the ICM of the mouse blastocyst. *Dev. Biol.* 384:65-71. (2013).

Kunath T, *et al.* 2007. FGF stimulation of the Erk1/2 signalling cascade triggers transition of pluripotent embryonic stem cells from self-renewal to lineage commitment. *Development.* 134:2895-2902. (2007).

Kwong WY, *et al.* Maternal undernutrition during the preimplantation period of rat development causes blastocyst abnormalities and programming of postnatal hypertension. *Development.* 127:4195–4202. (2000).

Kwong WY, *et al.* Imprinted gene expression in the rat embryo–fetal axis is altered in response to periconceptional maternal low protein diet. *Reproduction.* 132:265–277. (2006).

Kwong WY, *et al.* Maternal low protein diet restricted to the preimplantation period induces a gender-specific change on hepatic gene expression in rat fetuses. *Mol. Reprod. Dev.* 74:48–56. (2007).

Kyriakis JM, *et al.* The stress-activated protein kinase subfamily of c-Jun kinases. *Nature.* 369:156-160 (1994).

Lambert S, Frankart A, Poumay Y. p38 MAPK-regulated EGFR internalization takes place in keratinocyte monolayer during stress conditions. *Arch. Dermatol. Res.* 302:229-233 . (2010).

Lane M. and Gardner DK. Amino acids and vitamins prevent culture-induced metabolic perturbations and associated loss of viability of mouse blastocysts. *Human Reprod.* 13:991–997. (1998).

Lane M. and Gardner DK. Mitochondrial malate–aspartate shuttle regulates mouse embryo nutrient consumption. *J. Bio. Chem.* 280:18361–18367. (2005).

- Lanner F. and Rossant J. The role of FGF/Erk signaling in pluripotent cells. *Development*. 137:3351-3360. (2010).
- Laplante M. and Sabatini DM. mTOR signaling at a glance. *J. Cell Sci*. 122:3589–3594. (2009).
- Lavial F, *et al*. Bmi1 facilitates primitive endoderm formation by stabilizing Gata6 during early mouse development. *Genes & Dev*. 26:1445-1458. (2012).
- Lavoie J, *et al*. Modulation of actin microfilament dynamics and fluid phase pinocytosis by phosphorylation of heat shock protein 27. *J. Biol. Chem*. 268:24210-24214. (1993).
- Le Guezennec X. and Bulavin DV. WIP1 phosphatase at the crossroads of cancer and aging. *Trends Biochem. Sci*. 35:109–114. (2010).
- Lee JD, Ulevitch RJ, Han J. Primary structure of BMK1: a new mammalian map kinase. *Biochem. Biophys. Res. Commun*. 213:715-724. (1995).
- Lee MK, *et al*. TGF-beta activates Erk MAP kinase signalling through direct phosphorylation of ShcA. *EMBO J*. 26:3957–3967. (2007).
- Leese HJ. Metabolism of the preimplantation embryo: 40 years on. *Reproduction*. 143:417-27. (2012).
- Leung CY. and Zernicka-Goetz M. Angiotensin prevents pluripotent lineage differentiation in mouse embryos via Hippo pathway-dependent and -independent mechanisms. *Nat. Commun*. 4:2251-2259. (2013).
- Li SP, *et al*. p38 Mitogen-activated protein kinase pathway suppresses cell survival by inducing dephosphorylation of mitogen-activated protein/extracellular signal-regulated kinase kinase1,2. *Cancer Res*. 63:3473-3477. (2003).
- Liu J, *et al*. Integrins are required for the differentiation of visceral endoderm. *J. Cell. Sci*. 122:233-242. (2009).
- Liu Q. **and** Hofmann PA. Protein phosphatase 2A-mediated cross-talk between p38 MAPK and ERK in apoptosis of cardiac myocytes. *Am. J. Physiol. Heart Circ. Physiol*. 286:H2204-12. (2004).
- Lluis F, *et al*. Regulation of skeletal muscle gene expression by p38 MAP kinases. *Trends Cell Biol*. 16:36–44. (2006).
- Maekawa M, *et al*. Requirement of the MAP kinase signaling pathways for mouse preimplantation development. *Development*. 132:1773-1783. (2005).
- Urushihara M. and Kinoshita Y. Renin-Angiotensin System Activation and Extracellular Signal-Regulated Kinases in Glomerulonephritis, An Update on Glomerulopathies - Etiology and Pathogenesis. *InTech*. DOI: 10.5772/23393. (2011).

- Manes C. and Lai NC. Nonmitochondrial oxygen utilization by rabbit blastocysts and surface production of superoxide radicals. *J.Reprod. Fer.* 104:69–75. (1995).
- Manning BD. and Cantley LC. AKT/PKB signaling: navigating downstream. *Cell.* 129:1261–1274. (2007).
- Maryanovich M. and Gross A. A ROS rheostat for cell fate regulation. *Trends Cell Biol.* 23:129–134. (2013).
- Massague J, Seoane J, Wotton D. Smad transcription factors. *Genes & Dev.* 19:2783–2810. (2005).
- Massague J. and Wotton D. Transcriptional control by the TGF-beta/Smad signaling system. *EMBO J.* 19:1745–1754. (2000).
- McFalls EO, *et al.* Activation of p38 MAPK and increased glucose transport in chronic hibernating swine myocardium. *Am. J. Physiol .Heart. Circ .Physiol.* 287:H1328-34. (2004).
- Meilhac SM, *et al.* Active cell movements coupled to positional induction are involved in lineage segregation in the mouse blastocyst. *Dev.Biol.* 331: 210–221. (2009).
- Meininger CJ. and Wu G. L-Glutamine inhibits nitric oxide synthesis in bovine venular endothelial cells. *J. Pharm. Exp. Therap.* 281:448–453. (1997).
- Meng Z, Moroishi T, Guan KL. Mechanisms of Hippo pathway regulation. *Genes & Dev.* 30:1-17. (2016).
- Mihajlović AI. and Bruce AW. Rho-associated protein kinase regulates subcellular localisation of Angiotensin and Hippo-signalling during preimplantation mouse embryo development. *Reprod. Biomed. Online.* S1472-6483:30404-7. (2016).
- Mitsui K, *et al.* The homeoprotein Nanog is required for maintenance of pluripotency in mouse epiblast and ES cells. *Cell.* 113:631–642. (2003).
- Morris S A, *et al.* Origin and formation of the first two distinct cell types of the inner cell mass in the mouse embryo. *Proc. Natl. Acad. Sci. U. S. A.* 107:6364-6369. (2010).
- Moruno-Manchón JF, Pérez-Jiménez E, Knecht E. Glucose induces autophagy under starvation conditions by a p38 MAPK-dependent pathway. *Biochem J.* 449:497-506. (2013).
- Mudgett JS, *et al.* Essential role for p38alpha mitogen-activated protein kinase in placental angiogenesis. *Proc. Natl. Acad. Sci. U. S. A.* 97:10454-10459. (2000).
- Muniyappa H. and Das KC. Activation of c-Jun N-terminal kinase (JNK) by widely used specific p38 MAPK inhibitors SB202190 and SB203580: a MLK-3-MKK7-dependent mechanism. *Cell Signal.* 20:675-683. (2008).

Murakami M, *et al.* mTOR is essential for growth and proliferation in early mouse embryos and embryonic stem cells. *Mol. Cell Biol.* 24:6710–6718. (2004).

Naka K, *et al.* Dipeptide species regulate p38MAPK-Smad3 signalling to maintain chronic myelogenous leukaemia stem cells. *Nat. Commun.* 6:8039. (2015).

Natale DR, *et al.* p38 MAPK signaling during murine preimplantation development. *Dev. Biol.* 268:76–88. (2004).

Ng RK, *et al.* Epigenetic restriction of embryonic cell lineage fate by methylation of *Elf5*. *Nat. Cell Biol.* 10:1280–1290. (2008).

Niakan KK, *et al.* Sox17 promotes differentiation in mouse embryonic stem cells by directly regulating extraembryonic gene expression and indirectly antagonizing self-renewal. *Genes & Dev.* 24:312–326. (2010).

Nichols J, *et al.* Suppression of Erk signalling promotes ground state pluripotency in the mouse embryo. *Development.* 136:3215–3222. (2009).

Nichols J, *et al.* Formation of pluripotent stem cells in the mammalian embryo depends on the POU transcription factor Oct4. *Cell.* 95: 379–391. (1998).

Nishida K, *et al.* p38alpha mitogen-activated protein kinase plays a critical role in cardiomyocyte survival but not in cardiac hypertrophic growth in response to pressure overload. *Mol. Cell. Biol.* 24(24):10611–10620. (2004).

Nishioka N, *et al.* The Hippo signaling pathway components Lats and Yap pattern Tead4 activity to distinguish mouse trophectoderm from inner cell mass. *Dev. Cell.* 16:398–410. (2009).

Niwa H, *et al.* Interaction between Oct3/4 and Cdx2 determines trophectoderm differentiation. *Cell.* 123:917–929. (2005).

O'Brien PMS, Wheeler T, Barker DJP. Fetal Programming: Influences on Development and Disease in Later Life. *RCOG Press.* (1999).

O'Neill C. The potential roles for embryotrophic ligands in preimplantation embryo development. *Hum. Reprod. Update.* 14:275–288. (2008).

Ornitz DM. FGFs, heparan sulfate and FGFRs: complex interactions essential for development. *BioEssays.* 22:108–112. (2000).

Orsi NM. and Leese HJ. Protection against reactive oxygen species during mouse preimplantation embryo development: role of EDTA, oxygen tension, catalase, superoxide dismutase and pyruvate. *Mol. Reprod. Dev.* 59:44–53. (2001).

Owens DM. and Keyse SM. Differential regulation of MAP kinase signalling by dual-specificity protein phosphatases. *Oncogene.* 26:3203–3213. (2007).

- Paliga AJ, Natale DR, Watson AJ. p38 mitogen-activated protein kinase (MAPK) first regulates filamentous actin at the 8-16-cell stage during preimplantation development. *Biol. Cell.* 97:629-640. (2005).
- Palmieri SL, *et al.* Oct-4 transcription factor is differentially expressed in the mouse embryo during establishment of the first two extra-embryonic cell lineages involved in implantation. *Dev. Biol.* 166:259–267. (1994).
- Pargellis C, *et al.* Inhibition of p38 MAP kinase by utilizing a novel allosteric binding site. *Nat. Struct. Biol.* 9:268–272. (2002).
- Peregrin S, *et al.* Phosphorylation of p38 by GRK2 at the docking groove unveils a novel mechanism for inactivating p38MAPK. *Curr. Biol.* 16:2042–2047. (2006).
- Pereira SL, *et al.* Inhibition of mitochondrial complex III blocks neuronal differentiation and maintains embryonic stem cell pluripotency. *PLoS One.* 8:e82095. (2013).
- Plusa B, *et al.* Downregulation of Par3 and aPKC function directs cells towards the ICM in the preimplantation mouse embryo. *J. Cell Sci.* 118:505–515. (2005a).
- Plusa B, *et al.* Distinct sequential cell behaviours directing primitive endoderm formation in the mouse blastocyst revealed by live imaging. *Development.* 135: 3081 -3091. (2008).
- Qi X, *et al.* Simmons H, Miura S, Mishina Y, Zhao GQ. BMP4 supports self-renewal of embryonic stem cells by inhibiting mitogen-activated protein kinase pathways. *Proc. Natl. Acad. Sci. U. S. A.* 101:6027–6032. (2004).
- Qian X, *et al.* The Sos1 and Sos2 Ras-specific exchange factors: differences in placental expression and signaling properties. *EMBO J.* 19:642-654. (2000)
- Qiao L, MacDougald OA, Shao J. CCAAT/enhancer-binding protein alpha mediates induction of hepatic phosphoenolpyruvate carboxykinase by p38 mitogen-activated protein kinase. *J. Biol. Chem.* 281:24390–24397. (2006).
- Raingeaud J, *et al.* Pro-inflammatory cytokines and environmental stress cause p38 mitogen-activated protein kinase activation by dual phosphorylation on tyrosine and threonine. *J. Biol. Chem.* 270:7420–7426. (1995).
- Ralston A, *et al.* Gata3 regulates trophoblast development downstream of Tead4 and in parallel to Cdx2. *Development.* 137:395–403. (2010).
- Raman M, Chen W, Cobb MH. Differential regulation and properties of MAPKs. *Oncogene.* 26:3100-3112. (2007).

Rampalli S, *et al.* p38 MAPK signaling regulates recruitment of Ash2L-containing methyltransferase complexes to specific genes during differentiation. *Nat. Struct. Mol. Biol.* 14:1150–1156. (2007).

Ramsauer K, *et al.* p38 MAPK enhances STAT1-dependent transcription independently of Ser-727 phosphorylation. *Proc. Natl. Acad. Sci. U. S. A.* 99:12859-12864. (2002).

Reeve WJD. and Ziomek CA. Distribution of microvilli on dissociated blastomeres from mouse embryos: evidence for surface polarisation at compaction. *Development.* 62:339–350. (1981).

Reilly JF, Mickey G, Maher PA. Association of Fibroblast Growth Factor receptor 1 with the adaptor protein Grb14. Characterization of a new receptor binding partner. *J. Biol. Chem.* 275:7771–7778. (2000).

Roskoski R Jr. ERK1/2 MAP kinases: structure, function, and regulation. *Pharmacol. Res.* 66:105-43. (2012).

Russ AP, *et al.* Eomesodermin is required for mouse trophoblast development and mesoderm formation. *Nature.* 404:95–99. (2000).

Sabio G, *et al.* p38 $\gamma$  regulates the localisation of SAP97 in the cytoskeleton by modulating its interaction with GKAP. *EMBO J.* 24:1134–1145. (2005).

Saccani S, Pantano S, Natoli G. p38-Dependent marking of inflammatory genes for increased NF- $\kappa$ B recruitment. *Nat. Immunol.* 3:69–75. (2002).

Sakaki-Yumoto M, Katsuno Y, Derynck R. TGF- $\beta$  family signaling in stem cells. *Biochim. Biophys. Acta.* 1830;2:2280-2296. (2013).

Salvador JM, *et al.* Alternative p38 activation pathway mediated by T cell receptor-proximal tyrosine kinases. *Nat. Immunol.* 6:390–395. (2005).

Santinon G, Pocaterra A, Dupont S. Control of YAP/TAZ Activity by Metabolic and Nutrient-Sensing Pathways. *Trends Cell Biol.* 26:289-299. (2016).

Santos F, *et al.* Dynamic chromatin modifications characterise the first cell cycle in mouse embryos. *Dev. Biol.* 280:225–236. (2005).

Sefton M, Johnson MH, Clayton L. Synthesis and phosphorylation of uvomorulin during mouse early development. *Development.* 115:313–318. (1992).

Shaul Y D, and Seger R. The MEK/ERK cascade: from signaling specificity to diverse functions. *Biochim. Biophys. Acta.* 1773:1213-1226. (2007).

Shi X, *et al.* AICAR sustains J1 mouse embryonic stem cell self-renewal and pluripotency by regulating transcription factor and epigenetic modulator expression. *Cell Physiol. Biochem.* 32:459–475. (2013).

Shi Y. and Massague J. Mechanisms of TGF-beta signaling from cell membrane to the nucleus. *Cell*. 113:685–700. (2003).

Shirayoshi Y, *et al.* The calcium dependent cell-cell adhesion system regulates inner cell mass formation and cell surface polarization in early mouse development. *Cell*.35:631–638. (1983).

Schlessinger J. Cell signaling by receptor tyrosine kinases. *Cell*. 103:211–225. (2000).

Scholer HR, *et al.* New type of POU domain in germ line-specific protein Oct-4. *Nature*. 344:435–439. (1990a).

Silva J, *et al.* Nanog is the gateway to the pluripotent ground state. *Cell*. 138: 722–737. (2009).

Singh AM, *et al.* A heterogeneous expression pattern for Nanog in embryonic stem cells. *Stem Cells* 25:2534-2542. (2007).

Soloaga A, *et al.* MSK2 and MSK1 mediate the mitogen- and stress-induced phosphorylation of histone H3 and HMG-14. *EMBO J*. 22:2788–2279. (2003).

Sørensen V, *et al.* Phosphorylation of fibroblast growth factor (FGF) receptor 1 at Ser777 by p38 mitogen-activated protein kinase regulates translocation of exogenous FGF1 to the cytosol and nucleus. *Mol. Cell Biol*. 28:4129-4141. (2008).

Soudais C, *et al.* Targeted mutagenesis of the transcription factor GATA-4 gene in mouse embryonic stem cells disrupts visceral endoderm differentiation in vitro. *Development* .121: 3877-3888. (1995).

Sozen B, *et al.* The p38 MAPK signalling pathway is required for glucose metabolism, lineage specification and embryo survival during mouse preimplantation development. *Mech. Dev*. 138:375-398. (2015).

Sridharan R, *et al.* Role of the murine reprogramming factors in the induction of pluripotency. *Cell*. 136:364–377. (2009).

Steeves CL, *et al.* The glycine neurotransmitter transporter GLYT1 is an organic osmolyte transporter regulating cell volume in cleavage-stage embryos. *Proc. Natl. Acad. Sci. U S A*. 100:13982-13987. (2003).

Strumpf D, *et al.* Cdx2 is required for correct cell fate specification and differentiation of trophectoderm in the mouse blastocyst. *Development*. 132:2093–2102. (2005).

Sturmey RG, Brison DR, Leese HJ. Innovative techniques in human embryo viability assessment: assessing embryo viability by measurement of amino acid turnover. *Reprod. Biomed. Online*. 17:486–496. (2008).

Su WC, *et al.* Activation of Stat1 by mutant fibroblast growth-factor receptor in thanatophoric dysplasia type II dwarfism. *Nature*. 386:288–292. (1997).

- Sun C, *et al.* Mouse early extra-embryonic lineages activate compensatory endocytosis in response to poor maternal nutrition. *Development*. 141:1140–1150. (2014).
- Sun C, *et al.* Epigenetic regulation of histone modifications and *Gata6* gene expression induced by maternal diet in mouse embryoid bodies in a model of developmental programming. *BMC Dev. Biol.* 15:3. (2015).
- Sy JC, *et al.* Sustained release of a p38 inhibitor from non-inflammatory microspheres inhibits cardiac dysfunction. *Nat. Mater.* 7:863–868. (2008).
- Takahashi K, *et al.* Induction of pluripotent stem cells from mouse embryonic and adult fibroblast cultures by defined factors. *Cell*. 126: 663–676. (2006).
- Takubo K, *et al.* Regulation of glycolysis by Pdk functions as a metabolic checkpoint for cell cycle quiescence in hematopoietic stem cells. *Cell Stem Cell*. 12:49–61. (2013).
- Tan Y, *et al.* FGF and stress regulate CREB and ATF-1 via a pathway involving p38 MAP kinase and MAPKAP kinase-2. *EMBO J.* 15:4629–4642. (1996).
- Tanoue T, *et al.* A conserved docking motif in MAP kinases common to substrates, activators and regulators. *Nat. Cell Biol.* 2:110–116. (2000).
- Tarkowski AK. Experiments on the development of isolated blastomeres of mouse eggs. *Nature*. 184:1286–1287. (1959).
- Tarkowski AK. Mouse chimaeras developed from fused eggs. *Nature*. 190:857–860. (1961).
- Teslaa T. and Teitell MA. Pluripotent stem cell energy metabolism: an update. *EMBO J.* 34:138–153. (2015).
- Thamodaran V. and Bruce AW. p38 (Mapk14/11) occupies a regulatory node governing entry into primitive endoderm differentiation during preimplantation mouse embryo development. *Open Biol.* rsob.160190.
- Thannickal VJ. and Fanburg BL. Reactive oxygen species in cell signaling. *Am. J. Physiol. Lung Cell Mol. Physiol.* 279:L1005–28. (2000).
- Thompson JG, *et al.* Total protein content and protein synthesis within pre-elongation stage bovine embryos. *Mol. Reprod. Dev.* 50:139–145. (1998).
- Udenigwe CC. and Aluko RE. Chemometric analysis of the amino acid requirements of antioxidant food protein hydrolysates. *Int. J. Mol. Sci.* 12:3148–161. (2011).
- Varelas X, *et al.* TAZ controls Smad nucleocytoplasmic shuttling and regulates human embryonic stem-cell self-renewal. *Nat. Cell. Biol.* 10: 837–848. (2008).

- Varelas X, *et al.* The Crumbs complex couples cell density sensing to Hippo-dependent control of the TGF- $\beta$ -SMAD pathway. *Dev. Cell.* 19: 831–844. (2010).
- Vazquez-Martin A, *et al.* Activation of AMP-activated protein kinase (AMPK) provides a metabolic barrier to reprogramming somatic cells into stem cells. *Cell Cycle.* 11:974–989. (2012).
- Venkatakrishnan CD, *et al.* HSP27 regulates p53 transcriptional activity in doxorubicin-treated fibroblasts and cardiac H9c2 cells: p21 upregulation and G2/M phase cell cycle arrest. *Am. J. Physiol. Heart. Circ. Physiol.* 294:H1736-44. (2008).
- Vermilyea MD, O'Neill LP, Turner BM. Transcription-independent heritability of induced histone modifications in the mouse preimplantation embryo. *PLoS ONE* 4:e6086. (2009).
- Vinot S, *et al.* Two PAR6 proteins become asymmetrically localized during establishment of polarity in mouse oocytes. *Curr. Biol.* 14:52–55. (2004).
- Vinot S, *et al.* Asymmetric distribution of PAR proteins in the mouse embryo begins at the 8-cell stage during compaction. *Dev. Biol.* 282:307–319. (2005).
- Wang QT, *et al.* Genome-wide study of gene activity reveals developmental signaling pathways in the preimplantation mouse embryo. *Dev. Cell.* 6:133–144. (2004).
- Wang K, *et al.* Brg1 is required for Cdx2-mediated repression of Oct4 expression in mouse blastocysts. *PLoS One.* 5:e10622. (2010).
- Wang S, *et al.* Transient activation of autophagy via Sox2-mediated suppression of mTOR is an important early step in reprogramming to pluripotency. *Cell Stem Cell.* 13:617–625. (2013a).
- Wang X, *et al.* Targeted deletion of mek5 causes early embryonic death and defects in the extracellular signal-regulated kinase 5/myocyte enhancer factor 2 cell survival pathway. *Mol. Cell. Biol.* 25:336-345. (2005).
- Wang Y, *et al.* Entire mitogen activated protein kinase (MAPK) pathway is present in preimplantation mouse embryos. *Dev. Dyn.* 231:72-87. (2004).
- Webber JL and Tooze SA. Coordinated regulation of autophagy by p38 $\alpha$  MAPK through mAtg9 and p38IP. *EMBO J.* 29:27–40. (2010).
- Wei Y, An Z, *et al.* The stress-responsive kinases MAPKAPK2/MAPKAPK3 activate starvation-induced autophagy through Beclin 1 phosphorylation. *Elife.* 18;4. (2015).
- Weston CR. and Davis RJ. The JNK signal transduction pathway. *Curr. Opin. Genet. Dev.* 12:14-21. (2002),
- Wharton K. and Derynck R. TGFbeta family signaling: novel insights in development and disease. *Development.* 136:3691-3697. (2009).

- Whitman M. Smads and early developmental signaling by the TGF-beta superfamily. *Genes & Dev.* 12:2445–2462. (1998).
- Whitmarsh AJ and Davis RJ. Transcription factor AP-1 regulation by mitogen-activated protein kinase signal transduction pathways. *J. Mol. Med.* 74:589-607. (1996).
- Williamson DL, Butler DC, Alway SE. AMPK inhibits myoblast differentiation through a PGC-1alpha-dependent mechanism. *Am. J. Physiol. Endocrinol. Metab.* 297:E304–E314. (2009).
- Winkel GK, *et al.* Activation of protein kinase C triggers premature compaction in the four-cell stage mouse embryo. *Dev. Biol.* 138:1–15. (1990).
- Wood GW, *et al.* Expression and regulation of histidine decarboxylase mRNA expression in the uterus during pregnancy in the mouse. *Cytokine.* 12 :622–629. (2000).
- Wright DC, *et al.* Calcium induces increases in peroxisome proliferator-activated receptor  $\gamma$  coactivator-1 $\alpha$  and mitochondrial biogenesis by a pathway leading to p38 mitogen-activated protein kinase activation. *J. Biol. Chem.* 282: 18793–18799. (2007).
- Wu MY, Hill CS. TGF-beta superfamily signaling in embryonic development and homeostasis. *Dev. Cell.* 16:329–343. (2009).
- Xie Y, Puscheck EE, Rappolee DA. Effects of SAPK/JNK inhibitors on preimplantation mouse embryo development are influenced greatly by the amount of stress induced by the media. *Mol. Hum. Reprod.* 12:217-224. (2006).
- Xiong Y, *et al.* p38 mitogen-activated protein kinase plays an inhibitory role in hepatic lipogenesis. *J. Biol. Chem.* 282:4975–4982. (2007).
- Yagi R, *et al.* Transcription factor TEAD4 specifies the trophectoderm lineage at the beginning of mammalian development. *Development.* 134: 3827–3836. (2007).
- Yamanaka Y, Lanner F, Rossant J. FGF signal-dependent segregation of primitive endoderm and epiblast in the mouse blastocyst. *Development.* 137:715-724. (2010).
- Yamashita M, *et al.* TRAF6 mediates Smad-independent activation of JNK and p38 by TGF-beta. *Mol. Cell.* 31:918–924. (2008).
- Yan C, *et al.* Molecular cloning of mouse ERK5/BMK1 splice variants and characterization of ERK5 functional domains. *J. Biol. Chem.* 276:10870-10878. (2001).
- Yang J, *et al.* Binding of FGF2 to FGFR2 in an autocrine mode in trophectoderm cells is indispensable for mouse blastocyst formation through PKC-p38 pathway. *Cell Cycle.* 14:3318-3330. (2015).
- Ying QL, *et al.* The ground state of embryonic stem cell self-renewal. *Nature.* 453:519-523. (2008).

- Yu FX, *et al.* Regulation of the Hippo-YAP pathway by G-protein-coupled receptor signaling. *Cell*. 150:780-791. (2012).
- Yu FX. and Guan KL. The Hippo pathway: regulators and regulations. *Genes & Dev*. 27:355-71. (2013).
- Zeke A, *et al.* JNK Signaling: Regulation and Functions Based on Complex Protein-Protein Partnerships. *Microbiol. Mol. Biol. Rev.* 80:793-835. (2016).
- Zernicka-Goetz M. Fertile offspring derived from mammalian eggs lacking either animal or vegetal poles. *Development*. 125:4803–4808. (1998).
- Zernicka-Goetz M, Morris SA, Bruce AW. Making a firm decision: multifaceted regulation of cll fate in the early embryo. *Nat. Rev. Genet.* 10:467-477. (2009).
- Zhang J, *et al.* UCP2 regulates energy metabolism and differentiation potential of human pluripotent stem cells. *EMBO J.* 30:4860-4873. (2011).
- Zhang X, *et al.* Receptor specificity of the fibroblast growth factor family. The complete mammalian FGF family. *J. Biol. Chem.* 281:15694–15700. (2006).
- Zhang X, *et al.* Roles of intracellular fibroblast growth factors in neural development and functions. *Sci. Chin. Life Sci.* 55: 1038-1044. (2012).
- Zhang YY, *et al.* Enzymatic activity and substrate specificity of mitogen-activated protein kinase p38 $\alpha$  in different phosphorylation states. *J. Biol. Chem.* 283:26591–26601. (2008).
- Zhao B, *et al.* TEAD mediates YAP-dependent gene induction and growth control. *Genes & Dev.* 22:1962-1971. (2008).
- Zhao Q, *et al.* The p38 mitogen-activated protein kinase augments nucleotide excision repair by mediating DDB2 degradation and chromatin relaxation. *J. Biol. Chem.* 283:32553–32561. (2008).
- Zhong W, *et al.* FGF ligand family mRNA expression profile for mouse preimplantation embryos, early gestation human placenta, and mouse trophoblast stem cells. *Mol. Reprod. Dev.* 73:540-50. (2006).
- Zhou G, Bao ZQ, Dixon JE. Components of a new human protein kinase signal transduction pathway. *J. Biol. Chem.* 270:12665-12669. (1995).
- Zhu J, Blenis J, Yuan J. Activation of PI3K/Akt and MAPK pathways regulates Myc-mediated transcription by phosphorylating and promoting the degradation of Mad1. *Proc. Natl. Acad. Sci. U. S. A.* 105:6584-6589. (2008).

## **10. Appendix**

**Tables T1 (a&b)**

<b>+DMSO</b>			
<b>#</b>	<b>TOTAL NUMBER OF CELLS</b>		
	<b>EMBRYO</b>	<b>TE</b>	<b>ICM TOTAL</b>
1	89	66	23
2	59	41	18
3	89	68	21
4	67	47	20
5	90	66	24
6	64	49	15
7	70	50	20
8	104	88	16
9	80	59	21
10	75	51	24
11	79	62	17
12	79	49	30
13	73	54	19
14	87	61	26
15	94	78	16
16	93	75	18
17	42	33	9
18	101	83	18
19	82	66	16
20	110	87	23
21	73	52	21
22	82	70	12
23	101	78	23
24	100	85	15
25	99	80	19
26	80	65	15
27	79	65	14
28	97	70	27
29	103	83	20
30	75	62	13
31	81	62	19
32	103	78	25
33	90	67	23
34	101	85	16
35	99	75	24
36	103	76	27
37	93	77	16
38	85	63	22
39	76	52	24
40	99	79	20
41	92	68	24
42			
43			
44			
45			
<b>TOTAL</b>	3538	2725	813
<b>AVERAGE</b>	86.3	66.5	19.8
<b>SEM</b>	2.2	2.1	0.7

**Table T1a**

<b>+p38-Mapk14/11inhibitor (SB220025)</b>			
#	TOTAL NUMBER OF CELLS		
	EMBRYO	TE	ICM TOTAL
1	20	14	6
2	35	25	10
3	22	12	10
4	31	17	14
5	26	14	12
6	43	25	18
7	19	13	6
8	23	12	11
9	15	11	4
10	27	19	8
11	32	22	10
12	23	17	6
13	27	20	7
14	33	23	14
15	13	9	4
16	40	22	20
17	30	20	10
18	42	25	17
19	18	13	5
20	26	17	10
21	31	22	9
22	27	21	7
23	33	24	9
24	50	30	20
25	19	13	6
26	21	13	8
27	53	43	10
28	26	15	11
29	53	41	12
30	16	13	3
31	15	10	5
32	33	21	12
33	43	31	12
34	26	18	8
35	36	25	11
36	26	17	9
37	40	27	13
38	54	42	12
39	31	18	13
40	44	27	17
41	19	11	8
42	56	42	14
43	28	14	14
44	21	15	6
45	25	18	7
<b>TOTAL</b>	1371	921	458
<b>AVERAGE</b>	30.5	20.5	10.2
<b>SEM</b>	1.7	1.3	0.6
Stat. sig. (exp. vs. con embryo; T1a) *p<0.05, **p<0.005	**	**	**
p-value (2-tailed students t-test)	7.82E-34	4.08E-32	1.70E-16

**Table T1b**

**Tables T1 (a & b): Individual embryo data used to generate averaged data presented in figure 7 b;** the average number of outer and inner cells in embryos *in vitro* cultured in the presence of vehicle control (+DMSO) or p38-Mapk14/11 inhibitor (+SB220025) from the 8-cell (E2.5) to late blastocyst (E4.5) stages (averaged from three-data sets of embryos immuno-fluorescently stained for Nanog in combination with either Cdx2, Sox17 or Gata6).

Tables T2 (a-f)

+DMSO (IF: Nanog/ Cdx2)							
#	TOTAL NUMBER OF CELLS						TOTAL
	EMBRYO	TE (Cdx2 +ve)	Cdx2 +ve Inner cells	Nanog +ve outer cells	EPI (Nanog +ve)	ICM PrE (Nanog -ve)	
1	97	70	0	11	15	12	27
2	103	83	0	30	13	7	20
3	75	62	0	20	6	7	13
4	81	62	0	3	10	9	19
5	103	78	0	10	17	8	25
6	90	67	0	8	15	8	23
7	101	85	0	12	9	7	16
8	99	75	0	25	12	12	24
9	103	76	0	7	14	13	27
10	93	77	0	18	8	8	16
11	85	63	0	12	12	10	22
12	76	52	0	9	16	8	24
13	99	79	0	9	7	13	20
14	92	68	0	2	11	13	24
15							
16							
17							
18							
<b>TOTAL</b>	1297	997	0	176	165	135	300
<b>AVERAGE</b>	92.6	71.2	0.0	12.6	11.8	9.6	21.4
<b>SEM</b>	2.7	2.5	0.0	2.1	0.9	0.7	1.1

Table T2a

+p38-Mapk14/11inhibitor (SB220025, IF: Nanog/ Cdx2)							
#	TOTAL NUMBER OF CELLS						TOTAL
	EMBRYO	TE (Cdx2 +ve)	Cdx2 +ve Inner cells	Nanog +ve outer cells	EPI (Nanog +ve)	ICM PrE (Nanog -ve)	
1	26	15	8	15	11	0	11
2	53	41	3	41	12	0	12
3	16	13	0	13	3	0	3
4	15	10	2	10	5	0	5
5	33	21	0	21	12	0	12
6	43	31	1	31	12	0	12
7	26	18	6	18	8	0	8
8	36	25	0	25	11	0	11
9	26	17	2	17	9	0	9
10	40	27	0	25	12	0	13
11	54	42	4	16	12	0	12
12	31	18	5	17	13	0	13
13	44	27	3	16	17	0	17
14	19	11	4	11	8	0	8
15	56	42	1	13	14	0	14
16	28	14	0	7	14	0	14
17	21	15	3	15	6	0	6
18	25	18	1	14	7	0	7
<b>TOTAL</b>	592	405	43	325	186	0	187
<b>AVERAGE</b>	32.9	22.5	2.4	18.1	10.4	0.0	10.4
<b>SEM</b>	3.0	2.5	0.5	1.9	0.8	0.0	0.9
Stat. sig. (exp. vs. con embryo; T2a) *p<0.05, **p<0.005	**	**	**			**	**
p-value (2-tailed students t-test)	6.16E-15	2.20E-14	6.21E-04	6.70E-02	2.56E-01	7.46E-17	7.83E-09

Table T2b

<b>+DMSO (IF: Nanog/ Sox17)</b>								
#	TOTAL NUMBER OF CELLS							
	EMBRYO	TE	Nanog +ve TE cells	Nanog	Sox17	ICM Nanog/Sox17 (co-expressed)	Nanog/Sox17 ve	TOTAL
1	87	61	17	18	5	3	0	26
2	94	78	32	10	4	2	0	16
3	93	75	10	7	10	1	0	18
4	42	33	17	6	2	1	0	9
5	101	83	20	6	9	3	0	18
6	82	66	14	8	3	4	1	16
7	110	87	10	13	9	1	0	23
8	73	52	11	13	4	3	1	21
9	82	70	16	8	4	0	0	12
10	101	78	7	11	8	2	2	23
11	100	85	14	8	7	0	0	15
12	99	80	5	10	7	2	0	19
13	80	65	12	5	7	3	0	15
14	79	65	28	11	2	1	0	14
15								
<b>TOTAL</b>	1223	978	213	134	81	26	4	245
<b>AVERAGE</b>	87.4	69.9	15.2	9.6	5.8	1.9	0.3	17.5
<b>SEM</b>	4.5	3.9	2.0	0.9	0.7	0.3	0.2	1.2

Table T2c

<b>+p38-Mapk14/11 inhibitor (SB220025, IF: Nanog/ Sox17)</b>								
#	TOTAL NUMBER OF CELLS							
	EMBRYO	TE	Nanog +ve TE cells	Nanog	Sox17	ICM Nanog/Sox17 (co-expressed)	Nanog/Sox17 ve	TOTAL
1	27	20	16	7	0	0	0	7
2	33	23	12	13	0	0	1	14
3	13	9	4	4	0	0	0	4
4	40	22	22	18	0	0	2	20
5	30	20	19	10	0	0	0	10
6	42	25	18	17	0	0	0	17
7	18	13	13	5	0	0	0	5
8	26	17	13	9	0	0	1	10
9	31	22	22	9	0	0	0	9
10	27	21	13	6	0	0	1	7
11	33	24	12	9	0	0	0	9
12	50	30	17	20	0	0	0	20
13	19	13	13	6	0	0	0	6
14	21	13	10	8	0	0	0	8
15	53	43	35	10	0	0	0	10
<b>TOTAL</b>	463	315	239	151	0	0	5	156
<b>AVERAGE</b>	30.9	21.0	15.9	10.1	0.0	0.0	0.3	10.4
<b>SEM</b>	3.0	2.1	1.8	1.3	0.0	0.0	0.2	1.3
Stat. sig. (exp. vs. con embryos; T2c) *p<0.05, **p<0.005	**	**			**	**		**
p-value (2-tailed students t-test)	3.99E-11	1.20E-11	7.92E-01	7.57E-01	6.15E-09	3.16E-06	8.36E-01	5.54E-04

Table T2d

+DMSO (IF: Nanog/ Gata6)								
#	TOTAL NUMBER OF CELLS							
	EMBRYO	TE	Nanog +ve TE cells	Nanog	Gata6	ICM Nanog/Gata6 (co-expressed)	Nanog/Gata6-ve	TOTAL
1	89	66	0	9	13	1	0	23
2	59	41	6	9	5	4	0	18
3	89	68	0	6	7	8	0	21
4	67	47	1	6	6	8	0	20
5	90	66	0	10	5	9	0	24
6	64	49	0	11	1	3	0	15
7	70	50	0	8	8	4	0	20
8	104	88	1	6	8	2	0	16
9	80	59	0	8	11	2	0	21
10	75	51	0	8	6	10	0	24
11	79	62	0	5	9	3	0	17
12	79	49	0	11	17	2	0	30
13	73	54	0	5	3	11	0	19
<b>TOTAL</b>	<b>1018</b>	<b>750</b>	<b>8</b>	<b>102</b>	<b>99</b>	<b>67</b>	<b>0</b>	<b>268</b>
<b>AVERAGE</b>	<b>78.3</b>	<b>57.7</b>	<b>0.6</b>	<b>7.8</b>	<b>7.6</b>	<b>5.2</b>	<b>0.0</b>	<b>20.6</b>
<b>SEM</b>	<b>3.4</b>	<b>3.4</b>	<b>0.5</b>	<b>0.6</b>	<b>1.2</b>	<b>1.0</b>	<b>0.0</b>	<b>1.1</b>

Table T2e

p38-Mapk14/11 inhibitor (SB220025, IF: Nanog/ Gata6)								
#	TOTAL NUMBER OF CELLS							
	EMBRYO	TE	Nanog +ve TE cells	Nanog	Gata6	ICM Nanog/Gata6 (co-expressed)	Nanog/Gata6-ve	TOTAL
1	20	14	4	3	0	3	0	6
2	35	25	3	7	0	3	0	10
3	22	12	0	1	0	9	0	10
4	31	17	0	0	1	13	0	14
5	26	14	0	3	0	9	0	12
6	43	25	0	1	2	15	0	18
7	19	13	2	1	1	4	0	6
8	23	12	0	0	0	11	0	11
9	15	11	0	0	0	4	0	4
10	27	19	2	1	0	0	7	8
11	32	22	0	0	0	10	0	10
12	23	17	0	0	0	6	0	6
13								
<b>TOTAL</b>	<b>316</b>	<b>201</b>	<b>11</b>	<b>17</b>	<b>4</b>	<b>87</b>	<b>7</b>	<b>115</b>
<b>AVERAGE</b>	<b>26.3</b>	<b>16.8</b>	<b>0.9</b>	<b>1.4</b>	<b>0.3</b>	<b>7.3</b>	<b>0.6</b>	<b>9.6</b>
<b>SEM</b>	<b>2.3</b>	<b>1.4</b>	<b>0.4</b>	<b>0.6</b>	<b>0.2</b>	<b>1.3</b>	<b>0.6</b>	<b>1.1</b>
Stat. sig. (exp. vs. con embryo; T2e) *p<0.05, **p<0.005	<b>**</b>	<b>**</b>		<b>**</b>	<b>**</b>			<b>**</b>
p-value (2-tailed students t-test)	1.11E-11	2.30E-10	6.34E-01	8.59E-08	5.35E-06	2.10E-01	3.08E-01	4.62E-07

Table T2f

Tables T2 (a - f): Individual embryo data used to generate averaged data presented in figure 7d, d', e & e'; the average number of cells contributing to ICM cell lineages in embryos *in vitro* cultured in the presence of vehicle control (+DMSO) or p38-Mapk14/11 inhibitor (+SB220025) from the 8-cell (E2.5) to late blastocyst (E4.5) stages in embryos immuno-fluorescently stained for Nanog in combination with either Cdx2 (a & b), Sox17 (c & d) or Gata6 (e & f).

**Tables T3 (a-f)**

<b>+DMSO (IF: Nanog/ Gata4)</b>								
#	TOTAL NUMBER OF CELLS							
	EMBRYO	TE	Nanog +ve TE cells	Nanog	Gata4	ICM Nanog/Gata4 (co expressed)	Nanog/Gata4 ve	TOTAL
1	83	61	6	10	12	0	0	22
2	101	67	0	17	7	10	0	34
3	93	70	12	8	10	5	0	23
4	75	50	11	10	8	6	1	25
5	78	55	5	10	13	0	0	23
6	82	58	12	9	12	3	0	24
7	87	65	13	7	14	0	1	22
8	105	85	0	7	10	2	1	20
9	99	79	0	8	11	0	1	20
10	91	72	0	7	7	5	0	19
11	85	69	0	10	6	0	0	16
12	78	54	2	18	6	0	0	24
13	112	95	8	8	6	3	0	17
14	113	92	10	5	14	1	1	21
15	74	53	0	14	4	2	1	21
16	92	74	17	9	6	3	0	18
17	83	60	0	9	12	1	1	23
18	82	56	0	13	8	3	2	26
19	106	80	2	12	11	3	0	26
20	56	37	6	6	9	2	2	19
21	84	58	7	15	8	3	0	26
22	99	76	20	10	7	3	3	23
23	83	57	3	12	12	2	0	26
24	90	64	7	17	8	0	1	26
25	109	82	0	15	11	0	1	27
26	103	83	0	12	6	2	0	20
27	70	54	19	9	6	1	0	16
28								
29								
30								
31								
32								
33								
<b>TOTAL</b>	2413	1806	160	287	244	60	16	607
<b>AVERAGE</b>	89.4	66.9	5.9	10.6	9.0	2.2	0.6	22.5
<b>SEM</b>	2.7	2.7	1.2	0.7	0.5	0.4	0.2	0.8

**Table T3a**

<b>+p38-Mapk14/11 inhibitor (SB220025, IF: Nanog/ Gata4)</b>									
#	TOTAL NUMBER OF CELLS								
	EMBRYO	TE	Nanog +ve TE cells	ICM				TOTAL	
				Nanog	Gata4	Nanog/Gata4 (co- expressed)	Nanog/Gata4- ve		
1	66	55	19	6	2	1	2	11	
2	75	52	11	17	4	2	0	23	
3	65	49	25	15	0	0	1	16	
4	73	50	30	17	4	2	0	23	
5	105	82	20	16	6	0	1	23	
6	59	43	19	15	0	0	1	16	
7	51	38	10	8	4	1	0	13	
8	69	56	26	13	0	0	0	13	
9	41	31	14	9	0	0	1	10	
10	84	62	24	15	2	5	0	22	
11	91	73	15	8	6	2	2	18	
12	64	51	26	11	0	2	0	13	
13	71	54	12	8	7	1	1	17	
14	117	98	8	13	5	0	1	19	
15	67	55	8	6	0	6	0	12	
16	107	82	14	16	7	2	0	25	
17	80	60	20	13	3	3	1	20	
18	117	97	0	8	10	2	0	20	
19	73	55	10	7	4	5	2	18	
20	78	49	19	25	2	0	2	29	
21	87	63	48	24	0	0	0	24	
22	95	71	5	14	7	2	1	24	
23	52	42	11	10	0	0	0	10	
24	92	82	35	9	0	0	1	10	
25	72	50	31	15	3	3	1	22	
26	85	68	35	14	2	0	1	17	
27	64	47	19	15	0	2	0	17	
28	82	65	25	12	4	1	0	17	
29	83	62	26	21	0	0	0	21	
30	79	59	42	20	0	0	0	20	
31	72	46	23	22	2	2	0	26	
32	91	72	28	13	3	1	2	19	
33	56	38	28	16	0	0	2	18	
<b>TOTAL</b>	<b>2563</b>	<b>1957</b>	<b>606</b>	<b>451</b>	<b>87</b>	<b>45</b>	<b>23</b>	<b>606</b>	
<b>AVERAGE</b>	<b>77.7</b>	<b>59.3</b>	<b>20.8</b>	<b>13.7</b>	<b>2.6</b>	<b>1.4</b>	<b>0.7</b>	<b>18.4</b>	
<b>SEM</b>	<b>3.1</b>	<b>2.8</b>	<b>1.9</b>	<b>0.9</b>	<b>0.5</b>	<b>0.3</b>	<b>0.1</b>	<b>0.9</b>	
Stat. sig. (exp. vs. con. embryos; T3e) *p<0.05, **p<0.005	*		**	*	**			**	
p-value (2-tailed students t-test)	7.43E-03	5.88E-02	3.65E-08	1.02E-02	2.54E-12	9.64E-02	6.09E-01	9.52E-04	

**Table T3b**

+DMSO (IF: Nanog/ Sox17)								
#	TOTAL NUMBER OF CELLS							
	EMBRYO	TE	Nanog +ve TE cells	ICM				TOTAL
				Nanog	Sox17	Nanog/Sox17 (co-expressed)	Nanog/Sox17 -ve	
1	100	78	22	12	6	3	1	22
2	85	63	12	8	6	8	0	22
3	88	64	4	15	5	4	0	24
4	74	56	6	8	3	7	0	18
5	67	46	4	13	2	6	0	21
6	87	66	22	9	8	3	1	21
7	88	67	7	11	7	2	1	21
8	82	62	13	10	5	4	1	20
9	80	53	15	14	6	6	1	27
10	75	48	9	14	8	5	0	27
11	89	61	7	10	10	8	0	28
12	92	70	16	11	8	3	0	22
13	112	90	8	9	12	1	0	22
14	85	68	14	6	11	0	0	17
15	96	77	6	8	11	0	0	19
16	92	73	13	7	10	1	1	19
17	76	56	6	11	5	2	2	20
18	100	83	12	6	11	0	0	17
19								
20								
<b>TOTAL</b>	1568	1181	196	182	134	63	8	387
<b>AVERAGE</b>	87.1	65.6	10.9	10.1	7.4	3.5	0.4	21.5
<b>SEM</b>	2.6	2.8	1.3	0.6	0.7	0.6	0.1	0.8

Table T3c

+p38-Mapk14/11 inhibitor (SB220025, IF: Nanog/ Sox17)								
#	TOTAL NUMBER OF CELLS							
	EMBRYO	TE	Nanog +ve TE cells	ICM				TOTAL
				Nanog	Sox17	Nanog/Sox17 (co-expressed)	Nanog/Sox17 -ve	
1	71	42	19	25	0	2	2	29
2	76	52	21	17	0	5	2	24
3	77	55	29	17	0	3	2	22
4	75	54	26	21	0	0	0	21
5	77	55	48	22	0	0	0	22
6	92	70	35	14	2	6	0	22
7	73	56	33	16	0	1	0	17
8	78	62	19	8	3	5	0	16
9	84	58	25	16	3	7	0	26
10	81	63	20	9	8	0	1	18
11	72	55	27	16	1	0	0	17
12	92	68	30	15	9	0	0	24
13	76	60	23	11	1	1	3	16
14	73	57	12	9	2	5	0	16
15	91	66	26	16	4	5	0	25
16	78	63	35	12	0	3	0	15
17	78	69	22	5	0	4	0	9
18	85	64	17	12	2	5	2	21
19	77	65	24	8	4	0	0	12
20	72	57	32	7	3	3	2	15
<b>TOTAL</b>	1578	1191	523	276	42	55	14	387
<b>AVERAGE</b>	78.9	59.6	26.2	13.8	2.1	2.8	0.7	19.4
<b>SEM</b>	1.5	1.5	1.8	1.2	0.6	0.5	0.2	1.1
Stat. sig. (exp. vs. con. embryos; T3c) *p<0.05, **p<0.005	*		**	*	**			
p-value (2-tailed students t-test)	7.33E-03	5.63E-02	6.96E-08	1.21E-02	8.40E-07	3.67E-01	3.67E-01	1.32E-01

Table T3d

+DMSO (IF: Nanog/ Gata6)								
#	TOTAL NUMBER OF CELLS							
	EMBRYO	TE	Nanog +ve TE cells	Nanog	Gata6	ICM Nanog/Gata6 co-expressed)	Nanog/Gata6 ve	TOTAL
1	107	78	17	14	7	8	0	29
2	103	73	6	10	9	11	0	30
3	92	73	14	1	7	11	0	19
4	80	56	24	8	7	9	0	24
5	90	67	14	9	7	7	0	23
6	75	46	4	9	10	10	0	29
7	94	75	5	7	6	6	0	19
8	92	69	7	10	5	8	0	23
9	86	63	1	11	9	3	0	23
10	77	52	4	6	9	10	0	25
11	86	63	13	12	6	5	0	23
12	103	81	2	5	14	3	0	22
13	75	56	4	10	5	4	0	19
14	86	68	10	8	8	2	0	18
15	97	76	23	7	7	7	0	21
16	81	63	25	8	5	5	0	18
17	87	66	15	6	8	8	0	21
18	91	68	19	6	16	1	0	23
19	93	63	3	12	13	5	0	30
20	99	71	22	11	9	8	0	28
21	94	69	5	9	10	6	0	25
22	95	68	3	11	13	3	0	27
23	87	66	20	7	9	5	0	21
24	88	63	10	15	6	4	0	25
25								
26								
27								
<b>TOTAL</b>	2158	1593	270	85	76	83	0	244
<b>AVERAGE</b>	89.9	66.4	11.3	8.8	8.5	6.2	0.0	23.5
<b>SEM</b>	1.8	1.7	1.6	0.6	0.6	0.6	0.0	1.2

Table T3e

+p38-Mapk14/11 inhibitor (SB220025, IF: Nanog/ Gata6)								
#	TOTAL NUMBER OF CELLS							
	EMBRYO	TE	Nanog +ve TE cells	Nanog	Gata6	ICM Nanog/Gata6 co-expressed)	Nanog/Gata6 ve	TOTAL
1	91	66	47	9	4	12	0	25
2	65	50	26	4	3	8	0	15
3	90	65	52	9	3	13	0	25
4	79	59	42	6	1	13	0	20
5	88	67	35	5	3	13	0	21
6	91	75	18	5	4	7	0	16
7	87	67	45	6	5	9	0	20
8	80	67	43	0	2	11	0	13
9	65	42	36	0	0	23	0	23
10	81	56	34	10	1	14	0	25
11	80	59	29	7	4	10	0	21
12	65	55	19	3	3	4	0	10
13	73	60	35	8	1	4	0	13
14	48	38	21	4	1	5	0	10
15	61	47	24	5	2	7	0	14
16	88	63	25	13	4	8	0	25
17	79	60	12	8	1	10	0	19
18	75	62	36	6	3	4	0	13
19	84	63	39	5	3	13	0	21
20	73	55	23	6	2	10	0	18
21	100	80	44	8	0	12	0	20
22	88	71	40	6	2	9	0	17
23	82	62	29	6	4	10	0	20
24	83	67	26	8	5	3	0	16
25	91	75	68	4	2	10	0	16
26	87	68	28	9	5	5	0	19
27	82	62	19	9	1	10	0	20
<b>TOTAL</b>	2156	1661	895	169	69	257	0	495
<b>AVERAGE</b>	79.9	61.5	33.1	6.3	2.6	9.5	0.0	18.3
<b>SEM</b>	2.2	1.9	2.4	0.6	0.3	0.8	0.0	0.9
Stat. sig. (exp. vs. con. embryos; T3e) *p<0.05, **p<0.005	**		**	**	**	**		**
p-value (2-tailed students t-test)	9.27E-04	5.95E-02	1.28E-09	3.18E-03	2.21E-12	1.83E-03	n/a	4.27E-05

Table T3f

Tables T3 (a - f): Individual embryo data used to generate averaged data presented in figure 8c & d; the average number of cells contributing to all blastocyst cell lineages in embryos *in vitro* cultured in the presence of vehicle control (+DMSO) or p38-Mapk14/11 inhibitor (+SB220025) from the early (E3.5) to late blastocyst (E4.5) stages in embryos immuno-fluorescently stained for Nanog in combination with either Gata4 (a & b), Sox17 (c & d) or Gata6 (e & f).

Tables T4 (a-b)

+DMSO (IF: Nanog/ Cdx2)									
#	TOTAL NUMBER OF CELLS								
	EMBRYO	TE (Cdx2 +ve )	Nanog +ve TE cells	Nanog	Nanog/ Cdx2 -ve (PrE)	ICM Nanog/Cdx2 (co-expressed)	Cdx2 +ve	TOTAL	
1	79	63	35	11	5	0	0	16	
2	109	75	15	20	13	0	1	34	
3	92	69	12	15	7	0	1	23	
4	56	42	6	10	3	0	1	14	
5	84	62	9	15	7	0	0	22	
6	94	70	5	13	11	0	0	24	
7	76	58	10	12	6	0	0	18	
8	61	40	7	12	9	0	0	21	
9	80	70	8	6	4	0	0	10	
10	92	73	30	10	9	0	0	19	
11	90	66	15	16	8	0	0	24	
12	100	77	21	13	10	0	0	23	
13	90	63	5	13	14	0	0	27	
14	54	48	8	4	2	0	0	6	
15	60	45	1	11	3	0	1	15	
16	90	70	10	6	14	0	0	20	
17	83	61	11	14	8	0	0	22	
18									
19									
20									
21									
22									
23									
24									
25									
26									
<b>TOTAL</b>	1390	1052	208	201	133	0		338	
<b>AVERAGE</b>	81.8	61.9	12.2	11.8	7.8	0.0		19.9	
<b>SEM</b>	3.8	2.8	2.2	1.0	0.9	0.0		1.6	

Table T4a

+p38-Mapk14/11 inhibitor (SB220025, IF: Nanog/ Cdx2)								
#	TOTAL NUMBER OF CELLS							
	EMBRYO	TE (Cdx2 +ve )	Nanog +ve TE cells	ICM				TOTAL
				Nanog	Nanog/ Cdx2 -ve (PrE)	Nanog/Cdx2 (co-expressed)	Cdx2 +ve	
1	80	67	28	11	2	0	0	13
2	89	67	50	18	0	3	1	22
3	71	57	25	11	0	2	1	14
4	73	60	38	11	0	0	2	13
5	64	50	34	10	1	3	0	14
6	91	66	26	22	1	1	1	25
7	71	48	23	18	3	0	2	23
8	71	52	25	15	2	1	1	19
9	74	46	25	20	2	2	4	28
10	75	58	30	14	2	1	0	17
11	77	64	8	11	2	0	0	13
12	66	58	26	6	2	0	0	8
13	72	58	21	9	5	0	0	14
14	83	64	41	14	1	2	2	19
15	97	84	15	7	6	0	0	13
16	74	61	25	9	2	1	1	13
17	67	52	36	14	0	1	0	15
18	97	69	30	21	5	2	0	28
19	91	65	27	17	3	2	4	26
20	81	71	42	9	0	1	0	10
21	65	43	23	11	5	5	1	22
22	83	58	28	20	0	3	2	25
23	56	47	18	6	3	0	0	9
24	90	79	37	7	0	0	4	11
25	67	59	36	6	0	0	2	8
26	76	50	22	21	3	1	1	26
<b>TOTAL</b>	2001	1553	739	338	50	31	29	448
<b>AVERAGE</b>	77.0	59.7	28.4	13.0	1.9	1.2	1.1	17.2
<b>SEM</b>	2.1	2.0	1.8	1.0	0.4	0.3	0.3	1.3
Stat. sig. (exp. vs. con. embryos; T4a) *p<0.05, **p<0.005			**		**	**	*	
p-value (2-tailed students t-test)	2.41E-01	5.20E-01	9.46E-07	4.32E-01	2.46E-08	5.08E-04	1.08E-02	1.98E-01

**Table T4b**

**Tables T4 (a & b): Individual embryo data used to generate averaged data presented in figure 9;** the average number of cells contributing to all blastocyst cell lineages in embryos *in vitro* cultured in the presence of vehicle control (+DMSO) or p38-Mapk14/11 inhibitor (+SB220025) from the early (E3.5) to late blastocyst (E4.5) stages in embryos immuno-fluorescently stained for Nanog and Cdx2.

**Tables T5 (a-c)**

p38-Mapk $\alpha/\beta$ inhibitor (SB203580) inactive analogue (SB202474, IF: Nanog/ Gata4)									
#	TOTAL NUMBER OF CELLS								
	EMBRYO	TE	Nanog -ve TE cells	Nanog +ve TE cells	ICM				TOTAL
					Nanog	Gata4	Nanog/Gata4 (co-expressed)	Nanog/Gata4 -ve	
1	80	69	56	13	5	4	2	0	11
2	94	73	69	4	7	13	1	0	21
3	85	71	51	20	5	8	1	0	14
4	102	80	70	10	12	7	2	1	22
5	83	66	63	3	7	9	1	0	17
6	96	77	73	4	12	7	0	0	19
7	101	76	54	22	12	12	1	0	25
8	85	65	61	4	8	10	2	0	20
9	94	72	66	6	12	10	0	0	22
10	86	67	58	9	8	11	0	0	19
11	110	89	80	9	6	14	1	0	21
12	106	75	66	9	17	12	2	0	31
13	106	82	72	10	10	13	0	1	24
14	92	71	64	7	14	6	1	0	21
15	104	79	76	3	17	8	0	0	25
16	82	58	54	4	16	7	1	0	24
17	89	67	62	5	11	11	0	0	22
18	90	69	68	1	16	4	1	0	21
19	100	79	65	14	11	9	1	0	21
20									
21									
22									
23									
24									
25									
26									
27									
28									
29									
30									
31									
32									
<b>TOTAL</b>	1785	1385	1228	157	206	175	17	2	400
<b>AVERAGE</b>	93.9	72.9	64.6	8.3	10.8	9.2	0.9	0.1	21.1
<b>SEM</b>	2.1	1.7	1.8	1.3	0.9	0.7	0.2	0.1	1.0
Stat. sig. (con. vs. con. embryos; T5a) *p<0.05, **p<0.005							*		
p-value (2-tailed students t-test)	7.82E-01	9.36E-01	7.71E-01	5.66E-01	5.17E-01	2.26E-01	1.81E-02	8.60E-01	6.31E-01

**Table T5a**

DMSO (IF: Nanog/ Gata4)									
#	TOTAL NUMBER OF CELLS								
	EMBRYO	TE	Nanog -ve TE cells	Nanog +ve TE cells	ICM				TOTAL
					Nanog	Gata4	Nanog/Gata4 (co-expressed)	Nanog/Gata4 -ve	
1	97	72	59	13	16	7	2	0	25
2	99	81	61	20	12	6	0	0	18
3	92	67	54	13	18	7	0	0	25
4	106	84	71	13	9	10	3	0	22
5	104	81	72	9	13	10	0	0	23
6	103	87	82	5	8	6	2	0	16
7	110	85	77	8	14	8	3	0	25
8	95	73	65	8	13	7	2	0	22
9	83	64	55	9	9	9	1	0	19
10	75	58	50	8	11	2	2	2	17
11	108	78	77	1	18	10	2	0	30
12	87	67	62	5	12	8	0	0	20
13	115	90	87	3	15	9	1	0	25
14	85	63	59	4	11	9	2	0	22
15	101	82	66	16	9	7	3	0	19
16	89	66	56	10	12	6	5	0	23
17	93	69	57	12	12	10	2	0	24
18	76	60	55	5	5	9	2	0	16
19	84	65	47	18	8	8	2	1	19
20	102	88	73	15	6	8	0	0	14
21	98	79	78	1	8	9	2	0	19
22	107	76	72	4	15	14	2	0	31
23	76	59	57	2	9	5	3	0	17
24	99	76	71	5	13	9	1	0	23
25	83	65	58	7	11	5	2	0	18
26	105	76	61	15	17	12	0	0	29
27	92	75	48	27	8	8	0	1	17
28	95	70	66	4	15	8	2	0	25
29	85	64	54	10	12	4	5	0	21
30	98	77	69	8	8	10	3	0	21
31	99	80	66	14	5	14	0	0	19
32	91	62	58	4	18	10	1	0	29
<b>TOTAL</b>	<b>3032</b>	<b>2339</b>	<b>2043</b>	<b>296</b>	<b>370</b>	<b>264</b>	<b>55</b>	<b>4</b>	<b>693</b>
<b>AVERAGE</b>	<b>94.8</b>	<b>73.1</b>	<b>63.8</b>	<b>9.3</b>	<b>11.6</b>	<b>8.3</b>	<b>1.7</b>	<b>0.1</b>	<b>21.7</b>
<b>SEM</b>	<b>1.8</b>	<b>1.6</b>	<b>1.8</b>	<b>1.1</b>	<b>0.7</b>	<b>0.5</b>	<b>0.2</b>	<b>0.1</b>	<b>0.8</b>

Table T5b

p38-Mapk $\alpha/\beta$ inhibitor (SB203580, IF: Nanog/ Gata4)									
#	TOTAL NUMBER OF CELLS								
	EMBRYO	TE	Nanog -ve TE cells	Nanog +ve TE cells	ICM				TOTAL
					Nanog	Gata4	Nanog/Gata4 (co-expressed)	Nanog/Gata4 -ve	
1	95	61	60	1	31	2	1	0	34
2	83	47	39	8	30	6	0	0	36
3	66	42	39	3	19	3	1	1	24
4	97	67	65	2	24	5	0	1	30
5	92	59	57	2	27	4	0	2	33
6	72	53	48	5	17	2	0	0	19
7	94	63	62	1	26	1	1	3	31
8	86	62	58	4	16	8	0	0	24
9	85	55	53	2	23	3	3	1	30
10	87	53	51	2	30	2	1	1	34
11	87	60	47	13	24	0	3	0	27
12	66	38	35	3	22	6	0	0	28
13	88	50	47	3	32	1	4	1	38
14	87	57	56	1	28	0	2	0	30
15	66	37	32	5	26	1	2	0	29
16	108	83	81	2	21	2	2	0	25
17	88	58	57	1	24	5	1	0	30
18	99	65	60	5	27	4	2	1	34
19									
20									
21									
22									
23									
24									
25									
26									
27									
28									
29									
30									
31									
32									
<b>TOTAL</b>	1546	1010	947	63	447	55	23	11	536
<b>AVERAGE</b>	85.9	56.1	52.6	3.5	24.8	3.1	1.3	0.6	29.8
<b>SEM</b>	2.8	2.6	2.8	0.7	1.1	0.5	0.3	0.2	1.1
Stat. sig. (exp. vs. con. embryos; T5a) *p<0.05, **p<0.005	*	**	**	**	**	**		*	**
p-value (2-tailed students t-test)	8.15E-03	4.40E-07	9.02E-04	4.12E-04	8.50E-15	3.82E-09	2.58E-01	9.28E-03	1.65E-07
Stat. sig. (exp. vs. con. embryos; T5b) §p<0.05, §§p<0.005	§	§§	§§	§§	§§	§§		§	§§
p-value (2-tailed students t-test)	2.63E-02	3.65E-06	8.80E-04	3.38E-03	1.17E-11	2.96E-08	2.55E-01	2.06E-02	1.16E-06

**Table T5c**

**Tables T5 (a – c): Individual embryo data used to generate averaged data presented in figure 10;** the average number of cells contributing to all blastocyst cell lineages in embryos *in vitro* cultured in the presence of vehicle control (+DMSO), the inactive analog of the p38-Mapk14/11 inhibiting drug SB203580 (+SB202474) or the p38-Mapk14/11 inhibiting drug itself (+S203580), from the early (E3.5) to late blastocyst (E4.5) stages in embryos immuno-fluorescently stained for Nanog and Gata4.

Tables T6 (a-b)

DMSO (IF: Nanog/ Gata6)									
#	TOTAL NUMBER OF CELLS								
	EMBRYO	TE	Nanog -ve TE cells	Nanog +ve TE cells	ICM				TOTAL
					Nanog	Gata6	Nanog/Gata6 (co-expressed)	Nanog/Gata6 -ve	
1	104	89	65	24	5	9	1	0	15
2	114	92	71	21	7	13	2	0	22
3	80	64	50	14	9	7	0	0	16
4	103	86	81	5	4	8	5	0	17
5	94	72	59	13	6	12	4	0	22
6	96	72	63	9	6	14	4	0	24
7	86	66	53	13	4	10	6	0	20
8	94	76	60	16	4	10	4	0	18
9	89	72	62	10	7	10	0	0	17
10	73	55	46	9	4	7	7	0	18
11	80	64	42	22	5	9	2	0	16
12	99	81	59	22	7	7	4	0	18
13									
14									
<b>TOTAL</b>	1112	889	711	178	68	116	39	0	223
<b>AVERAGE</b>	92.7	74.1	59.3	14.8	5.7	9.7	3.3	0.0	18.6
<b>SEM</b>	3.4	3.2	3.1	1.8	0.5	0.7	0.7	0.0	0.8

Table T6a

p38-Mapk $\alpha/\beta$ inhibitor (SB203580, IF: Nanog/ Gata6)									
#	TOTAL NUMBER OF CELLS								
	EMBRYO	TE	Nanog -ve TE cells	Nanog +ve TE cells	ICM				TOTAL
					Nanog	Gata6	Nanog/Gata6 (co-expressed)	Nanog/Gata6 -ve	
1	95	62	41	21	3	7	23	0	33
2	63	42	40	2	0	7	14	0	21
3	95	65	50	15	0	2	28	0	30
4	99	70	57	13	3	8	18	0	29
5	89	65	51	14	4	4	16	0	24
6	47	30	22	8	1	4	12	0	17
7	99	75	66	9	1	5	18	0	24
8	96	61	60	1	5	15	15	0	35
9	91	71	64	7	1	1	18	0	20
10	94	51	43	8	3	5	35	0	43
11	105	67	65	2	2	4	32	0	38
12	90	65	64	1	4	8	13	0	25
13	101	74	72	2	2	7	18	0	27
14	97	75	62	13	4	7	11	0	22
<b>TOTAL</b>	1261	873	757	116	33	84	271	0	388
<b>AVERAGE</b>	90.1	62.4	54.1	8.3	2.4	6.0	19.4	0.0	27.7
<b>SEM</b>	4.2	3.5	3.7	1.7	0.4	0.9	2.0	0.0	2.0
Stat. sig. (exp. vs. con. embryos; T6a) *p<0.05, **p<0.005		*		*	**	**	**		**
p-value (2-tailed students t-test)	6.43E-01	2.29E-02	2.99E-01	1.34E-02	2.27E-05	4.22E-03	2.00E-07	-	5.06E-04

Table T6b

Tables T6 (a & b): Individual embryo data used to generate averaged data presented in figure 11; the average number of cells contributing to all blastocyst cell lineages in embryos *in vitro* cultured in the presence of vehicle control (+DMSO) or the p38-Mapk14/11 inhibiting drug S203580, from the early (E3.5) to late blastocyst (E4.5) stages in embryos immuno-fluorescently stained for Nanog and Gata6.

Tables T7 (a-h)

<b>+DMSO E3.5 - E4.5, IF: (Nanog/ Gata4)</b>										
#	TOTAL NUMBER OF CELLS									
	EMBRYO	TE	Nanog -ve TE cells	Nanog +ve TE cells	ICM				TOTAL	
					Nanog	Gata4	Nanog/Gata4 (co-expressed)	Nanog/Gata4 -ve		
1	69	44	31	13	15	3	6	1	25	
2	96	69	59	10	14	8	5	0	27	
3	86	64	57	7	14	8	0	0	22	
4	90	66	48	18	11	6	7	0	24	
5	78	56	39	17	10	12	0	0	22	
6	81	62	37	25	13	5	1	0	19	
7	83	57	54	3	11	8	5	2	26	
8	104	85	66	19	8	10	1	0	19	
9	64	52	50	2	5	4	3	0	12	
10	87	67	55	12	11	7	2	0	20	
11	85	71	69	2	4	9	1	0	14	
12	101	75	69	6	11	11	4	0	26	
13										
14										
15										
<b>TOTAL</b>	1024	768	634	134	127	91	35	3	256	
<b>AVERAGE</b>	85.3	64.0	52.8	11.2	10.6	7.6	2.9	0.3	21.3	
<b>SEM</b>	3.4	3.2	3.6	2.2	1.0	0.8	0.7	0.2	1.4	

Table T7a

<b>+DMSO E3.5 - E4.0 &amp; KSOM alone E4.0 - E4.5, (IF: Nanog/ Gata4)</b>										
#	TOTAL NUMBER OF CELLS									
	EMBRYO	TE	Nanog -ve TE cells	Nanog +ve TE cells	ICM				TOTAL	
					Nanog	Gata4	Nanog/Gata4 (co-expressed)	Nanog/Gata4 -ve		
1	62	43	29	14	15	4	0	0	19	
2	119	87	85	2	6	26	0	0	32	
3	99	78	63	15	8	10	3	0	21	
4	63	34	27	7	22	5	2	0	29	
5	87	66	45	21	13	6	2	0	21	
6	100	80	73	7	7	12	1	0	20	
7	90	60	49	11	17	9	4	0	30	
8	99	75	47	28	13	11	0	0	24	
9	96	70	50	20	12	7	7	0	26	
10	94	67	44	23	19	6	0	2	27	
11	86	68	61	7	6	11	1	0	18	
12	72	48	35	13	13	7	4	0	24	
13	86	61	40	21	18	6	0	1	25	
14	58	34	29	5	18	4	0	2	24	
15	92	70	56	14	10	11	1	0	22	
16	87	63	58	5	9	15	0	0	24	
17	102	79	71	8	10	13	0	0	23	
18	86	66	55	11	5	14	1	0	20	
19	49	31	30	1	8	9	1	0	18	
20	91	69	55	14	14	6	2	0	22	
21	102	74	51	23	11	15	2	0	28	
22	76	60	50	10	7	7	2	0	16	
23	81	64	63	1	7	10	0	0	17	
<b>TOTAL</b>	1977	1447	1166	281	268	224	33	5	530	
<b>AVERAGE</b>	86.0	62.9	50.7	12.2	11.7	9.7	1.4	0.2	23.0	
<b>SEM</b>	3.4	3.2	3.1	1.6	1.0	1.0	0.4	0.1	0.9	
Stat. sig. (con vs. con embryos; T7a) *p<0.05, **p<0.005										
p-value (2-tailed students t-test)	9.08E-01	9.08E-01	9.08E-01	9.08E-01	9.08E-01	9.08E-01	9.08E-01	9.08E-01	9.08E-01	

Table T7b

<b>+DMSO E3.75 - E4.5, (IF: Nanog/ Gata4)</b>									
#	TOTAL NUMBER OF CELLS								
	EMBRYO	TE	Nanog -ve TE cells	Nanog +ve TE cells	Nanog	Gata4	ICM		TOTAL
							Nanog/Gata4 (co-expressed)	Nanog/Gata4 -ve	
1	83	71	45	26	7	5	0	0	12
2	70	53	41	12	8	8	1	0	17
3	92	70	55	15	11	9	2	0	22
4	87	65	54	11	7	10	5	0	22
5	88	64	64	0	15	6	3	0	24
6	88	70	55	15	11	7	0	0	18
7	87	59	55	4	18	9	1	0	28
8	87	68	58	10	9	6	4	0	19
9	69	56	55	1	6	7	0	0	13
10	87	60	45	15	14	11	2	0	27
11	98	74	54	20	15	7	2	0	24
12									
13									
14									
15									
<b>TOTAL</b>	936	710	581	129	121	85	20	0	226
<b>AVERAGE</b>	85.1	64.5	52.8	11.7	11.0	7.7	1.8	0.0	20.9
<b>SEM</b>	2.6	2.0	2.0	2.4	1.2	0.6	0.5	0.0	1.6
Stat. sig. (con vs. con embryos; T7a) *p<0.05, **p<0.005									
p-value (2-tailed students t-test)	9.56E-01	8.88E-01	9.97E-01	8.63E-01	7.91E-01	8.85E-01	2.24E-01	1.97E-01	7.10E-01
Stat. sig. (con vs. con embryos; T7b) §p<0.05, §§p<0.005									
p-value (2-tailed students t-test)	8.71E-01	7.39E-01	6.60E-01	8.63E-01	6.99E-01	1.99E-01	5.49E-01	2.42E-01	1.49E-01

Table T7c

<b>+DMSO E4.0 - E4.5, (IF: Nanog/ Gata4)</b>									
#	TOTAL NUMBER OF CELLS								
	EMBRYO	TE	Nanog -ve TE cells	Nanog +ve TE cells	Nanog	Gata4	ICM		TOTAL
							Nanog/Gata4 (co-expressed)	Nanog/Gata4 -ve	
1	106	81	73	8	9	13	3	0	25
2	79	63	57	6	11	5	0	0	16
3	82	59	46	13	10	9	4	0	23
4	99	69	63	6	15	11	4	0	30
5	48	38	31	7	8	2	0	0	10
6	105	83	77	6	10	10	2	0	22
7	96	70	54	16	16	9	1	0	26
8	85	58	51	7	17	5	4	1	27
9	94	74	71	3	6	11	3	0	20
10	88	68	57	11	7	11	1	1	20
11	75	53	47	6	11	7	4	0	22
12	88	58	53	5	13	9	8	0	30
13									
14									
15									
<b>TOTAL</b>	1045	774	680	94	133	102	34	2	271
<b>AVERAGE</b>	87.1	64.5	56.7	7.8	11.1	8.5	2.8	0.2	22.6
<b>SEM</b>	4.5	3.6	3.7	1.1	1.0	0.9	0.6	0.1	1.7
Stat. sig. (con vs. con embryos; T7a) *p<0.05, **p<0.005									
p-value (2-tailed students t-test)	7.61E-01	7.61E-01	7.61E-01	7.61E-01	7.61E-01	7.61E-01	7.61E-01	7.61E-01	7.61E-01
Stat. sig. (con vs. con embryos; T7b) §p<0.05, §§p<0.005									
p-value (2-tailed students t-test)	8.46E-01	8.46E-01	8.46E-01	8.46E-01	8.46E-01	8.46E-01	8.46E-01	8.46E-01	8.46E-01
Stat. sig. (con vs. con embryos; T7c) p<0.05, ††p<0.005									
p-value (2-tailed students t-test)	7.14E-01	9.92E-01	3.86E-01	1.38E-01	9.58E-01	4.89E-01	2.36E-01	1.71E-01	3.86E-01

Table T7d

<b>+DMSO E4.0 - E4.5, (IF: Nanog/ Gata4)</b>									
#	TOTAL NUMBER OF CELLS								
	EMBRYO	TE	Nanog -ve TE cells	Nanog +ve TE cells	Nanog	Gata4	ICM Nanog/Gata4 (co-expressed)	Nanog/Gata4 -ve	TOTAL
1	106	81	73	8	9	13	3	0	25
2	79	63	57	6	11	5	0	0	16
3	82	59	46	13	10	9	4	0	23
4	99	69	63	6	15	11	4	0	30
5	48	38	31	7	8	2	0	0	10
6	105	83	77	6	10	10	2	0	22
7	96	70	54	16	16	9	1	0	26
8	85	58	51	7	17	5	4	1	27
9	94	74	71	3	6	11	3	0	20
10	88	68	57	11	7	11	1	1	20
11	75	53	47	6	11	7	4	0	22
12	88	58	53	5	13	9	8	0	30
13									
14									
15									
<b>TOTAL</b>	1045	774	680	94	133	102	34	2	271
<b>AVERAGE</b>	87.1	64.5	56.7	7.8	11.1	8.5	2.8	0.2	22.6
<b>SEM</b>	4.5	3.6	3.7	1.1	1.0	0.9	0.6	0.1	1.7
Stat. sig. (con vs. con embryos; T7a) *p<0.05, **p<0.005									
p-value (2-tailed students t-test)	7.61E-01	7.61E-01	7.61E-01	7.61E-01	7.61E-01	7.61E-01	7.61E-01	7.61E-01	7.61E-01
Stat. sig. (con vs. con embryos; T7b) \$p<0.05, \$\$p<0.005									
p-value (2-tailed students t-test)	8.46E-01	8.46E-01	8.46E-01	8.46E-01	8.46E-01	8.46E-01	8.46E-01	8.46E-01	8.46E-01
Stat. sig. (con vs. con embryos; T7c) p<0.05, ++p<0.005									
p-value (2-tailed students t-test)	7.14E-01	9.92E-01	3.86E-01	1.38E-01	9.58E-01	4.89E-01	2.36E-01	1.71E-01	3.86E-01

Table T7e

<b>+p38-Mapk14/11 (SB220025) E3.5 - E4.0 &amp; KSOM alone E4.0 to E4.5, (IF: Nanog/ Gata4)</b>									
#	TOTAL NUMBER OF CELLS								
	EMBRYO	TE	Nanog -ve TE cells	Nanog +ve TE cells	Nanog	Gata4	ICM Nanog/Gata4 (co-expressed)	Nanog/Gata4 -ve	TOTAL
1	78	63	50	13	13	0	0	2	15
2	79	64	55	9	9	4	2	0	15
3	85	68	34	34	13	2	0	2	17
4	84	62	29	33	16	2	2	2	22
5	69	57	28	29	11	0	0	1	12
6	71	60	37	23	8	2	1	0	11
7	70	53	30	23	9	3	5	0	17
8	51	31	17	14	18	1	1	0	20
9	80	60	49	11	12	6	0	2	20
10	71	55	52	3	12	4	0	0	16
11	75	46	36	10	25	2	0	2	29
12	70	54	34	20	16	0	0	0	16
13	85	69	53	16	12	3	0	1	16
14	74	55	10	45	16	2	1	0	19
15	51	41	18	23	10	0	0	0	10
16	86	54	32	22	27	2	3	0	32
17	83	52	28	24	26	2	2	1	31
18	92	73	38	35	11	6	1	1	19
19	82	57	30	27	21	3	0	1	25
20	91	62	28	34	26	1	2	0	29
21	89	64	36	28	17	6	2	0	25
22	63	49	22	27	9	4	0	1	14
23	83	65	33	32	13	3	2	0	18
24	79	67	27	40	8	3	1	0	12
25	65	51	21	30	13	0	0	1	14
<b>TOTAL</b>	1906	1432	827	605	371	61	25	17	474
<b>AVERAGE</b>	76.2	57.3	33.1	24.2	14.8	2.4	1.0	0.7	19.0
<b>SEM</b>	2.2	1.9	2.3	2.1	1.2	0.4	0.3	0.2	1.3
Stat. sig. (exp. vs. con. embryos; T7b) *p<0.05, **p<0.005	*		**	**	*	**		*	*
p-value (2-tailed students t-test)	1.91E-02	1.28E-01	3.96E-05	4.36E-05	4.74E-02	1.10E-08	3.26E-01	2.95E-02	1.25E-02
Stat. sig. (exp. vs. exp. embryos; T7e) \$p<0.05, \$\$p<0.005									
p-value (2-tailed students t-test)	3.62E-01	3.62E-01	3.62E-01	3.62E-01	3.62E-01	3.62E-01	3.62E-01	3.62E-01	3.62E-01

Table T7f

<b>+p38-Mapk14/11 inhibitor (SB220025) E3.75 - E4.5, (IF: Nanog/ Gata4)</b>									
#	TOTAL NUMBER OF CELLS								
	EMBRYO	TE	Nanog -ve TE cells	Nanog +ve TE cells	Nanog	Gata4	ICM Nanog/Gata4 (co-expressed)	Nanog/Gata4 -ve	TOTAL
1	97	76	71	5	14	7	0	0	21
2	71	53	51	2	9	7	0	2	18
3	101	73	65	8	13	12	3	0	28
4	64	42	36	6	13	2	5	2	22
5	76	54	39	15	12	5	5	0	22
6	78	58	48	10	10	4	3	3	20
7	73	54	53	1	10	7	0	2	19
8	77	60	49	11	6	10	1	0	17
9	83	62	42	20	11	6	4	0	21
10	80	58	53	5	10	9	2	1	22
11	85	61	41	20	16	5	3	0	24
12	106	82	80	2	10	14	0	0	24
13									
14									
15									
<b>TOTAL</b>	991	733	628	105	134	88	26	10	258
<b>AVERAGE</b>	82.6	61.1	52.3	8.8	11.2	7.3	2.2	0.8	21.5
<b>SEM</b>	3.5	3.1	3.7	1.8	0.7	0.9	0.5	0.3	0.8
Stat. sig. (exp. vs. con. embryos; T7c) *p<0.05, **p<0.005								*	
p-value (2-tailed students t-test)	5.89E-01	3.82E-01	9.15E-01	3.37E-01	9.06E-01	7.38E-01	6.51E-01	2.19E-02	5.93E-01
Stat. sig. (exp. vs. exp. embryos; T7e) §p<0.05, §§p<0.005			§§	§		§§	§§		
p-value (2-tailed students t-test)	5.66E-02	7.49E-02	2.50E-03	3.03E-02	6.74E-02	7.56E-06	4.63E-03	9.48E-01	4.68E-01
Stat. sig. (exp. vs. exp. embryos; T7f) †p<0.05, ††p<0.005			††	††	†	††	†		
p-value (2-tailed students t-test)	1.26E-01	2.83E-01	7.80E-05	4.10E-05	4.88E-02	2.06E-06	3.44E-02	6.35E-01	1.96E-01

Table T7g

<b>+p38-Mapk14/11 inhibitor (SB220025) E4.0 - E4.5, (IF: Nanog/ Gata4)</b>									
#	TOTAL NUMBER OF CELLS								
	EMBRYO	TE	Nanog -ve TE cells	Nanog +ve TE cells	Nanog	Gata4	ICM Nanog/Gata4 (co-expressed)	Nanog/Gata4 -ve	TOTAL
1	111	84	71	13	12	14	0	1	27
2	71	56	43	13	10	5	0	0	15
3	82	50	42	8	26	5	1	0	32
4	109	80	76	4	17	9	2	1	29
5	82	60	49	11	9	8	5	0	22
6	97	72	60	12	14	9	2	0	25
7	94	67	47	20	21	6	0	0	27
8	86	76	74	2	4	5	1	0	10
9	98	67	60	7	18	11	2	0	31
10	104	81	72	9	13	9	1	0	23
11	89	65	55	10	12	9	3	0	24
12	91	67	55	12	11	8	5	0	24
13	88	71	65	6	9	8	0	0	17
14	92	76	65	11	7	7	2	0	16
15									
<b>TOTAL</b>	1294	972	834	138	183	113	24	2	322
<b>AVERAGE</b>	92.4	69.4	59.6	9.9	13.1	8.1	1.7	0.1	23.0
<b>SEM</b>	2.9	2.6	3.1	1.2	1.6	0.7	0.5	0.1	1.7
Stat. sig. (exp. vs. con embryos; T7d) *p<0.05, **p<0.005									
p-value (2-tailed students t-test)	3.19E-01	2.70E-01	5.50E-01	2.24E-01	3.12E-01	7.03E-01	1.60E-01	8.73E-01	8.64E-01
Stat. sig. (exp. vs. exp. embryos; T7e) §p<0.05, §§p<0.005	§§	§§	§§	§		§§	§		
p-value (2-tailed students t-test)	1.05E-04	2.11E-04	5.94E-06	3.60E-02	2.70E-01	1.40E-08	2.13E-02	6.12E-02	2.10E-01
Stat. sig. (exp. vs. exp. embryos; T7f) †p<0.05, ††p<0.005	††	††	††	††		††		†	
p-value (2-tailed students t-test)	7.93E-05	4.81E-04	4.72E-08	1.97E-05	3.74E-01	1.24E-09	1.41E-01	2.35E-02	6.47E-02
Stat. sig. (exp. vs. exp. embryos; T7g) #p<0.05, ##p<0.005	#							#	
p-value (2-tailed students t-test)	4.42E-02	5.23E-02	1.52E-01	6.18E-01	3.06E-01	5.32E-01	5.31E-01	3.83E-02	4.66E-01

Table T7h

Tables T7 (a - h): Individual embryo data used to generate averaged data presented in figure 15c (p38-Mapk14/11 inhibition); the average number of cells contributing to all blastocyst cell lineages in embryos *in vitro* cultured to the late blastocyst (E4.5) stage in the presence of vehicle control (+DMSO) or p38-Mapk14/11 inhibitor (+SB220025) from the following blastocyst stage; E3.5, E3.75 and E4.0. Note an additional condition, in which embryos were cultured in control or inhibitor from the early blastocyst (E3.5) stage until the mid blastocyst (E4.0) stage and then transferred back to conventional growth media before continued culture to the late blastocyst (E4.5) stage, was also included. Embryos were immuno-fluorescently stained for Nanog and Gata4.

Tables T8 (a – h)

+DMSO E3.5 - E4.5, IF: (Nanog/ Gata4)									
#	TOTAL NUMBER OF CELLS								
	EMBRYO	TE	Nanog - ve TE cells	Nanog +ve TE cells	ICM				TOTAL
					Nanog	Gata4	Nanog/Gata4 co-expressed)	Nanog/Gata4 ve	
1	89	58	47	11	19	12	0	0	31
2	78	53	39	14	13	8	4	0	25
3	92	71	52	19	11	8	2	0	21
4	85	64	47	17	5	13	2	1	21
5	79	52	47	5	12	10	4	1	27
6	91	65	50	10	17	6	3	0	26
7	92	61	60	1	17	5	8	1	31
8	70	44	43	1	16	8	2	0	26
9	86	61	51	10	12	4	9	0	25
10	82	58	41	17	14	7	3	0	24
11	107	83	72	11	12	10	2	0	24
12	93	75	59	16	12	2	2	2	18
13	90	70	46	24	14	4	2	0	20
14									
15									
<b>TOTAL</b>	1134	815	654	156	174	97	43	5	319
<b>AVERAGE</b>	87.2	62.7	50.3	12.0	13.4	7.5	3.3	0.4	24.5
<b>SEM</b>	2.5	2.9	2.5	1.9	1.0	0.9	0.7	0.2	1.1

Table T8a

+DMSO E3.5 - E4.0 & KSOM alone E4.0 - E4.5, (IF: Nanog/ Gata4)									
#	TOTAL NUMBER OF CELLS								
	EMBRYO	TE	Nanog - ve TE cells	Nanog +ve TE cells	ICM				TOTAL
					Nanog	Gata4	Nanog/Gata4 co-expressed)	Nanog/Gata4 ve	
1	93	67	62	5	15	7	4	0	26
2	119	88	75	13	11	19	1	0	31
3	73	56	40	16	13	2	1	1	17
4	83	58	43	15	18	2	5	0	25
5	81	60	46	14	8	11	1	1	21
6	68	46	44	2	9	12	1	0	22
7	98	65	65	0	11	22	0	0	33
8	108	79	70	9	15	12	2	0	29
9	98	79	60	19	7	9	3	0	19
10	58	39	34	5	12	6	1	0	19
11	69	45	25	20	21	1	2	0	24
12	75	53	28	25	15	4	0	3	22
13	82	64	59	5	6	10	2	0	18
14	78	54	41	13	14	6	4	0	24
15	87	62	49	13	19	6	0	0	25
16	78	54	45	9	14	5	5	0	24
17	89	69	65	4	10	8	2	0	20
18	67	50	42	8	10	6	1	0	17
19	70	50	44	6	12	8	0	0	20
20	87	59	44	15	17	9	2	0	28
21									
22									
23									
24									
25									
<b>TOTAL</b>	1661	1197	981	216	257	165	37	5	464
<b>AVERAGE</b>	83.1	59.9	49.1	10.8	12.9	8.3	1.9	0.3	23.2
<b>SEM</b>	3.3	2.8	3.1	1.5	0.9	1.2	0.4	0.2	1.0
Stat. sig. (con vs. con embryos; T8a) *p<0.05, **p<0.005							*		
p-value (2-tailed students t-test)	3.24E-01	4.52E-01	6.59E-01	7.13E-01	6.47E-01	6.14E-01	3.74E-02	6.34E-01	3.52E-01

Table T8b

+DMSO E3.75 - E4.5, (IF: Nanog/ Gata4)									
#	TOTAL NUMBER OF CELLS								
	EMBRYO	TE	Nanog - ve TE cells	Nanog +ve TE cells	Nanog	Gata4	ICM Nanog/Gata4 co-expressed)	Nanog/Gata4 ve	TOTAL
1	64	50	47	3	6	7	1	0	14
2	89	68	59	9	12	7	2	0	21
3	81	63	59	4	6	10	2	0	18
4	80	60	46	14	8	9	3	0	20
5	77	54	47	7	11	6	5	1	23
6	95	69	54	15	15	9	2	0	26
7	78	58	48	10	9	9	2	0	20
8	78	51	39	12	14	11	2	0	27
9	80	68	61	7	7	5	0	0	12
10	77	60	41	19	7	8	2	0	17
11	94	76	68	8	5	13	0	0	18
12	78	59	39	20	10	6	3	0	19
13	93	62	56	6	19	8	4	0	31
14	91	72	35	37	9	6	3	1	19
15									
<b>TOTAL</b>	1155	870	699	171	138	114	31	2	285
<b>AVERAGE</b>	82.5	62.1	49.9	12.2	9.9	8.1	2.2	0.1	20.4
<b>SEM</b>	2.3	2.1	2.6	2.4	1.1	0.6	0.4	0.1	1.4
Stat. sig. (con vs. con embryos; T8a) *p<0.05, **p<0.005					*				
p-value (2-tailed students t-test)	1.79E-01	8.77E-01	9.17E-01	9.45E-01	2.29E-02	5.28E-01	1.70E-01	2.40E-01	2.48E-02
Stat. sig. (con vs. con embryos; T8b) \$p<0.05, \$\$p<0.005					*				
p-value (2-tailed students t-test)	9.02E-01	5.43E-01	8.39E-01	5.95E-01	4.02E-02	9.43E-01	4.94E-01	6.11E-01	9.74E-02

Table T8c

+DMSO E4.0 - E4.5, (IF: Nanog/ Gata4)									
#	TOTAL NUMBER OF CELLS								
	EMBRYO	TE	Nanog - ve TE cells	Nanog +ve TE cells	Nanog	Gata4	ICM Nanog/Gata4 co-expressed)	Nanog/Gata4 ve	TOTAL
1	73	51	39	12	13	7	2	0	22
2	102	73	56	17	13	11	5	0	29
3	88	74	52	22	9	5	0	0	14
4	84	59	55	4	10	13	2	0	25
5	87	70	52	18	6	11	0	0	17
6	90	65	53	12	8	13	4	0	25
7	92	70	63	7	12	5	5	0	22
8	95	75	48	27	8	7	4	1	20
9	83	61	60	1	9	11	2	0	22
10	85	61	57	4	10	13	0	1	24
11	83	65	43	22	12	4	2	0	18
12	102	71	67	4	15	15	1	0	31
13	92	63	46	17	16	8	5	0	29
14									
15									
<b>TOTAL</b>	1156	858	691	167	141	123	32	2	298
<b>AVERAGE</b>	88.9	66.0	53.2	12.8	10.8	9.5	2.5	0.2	22.9
<b>SEM</b>	2.2	1.9	2.2	2.3	0.8	1.0	0.5	0.1	1.4
Stat. sig. (con vs. con embryos; T8a) *p<0.05, **p<0.005									
p-value (2-tailed students t-test)	6.18E-01	3.51E-01	3.98E-01	7.80E-01	5.76E-02	1.53E-01	3.48E-01	2.79E-01	3.67E-01
Stat. sig. (con vs. con embryos; T8b) \$p<0.05, \$\$p<0.005									
p-value (2-tailed students t-test)	2.04E-01	1.13E-01	3.38E-01	4.38E-01	1.33E-01	4.75E-01	3.31E-01	6.60E-01	8.71E-01
Stat. sig. (con vs. con embryos; T8c) †p<0.05, ††p<0.005									
p-value (2-tailed students t-test)	5.78E-02	1.88E-01	3.57E-01	8.50E-01	4.74E-01	2.62E-01	7.04E-01	9.39E-01	1.97E-01

Table T8d

<b>+Mek1/2 inhibitor (SB220025) E3.5 - E4.5, (IF: Nanog/ Gata4)</b>									
#	TOTAL NUMBER OF CELLS								TOTAL
	EMBRYO	TE	Nanog - ve TE cells	Nanog +ve TE cells	Nanog	Gata4	ICM Nanog/Gata4 co-expressed)	Nanog/Gata4 ve	
1	90	55	51	4	35	0	0	0	35
2	97	70	63	7	27	0	0	0	27
3	88	54	49	5	32	0	1	1	34
4	105	73	67	6	32	0	0	0	32
5	71	65	51	14	6	0	0	0	6
6	103	66	51	15	35	0	2	0	37
7	75	52	44	8	23	0	0	0	23
8	93	67	67	0	25	0	0	1	26
9	82	59	59	0	23	0	0	0	23
10	102	59	54	5	43	0	0	0	43
11	95	57	55	2	38	0	0	0	38
12	78	48	43	5	24	4	2	0	30
13	105	72	69	3	33	0	0	0	33
14	134	79	73	6	55	0	0	0	55
15	92	56	53	3	36	0	0	0	36
16	98	80	65	15	18	0	0	0	18
17	104	60	51	9	42	0	0	2	44
18	107	83	64	19	24	0	0	0	24
19	110	69	62	7	41	0	0	0	41
20	99	71	60	11	27	0	1	0	28
21	82	54	44	10	25	3	0	0	28
22	82	53	40	13	29	0	0	0	29
23	73	53	44	9	20	0	0	0	20
24									
25									
<b>TOTAL</b>	2165	1455	1279	176	693	7	6	4	710
<b>AVERAGE</b>	94.1	63.3	55.6	7.7	30.1	0.3	0.3	0.2	30.9
<b>SEM</b>	3.0	2.1	2.0	1.1	2.1	0.2	0.1	0.1	2.1
Stat. sig. (exp vs. con embryos; T8a) *p<0.05, **p<0.005				*	**	**	**		*
p-value (2-tailed students t-test)	1.31E-01	8.73E-01	1.09E-01	3.63E-02	2.09E-06	1.87E-11	3.34E-06	2.80E-01	3.95E-02

Table T8e

<b>+Mek1/2 (SB220025) E3.5 - E4.0 &amp; KSOM alone E4.0 to E4.5, (IF: Nanog/ Gata4)</b>									
#	TOTAL NUMBER OF CELLS								TOTAL
	EMBRYO	TE	Nanog - ve TE cells	Nanog +ve TE cells	Nanog	Gata4	ICM Nanog/Gata4 co-expressed)	Nanog/Gata4 ve	
1	78	64	53	11	5	5	4	0	14
2	70	45	31	14	17	5	2	1	25
3	72	55	53	2	7	9	1	0	17
4	91	59	57	2	31	0	0	1	32
5	86	60	54	6	12	14	0	0	26
6	75	56	39	17	10	5	2	2	19
7	91	58	58	0	20	11	0	2	33
8	73	52	51	1	13	7	0	1	21
9	83	58	55	3	10	12	3	0	25
10	97	70	70	0	25	0	0	2	27
11	82	64	54	10	6	12	0	0	18
12	95	66	60	6	11	14	4	0	29
13	82	64	47	17	9	5	2	2	18
14	61	44	36	8	11	4	2	0	17
15	98	70	60	10	20	8	0	0	28
16	68	50	45	5	12	5	0	1	18
17	92	69	66	3	20	1	2	0	23
18	121	93	91	2	21	7	0	0	28
19	87	63	59	4	13	8	3	0	24
20	76	60	52	8	7	9	0	0	16
21	93	74	52	22	8	10	1	0	19
22	56	34	31	3	12	6	4	0	22
23	60	42	25	17	14	3	1	0	18
24									
25									
<b>TOTAL</b>	1887	1370	1199	171	314	160	31	12	517
<b>AVERAGE</b>	82.0	59.6	52.1	7.4	13.7	7.0	1.3	0.5	22.5
<b>SEM</b>	3.1	2.6	3.0	1.3	1.4	0.8	0.3	0.2	1.1
Stat. sig. (exp vs. con embryos; T8b) *p<0.05, **p<0.005									
p-value (2-tailed students t-test)	8.26E-01	9.40E-01	4.75E-01	9.47E-02	6.37E-01	3.69E-01	2.89E-01	2.47E-01	6.40E-01
Stat. sig. (exp. vs. exp embryos; T8e) \$p<0.05, \$\$p<0.005					\$\$	\$\$	\$\$		\$\$
p-value (2-tailed students t-test)	7.65E-03	2.71E-01	3.33E-01	8.98E-01	5.67E-08	1.44E-09	2.05E-03	7.99E-02	1.10E-03

Table T8f

<b>+Mek1/2 (SB220025) E3.75 - E4.5, (IF: Nanog/ Gata4)</b>									
#	TOTAL NUMBER OF CELLS								
	EMBRYO	TE	Nanog - ve TE cells	Nanog +ve TE cells	Nanog	Gata4	ICM Nanog/Gata4 co-expressed)	Nanog/Gata4 ve	TOTAL
1	99	70	59	11	27	2	0	0	29
2	81	55	35	20	18	2	6	0	26
3	108	64	57	7	42	2	0	0	44
4	109	58	58	0	51	0	0	0	51
5	106	61	60	1	38	7	0	0	45
6	75	48	42	6	25	2	0	0	27
7	102	71	68	3	21	9	0	1	31
8	87	55	52	3	30	2	0	0	32
9	82	47	47	0	34	0	0	1	35
10	103	61	58	3	42	0	0	0	42
11	90	63	55	8	25	2	0	0	27
12	108	57	55	2	46	3	1	1	51
13	97	57	57	0	40	0	0	0	40
14	68	47	38	9	21	0	0	0	21
15									
<b>TOTAL</b>	1315	814	741	73	460	31	7	3	501
<b>AVERAGE</b>	93.9	58.1	52.9	5.2	32.9	2.2	0.5	0.2	35.8
<b>SEM</b>	3.6	2.0	2.5	1.5	2.8	0.7	0.4	0.1	2.6
Stat. sig. (exp. vs. con embryos; T8c) *p<0.05, **p<0.005	**			*	**	**	**		**
p-value (2-tailed students t-test)	2.25E-03	2.86E-01	2.52E-01	1.80E-02	1.91E-08	2.56E-06	8.30E-03	5.74E-01	3.58E-06
Stat. sig. (exp. vs. exp embryos; T8e) \$p<0.05, \$\$p<0.005						\$\$			
p-value (2-tailed students t-test)	9.67E-01	1.09E-01	4.05E-01	1.79E-01	4.39E-01	4.03E-03	5.23E-01	8.01E-01	1.56E-01
Stat. sig. (exp. vs. exp embryos; T8f) †p<0.05, ††p<0.005	†				††	††			††
p-value (2-tailed students t-test)	1.95E-02	7.01E-01	8.52E-01	2.86E-01	5.08E-08	4.54E-04	1.09E-01	1.90E-01	4.95E-06

Table T8g

<b>+Mek1/2 (SB220025) E4.0 - E4.5, (IF: Nanog/ Gata4)</b>									
#	TOTAL NUMBER OF CELLS								
	EMBRYO	TE	Nanog - ve TE cells	Nanog +ve TE cells	Nanog	Gata4	ICM Nanog/Gata4 co-expressed)	Nanog/Gata4 ve	TOTAL
1	87	59	48	11	22	3	3	0	28
2	101	59	51	8	38	4	0	0	42
3	89	54	51	3	33	0	2	0	35
4	84	53	47	6	26	2	3	0	31
5	83	45	31	14	38	0	0	0	38
6	94	70	62	8	17	5	2	0	24
7	111	74	69	5	28	8	0	1	37
8	88	53	51	2	32	2	1	0	35
9	101	81	72	9	18	1	1	0	20
10	84	55	50	5	21	8	0	0	29
11	54	37	33	4	17	0	0	0	17
12	95	55	44	11	39	0	0	1	40
13	101	75	70	5	22	4	0	0	26
14									
15									
<b>TOTAL</b>	1172	770	679	91	351	37	12	2	402
<b>AVERAGE</b>	90.2	59.2	52.2	7.0	27.0	2.8	0.9	0.2	30.9
<b>SEM</b>	3.8	3.5	3.6	1.0	2.3	0.8	0.3	0.1	2.2
Stat. sig. (exp. vs. con embryos; T8d) *p<0.05, **p<0.005				*	**	**	*		**
p-value (2-tailed students t-test)	7.83E-01	1.03E-01	8.29E-01	2.91E-02	7.00E-07	2.81E-05	2.26E-02	1.00E+00	4.59E-03
Stat. sig. (exp. vs. exp embryos; T8e) \$p<0.05, \$\$p<0.005						\$\$	\$		
p-value (2-tailed students t-test)	4.27E-01	2.97E-01	3.76E-01	6.83E-01	3.51E-01	4.43E-04	3.40E-02	8.99E-01	9.87E-01
Stat. sig. (exp. vs. exp embryos; T8f) †p<0.05, ††p<0.005					††	††			††
p-value (2-tailed students t-test)	1.15E-01	9.39E-01	9.83E-01	8.21E-01	6.02E-06	2.83E-03	3.79E-01	1.25E-01	4.93E-04
Stat. sig. (exp. vs. exp embryos; T8g) #p<0.05, ##p<0.005									
p-value (2-tailed students t-test)	4.78E-01	7.86E-01	8.73E-01	3.33E-01	1.20E-01	5.59E-01	4.47E-01	7.00E-01	1.65E-01

Table T8h

Tables T8 (a - h): Individual embryo data used to generate averaged data presented in figure 15c (Mek1/2 inhibition); the average number of cells contributing to all blastocyst cell lineages in embryos *in vitro* cultured to the late blastocyst (E4.5) stage in the presence of vehicle control (+DMSO) or Mek1/2 inhibitor (+PD0325901) from the following blastocyst stage; E3.5, E3.75 and E4.0. Note an additional condition, in which embryos were cultured in control or inhibitor from the early blastocyst (E3.5) stage until the mid blastocyst (E4.0) stage and then transferred back to conventional growth media before continued culture to the late blastocyst (E4.5) stage, was also included. Embryos were immuno-fluorescently stained for Nanog and Gata4.

Tables T9 (a&b)

+DMSO E3.5 - E4.0, IF: (Nanog/ Sox17)									
#	TOTAL NUMBER OF CELLS								
	EMBRYO	TE	Nanog -ve TE cells	Nanog +ve TE cells	ICM				TOTAL
					Nanog	Sox17	Nanog/Sox17 (co-expressed)	Nanog/Sox17 -ve	
1	60	36	18	18	11	3	10	0	24
2	59	32	29	3	14	4	8	1	27
3	62	37	30	7	6	7	12	0	25
4	45	34	24	10	2	3	6	0	11
5	53	30	14	16	7	2	14	0	23
6	64	42	30	12	3	3	16	0	22
7	56	36	22	14	5	4	11	0	20
8	66	43	36	7	4	3	16	0	23
9	65	34	18	16	11	5	15	0	31
10	58	40	30	10	5	3	10	0	18
11	66	49	43	6	10	5	2	0	17
12	57	36	30	6	7	5	8	1	21
13	53	31	25	6	5	10	7	0	22
<b>TOTAL</b>	764	480	349	131	90	57	135	2	284
<b>AVERAGE</b>	58.8	36.9	26.8	10.1	6.9	4.4	10.4	0.2	21.8
<b>SEM</b>	1.7	1.5	2.2	1.3	1.0	0.6	1.2	0.1	1.4

Table T9a

+p38 Mapk14/11 inhibitor (SB220025) E3.5 - E4.0, (IF: Nanog/ Sox17)									
#	TOTAL NUMBER OF CELLS								
	EMBRYO	TE	Nanog -ve TE cells	Nanog +ve TE cells	ICM				TOTAL
					Nanog	Sox17	Nanog/Sox17 (co-expressed)	Nanog/Sox17 -ve	
1	61	38	20	18	4	3	16	0	23
2	54	31	12	19	0	0	21	2	23
3	51	33	19	14	5	4	8	1	18
4	48	24	16	8	0	4	20	0	24
5	57	31	27	4	7	2	17	0	26
6	62	43	33	10	3	4	10	2	19
7	65	39	29	10	2	3	21	0	26
8	53	30	16	14	0	1	22	0	23
9	51	27	18	9	0	5	19	0	24
10	44	30	27	3	0	2	12	0	14
11	55	35	29	6	0	5	15	0	20
12	52	32	19	13	0	3	17	0	20
13	45	26	18	8	0	2	17	0	19
<b>TOTAL</b>	698	419	283	136	21	38	215	5	279
<b>AVERAGE</b>	53.7	32.2	21.8	10.5	1.6	2.9	16.5	0.4	21.5
<b>SEM</b>	1.8	1.5	1.8	1.4	0.7	0.4	1.2	0.2	1.0
Stat. sig. (exp vs. con embryos; T9a) *p<0.05, **p<0.005	*	*			**	*	**		
p-value (2-tailed students t-test)	4.88E-02	3.59E-02	8.43E-02	8.41E-01	1.69E-04	5.51E-02	1.23E-03	3.40E-01	8.19E-01

Table T9b

Tables T9 (a & b): Individual embryo data used to generate averaged data presented in figure 16b (p38-Mapk14/11 inhibition); the average number of cells contributing to all blastocyst cell lineages in embryos *in vitro* cultured from the early blastocyst (E3.5) stage until the mid-blastocyst (E4.0) stage in the presence of vehicle control (+DMSO) or p38-Mapk14/11 inhibitor (+SB220025) and immuno-fluorescently stained for Nanog and Sox17.

Tables T10 (a&b)

+DMSO E3.5 - E4.0, IF: (Nanog/ Sox17)									
#	TOTAL NUMBER OF CELLS								
	EMBRYO	TE	Nanog -ve TE cells	Nanog +ve TE cells	ICM				TOTAL
					Nanog	Sox17	Nanog/Sox17 (co-expressed)	Nanog/Sox17 -ve	
1	60	37	21	16	10	5	8	0	23
2	61	37	23	14	11	3	10	0	24
3	54	34	19	15	11	1	8	0	20
4	60	35	12	23	7	7	11	0	25
5	62	36	20	16	17	3	6	0	26
6	62	40	24	16	14	4	4	0	22
7	57	33	16	17	9	7	8	0	24
8	47	26	10	16	12	2	7	0	21
9	53	34	18	16	11	3	5	0	19
10	55	31	26	5	15	2	7	0	24
11	69	47	34	13	9	7	6	0	22
12	58	32	15	17	7	12	7	0	26
13									
<b>TOTAL</b>	698	422	238	184	133	56	87	0	276
<b>AVERAGE</b>	58.2	35.2	19.8	15.3	11.1	4.7	7.3	0.0	23.0
<b>SEM</b>	1.6	1.5	1.9	1.2	0.9	0.9	0.6	0.0	0.7

Table T10a

+Mek1/2 inhibitor (SB220025) E3.5 - E4.0, (IF: Nanog/ Sox17)									
#	TOTAL NUMBER OF CELLS								
	EMBRYO	TE	Nanog -ve TE cells	Nanog +ve TE cells	ICM				TOTAL
					Nanog	Sox17	Nanog/Sox17 (co-expressed)	Nanog/Sox17 -ve	
1	56	33	21	12	11	4	8	0	23
2	54	28	18	10	23	0	3	0	26
3	62	35	31	4	8	3	16	0	27
4	67	32	20	12	20	3	12	0	35
5	57	37	28	9	10	0	10	0	20
6	60	37	33	4	12	3	8	0	23
7	51	28	18	10	19	0	4	0	23
8	64	39	35	4	12	5	6	2	25
9	48	32	25	7	13	0	3	0	16
10	55	26	13	13	13	1	14	1	29
11	59	35	21	14	20	0	3	1	24
12	60	33	20	13	16	4	6	1	27
13	60	34	18	16	18	2	5	1	26
<b>TOTAL</b>	753	429	301	128	195	25	98	6	324
<b>AVERAGE</b>	57.9	33.0	23.2	9.8	15.0	1.9	7.5	0.5	24.9
<b>SEM</b>	1.4	1.1	1.9	1.1	1.3	0.5	1.2	0.2	1.3
Stat. sig. (exp vs. con embryo; T10a) *p<0.05, **p<0.005				**	*	*		*	
p-value (2-tailed students t-test)	8.54E-01	2.44E-01	1.82E-01	1.07E-03	3.45E-02	1.63E-02	7.25E-01	4.20E-02	2.37E-01

Table T10b

Tables T10 (a & b): Individual embryo data used to generate averaged data presented in figure 16c (Mek1/2 inhibition); the average number of cells contributing to all blastocyst cell lineages in embryos *in vitro* cultured from the early blastocyst (E3.5) stage until the mid-blastocyst (E4.0) stage in the presence of vehicle control (+DMSO) or Mek1/2 inhibitor (+PD0325901) and immunofluorescently stained for Nanog and Sox17.

Tables T11 (a-e)

+DMSO, GFP mRNA (+OGDB) microinjected									
#	TOTAL NUMBER OF CELLS								
	EMBRYO	TE	Nanog -ve TE cells	Nanog +ve TE cells	Nanog	Gata4	ICM Nanog/Gata4 (co-expressed)	Nanog/Gata4 -ve	TOTAL
1	69	56	46	10	8	3	2	0	13
2	75	58	47	11	9	8	0	0	17
3	79	58	51	7	11	8	2	0	21
4	91	67	64	3	16	7	1	0	24
5	96	75	55	20	15	4	1	1	21
6	91	66	60	6	11	8	6	0	25
7	78	58	52	6	7	11	1	1	20
8	76	54	46	8	12	8	2	0	22
9	119	103	89	14	4	11	1	0	16
10	74	47	41	6	16	8	2	1	27
11	57	39	29	10	13	3	2	0	18
12	79	62	45	17	9	6	2	0	17
13	88	69	64	5	9	8	1	1	19
14	85	53	44	9	24	7	1	0	32
15	91	70	58	12	11	10	0	0	21
16	67	46	38	8	15	5	0	1	21
17	81	58	52	6	13	7	3	0	23
18	93	73	59	14	12	7	0	1	20
19	85	56	50	6	16	10	1	2	29
20	76	58	48	10	11	7	0	0	18
21	70	49	40	9	15	5	0	1	21
22	97	67	64	3	16	13	0	1	30
23	91	70	64	6	12	9	0	0	21
24									
<b>TOTAL</b>	1908	1412	1206	206	285	173	28	10	496
<b>AVERAGE</b>	83.0	61.4	52.4	9.0	12.4	7.5	1.2	0.4	21.6
<b>SEM</b>	2.7	2.7	2.6	0.9	0.9	0.5	0.3	0.1	1.0

Table T11a

+Fgf-receptor inhibitor (SU5402), GFP mRNA (+OGDB) microinjected									
#	TOTAL NUMBER OF CELLS								
	EMBRYO	TE	Nanog -ve TE cells	Nanog +ve TE cells	Nanog	Gata4	ICM Nanog/Gata4 (co-expressed)	Nanog/Gata4 -ve	TOTAL
1	74	68	53	15	5	0	0	1	6
2	81	49	33	16	25	7	0	0	32
3	75	57	52	5	15	0	1	2	18
4	74	55	45	10	19	0	0	0	19
5	49	41	28	13	5	0	2	1	8
6	55	34	25	9	15	4	2	0	21
7	72	54	42	12	17	0	0	1	18
8	73	51	47	4	16	5	1	0	22
9	85	56	46	10	20	5	3	1	29
10	94	61	55	6	25	6	2	0	33
11	44	26	17	9	16	0	0	2	18
12	68	51	37	14	17	0	0	0	17
13	92	71	61	10	15	4	1	1	21
14	65	47	37	10	18	0	0	0	18
15	66	48	35	13	16	1	1	0	18
16	67	41	18	23	25	0	0	1	26
17	91	70	61	9	13	5	1	2	21
18	96	67	63	4	25	1	1	2	29
19	57	36	22	14	20	0	0	1	21
20	62	41	26	15	18	0	2	1	21
21	64	57	41	16	7	0	0	0	7
22	66	53	36	17	10	2	0	1	13
23	82	63	41	22	13	3	2	1	19
24									
<b>TOTAL</b>	1652	1197	921	276	375	43	19	18	455
<b>AVERAGE</b>	71.8	52.0	40.0	12.0	16.3	1.9	0.8	0.8	19.8
<b>SEM</b>	2.9	2.5	2.8	1.1	1.2	0.5	0.2	0.2	1.5
Stat. sig. (exp. vs. con. embryos; T11a) *p<0.05, **p<0.005	**	*	**	*	*	**			
p-value (2-tailed students t-test)	7.55E-03	1.43E-02	2.27E-03	3.25E-02	1.18E-02	8.08E-10	2.67E-01	8.38E-02	3.18E-01

Table T11b

<b>+DMSO, Mkk6-EE mRNA (+OGDBs) microinjected</b>									
#	TOTAL NUMBER OF CELLS								
	EMBRYO	TE	Nanog -ve TE cells	Nanog +ve TE cells	Nanog	Gata4	ICM Nanog/Gata4 (co-expressed)	Nanog/Gata4 -ve	TOTAL
1	70	60	58	2	4	6	0	0	10
2	67	58	58	0	2	7	0	0	9
3	89	74	74	0	5	7	2	1	15
4	66	49	41	8	8	8	1	0	17
5	57	49	48	1	4	3	1	0	8
6	45	34	30	4	1	9	0	1	11
7	73	63	54	9	1	8	1	0	10
8	64	52	50	2	0	12	0	0	12
9	73	57	52	5	4	12	0	0	16
10	88	74	74	0	0	13	0	1	14
11	72	67	65	2	0	5	0	0	5
12	84	74	72	2	1	9	0	0	10
13	45	38	38	0	2	5	0	0	7
14	73	59	58	1	3	11	0	0	14
15	62	55	53	2	1	6	0	0	7
16	85	75	72	3	0	10	0	0	10
17	78	65	64	1	2	10	0	1	13
18	59	47	47	0	2	10	0	0	12
19	55	48	43	5	0	7	0	0	7
20	66	51	41	10	9	6	0	0	15
21	66	57	56	1	0	9	0	0	9
22	70	60	60	0	0	10	0	0	10
23	50	36	28	8	9	4	0	1	14
24	70	61	57	4	0	9	0	0	9
<b>TOTAL</b>	<b>1627</b>	<b>1363</b>	<b>1293</b>	<b>70</b>	<b>58</b>	<b>196</b>	<b>5</b>	<b>5</b>	<b>264</b>
<b>AVERAGE</b>	<b>67.8</b>	<b>56.8</b>	<b>53.9</b>	<b>2.9</b>	<b>2.4</b>	<b>8.2</b>	<b>0.2</b>	<b>0.2</b>	<b>11.0</b>
<b>SEM</b>	<b>2.5</b>	<b>2.4</b>	<b>2.6</b>	<b>0.6</b>	<b>0.6</b>	<b>0.5</b>	<b>0.1</b>	<b>0.1</b>	<b>0.7</b>
Stat. sig. (exp. vs. con. embryos; T11a) *p<0.05, **p<0.005	<b>**</b>			<b>**</b>	<b>**</b>		<b>**</b>		<b>**</b>
p-value (2-tailed students t-test)	1.46E-04	2.07E-01	6.97E-01	1.30E-06	1.28E-12	3.96E-01	1.63E-03	1.34E-01	7.96E-12

Table T11c

<b>+Fgf-receptor inhibitor (SU5402), Mkk6-EE mRNA (+OGDBs) microinjected</b>									
#	TOTAL NUMBER OF CELLS								
	EMBRYO	TE	Nanog -ve TE cells	Nanog +ve TE cells	Nanog	Gata4	ICM Nanog/Gata4 (co-expressed)	Nanog/Gata4 -ve	TOTAL
1	70	60	60	0	0	10	0	0	10
2	69	58	56	2	3	8	0	0	11
3	61	52	52	0	0	9	0	0	9
4	79	74	74	0	1	4	0	0	5
5	42	22	14	8	16	2	1	1	20
6	75	65	65	0	0	10	0	0	10
7	42	33	29	4	4	2	3	0	9
8	66	56	51	5	4	4	0	2	10
9	81	57	56	1	11	11	1	1	24
10	61	52	50	2	4	4	1	0	9
11	74	60	60	0	7	7	0	0	14
12	72	62	62	0	4	4	1	1	10
13	60	50	46	4	6	4	0	0	10
14	71	62	59	3	0	9	0	0	9
15	79	65	65	0	8	5	0	1	14
16	53	46	43	3	2	5	0	0	7
17	41	35	35	0	3	3	0	0	6
18	91	74	74	0	10	6	1	0	17
19	57	50	46	4	4	3	0	0	7
20	77	54	52	2	6	8	1	8	23
21	65	51	51	0	7	7	0	0	14
22	33	27	24	3	3	0	2	1	6
23	55	48	33	15	5	2	0	0	7
24									
<b>TOTAL</b>	<b>1474</b>	<b>1213</b>	<b>1157</b>	<b>56</b>	<b>108</b>	<b>127</b>	<b>11</b>	<b>15</b>	<b>261</b>
<b>AVERAGE</b>	<b>64.1</b>	<b>52.7</b>	<b>50.3</b>	<b>2.4</b>	<b>4.7</b>	<b>5.5</b>	<b>0.5</b>	<b>0.7</b>	<b>11.3</b>
<b>SEM</b>	<b>3.1</b>	<b>2.8</b>	<b>3.2</b>	<b>0.7</b>	<b>0.8</b>	<b>0.6</b>	<b>0.2</b>	<b>0.4</b>	<b>1.1</b>
Stat. sig. (exp. vs. con. embryos; T11a) *p<0.05, **p<0.005	<b>**</b>	<b>*</b>		<b>**</b>	<b>**</b>	<b>*</b>	<b>*</b>		<b>**</b>
p-value (2-tailed students t-test)	3.31E-05	3.09E-02	6.04E-01	9.60E-07	6.31E-08	1.94E-02	3.10E-02	5.64E-01	1.15E-08
Stat. sig. (exp. vs. exp embryos; T11b) \$p<0.05, \$\$p<0.005			<b>\$</b>	<b>\$\$</b>	<b>\$\$</b>	<b>\$\$</b>			<b>\$\$</b>
p-value (2-tailed students t-test)	9.92E-02	7.54E-01	2.27E-02	2.89E-09	7.50E-10	5.28E-05	2.56E-01	7.61E-01	5.18E-05
Stat. sig. (exp. vs. exp embryos; T11c) †p<0.05, ††p<0.005					<b>†</b>	<b>††</b>			
p-value (2-tailed students t-test)	3.52E-01	2.74E-01	3.90E-01	6.18E-01	2.75E-02	2.58E-03	1.69E-01	2.20E-01	7.85E-01

Table T11d

+Fgf-receptor inhibitor (SU5402) + p38-Mapk14/11 (SB22025) inhibitors, Mkk6-EE mRNA (+OGDB) microinjected									
#	TOTAL NUMBER OF CELLS								
	EMBRYO	TE	Nanog -ve TE cells	Nanog +ve TE cells	Nanog	Gata4	ICM Nanog/Gata4 (co-expressed)	Nanog/Gata4-ve	TOTAL
1	52	40	27	13	9	2	0	1	12
2	42	32	9	23	10	0	0	0	10
3	57	40	30	10	15	2	0	0	17
4	72	59	22	37	11	0	0	2	13
5	59	50	25	25	6	3	0	0	9
6	52	40	31	9	12	0	0	0	12
7	39	30	12	18	8	1	0	0	9
8	59	43	15	28	12	2	0	2	16
9	38	20	8	12	15	2	0	1	18
10	38	27	20	7	11	0	0	0	11
11	48	36	28	8	2	8	0	2	12
12	68	46	28	18	19	0	0	3	22
13	44	30	15	15	11	0	0	3	14
14	61	48	24	24	12	0	0	1	13
15	58	47	31	16	11	0	0	0	11
16	47	30	12	18	15	0	0	2	17
17	43	27	18	9	15	1	0	0	16
18	28	21	12	9	6	0	0	1	7
19	54	36	26	10	11	5	0	2	18
20	42	26	9	17	15	0	0	1	16
21	55	29	11	18	23	0	0	3	26
22	50	43	38	5	6	1	0	0	7
23									
24									
<b>TOTAL</b>	1106	800	451	349	255	27	0	24	306
<b>AVERAGE</b>	50.3	36.4	20.5	15.9	11.6	1.2	0.0	1.1	13.9
<b>SEM</b>	2.3	2.2	1.9	1.7	1.0	0.4	0.0	0.2	1.0
Stat. sig. (exp. vs. con. embryos; T11a) *p<0.05, **p<0.005	**	**	**	**		**	**	*	**
p-value (2-tailed students t-test)	8.40E-12	6.46E-09	9.18E-13	6.50E-04	5.43E-01	8.55E-12	1.62E-04	1.66E-02	1.91E-06
Stat. sig. (exp. vs. exp embryos; T11b) §p<0.05, §§p<0.005	§§	§§	§§	§	§§		§§		§§
p-value (2-tailed students t-test)	7.51E-07	2.28E-05	1.03E-06	5.59E-02	4.67E-03	3.36E-01	1.62E-04	2.76E-01	2.21E-03
Stat. sig. (exp. vs. exp embryos; T11c) †p<0.05, ††p<0.005	††	††	††	††	††	††		††	†
p-value (2-tailed students t-test)	5.31E-06	1.16E-07	4.33E-13	2.54E-09	2.52E-10	6.68E-13	6.16E-02	7.24E-04	1.76E-02
Stat. sig. (exp. vs. exp embryos; T11d) ##p<0.05, ###p<0.005	###	###	###	###	###	###	#		
p-value (2-tailed students t-test)	8.37E-04	3.53E-05	5.08E-10	2.92E-09	2.89E-06	1.55E-06	6.92E-03	3.12E-01	9.30E-02

Table T11e

Tables T11 (a - e): Individual embryo data used to generate averaged data presented in figure 19 (Fgfr inhibition and Mkk6-EE rescue/p38-Mapk14/11 inhibition ablation); the average number of cells contributing to all blastocyst cell lineages in embryos microinjected in both blastomeres at the 2-cell (E1.5) stage with either control GFP or constitutively active Mkk6-EE mutant mRNA (plus Oregon-green conjugated dextran beads/ OGDBs; injection marker), *in vitro* cultured to the 16-cell (E3.0) stage and transferred into growth media supplemented with either Fgfr inhibitor (+SU5402) or vehicle control (DMSO) before being further cultured until the late-blastocyst (E4.5) stage and immuno-fluorescently stained for Nanog and Gata4. Note an additional group of Mkk6-EE microinjected embryos that had been transferred to Fgfr specific inhibitor, were further transferred into media supplemented with both Fgfr and p38-Mapk14/11 inhibitor (+SU5402 +SB220025) at the early-blastocyst (E3.5) stage before continued culture to the late-blastocyst (E4.5) cell stage and identical immuno-fluorescent staining as the other described groups.

Tables T12 (a-e)

<b>+DMSO, GFP mRNA (+OGDB) microinjected</b>										
#	TOTAL NUMBER OF CELLS									
	EMBRYO	TE	Nanog -ve TE cells	Nanog +ve TE cells	Nanog	Gata4	ICM Nanog/Gata4 (co-expressed)	Nanog/Gata4 -ve	TOTAL	
1	85	64	46	18	11	8	2	0	21	
2	49	34	29	5	8	5	1	1	15	
3	90	70	57	13	9	11	0	0	20	
4	78	56	53	3	15	6	0	1	22	
5	79	57	34	23	12	6	3	1	22	
6	72	56	45	11	6	10	0	0	16	
7	69	49	39	10	11	5	3	1	20	
8	64	51	45	6	5	7	1	0	13	
9	74	60	55	5	4	9	1	0	14	
10	66	52	42	10	8	3	2	1	14	
11	79	61	57	4	8	9	1	0	18	
12	87	61	55	6	15	7	4	0	26	
13	102	79	77	2	12	11	0	0	23	
14	100	74	71	3	11	13	1	1	26	
15	94	73	70	3	13	7	0	1	21	
16	100	78	77	1	8	14	0	0	22	
17	79	50	45	5	17	8	3	1	29	
18	95	75	73	2	7	9	4	0	20	
19	83	58	56	2	18	6	1	0	25	
20	63	46	40	6	8	8	1	0	17	
21	90	60	53	7	16	10	3	1	30	
22	105	81	78	3	10	14	0	0	24	
23										
24										
25										
<b>TOTAL</b>	1803	1345	1197	148	232	186	31	9	458	
<b>AVERAGE</b>	82.0	61.1	54.4	6.7	10.5	8.5	1.4	0.4	20.8	
<b>SEM</b>	3.1	2.6	3.1	1.2	0.8	0.6	0.3	0.1	1.0	

Table T12a

<b>+Tak1 inhibitor (5Z-7-Oxo), GFP mRNA (+OGDB) microinjected</b>										
#	TOTAL NUMBER OF CELLS									
	EMBRYO	TE	Nanog -ve TE cells	Nanog +ve TE cells	Nanog	Gata4	ICM Nanog/Gata4 (co-expressed)	Nanog/Gata4 -ve	TOTAL	
1	70	54	44	10	10	3	3	0	16	
2	54	36	35	1	13	1	4	0	18	
3	70	50	40	10	14	3	2	1	20	
4	62	45	28	17	14	0	1	2	17	
5	87	71	57	14	9	4	3	0	16	
6	67	51	47	4	12	1	1	2	16	
7	64	51	39	12	8	4	0	1	13	
8	73	59	57	2	6	6	2	0	14	
9	85	56	49	7	21	5	3	0	29	
10	63	47	43	4	11	1	3	1	16	
11	86	64	60	4	13	8	1	0	22	
12	87	58	52	6	18	7	3	1	29	
13	84	64	58	6	14	6	0	0	20	
14	84	69	64	5	12	2	0	1	15	
15	76	68	50	18	8	0	0	0	8	
16	81	61	53	8	18	2	0	0	20	
17	76	53	46	7	18	3	2	0	23	
18	92	67	63	4	17	3	4	1	25	
19	79	63	55	8	13	2	0	1	16	
20	90	70	67	3	12	7	1	0	20	
21	70	54	50	4	9	4	3	0	16	
22	42	34	26	8	5	3	0	0	8	
23	76	60	53	7	13	2	1	0	16	
24										
25										
<b>TOTAL</b>	1718	1305	1136	169	288	77	37	11	413	
<b>AVERAGE</b>	74.7	56.7	49.4	7.3	12.5	3.3	1.6	0.5	18.0	
<b>SEM</b>	2.6	2.1	2.3	0.9	0.8	0.5	0.3	0.1	1.1	
Stat. sig. (exp. vs. con. embryos; T12a) *p<0.05, **p<0.005						**				
p-value (2-tailed students t-test)	7.78E-02	1.93E-01	1.95E-01	6.81E-01	1.04E-01	5.53E-08	6.32E-01	6.97E-01	6.50E-02	

Table T12b

+DMSO, Mkk6-EE mRNA (+OGDB) microinjected									
#	TOTAL NUMBER OF CELLS								TOTAL
	EMBRYO	TE	Nanog -ve TE cells	Nanog +ve TE cells	Nanog	Gata4	ICM Nanog/Gata4 (co-expressed)	Nanog/Gata4 -ve	
1	72	54	54	0	9	8	1	0	18
2	47	36	29	7	3	6	2	0	11
3	64	51	48	3	3	8	0	2	13
4	67	50	50	0	9	8	0	0	17
5	51	42	36	6	3	5	0	1	9
6	54	43	41	2	6	4	1	0	11
7	48	45	44	1	1	2	0	0	3
8	59	53	50	3	1	5	0	0	6
9	77	57	55	2	4	16	0	0	20
10	39	32	32	0	0	7	0	0	7
11	56	45	32	13	5	3	1	2	11
12	41	31	16	15	0	6	4	0	10
13	97	84	84	0	3	10	0	0	13
14	62	49	47	2	4	9	0	0	13
15	57	43	30	13	4	7	3	0	14
16	81	64	64	0	7	10	0	0	17
17	81	70	70	0	0	11	0	0	11
18	68	51	45	6	12	4	0	1	17
19	74	66	62	4	2	6	0	0	8
20	78	66	66	0	1	11	0	0	12
21	51	40	38	2	0	9	2	0	11
22	76	67	67	0	3	6	0	0	9
23	55	44	31	13	4	7	0	0	11
24	46	24	9	15	6	13	2	1	22
25	83	66	66	0	2	15	0	0	17
<b>TOTAL</b>	<b>1584</b>	<b>1273</b>	<b>1166</b>	<b>107</b>	<b>92</b>	<b>196</b>	<b>16</b>	<b>7</b>	<b>311</b>
<b>AVERAGE</b>	<b>63.4</b>	<b>50.9</b>	<b>46.6</b>	<b>4.3</b>	<b>3.7</b>	<b>7.8</b>	<b>0.6</b>	<b>0.3</b>	<b>12.4</b>
<b>SEM</b>	<b>3.0</b>	<b>2.8</b>	<b>3.6</b>	<b>1.1</b>	<b>0.6</b>	<b>0.7</b>	<b>0.2</b>	<b>0.1</b>	<b>0.9</b>
Stat. sig. (exp. vs. con. embryos; T12a) *p<0.05, **p<0.005	<b>**</b>	<b>*</b>			<b>**</b>		<b>*</b>		<b>**</b>
p-value (2-tailed students t-test)	9.13E-05	1.12E-02	1.12E-01	1.29E-01	2.84E-08	5.21E-01	3.92E-02	4.38E-01	1.64E-07

Table T12c

+Tak1 inhibitor (5Z-7-Oxo), Mkk6-EE mRNA (+OGDBs) microinjected									
#	TOTAL NUMBER OF CELLS								TOTAL
	EMBRYO	TE	Nanog -ve TE cells	Nanog +ve TE cells	Nanog	Gata4	ICM Nanog/Gata4 (co-expressed)	Nanog/Gata4 -ve	
1	56	42	41	1	4	9	1	0	14
2	56	45	37	8	4	5	2	0	11
3	74	56	53	3	7	7	3	1	18
4	72	63	63	0	2	7	0	0	9
5	50	38	31	7	9	2	0	1	12
6	64	51	45	6	10	1	1	1	13
7	63	54	53	1	3	6	0	0	9
8	59	45	40	5	5	3	4	2	14
9	61	51	49	2	6	4	0	0	10
10	54	50	49	1	1	3	0	0	4
11	54	40	38	2	9	4	1	0	14
12	79	65	64	1	7	7	0	0	14
13	75	49	49	0	14	9	2	1	26
14	87	75	71	4	4	8	0	0	12
15	66	47	36	11	9	2	5	3	19
16	79	72	72	0	0	7	0	0	7
17	87	70	69	1	7	10	0	0	17
18	61	47	43	4	6	6	0	2	14
19	107	86	79	7	6	15	0	0	21
20	87	66	63	3	13	7	1	0	21
21	76	60	49	11	11	3	1	1	16
22	64	45	37	8	16	3	0	0	19
23	71	53	52	1	8	7	3	0	18
24	90	73	69	4	6	9	2	0	17
25	83	66	64	2	4	13	0	0	17
<b>TOTAL</b>	<b>1775</b>	<b>1409</b>	<b>1316</b>	<b>93</b>	<b>171</b>	<b>157</b>	<b>26</b>	<b>12</b>	<b>366</b>
<b>AVERAGE</b>	<b>71.0</b>	<b>56.4</b>	<b>52.6</b>	<b>3.7</b>	<b>6.8</b>	<b>6.3</b>	<b>1.0</b>	<b>0.5</b>	<b>14.6</b>
<b>SEM</b>	<b>2.8</b>	<b>2.5</b>	<b>2.7</b>	<b>0.7</b>	<b>0.8</b>	<b>0.7</b>	<b>0.3</b>	<b>0.2</b>	<b>1.0</b>
Stat. sig. (exp. vs. con. embryos; T12a) *p<0.05, **p<0.005	<b>*</b>			<b>*</b>	<b>**</b>	<b>*</b>			<b>**</b>
p-value (2-tailed students t-test)	1.20E-02	1.93E-01	6.68E-01	2.70E-02	2.31E-03	2.49E-02	3.72E-01	7.28E-01	7.36E-05
Stat. sig. (exp. vs. exp embryos; T12b) *p<0.05, **p<0.005				<b>\$\$</b>	<b>\$\$</b>	<b>\$\$</b>			<b>\$</b>
p-value (2-tailed students t-test)	3.40E-01	9.09E-01	3.65E-01	2.49E-03	1.18E-05	1.18E-03	1.72E-01	9.94E-01	2.98E-02
Stat. sig. (exp. vs. exp embryos; T12c) *p<0.05, **p<0.005					<b>++</b>				
p-value (2-tailed students t-test)	6.93E-02	1.56E-01	1.86E-01	6.56E-01	2.87E-03	1.19E-01	2.75E-01	3.35E-01	1.05E-01

Table T12d

<b>+Tak1 (5Z-7-Oxo) + p38-Mapk14/11 inhibitors, Mkk6-EE mRNA (+OGDBs) microinjected</b>										
#	TOTAL NUMBER OF CELLS									TOTAL
	EMBRYO	TE	Nanog -ve TE cells	Nanog +ve TE cells	Nanog	Gata4	ICM Nanog/Gata4 (co-expressed)	Nanog/Gata4 -ve		
1	84	58	21	37	21	2	1	2	26	
2	29	25	16	9	2	2	0	0	4	
3	72	52	27	25	18	0	0	2	20	
4	51	46	32	14	5	0	0	0	5	
5	73	58	24	34	15	0	0	0	15	
6	68	48	24	24	17	0	2	1	20	
7	61	45	13	32	12	2	2	0	16	
8	65	43	40	3	18	4	0	0	22	
9	56	41	27	14	14	0	0	1	15	
10	63	49	39	10	12	0	0	2	14	
11	64	46	25	21	15	1	0	2	18	
12	73	41	24	17	32	0	0	0	32	
13	56	48	36	12	8	0	0	0	8	
14	70	37	22	15	29	0	0	4	33	
15	47	38	27	11	9	0	0	0	9	
16	42	30	26	4	10	0	0	2	12	
17	62	32	15	17	29	0	0	1	30	
18	52	36	23	13	11	3	1	1	16	
19	68	58	38	20	7	2	0	1	10	
20	60	41	20	21	16	0	2	1	19	
21	55	37	13	24	18	0	0	0	18	
22										
23										
24										
25										
<b>TOTAL</b>	1271	909	532	377	318	16	8	20	362	
<b>AVERAGE</b>	60.5	43.3	25.3	18.0	15.1	0.8	0.4	1.0	17.2	
<b>SEM</b>	2.7	2.0	1.8	2.0	1.7	0.3	0.2	0.2	1.8	
Stat. sig. (exp. vs. con. embryos; T12a) *p<0.05, **p<0.005	**	**	**	**	*	**	**	*		
p-value (2-tailed students t-test)	5.67E-06	2.60E-06	5.78E-10	1.59E-05	1.85E-02	5.30E-14	4.07E-03	3.80E-02	8.46E-02	
Stat. sig. (exp. vs. exp embryos; T12b) \$p<0.05, \$\$p<0.005	\$\$	\$\$	\$\$	\$\$		\$\$	\$\$			
p-value (2-tailed students t-test)	4.30E-04	3.53E-05	2.10E-10	1.25E-05	1.66E-01	3.37E-05	9.02E-04	8.22E-02	7.29E-01	
Stat. sig. (exp. vs. exp embryos; T12c) †p<0.05, ††p<0.005		†	††	††		††		†	†	
p-value (2-tailed students t-test)	4.91E-01	3.81E-02	8.14E-06	1.12E-07	2.92E-08	2.99E-11	3.68E-01	1.08E-02	1.54E-02	
Stat. sig. (exp. vs. exp embryos; T12d) #p<0.05, ##p<0.005	#	##	##	##	##	##				
p-value (2-tailed students t-test)	1.06E-02	2.57E-04	2.60E-10	5.14E-09	3.02E-05	1.18E-08	6.29E-02	9.79E-02	1.89E-01	

**Table T12e**

**Tables T12 (a - e): Individual embryo data used to generate averaged data presented in figure 20 (Tak1 inhibition and Mkk6-EE rescue/p38-Mapk14/11 inhibition ablation);** the average number of cells contributing to all blastocyst cell lineages in embryos microinjected in both blastomeres at the 2-cell (E1.5) stage with either control GFP or constitutively active Mkk6-EE mutant mRNA (plus Oregon-green conjugated dextran beads/ OGDBs; injection marker), *in vitro* cultured to the 8-cell (E2.5) stage and transferred into growth media supplemented with either Tak1 inhibitor (+5Z-7-Oxo) or vehicle control (+DMSO) before being further cultured until the late-blastocyst (E4.5) stage and immuno-fluorescently stained for Nanog and Gata4. Note an additional group of Mkk6-EE microinjected embryos that had been transferred to Tak1 specific inhibitor, were further transferred into media supplemented with both Tak1 and p38-Mapk14/11 inhibitor (+5Z-7-Oxo +SB220025) at the early-blastocyst (E3.5) stage before continued culture to the late-blastocyst (E4.5) cell stage and identical immuno-fluorescent staining as the other described groups.

Tables 13 (a-d)

<b>+DMSO (IF: Nanog/Gata4)</b>								
#	TOTAL NUMBER OF CELLS							
	EMBRYO	TE	Nanog +ve TE cells	ICM				TOTAL
				Nanog	Gata4	Nanog/Gata4 (co-expressed)	Nanog/Gata4 -Ve	
1	99	80	7	8	11	0	0	19
2	90	59	4	19	11	1	0	31
3	97	75	15	9	13	0	0	22
4	90	74	19	7	7	2	0	16
5	56	47	5	7	2	0	0	9
6	88	58	10	17	9	3	1	30
7	70	48	3	12	7	3	0	22
8	77	53	8	13	8	3	0	24
9	90	58	6	18	14	0	0	32
10	85	64	4	10	11	0	0	21
11	62	51	13	7	4	0	0	11
12	82	60	3	7	15	0	0	22
13	105	74	2	14	17	0	0	31
14	87	70	20	10	7	0	0	17
15	84	63	3	14	7	0	0	21
16								
17								
<b>TOTAL</b>	1262	934	122	172	143	12	1	328
<b>AVERAGE</b>	84.1	62.3	8.1	11.5	9.5	0.8	0.1	21.9
<b>SEM</b>	3.4	2.7	1.5	1.1	1.1	0.3	0.1	1.8

Table T13a

<b>+p38-Mapk14/11 inhibitor (SB220025, IF: Nanog/Gata4)</b>								
#	TOTAL NUMBER OF CELLS							
	EMBRYO	TE	Nanog +ve TE cells	ICM				TOTAL
				Nanog	Gata4	Nanog/Gata4 (co-expressed)	Nanog/Gata4 -Ve	
1	66	51	26	11	3	0	1	15
2	82	54	20	27	1	0	0	28
3	89	57	29	30	0	2	0	32
4	74	53	12	17	3	0	1	21
5	79	48	18	27	1	1	2	31
6	48	35	27	13	0	0	0	13
7	70	59	26	7	2	1	1	11
8	95	73	16	16	5	0	1	22
9	80	63	26	12	3	2	0	17
10	92	78	14	12	2	0	0	14
11	75	46	22	23	2	2	2	29
12	56	34	13	21	1	0	0	22
13	88	60	11	22	6	0	0	28
14	64	38	20	21	2	0	3	26
15	64	49	13	10	0	0	5	15
16	72	61	18	9	0	0	2	11
17	50	38	24	12	0	0	0	12
<b>TOTAL</b>	1244	897	335	290	31	8	18	347
<b>AVERAGE</b>	73.2	52.8	19.7	17.1	1.8	0.5	1.1	20.4
<b>SEM</b>	3.4	3.0	1.4	1.7	0.4	0.2	0.3	1.8
Stat. sig. (exp. vs. con embryo; T13a) *p<0.05, **p<0.005	*	*	**	*	**		*	
p-value (2-tailed students t-test)	3.16E-02	2.78E-02	5.72E-06	1.22E-02	8.93E-08	3.80E-01	1.08E-02	5.75E-01

Table T13b

<b>+GSK-3<math>\beta</math> inhibitor (CHIR99021, IF: Nanog/Gata4)</b>									
#	TOTAL NUMBER OF CELLS								
	EMBRYO	TE	Nanog +ve TE cells	ICM				TOTAL	
				Nanog	Gata4	Nanog/Gata4 (co-expressed)	Nanog/Gata4 -Ve		
1	94	65	6	17	11	1	0	29	
2	88	72	8	6	10	0	0	16	
3	45	35	5	5	4	1	0	10	
4	82	67	22	7	8	0	0	15	
5	72	52	8	13	5	1	1	20	
6	96	76	5	8	11	1	0	20	
7	79	65	9	5	9	0	0	14	
8	85	62	6	9	12	2	0	23	
9	75	56	2	13	5	0	1	19	
10	67	45	4	13	8	0	1	22	
11	84	66	4	9	8	1	0	18	
12	84	68	5	6	8	2	0	16	
13	92	67	8	11	10	3	1	25	
14	69	52	1	8	8	1	0	17	
15	71	50	5	12	6	3	0	21	
16									
17									
<b>TOTAL</b>	<b>1183</b>	<b>898</b>	<b>98</b>	<b>142</b>	<b>123</b>	<b>16</b>	<b>4</b>	<b>285</b>	
<b>AVERAGE</b>	<b>78.9</b>	<b>59.9</b>	<b>6.5</b>	<b>9.5</b>	<b>8.2</b>	<b>1.1</b>	<b>0.3</b>	<b>19.0</b>	
<b>SEM</b>	<b>3.4</b>	<b>2.9</b>	<b>1.2</b>	<b>0.9</b>	<b>0.6</b>	<b>0.3</b>	<b>0.1</b>	<b>1.2</b>	

Table T13c

<b>+GSK-3<math>\beta</math> inhibitor (CHIR99021, E2.5-E3.5) co-inhibition (CHIR99021+SB220025, E3.5-E4.5); (IF: Nanog/Gata4)</b>									
#	TOTAL NUMBER OF CELLS								
	EMBRYO	TE	Nanog +ve TE cells	ICM				TOTAL	
				Nanog	Gata4	Nanog/Gata4 (co-expressed)	Nanog/Gata4 -Ve		
1	39	30	15	9	0	0	0	9	
2	47	32	21	13	0	0	2	15	
3	48	38	14	6	3	0	1	10	
4	55	40	15	11	1	1	2	15	
5	46	35	14	8	0	0	3	11	
6	51	41	6	9	0	0	1	10	
7	19	18	7	1	0	0	0	1	
8	47	31	7	11	3	2	0	16	
9	52	43	8	2	7	0	0	9	
10	46	33	15	12	0	0	1	13	
11	47	35	9	7	3	0	2	12	
12	61	46	20	14	1	0	0	15	
13									
14									
15									
16									
17									
<b>TOTAL</b>	<b>558</b>	<b>422</b>	<b>151</b>	<b>103</b>	<b>18</b>	<b>3</b>	<b>12</b>	<b>136</b>	
<b>AVERAGE</b>	<b>46.5</b>	<b>35.2</b>	<b>12.6</b>	<b>8.6</b>	<b>1.5</b>	<b>0.3</b>	<b>1.0</b>	<b>11.3</b>	
<b>SEM</b>	<b>3.0</b>	<b>2.1</b>	<b>1.5</b>	<b>1.2</b>	<b>0.6</b>	<b>0.2</b>	<b>0.3</b>	<b>1.2</b>	
Stat. sig. (exp. vs. exp. Embryo; T13b) $5p < 0.05$ , $55p < 0.005$	<b>55</b>	<b>55</b>	<b>55</b>	<b>55</b>				<b>55</b>	
p-value (2-tailed students t-test)	6.10E-06	1.77E-04	2.26E-03	9.24E-04	6.62E-01	4.31E-01	9.02E-01	7.11E-04	

Table T13d

Tables T13 (a - d): Individual embryo data used to generate averaged data presented in figure 22 (Gsk-3 $\beta$ , p38-Mapk14/11 inhibition and Gsk-3 $\beta$  + p38-Mapk14/11 double inhibition); the average number of cells contributing to all blastocyst cell lineages in embryos *in vitro* cultured in the presence of vehicle control (+DMSO) or p38-Mapk14/11 inhibitor (+SB220025) from the early (E3.5) to late blastocyst (E4.5). For Gsk-3 $\beta$  inhibition the embryos were cultured to the 8-cell stage (E2.5) before being further cultured until the late-blastocyst (E4.5) stage and all the groups are immuno-fluorescently stained for Nanog and Gata4. For double inhibition embryos that had been transferred to Gsk-3 $\beta$  (+CHIR99021) specific inhibitor, were further transferred into media supplemented with both Tak1 and p38-Mapk14/11 inhibitor (+CHIR99021 +SB220025) at the early-blastocyst (E3.5) stage before continued culture to the late-blastocyst (E4.5) cell stage and identical immuno-fluorescent staining as the other described groups.

Tables 14 (a-d)

<b>+DMSO, GFP mRNA (+OGDB) microinjected</b>									
#	TOTAL NUMBER OF CELLS								
	EMBRYO	TE	Nanog +ve TE cells	ICM				TOTAL	
				Nanog	Gata4	Nanog/Gata4 (co-expressed)	Nanog/Gata4 - Ve		
1	78	58	14	8	10	2	0	20	
2	88	73	18	5	8	2	0	15	
3	73	49	2	13	9	2	0	24	
4	90	69	7	11	8	2	0	21	
5	77	57	4	9	8	3	0	20	
6	74	50	1	8	10	6	0	24	
7	71	56	14	9	5	0	1	15	
8	77	58	6	9	10	0	0	19	
9	70	53	10	9	8	0	0	17	
10	69	52	5	13	3	1	0	17	
11	85	77	10	3	4	1	0	8	
12	96	72	20	10	12	1	1	24	
13									
14									
<b>TOTAL</b>	948	724	111	107	95	20	2	224	
<b>AVERAGE</b>	79.0	60.3	9.3	8.9	7.9	1.7	0.2	18.7	
<b>SEM</b>	2.5	2.8	1.8	0.8	0.8	0.5	0.1	1.4	

Table 14a

<b>+DMSO, CA-ATF2 mRNA (+OGDB) microinjected</b>									
#	TOTAL NUMBER OF CELLS								
	EMBRYO	TE	Nanog +ve TE cells	ICM				TOTAL	
				Nanog	Gata4	Nanog/Gata4 (co-expressed)	Nanog/Gata4 - Ve		
1	69	43	20	18	6	2	0	26	
2	57	37	10	16	2	2	0	20	
3	51	42	7	4	2	2	1	9	
4	59	35	14	17	2	3	2	24	
5	49	30	16	18	0	0	1	19	
6	62	57	8	2	3	0	0	5	
7	79	65	9	6	7	1	0	14	
8	56	31	21	18	1	6	0	25	
9	63	39	12	20	1	2	1	24	
10	76	59	7	10	7	0	0	17	
11	47	29	3	12	1	2	3	18	
12	59	42	6	10	5	2	0	17	
13									
14									
<b>TOTAL</b>	727	509	133	151	37	22	8	218	
<b>AVERAGE</b>	60.6	42.4	11.1	12.6	3.1	1.8	0.7	18.2	
<b>SEM</b>	2.9	3.4	1.6	1.8	0.7	0.5	0.3	1.9	
Stat. sig. (exp. vs. con embryo; T14a) #p<0.05, ##p<0.005	##	##			##				
p-value (2-tailed students t-test)	8.66E-05	5.59E-04	4.56E-01	7.49E-02	1.51E-04	8.08E-01	1.16E-01	8.30E-01	

Table 14b

<b>+p38-Mapk14/11 (SB220025), GFP mRNA (+OGDB) microinjected</b>									
#	TOTAL NUMBER OF CELLS								TOTAL
	EMBRYO	TE	Nanog +ve TE cells	ICM					
				Nanog	Gata4	Nanog/Gata4 (co-expressed)	Nanog/Gata4 -Ve		
1	89	66	9	12	9	1	1	23	
2	48	34	17	11	0	0	3	14	
3	87	62	42	23	0	0	2	25	
4	89	61	21	21	2	4	1	28	
5	42	33	20	9	0	0	0	9	
6	74	53	38	18	2	1	0	21	
7	80	62	40	16	1	0	1	18	
8	65	47	22	15	0	0	3	18	
9	54	34	24	19	0	0	1	20	
10	80	57	21	18	4	0	1	23	
11	56	38	31	12	4	2	0	18	
12	60	53	28	5	2	0	0	7	
13	59	43	18	14	0	2	0	16	
14	69	62	19	5	0	0	2	7	
15	55	36	16	17	0	0	2	19	
<b>TOTAL</b>	<b>1007</b>	<b>741</b>	<b>366</b>	<b>215</b>	<b>24</b>	<b>10</b>	<b>17</b>	<b>266</b>	
<b>AVERAGE</b>	<b>67.1</b>	<b>49.4</b>	<b>24.4</b>	<b>14.3</b>	<b>1.6</b>	<b>0.7</b>	<b>1.1</b>	<b>17.7</b>	
<b>SEM</b>	<b>4.0</b>	<b>3.1</b>	<b>2.5</b>	<b>1.4</b>	<b>0.6</b>	<b>0.3</b>	<b>0.3</b>	<b>1.6</b>	
Stat. sig. (exp. vs. con embryo; T14a) *p<0.05, **p<0.005	*	*	**	**	**		*		
p-value (2-tailed students t-test)	2.52E-02	1.82E-02	7.13E-05	4.25E-03	1.30E-06	7.99E-02	6.16E-03	6.73E-01	

Table 14c

<b>+p38-Mapk14/11 (SB220025), CA-ATF2 mRNA (+OGDB) microinjected</b>									
#	TOTAL NUMBER OF CELLS								TOTAL
	EMBRYO	TE	Nanog +ve TE cells	ICM					
				Nanog	Gata4	Nanog/Gata4 (co-expressed)	Nanog/Gata4 -Ve		
1	51	39	14	8	1	1	2	12	
2	52	36	22	16	0	0	0	16	
3	34	23	14	9	0	2	0	11	
4	40	33	27	7	0	0	0	7	
5	41	27	20	11	0	3	0	14	
6	52	43	29	9	0	0	0	9	
7	72	51	33	16	2	3	0	21	
8	57	41	15	16	0	0	0	16	
9	40	34	25	6	0	0	0	6	
10	66	53	28	7	2	4	0	13	
11	65	49	28	11	3	1	1	16	
12	39	32	13	7	0	0	0	7	
13	49	35	25	14	0	0	0	14	
14	74	55	21	10	3	3	3	19	
15									
<b>TOTAL</b>	<b>732</b>	<b>551</b>	<b>314</b>	<b>147</b>	<b>11</b>	<b>17</b>	<b>6</b>	<b>181</b>	
<b>AVERAGE</b>	<b>52.3</b>	<b>39.4</b>	<b>22.4</b>	<b>10.5</b>	<b>0.8</b>	<b>1.2</b>	<b>0.4</b>	<b>12.9</b>	
<b>SEM</b>	<b>3.5</b>	<b>2.6</b>	<b>1.7</b>	<b>1.0</b>	<b>0.3</b>	<b>0.4</b>	<b>0.3</b>	<b>1.2</b>	
Stat. sig. (exp. Vs. exp embryo; T14b) §p<0.05, §§p<0.005	§	§		§				§	
p-value (2-tailed students t-test)	9.23E-03	2.17E-02	5.24E-01	3.38E-02	2.78E-01	2.77E-01	6.94E-02	2.71E-02	

Table 14d

Tables T14 (a - d): Individual embryo data used to generate averaged data presented in figure 23 (CA-ATF2 and p38-Mapk14/11 inhibition); the average number of cells contributing to all blastocyst cell lineages in embryos microinjected in both blastomeres at the 2-cell (E1.5) stage with either control GFP or constitutively active CA-ATF2 mutant mRNA (plus Oregon-green conjugated dextran beads/ OGDBs; injection marker), *in vitro* cultured to the early blastocyst (E3.5) stage and transferred into growth media supplemented with either p38-Mapk14/11 inhibitor (+SB220025) or vehicle control (+DMSO) before being further cultured until the late-blastocyst (E4.5) stage and immuno-fluorescently stained for Nanog and Gata4.

Tables 15 (a-d)

+DMSO, GFP mRNA (+OGDB) microinjected								
#	TOTAL NUMBER OF CELLS							
	EMBRYO	TE	Nanog +ve TE cells	ICM				TOTAL
				Nanog	Gata4	Nanog/Gata4 (co-expressed)	Nanog/Gata4 -Ve	
1	71	58	14	8	4	1	0	13
2	65	50	9	5	4	6	0	15
3	86	64	12	16	5	0	1	22
4	80	60	15	13	6	0	1	20
5	89	51	6	30	5	3	0	38
6	91	70	8	11	7	3	0	21
7	80	64	3	8	7	1	0	16
8	88	65	6	17	4	2	0	23
9	84	60	10	15	6	1	2	24
10	76	57	3	12	5	2	0	19
11	60	42	4	8	6	0	4	18
12	79	61	7	11	7	0	0	18
13	73	55	2	8	8	2	0	18
14								
15								
<b>TOTAL</b>	1022	757	99	162	74	21	8	265
<b>AVERAGE</b>	78.6	58.2	7.6	12.5	5.7	1.6	0.6	20.4
<b>SEM</b>	2.6	2.1	1.2	1.8	0.4	0.5	0.3	1.7

Table 15a

+p38-Mapk14/11 (SB220025), GFP mRNA (+OGDB) microinjected								
#	TOTAL NUMBER OF CELLS							
	EMBRYO	TE	Nanog +ve TE cells	ICM				TOTAL
				Nanog	Gata4	Nanog/Gata4 (co-expressed)	Nanog/Gata4 -Ve	
1	75	50	42	24	0	1	0	25
2	59	41	31	18	0	0	0	18
3	66	53	19	13	0	0	0	13
4	65	45	22	13	0	5	2	20
5	82	54	15	20	3	4	1	28
6	70	51	10	16	0	0	3	19
7	69	54	34	10	4	1	0	15
8	77	62	19	9	5	1	0	15
9	70	54	13	13	3	0	0	16
10	59	49	22	10	0	0	0	10
11	66	45	26	18	2	1	0	21
12	74	56	27	12	3	1	2	18
13	59	39	15	16	1	0	3	20
14	57	36	14	19	0	0	2	21
15	41	35	24	6	0	0	0	6
<b>TOTAL</b>	989	724	333	217	21	14	13	265
<b>AVERAGE</b>	65.9	48.3	22.2	14.5	1.4	0.9	0.9	17.7
<b>SEM</b>	2.6	2.0	2.3	1.2	0.5	0.4	0.3	1.4
Stat. sig. (exp. vs. con embryo; T15a) *p<0.05, **p<0.005	**	**	**		**			
p-value (2-tailed students t-test)	2.05E-03	2.02E-03	9.89E-06	3.53E-01	1.21E-07	2.76E-01	5.82E-01	2.30E-01

Table 15b

+DMSO, CA-Mk3 mRNA (+OGDB) microinjected								
#	TOTAL NUMBER OF CELLS							
	EMBRYO	TE	Nanog +ve TE cells	ICM				TOTAL
				Nanog	Gata4	Nanog/Gata4 (co-expressed)	Nanog/Gata4 -Ve	
1	35	27	8	6	2	0	0	8
2	85	67	9	10	8	0	0	18
3	65	45	0	10	8	2	0	20
4	68	56	4	6	4	2	0	12
5	77	45	11	22	4	4	2	32
6	72	55	12	14	2	1	0	17
7	69	46	8	17	5	1	0	23
8	62	45	4	9	5	2	1	17
9	51	42	13	7	1	1	0	9
10	70	47	8	14	9	0	0	23
11	46	33	5	11	2	0	0	13
12								
13								
14								
15								
<b>TOTAL</b>	700	508	82	126	50	13	3	192
<b>AVERAGE</b>	63.6	46.2	7.5	11.5	4.5	1.2	0.3	17.5
<b>SEM</b>	4.4	3.3	1.2	1.5	0.8	0.4	0.2	2.1
Stat. sig. (exp. vs. con embryo; T15a) #p<0.05, ##p<0.005	#	##						
p-value (2-tailed students t-test)	5.02E-03	3.91E-03	9.24E-01	6.74E-01	1.97E-01	4.93E-01	4.04E-01	2.87E-01

Table 15c

+p38-Mapk14/11 (SB220025), CA-Mk3 mRNA (+OGDB) microinjected								
#	TOTAL NUMBER OF CELLS							
	EMBRYO	TE	Nanog +ve TE cells	ICM				TOTAL
				Nanog	Gata4	Nanog/Gata4 (co-expressed)	Nanog/Gata4 -Ve	
1	36	28	14	6	1	1	0	8
2	76	52	17	19	4	1	0	24
3	40	27	16	11	0	2	0	13
4	66	46	24	20	0	0	0	20
5	69	52	28	13	0	0	4	17
6	51	39	9	12	0	0	0	12
7	55	45	15	7	3	0	0	10
8	52	35	19	17	0	0	0	17
9	58	42	23	13	2	1	0	16
10	44	32	11	12	0	0	0	12
11	73	55	19	10	4	4	0	18
12	69	41	19	28	0	0	0	28
13								
14								
15								
<b>TOTAL</b>	689	494	214	168	14	9	4	195
<b>AVERAGE</b>	57.4	41.2	17.8	14.0	1.2	0.8	0.3	16.3
<b>SEM</b>	3.8	2.7	1.6	1.8	0.5	0.4	0.3	1.7
Stat. sig. (exp. vs. con embryo; T15b) §p<0.05, §§p<0.005		§						
p-value (2-tailed students t-test)	6.97E-02	4.22E-02	1.44E-01	8.26E-01	7.28E-01	7.39E-01	2.51E-01	5.24E-01

Table 15d

Tables T15 (a - d): Individual embryo data used to generate averaged data presented in figure 24 (CA-Mk3 and p38-Mapk14/11 inhibition); the average number of cells contributing to all blastocyst cell lineages in embryos microinjected in both blastomeres at the 2-cell (E1.5) stage with either control GFP or constitutively active CA-Mk3 mutant mRNA (plus Oregon-green conjugated dextran beads/ OGDBs; injection marker), *in vitro* cultured to the early blastocyst (E3.5) stage and transferred into growth media supplemented with either p38-Mapk14/11 inhibitor (+SB220025) or vehicle control (+DMSO) before being further cultured until the late-blastocyst (E4.5) stage and immuno-fluorescently stained for Nanog and Gata4.

Tables 16 (a-d)

cKSOM +DMSO (IF: Nanog/ Gata4)								
#	TOTAL NUMBER OF CELLS							
	EMBRYO	TE	Nanog +ve TE cells	ICM				TOTAL
				Nanog	Gata4	Nanog/Gata4 (co-expressed)	Nanog/Gata4 -ve	
1	67	51	0	11	5	0	1	17
2	89	58	0	17	3	11	0	31
3	89	61	5	13	10	5	1	29
4	97	68	0	11	11	7	0	29
5	83	55	10	12	10	6	1	29
6	88	60	8	12	10	6	1	29
7	68	54	17	7	4	3	1	15
8	71	61	0	6	1	3	1	11
9	67	51	6	12	3	1	0	16
10	92	68	8	12	6	6	0	24
11	83	69	15	7	4	3	1	15
12	90	70	6	15	4	1	2	22
13	102	79	7	10	11	2	0	23
14	82	59	5	12	8	3	0	23
15	98	75	0	10	10	3	0	23
16	77	63	3	7	6	1	0	14
17	85	55	0	14	15	1	1	31
18	78	61	0	14	1	2	0	17
19	80	65	4	10	5	0	1	16
20	90	66	1	15	7	2	0	24
21	95	73	3	16	6	0	0	22
22	78	58	7	10	10	0	1	21
<b>TOTAL</b>	<b>1849</b>	<b>1380</b>	<b>105</b>	<b>253</b>	<b>150</b>	<b>66</b>	<b>12</b>	<b>481</b>
<b>AVERAGE</b>	<b>84.0</b>	<b>62.7</b>	<b>4.8</b>	<b>11.5</b>	<b>6.8</b>	<b>3.0</b>	<b>0.5</b>	<b>21.9</b>
<b>SEM</b>	<b>2.2</b>	<b>1.6</b>	<b>1.0</b>	<b>0.6</b>	<b>0.8</b>	<b>0.6</b>	<b>0.1</b>	<b>1.3</b>

Table 16a

cKSOM +p38-Mapk14/11 inhibitor (SB220025, IF: Nanog/ Gata4)								
#	TOTAL NUMBER OF CELLS							
	EMBRYO	TE	Nanog +ve TE cells	ICM				TOTAL
				Nanog	Gata4	Nanog/Gata4 (co-expressed)	Nanog/Gata4 -ve	
1	50	25	20	25	0	0	0	25
2	87	70	38	11	2	4	1	18
3	60	48	15	12	0	0	2	14
4	62	52	34	4	4	2	0	10
5	84	65	31	11	4	4	0	19
6	55	41	15	11	3	0	2	16
7	70	50	26	18	0	2	2	22
8	52	36	18	16	0	0	0	16
9	55	45	18	8	0	2	1	11
10	62	53	17	6	3	0	5	14
11	54	43	19	11	0	0	4	15
12	56	47	13	7	0	2	0	9
13	46	37	14	9	0	0	0	9
14	87	66	17	18	2	1	2	23
15	65	54	11	11	0	0	1	12
16	37	30	8	7	0	0	1	8
17	45	35	7	10	0	0	0	10
18	52	43	16	8	1	0	1	10
19	66	55	20	11	0	0	1	12
20	46	35	16	8	1	2	0	11
21	59	53	19	6	0	0	0	6
22	48	37	4	9	0	2	2	13
23	49	41	5	7	1	0	0	8
24	45	36	9	9	0	0	0	9
<b>TOTAL</b>	<b>1392</b>	<b>1097</b>	<b>410</b>	<b>253</b>	<b>21</b>	<b>21</b>	<b>25</b>	<b>320</b>
<b>AVERAGE</b>	<b>58.0</b>	<b>45.7</b>	<b>17.1</b>	<b>10.5</b>	<b>0.9</b>	<b>0.9</b>	<b>1.0</b>	<b>13.3</b>
<b>SEM</b>	<b>2.7</b>	<b>2.3</b>	<b>1.7</b>	<b>1.0</b>	<b>0.3</b>	<b>0.3</b>	<b>0.3</b>	<b>1.0</b>
Stat. sig. (exp. vs. con embryo; T16a) *p<0.05, **p<0.005	<b>**</b>	<b>**</b>	<b>**</b>	<b>**</b>	<b>**</b>	<b>**</b>	<b>**</b>	<b>**</b>
p-value (2-tailed students t-test)	<b>2.84E-09</b>	<b>5.12E-07</b>	<b>3.95E-07</b>	<b>4.18E-01</b>	<b>2.99E-09</b>	<b>1.72E-03</b>	<b>1.16E-01</b>	<b>5.19E-06</b>

Table 16b

KSOM+AA +DMSO (IF: Nanog/ Gata4)								
#	TOTAL NUMBER OF CELLS							
	EMBRYO	TE	Nanog +ve TE cells	ICM				TOTAL
				Nanog	Gata4	Nanog/Gata4 (co-expressed)	Nanog/Gata4 -ve	
1	97	75	7	10	10	2	0	22
2	86	59	13	19	4	4	0	27
3	78	54	3	11	10	3	0	24
4	98	87	16	3	8	0	0	11
5	68	55	7	7	4	2	0	13
6	68	55	14	7	2	4	0	13
7	74	49	3	16	5	4	0	25
8	88	70	13	9	9	0	0	18
9	97	79	13	11	7	0	0	18
10	68	47	7	12	8	1	0	21
11	68	49	8	11	4	4	0	19
12	102	82	11	13	7	0	0	20
13	83	64	10	12	7	0	0	19
14	104	76	4	12	14	2	0	28
15								
16								
17								
18								
19								
20								
21								
22								
23								
24								
TOTAL	1179	901	129	153	99	26	0	278
AVERAGE	84.2	64.4	9.2	10.9	7.1	1.9	0.0	19.9
SEM	3.7	3.6	1.1	1.0	0.8	0.5	0.0	1.4

Table 16c

KSOM+AA +p38-Mapk14/11 inhibitor (SB220025, IF: Nanog/ Gata4)								
#	TOTAL NUMBER OF CELLS							
	EMBRYO	TE	Nanog +ve TE cells	ICM				TOTAL
				Nanog	Gata4	Nanog/Gata4 (co-expressed)	Nanog/Gata4 -ve	
1	79	50	21	28	1	0	0	29
2	54	42	19	12	0	0	0	12
3	82	51	29	31	0	0	0	31
4	55	33	18	18	2	2	0	22
5	87	69	22	12	3	3	0	18
6	54	35	10	16	0	0	3	19
7	73	61	35	8	2	2	0	12
8	82	62	25	10	6	2	2	20
9	71	54	14	8	6	2	1	17
10	67	49	16	13	3	0	2	18
11	67	54	40	13	0	0	0	13
12	69	43	9	16	2	1	7	26
13	82	62	18	15	3	2	0	20
14	76	50	23	26	0	0	0	26
15	80	60	39	18	0	1	1	20
16	79	52	29	26	0	1	0	27
17	90	72	32	13	4	0	1	18
18	98	71	24	25	0	0	2	27
19								
20								
21								
22								
23								
24								
TOTAL	1345	970	423	308	32	16	19	375
AVERAGE	74.7	53.9	23.5	17.1	1.8	0.9	1.1	20.8
SEM	2.9	2.7	2.1	1.7	0.5	0.2	0.4	1.4
Stat. sig. (exp. vs. con embryo; T1&C) #p<0.05, ##p<0.005	#	#	###	#	###		#	
p-value (2-tailed students t-test)	4.80E-02	2.42E-02	7.24E-06	6.53E-03	2.79E-06	5.49E-02	3.34E-02	6.23E-01
Stat. sig. (exp. vs. exp. Embryo; T1&B) \$p<0.05, \$\$p<0.005	\$	\$	\$	\$				\$
p-value (2-tailed students t-test)	1.63E-04	2.66E-02	2.39E-02	8.41E-04	9.37E-02	9.70E-01	9.77E-01	6.13E-05

Table 16d

Tables T16 (a - d): Individual embryo data used to generate averaged data presented in figure 26 (b & b'); the average number of cells contributing to all blastocyst cell lineages in embryos *in vitro* cultured in the presence of vehicle control (+DMSO) or p38-Mapk14/11 inhibitor (+SB220025) in both cKSOM and KSOM+AA from the early (E3.5) to late blastocyst (E4.5) stages in embryos immuno-fluorescently stained for Nanog in combination with Gata4.

Tables 17 (a-d)

cKSOM +DMSO (IF: Nanog/Sox17)										
#	TOTAL NUMBER OF CELLS									TOTAL
	EMBRYO	TE	Nanog -ve TE cells	Nanog +ve TE cells	ICM					
					Nanog	Sox17	Nanog/Sox17(co-expressed)	Nanog/Sox17 - Ve		
1	105	76	64	12	12	8	8	1	29	
2	103	82	62	20	12	9	0	0	21	
3	89	63	44	19	10	5	11	0	26	
4	94	72	57	15	8	6	8	0	22	
5	102	73	53	20	15	7	5	2	29	
6	74	57	36	21	9	4	4	0	17	
7	97	62	54	8	15	8	12	0	35	
8	98	62	44	18	16	8	10	2	36	
9	64	46	39	7	5	11	2	0	18	
10	82	64	51	13	11	6	1	0	18	
11	96	66	55	11	15	10	1	4	30	
12	82	61	55	6	9	8	4	0	21	
13	80	67	67	0	6	6	1	0	13	
14	95	75	74	1	7	12	0	1	20	
15	89	69	69	0	9	5	2	4	20	
16	99	81	79	2	6	12	0	0	18	
17	72	56	53	3	9	6	1	0	16	
18	92	71	62	9	9	9	3	0	21	
19	74	53	47	6	12	6	3	0	21	
20	97	75	73	2	9	11	0	2	22	
<b>TOTAL</b>	<b>1784</b>	<b>1331</b>	<b>1138</b>	<b>193</b>	<b>204</b>	<b>157</b>	<b>76</b>	<b>16</b>	<b>453</b>	
<b>AVERAGE</b>	<b>89.2</b>	<b>66.6</b>	<b>56.9</b>	<b>9.7</b>	<b>10.2</b>	<b>7.9</b>	<b>3.8</b>	<b>0.8</b>	<b>22.7</b>	
<b>SEM</b>	<b>2.6</b>	<b>2.1</b>	<b>2.6</b>	<b>1.6</b>	<b>0.7</b>	<b>0.5</b>	<b>0.9</b>	<b>0.3</b>	<b>1.4</b>	

Table 17a

cKSOM +p38-Mapk14/11 inhibitor (SB220025, IF: Nanog/Sox17)										
#	TOTAL NUMBER OF CELLS									TOTAL
	EMBRYO	TE	Nanog -ve TE cells	Nanog +ve TE cells	ICM					
					Nanog	Sox17	Nanog/Sox17(co-expressed)	Nanog/Sox17 - Ve		
1	52	37	20	17	13	0	2	0	15	
2	86	70	51	19	6	4	5	1	16	
3	48	35	15	20	11	0	0	2	13	
4	46	33	11	22	12	0	0	1	13	
5	61	47	39	8	8	3	3	0	14	
6	50	40	16	24	6	1	0	3	10	
7	55	38	15	23	15	0	0	2	17	
8	53	35	16	19	13	0	5	0	18	
9	44	31	13	18	13	0	0	0	13	
10	67	53	10	43	11	0	3	0	14	
11	53	37	7	30	9	0	6	1	16	
12	49	38	6	32	8	0	2	1	11	
13	48	39	14	25	8	0	0	1	9	
14	50	40	22	18	8	0	2	0	10	
15	60	49	18	31	11	0	0	0	11	
16	71	57	22	35	12	2	0	0	14	
17	54	51	21	30	3	0	0	0	3	
18	58	49	24	25	8	0	1	0	9	
19	72	58	37	21	12	2	0	0	14	
20	66	54	42	12	11	0	0	1	12	
21	62	48	24	24	9	0	5	0	14	
22	56	48	32	16	8	0	0	0	8	
23	56	47	27	20	8	0	0	1	9	
24	94	72	60	12	13	6	2	1	22	
<b>TOTAL</b>	<b>1411</b>	<b>1106</b>	<b>562</b>	<b>544</b>	<b>236</b>	<b>18</b>	<b>36</b>	<b>15</b>	<b>305</b>	
<b>AVERAGE</b>	<b>58.8</b>	<b>46.1</b>	<b>23.4</b>	<b>22.7</b>	<b>9.8</b>	<b>0.8</b>	<b>1.5</b>	<b>0.6</b>	<b>12.7</b>	
<b>SEM</b>	<b>2.5</b>	<b>2.2</b>	<b>2.8</b>	<b>1.6</b>	<b>0.6</b>	<b>0.3</b>	<b>0.4</b>	<b>0.2</b>	<b>0.8</b>	
Stat. sig. (exp. vs. con embryo; T17a) *p<0.05, **p<0.005	<b>**</b>	<b>**</b>	<b>**</b>	<b>**</b>	<b>**</b>	<b>**</b>	<b>*</b>		<b>**</b>	
p-value (2-tailed students t-test)	<b>1.77E-10</b>	<b>5.45E-08</b>	<b>9.67E-11</b>	<b>1.40E-06</b>	<b>6.92E-01</b>	<b>7.19E-15</b>	<b>1.58E-02</b>	<b>5.95E-01</b>	<b>8.51E-08</b>	

Table 17b

KSOM+AA +DMSO (IF: Nanog/Sox17)									
#	TOTAL NUMBER OF CELLS								
	EMBRYO	TE	Nanog -ve TE cells	Nanog +ve TE cells	ICM		Nanog/Sox17 (co-expressed)	Nanog/Sox17 - Ve	TOTAL
					Nanog	Sox17			
1	102	73	71	2	15	9	5	0	29
2	81	60	53	7	11	7	3	0	21
3	80	56	43	13	4	19	1	0	24
4	71	50	45	5	9	8	4	0	21
5	67	56	48	8	5	5	1	0	11
6	122	103	94	9	8	9	2	0	19
7	83	64	61	3	10	7	2	0	19
8	81	72	68	4	4	5	0	0	9
9	84	61	61	0	10	13	0	0	23
10	88	66	59	7	14	7	1	0	22
11	82	58	52	6	9	12	3	0	24
12	93	61	59	2	14	5	13	0	32
13	64	47	41	6	6	11	0	0	17
14	93	70	61	9	7	14	2	0	23
15	99	75	71	4	11	13	0	0	24
16	73	65	50	15	4	2	2	0	8
17	78	53	48	5	11	6	8	0	25
18									
19									
20									
21									
22									
23									
24									
<b>TOTAL</b>	1441	1090	985	105	152	152	47	0	351
<b>AVERAGE</b>	84.8	64.1	57.9	6.2	8.9	8.9	2.8	0.0	20.6
<b>SEM</b>	3.4	3.1	3.2	0.9	0.9	1.0	0.8	0.0	1.6

Table 17c

KSOM+AA +p38-Mapk14/11 inhibitor (SB220025, IF: Nanog/Sox17)									
#	TOTAL NUMBER OF CELLS								
	EMBRYO	TE	Nanog -ve TE cells	Nanog +ve TE cells	ICM		Nanog/Sox17 (co-expressed)	Nanog/Sox17 - Ve	TOTAL
					Nanog	Sox17			
1	76	55	28	27	16	4	1	0	21
2	63	48	23	25	15	0	0	0	15
3	66	50	36	14	7	0	6	3	16
4	83	67	51	16	13	2	1	0	16
5	94	71	58	13	14	5	4	0	23
6	75	59	51	8	15	0	0	1	16
7	78	62	40	22	9	5	2	0	16
8	71	53	48	5	12	4	2	0	18
9	66	53	38	15	12	0	0	1	13
10	68	43	29	14	19	0	6	0	25
11	88	69	44	25	16	0	3	0	19
12	71	54	47	7	12	2	2	1	17
13	72	60	51	9	11	0	1	0	12
14	80	52	33	19	27	0	0	1	28
15	90	62	46	16	22	1	5	0	28
16	62	43	20	23	18	0	1	0	19
17	81	57	49	8	10	10	4	0	24
18									
19									
20									
21									
22									
23									
24									
<b>TOTAL</b>	1284	958	692	266	248	33	38	7	326
<b>AVERAGE</b>	75.5	56.4	40.7	15.6	14.6	1.9	2.2	0.4	19.2
<b>SEM</b>	2.3	2.0	2.7	1.7	1.2	0.7	0.5	0.2	1.2
Stat. sig. (exp. vs. con embryo: T17c) #p<0.05, ##p<0.005	#	#	###	###	###	###		#	
p-value (2-tailed students t-test)	3.29E-02	4.37E-02	2.37E-04	2.59E-05	5.82E-04	2.90E-06	5.85E-01	4.05E-02	4.61E-01
Stat. sig. (exp. vs. exp. Embryo: T17b) \$p<0.05, \$\$p<0.005	\$	\$	\$	\$	\$				\$
p-value (2-tailed students t-test)	3.21E-05	2.23E-03	1.15E-04	5.60E-03	3.71E-04	9.11E-02	2.61E-01	4.13E-01	3.10E-05

Table 17d

Tables T17 (a - d): Individual embryo data used to generate averaged data presented in figure 26 (c & c'); the average number of cells contributing to all blastocyst cell lineages in embryos *in vitro* cultured in the presence of vehicle control (+DMSO) or p38-Mapk14/11 inhibitor (+SB220025) in both cKSOM and KSOM+AA from the early (E3.5) to late blastocyst (E4.5) stages in embryos immuno-fluorescently stained for Nanog in combination with Sox17.

Tables 18 (a-d)

cKSOM +DMSO (IF: Nanog/Gata6)										
#	TOTAL NUMBER OF CELLS									
	EMBRYO	TE	Nanog -ve TE cells	Nanog +ve TE cells	ICM				TOTAL	
					Nanog	Gata6	Nanog/Gata6(co-expressed)	Nanog/Gata6 -Ve		
1	84	70	58	12	4	10	0	0	14	
2	83	64	59	5	11	8	0	0	19	
3	71	49	39	10	6	6	10	0	22	
4	89	70	53	17	5	8	6	0	19	
5	104	79	75	4	12	10	3	0	25	
6	85	59	56	3	13	7	6	0	26	
7	73	53	43	10	8	8	4	0	20	
8	82	62	53	9	7	7	6	0	20	
9	63	37	29	8	11	2	13	0	26	
10	96	66	59	7	10	8	12	0	30	
11	94	74	72	2	8	5	7	0	20	
12	104	80	70	10	8	11	5	0	24	
13	96	69	60	9	14	11	2	0	27	
14	88	69	52	17	9	7	3	0	19	
15	96	73	60	13	8	12	3	0	23	
16	89	61	51	10	12	7	9	0	28	
17	105	83	63	20	8	12	2	0	22	
18	82	65	50	15	5	7	5	0	17	
19	95	61	57	4	10	13	11	0	34	
20	100	70	48	22	12	8	10	0	30	
21	87	71	47	24	7	5	4	0	16	
22	99	69	59	10	13	11	6	0	30	
23	73	60	40	20	5	5	3	0	13	
24	75	60	54	6	4	5	6	0	15	
<b>TOTAL</b>	<b>2113</b>	<b>1574</b>	<b>1307</b>	<b>267</b>	<b>210</b>	<b>193</b>	<b>136</b>	<b>0</b>	<b>539</b>	
<b>AVERAGE</b>	<b>88.0</b>	<b>65.6</b>	<b>54.5</b>	<b>11.1</b>	<b>8.8</b>	<b>8.0</b>	<b>5.7</b>	<b>0.0</b>	<b>22.5</b>	
<b>SEM</b>	<b>2.3</b>	<b>2.1</b>	<b>2.2</b>	<b>1.3</b>	<b>0.6</b>	<b>0.6</b>	<b>0.7</b>	<b>0.0</b>	<b>1.2</b>	

Table 18a

cKSOM +p38-Mapk14/11 inhibitor (SB220025, IF: Nanog/Gata6)										
#	TOTAL NUMBER OF CELLS									
	EMBRYO	TE	Nanog -ve TE cells	Nanog +ve TE cells	ICM				TOTAL	
					Nanog	Gata6	Nanog/Gata6(co-expressed)	Nanog/Gata6 -Ve		
1	46	30	17	13	5	2	9	0	16	
2	41	26	8	18	1	1	13	0	15	
3	48	35	14	21	0	0	13	0	13	
4	40	24	2	22	2	0	14	0	16	
5	72	58	25	33	2	2	10	0	14	
6	41	31	25	6	0	1	9	0	10	
7	38	30	10	20	0	0	8	0	8	
8	46	33	5	28	1	0	12	0	13	
9	59	49	22	27	0	0	10	0	10	
10	50	38	17	21	2	1	9	0	12	
11	52	36	16	20	4	0	12	0	16	
12	73	51	33	18	11	5	6	0	22	
13	43	33	12	21	2	1	7	0	10	
14	66	51	22	29	6	0	9	0	15	
15	51	41	21	20	6	0	4	0	10	
16	49	40	18	22	2	1	6	0	9	
17	69	61	27	34	2	2	4	0	8	
18	51	39	17	22	2	1	9	0	12	
19	47	32	13	19	1	2	12	0	15	
20	56	46	25	21	2	0	8	0	10	
21	62	44	11	33	6	2	10	0	18	
22	60	54	28	26	4	0	2	0	6	
<b>TOTAL</b>	<b>1160</b>	<b>882</b>	<b>388</b>	<b>494</b>	<b>61</b>	<b>21</b>	<b>196</b>	<b>0</b>	<b>278</b>	
<b>AVERAGE</b>	<b>52.7</b>	<b>40.1</b>	<b>17.6</b>	<b>22.5</b>	<b>2.8</b>	<b>1.0</b>	<b>8.9</b>	<b>0.0</b>	<b>12.6</b>	
<b>SEM</b>	<b>2.2</b>	<b>2.1</b>	<b>1.7</b>	<b>1.4</b>	<b>0.6</b>	<b>0.3</b>	<b>0.7</b>	<b>0.0</b>	<b>0.8</b>	
Stat. sig. (exp. vs. con embryo; T18a) *p<0.05, **p<0.005	<b>**</b>	<b>**</b>	<b>**</b>	<b>**</b>	<b>**</b>	<b>**</b>	<b>**</b>		<b>**</b>	
p-value (2-tailed students t-test)	4.86E-14	1.02E-10	5.05E-17	3.14E-07	1.01E-08	2.07E-14	2.35E-03	n/a	1.87E-08	

Table 18b

KSOM+AA +DMSO (IF: Nanog/Gata6)									
#	TOTAL NUMBER OF CELLS								
	EMBRYO	TE	Nanog -ve TE cells	Nanog +ve TE cells	ICM				TOTAL
					Nanog	Gata6	Nanog/Gata6 (Co-expressed)	Nanog/Gata6 - Ve	
1	95	70	58	12	9	14	2	0	25
2	121	94	76	18	10	13	4	0	27
3	82	59	47	12	7	10	6	0	23
4	83	62	60	2	4	10	7	0	21
5	100	71	51	20	12	9	8	0	29
6	86	63	42	21	9	7	7	0	23
7	86	67	28	39	8	9	2	0	19
8	76	55	43	12	9	10	2	0	21
9	94	63	59	4	12	16	3	0	31
10	80	58	43	15	7	11	4	0	22
11	103	77	72	5	9	15	2	0	26
12	90	58	52	6	9	12	11	0	32
13	74	52	49	3	7	8	7	0	22
14	99	82	67	15	6	9	2	0	17
15	75	58	42	16	7	3	7	0	17
16	87	61	55	6	6	14	6	0	26
17									
18									
19									
20									
21									
22									
23									
24									
<b>TOTAL</b>	1431	1050	844	206	131	170	80	0	381
<b>AVERAGE</b>	89.4	65.6	52.8	12.9	8.2	10.6	5.0	0.0	23.8
<b>SEM</b>	3.1	2.8	3.1	2.3	0.5	0.8	0.7	0.0	1.1

Table 18c

KSOM+AA +p38-Mapk14/11 inhibitor (SB220025, IF: Nanog/Gata6)									
#	TOTAL NUMBER OF CELLS								
	EMBRYO	TE	Nanog -ve TE cells	Nanog +ve TE cells	ICM				TOTAL
					Nanog	Gata6	Nanog/Gata6 (co-expressed)	Nanog/Gata6 - Ve	
1	81	56	39	17	5	3	17	0	25
2	66	48	21	27	1	4	13	0	18
3	79	61	46	15	7	10	1	0	18
4	78	55	44	11	6	2	15	0	23
5	60	39	27	12	4	3	14	0	21
6	60	49	22	27	2	1	8	0	11
7	87	72	30	42	2	2	11	0	15
8	64	44	37	7	5	3	12	0	20
9	98	70	39	31	11	4	13	0	28
10	86	64	48	16	5	3	14	0	22
11	74	61	35	26	0	0	13	0	13
12	46	30	18	12	1	6	9	0	16
13	89	69	42	27	6	3	11	0	20
14	72	49	30	19	4	1	18	0	23
15	57	47	45	2	1	3	6	0	10
16	77	55	39	16	4	5	13	0	22
17	68	47	21	26	2	1	18	0	21
18									
19									
20									
21									
22									
23									
24									
<b>TOTAL</b>	1242	916	583	333	66	54	206	0	326
<b>AVERAGE</b>	73.1	53.9	34.3	19.6	3.9	3.2	12.1	0.0	19.2
<b>SEM</b>	3.2	2.8	2.4	2.4	0.7	0.6	1.1	0.0	1.2
Stat. sig. (exp. vs. con embryo: T18c) #p<0.05, ##p<0.005	###	#	###		###	###	###	###	#
p-value (2-tailed students t-test)	9.56E-04	5.27E-03	4.34E-05	5.47E-02	2.38E-05	1.90E-06	4.07E-06	n/a	8.31E-03
Stat. sig. (exp. vs. exp. Embryo: T18b) \$p<0.05, \$\$p<0.005	\$\$	\$\$	\$\$	\$	\$\$	\$\$			\$\$
p-value (2-tailed students t-test)	5.39E-06	3.59E-04	8.92E-07	2.86E-01	2.16E-01	4.36E-04	1.11E-02	n/a	3.64E-05

Table 18d

Tables T18 (a - d): Individual embryo data used to generate averaged data presented in figure 26 (d & d'); the average number of cells contributing to all blastocyst cell lineages in embryos *in vitro* cultured in the presence of vehicle control (+DMSO) or p38-Mapk14/11 inhibitor (+SB220025) in both cKSOM and KSOM+AA from the early (E3.5) to late blastocyst (E4.5) stages in embryos immuno-fluorescently stained for Nanog in combination with Gata6.

Tables 19 (a-d)

cKSOM +DMSO (IF: Nanog/ Gata4)									
#	TOTAL NUMBER OF CELLS								
	EMBRYO	TE	Nanog +ve TE cells	ICM		Nanog/Gata4 (co-expressed)	Nanog/Gata4 - Ve	TOTAL	
				Nanog	Gata4				
1	99	69	7	15	12	3	0	30	
2	69	56	6	3	5	5	0	13	
3	77	56	7	13	4	4	0	21	
4	84	65	22	11	6	2	0	19	
5	87	68	7	10	7	2	0	19	
6	73	53	3	13	5	2	0	20	
7	70	55	13	11	4	0	2	15	
8	85	67	11	11	7	0	0	18	
9	52	41	9	9	2	0	0	11	
10	114	95	10	9	9	1	2	19	
11	74	51	0	17	3	3	1	23	
12	80	57	23	15	5	3	2	23	
13	81	52	10	17	10	2	0	29	
14	102	79	14	13	8	1	1	23	
15	89	69	2	9	9	1	1	20	
16	65	42	7	20	3	0	0	23	
17	94	70	14	17	6	1	0	24	
18	108	86	2	8	13	0	1	22	
19	95	62	8	25	5	3	0	33	
20	97	68	30	18	8	2	1	29	
21	92	67	0	12	7	3	3	25	
22	85	65	24	14	2	4	0	20	
23	94	72	12	11	10	1	0	22	
24	83	64	16	13	2	2	2	19	
25	108	84	3	10	12	1	1	24	
26	79	65	9	8	6	0	0	14	
27	89	72	8	11	4	0	2	17	
28									
<b>TOTAL</b>	2325	1750	277	343	174	46	19	575	
<b>AVERAGE</b>	86.1	64.8	10.3	12.7	6.4	1.7	0.7	21.3	
<b>SEM</b>	2.7	2.4	1.5	0.9	0.6	0.3	0.2	1.0	

Table 19a

cKSOM +p38-Mapk14/11 inhibitor (SB220025, IF: Nanog/ Gata4)									
#	TOTAL NUMBER OF CELLS								
	EMBRYO	TE	Nanog +ve TE cells	ICM		Nanog/Gata4 (co-expressed)	Nanog/Gata4 - Ve	TOTAL	
				Nanog	Gata4				
1	57	49	16	7	0	1	2	8	
2	65	49	34	13	0	3	0	16	
3	68	55	35	10	2	1	0	13	
4	47	36	24	11	0	0	2	11	
5	55	48	43	7	0	0	0	7	
6	56	47	35	9	0	0	0	9	
7	76	65	32	7	4	0	1	11	
8	60	50	30	10	0	0	0	10	
9	88	77	26	7	3	1	1	11	
10	56	42	22	8	2	4	0	14	
11	43	30	13	13	0	0	0	13	
12	83	56	24	22	2	0	3	27	
13	48	35	21	13	0	0	0	13	
14	63	40	22	21	0	0	2	23	
15	57	44	35	12	0	0	1	13	
16	43	29	25	14	0	0	0	14	
17	40	28	23	12	0	0	0	12	
18	26	14	14	12	0	0	0	12	
19	87	70	21	14	2	0	1	17	
20	70	53	15	16	0	0	1	17	
21	66	54	29	10	0	0	2	12	
22	30	19	19	11	0	0	0	11	
23	47	34	23	13	0	0	0	13	
24	65	51	28	13	1	0	0	14	
25	45	35	22	10	0	0	0	10	
26	53	43	30	10	0	0	0	10	
27	50	33	23	16	0	0	1	17	
28	70	56	35	14	0	0	0	14	
<b>TOTAL</b>	1614	1242	719	335	16	10	17	372	
<b>AVERAGE</b>	57.6	44.4	25.7	12.0	0.6	0.4	0.6	13.3	
<b>SEM</b>	2.9	2.7	1.4	0.7	0.2	0.2	0.2	0.8	
Stat. sig. (exp. vs. con embryo; T19a) *p<0.05, **p<0.005	**	**	**		**	**		**	
p-value (2-tailed students t-test)	3.03E-09	7.21E-07	3.87E-10	5.06E-01	1.06E-12	1.36E-04	6.90E-01	5.75E-08	

Table 19b

cKSOM +DMSO +1mM N-Acetyl Cysteine (IF: Nanog/ Gata4)								
#	TOTAL NUMBER OF CELLS							
	EMBRYO	TE	Nanog +ve TE cells	ICM				TOTAL
				Nanog	Gata4	Nanog/Gata4 (co-expressed)	Nanog/Gata4 - Ve	
1	95	78	29	7	8	2	0	17
2	65	48	16	13	3	1	0	17
3	93	74	13	13	4	2	0	19
4	108	89	18	9	8	2	0	19
5	92	70	4	12	9	1	0	22
6	86	75	19	5	6	0	0	11
7	89	58	11	24	2	5	0	31
8	88	62	12	19	5	2	0	26
9	103	79	25	10	10	4	0	24
10	92	73	10	7	11	1	0	19
11	100	68	3	21	10	1	0	32
12	105	75	10	21	7	2	0	30
13	101	77	6	10	10	2	2	24
<b>TOTAL</b>	<b>1217</b>	<b>926</b>	<b>176</b>	<b>171</b>	<b>93</b>	<b>25</b>	<b>2</b>	<b>291</b>
<b>AVERAGE</b>	<b>93.6</b>	<b>71.2</b>	<b>13.5</b>	<b>13.2</b>	<b>7.2</b>	<b>1.9</b>	<b>0.2</b>	<b>22.4</b>
<b>SEM</b>	<b>3.1</b>	<b>2.9</b>	<b>2.1</b>	<b>1.7</b>	<b>0.8</b>	<b>0.4</b>	<b>0.2</b>	<b>1.7</b>

Table 19c

cKSOM +p38-Mapk14/11 inhibitor +1mM N-Acetyl cysteine (SB220025, IF: Nanog/ Gata4)								
#	TOTAL NUMBER OF CELLS							
	EMBRYO	TE	Nanog +ve TE cells	ICM				TOTAL
				Nanog	Gata4	Nanog/Gata4 (co-expressed)	Nanog/Gata4 - Ve	
1	66	43	16	19	2	0	2	23
2	43	25	20	16	0	0	2	18
3	67	47	24	19	0	0	1	20
4	42	23	19	19	0	0	0	19
5	58	46	34	11	0	0	1	12
6	41	28	20	13	0	0	0	13
7	60	42	33	16	0	0	2	18
8	58	42	30	16	0	0	0	16
9	57	39	35	17	0	0	1	18
10	76	60	30	16	0	0	0	16
11	43	33	27	10	0	0	0	10
12	71	55	28	16	0	0	0	16
13	68	52	32	15	0	1	0	16
14	48	38	25	8	0	2	0	10
15	50	39	19	9	2	0	0	11
16	50	34	30	15	0	0	1	16
17	35	25	19	10	0	0	0	10
18	50	30	18	18	0	0	2	20
19	52	41	32	9	0	0	2	11
20	51	38	23	13	0	0	0	13
<b>TOTAL</b>	<b>1086</b>	<b>780</b>	<b>514</b>	<b>285</b>	<b>4</b>	<b>3</b>	<b>14</b>	<b>306</b>
<b>AVERAGE</b>	<b>54.3</b>	<b>39.0</b>	<b>25.7</b>	<b>14.3</b>	<b>0.2</b>	<b>0.2</b>	<b>0.7</b>	<b>15.3</b>
<b>SEM</b>	<b>2.5</b>	<b>2.3</b>	<b>1.4</b>	<b>0.8</b>	<b>0.1</b>	<b>0.1</b>	<b>0.2</b>	<b>0.9</b>
Stat. sig. (exp. vs. exp. Embryo; T19c) #p<0.05, ##p<0.005	<b>##</b>	<b>##</b>	<b>##</b>	<b>##</b>	<b>##</b>	<b>##</b>		<b>##</b>
p-value (2-tailed student's t-test)	3.77E-11	5.39E-10	2.03E-05	5.24E-01	1.50E-11	5.26E-06	5.23E-02	3.22E-04

Table 19d

Tables T19 (a - d): Individual embryo data used to generate averaged data presented in figure 27 (b & b'); the average number of cells contributing to all blastocyst cell lineages in embryos *in vitro* cultured in the presence of vehicle control (+DMSO) or p38-Mapk14/11 inhibitor (+SB220025) in both cKSOM from the early (E3.5) to late blastocyst (E4.5) stage. Similarly, embryos were cultured in cKSOM supplemented with 1mM N-acetyl cysteine (NAC) and p38-Mapk14/11 inhibitor (+SB220025) or vehicle control (+DMSO) from the early (E3.5) to late blastocyst (E4.5) stage. Embryos in all the groups are immuno-fluorescently stained for Nanog and Gata4.

Tables 20 (a-d)

KSOM+AA +DMSO (IF: Nanog/ Gata4)										
#	TOTAL NUMBER OF CELLS									
	EMBRYO	TE	Nanog -ve TE cells	Nanog +ve TE cells	ICM				TOTAL	
					Nanog	Gata4	Nanog/Gata4 (co-expressed)	Nanog/Gata4 - Ve		
1	93	73	64	9	12	5	1	2	20	
2	92	65	50	15	14	9	4	0	27	
3	82	57	43	14	15	7	2	1	25	
4	73	59	53	6	4	8	2	0	14	
5	55	42	36	6	4	4	4	1	13	
6	94	73	62	11	11	6	2	2	21	
7	96	77	71	6	7	10	2	0	19	
8	118	100	75	25	6	10	0	2	18	
9	102	71	45	26	18	10	3	0	31	
10	111	77	67	10	18	14	2	0	34	
11	110	96	79	17	6	7	0	1	14	
12	85	70	60	10	7	5	2	1	15	
13	75	54	53	1	13	5	2	1	21	
14	87	61	58	3	16	8	2	0	26	
15	88	66	46	20	12	9	1	0	22	
16	100	81	72	9	9	8	1	1	19	
17	88	73	57	16	8	7	0	0	15	
18	88	70	45	25	14	4	0	0	18	
19	83	57	49	8	17	9	0	0	26	
20	82	56	44	12	20	4	2	0	26	
21	78	57	46	11	12	7	1	1	21	
22	77	60	60	0	9	7	1	0	17	
23	76	57	51	6	13	4	1	1	19	
24	81	66	60	6	7	7	1	0	15	
<b>TOTAL</b>	2114	1618	1346	272	272	174	36	14	496	
<b>AVERAGE</b>	88.1	67.4	56.1	11.3	11.3	7.3	1.5	0.6	20.7	
<b>SEM</b>	2.8	2.7	2.3	1.5	0.9	0.5	0.2	0.1	1.1	

Table 20a

KSOM+AA +p38-Mapk14/11 inhibitor (SB220025, IF: Nanog/ Gata4)										
#	TOTAL NUMBER OF CELLS									
	EMBRYO	TE	Nanog -ve TE cells	Nanog +ve TE cells	ICM				TOTAL	
					Nanog	Gata4	Nanog/Gata4 (co-expressed)	Nanog/Gata4 - Ve		
1	59	40	10	30	15	0	2	2	19	
2	98	79	55	24	11	5	2	1	19	
3	46	40	30	10	6	0	0	0	6	
4	83	73	60	13	7	2	1	0	10	
5	93	72	50	22	14	4	3	0	21	
6	97	84	64	20	5	5	2	1	13	
7	83	69	36	33	8	5	0	1	14	
8	94	68	49	19	19	2	4	1	26	
9	84	66	30	36	14	2	1	1	18	
10	82	67	43	24	11	4	0	0	15	
11	93	72	31	41	17	3	0	1	21	
12	64	48	28	20	12	4	0	0	16	
13	84	70	50	20	5	8	1	0	14	
14	89	72	55	17	11	4	1	1	17	
15	92	79	39	40	9	3	1	0	13	
16	61	51	25	26	10	0	0	0	10	
17	66	52	26	26	13	0	0	1	14	
18	69	55	25	30	12	0	0	2	14	
19	62	52	18	34	9	0	0	1	10	
20	54	40	20	20	13	1	0	0	14	
21	58	43	6	37	14	0	1	0	15	
22	51	40	24	16	11	0	0	0	11	
23	69	55	15	40	14	0	0	0	14	
24	59	50	27	23	8	1	0	0	9	
<b>TOTAL</b>	1790	1437	816	621	268	53	19	13	353	
<b>AVERAGE</b>	74.6	59.9	34.0	25.9	11.2	2.2	0.8	0.5	14.7	
<b>SEM</b>	3.3	2.9	3.3	1.8	0.7	0.5	0.2	0.1	0.9	
Stat. sig. (exp. vs. con embryo; T20a) *p<0.05, **p<0.005	**			**		**	*		**	
p-value (2-tailed students t-test)	3.39E-03	6.16E-02		1.40E-07	8.90E-01	2.32E-09	3.39E-02	8.35E-01	1.71E-04	

Table 20b

KSOM+AA +DMSO +1mM N-Acetyl Cysteine (IF: Nanog/ Gata4)									
#	TOTAL NUMBER OF CELLS								
	EMBRYO	TE	Nanog -ve TE cells	Nanog +ve TE cells	ICM				TOTAL
					Nanog	Gata4	Nanog/Gata4 (co-expressed)	Nanog/Gata4 -Ve	
1	85	64	64	0	10	10	1	0	21
2	87	64	39	25	14	6	3	0	23
3	77	55	43	12	10	11	1	0	22
4	76	57	53	4	11	5	3	0	19
5	84	62	52	10	12	5	4	1	22
6	82	62	58	4	7	11	2	0	20
7	96	68	61	7	18	6	2	2	28
8	92	66	51	15	11	14	0	1	26
9	86	72	57	15	5	8	1	0	14
10	90	64	63	1	13	11	2	0	26
11	74	58	57	1	6	9	1	0	16
12	82	64	54	10	11	7	0	0	18
13	65	48	43	5	7	10	0	0	17
14	96	76	55	21	9	8	3	0	20
15	81	61	53	8	12	6	2	0	20
16	77	54	54	0	12	10	1	0	23
17	79	63	56	7	7	6	0	3	16
18									
19									
20									
21									
22									
23									
24									
<b>TOTAL</b>	1409	1058	913	145	175	143	26	7	351
<b>AVERAGE</b>	82.9	62.2	53.7	8.5	10.3	8.4	1.5	0.4	20.6
<b>SEM</b>	2.0	1.6	1.7	1.8	0.8	0.6	0.3	0.2	0.9

Table 20c

KSOM +p38-Mapk14/11 inhibitor +1mM N-Acetyl cysteine (SB220025, IF: Nanog/ Gata4)									
#	TOTAL NUMBER OF CELLS								
	EMBRYO	TE	Nanog -ve TE cells	Nanog +ve TE cells	ICM				TOTAL
					Nanog	Gata4	Nanog/Gata4 (weakly)	Nanog/Gata4 -Ve	
1	97	79	50	29	11	6	1	0	18
2	86	64	34	30	19	2	1	0	22
3	81	65	31	34	10	3	3	0	16
4	78	53	26	27	20	2	2	1	25
5	82	58	34	24	20	4	0	0	24
6	93	71	42	29	21	0	1	0	22
7	121	100	85	15	13	4	4	0	21
8	88	64	30	34	19	5	0	0	24
9	85	70	29	41	10	2	2	1	15
10	110	86	63	23	19	3	2	0	24
11	88	67	48	19	15	4	1	1	21
12	99	87	35	52	10	1	0	1	12
13	105	91	54	37	11	0	1	2	14
14	89	69	34	35	17	0	1	2	20
15	78	58	24	34	16	0	0	4	20
16	68	50	42	8	17	0	0	1	18
17	93	66	37	29	23	0	0	4	27
18	69	46	27	19	21	2	0	0	23
19	90	70	54	16	14	3	2	1	20
20	99	75	45	30	18	5	0	1	24
21	102	83	68	15	17	0	1	1	19
22	66	50	30	20	14	0	0	2	16
23	67	53	21	32	14	0	0	0	14
24									
<b>TOTAL</b>	2034	1575	943	632	369	46	22	22	459
<b>AVERAGE</b>	88.4	68.5	41.0	27.5	16.0	2.0	1.0	1.0	20.0
<b>SEM</b>	3.0	3.0	3.3	2.1	0.8	0.4	0.2	0.2	0.8
Stat. sig. (exp. vs. exp. Embryo; T20b) #p<0.05, ##p<0.005			##	##	##	##			
p-value (2-tailed students t-test)	1.56E-01	1.03E-01	3.49E-03	6.90E-08	1.96E-05	8.58E-11	1.31E-01	1.18E-01	5.89E-01
Stat. sig. (exp. vs. exp. Embryo; T20c) \$p<0.05, \$\$p<0.005	\$	\$			\$				\$
p-value (2-tailed students t-test)	3.34E-03	4.38E-02	1.38E-01	5.61E-01	6.36E-05	7.39E-01	6.12E-01	1.43E-01	1.17E-04

Table 20d

Tables T20 (a - d): Individual embryo data used to generate averaged data presented in figure 27 (c & c'); the average number of cells contributing to all blastocyst cell lineages in embryos *in vitro* cultured in the presence of vehicle control (+DMSO) or p38-Mapk14/11 inhibitor (+SB220025) in both KSOM+AA from the early (E3.5) to late blastocyst (E4.5) stage. Similarly, embryos where cultured in KSOM+AA supplemented with 1mM N-acetyl cysteine (NAC) and p38-Mapk14/11 inhibitor (+SB220025) or vehicle control (+DMSO) from the early (E3.5) to late blastocyst (E4.5) stage. Embryos in all the groups are immuno-fluorescently stained for Nanog and Gata4.